Design and Fabrication of a Post-Processing Furnace for 3D Printed Parts

by

Ram Chilukuri

Bachelor of Technology, Mechanical Engineering
Indian Institute of Technology, Delhi, 1998

Submitted to the Department of Mechanical Engineering
in Partial Fulfillment of the Requirements for the degree of

MASTER OF SCIENCE IN MECHANICAL ENGINEERING

at the

MASSACHUSETTS INSTITUTE OF TECHNOLOGY

MAY 2000

Signature of author: .....
Department of Mechanical Engineering
May 15, 2000

Certified by: .....
Emanuel M. Sachs
Professor of Mechanical Engineering
Thesis Supervisor

Accepted by: .....
Ain A. Sonin
Chairman, Graduate Committee

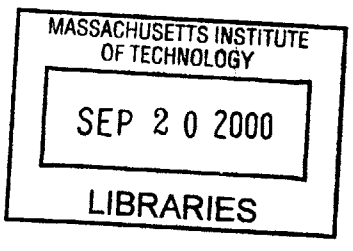

Design and Fabrication of a Post-Processing Furnace for 3D Printed Parts

by

Ram Chilukuri

Submitted to the Department of Mechanical Engineering on May 15, 2000
in Partial Fulfillment of the Requirements for the Degree of
Master of Science in Mechanical Engineering

ABSTRACT

Three dimensional printing is a rapid prototyping process that forms parts directly from a computer model by joining powdered material with a binder. The green part so obtained is subjected to post processing steps that include debinding, sintering and infiltration. Furnaces currently being used for post processing use a Hydrogen or a vacuum atmosphere and the cost of scaling them up to process large parts is prohibitively high. Previous work done at MIT came up with a design for an economical furnace, and a prototype small scale furnace. In this work, as a first step, the small scale furnace previously developed at MIT was optimized to yield good quality, oxide free sintered and infiltrated parts. The important thing learnt from the small scale furnace was that it in order to get oxide free parts, it was necessary to heat the furnace shell from the outside and allow the furnace to soak at 200 C until the dew point inside got to a low value like –25 C, before ramping the furnace to 1200 C.

Having learnt about the process and obtained design parameters from the small scale furnace, a large scale furnace was constructed. This furnace has a rectangular cross section and is more than 20 times bigger in volume than the small scale furnace, which had a circular cross section. This furnace has an Aluminum shell, uses Alumina and Graphite insulation and uses Kanthal heating elements embedded in high Alumina content heater plates to heat the inside of the furnace (12 internal heaters for a total of 10.2 kW). It is designed to operate in a Forming gas or Argon atmosphere. In addition to the internal heaters, it has eleven strip heaters on the shell (a total power of 11 kW) to expel moisture from the insulation during the purging phase of a furnace run. The furnace has a Honeywell controller that uses PID control to ensure the desired operation of the furnace. The controller has events that are used to control the switching of the strip heaters and gas solenoid valves. SS420 parts were successfully sintered and infiltrated using the large scale furnace. At 1200 C, excellent temperature uniformity (temperature in a 5 C band) was found to exist inside the furnace both in the vertical direction and along the furnace depth.

A second issue that was studied as part of this work was the effect of directional solidification on porosity in infiltrated parts. The small scale furnace was used to conduct directional solidification experiments on SS420 parts infiltrated with Bronze. These involved inducing a temperature gradient in a part (using a jet of Argon set up to strike the part on the top) at the end of an infiltration cycle. By comparing two extreme cases, directional solidification, in which the top of a solidifying part is kept cooler than the bottom, with reverse directional solidification, in which the bottom of the part is kept cooler than the top as it solidifies, it was established that directional solidification reduces porosity in parts.

Thesis Supervisor: Emanuel M. Sachs
Title: Professor of Mechanical Engineering

Acknowledgements

I would like to thank Prof. Emanuel Sachs for giving me a chance to work on this project. I am grateful to Prof. Sachs for all that he taught me over the last two years. I am truly impressed by his ability to come up with simple solutions to seemingly complex problems.

I would like to thank the following people who helped me during the course of my research:

Prof. Samuel Allen, for giving me ideas out of his infinite trove of material science knowledge.

Adam Lorenz, who helped me come up to speed with furnace design. I would like to thank him for being a good colleague, ever ready to use his expertise to help me solve problems.

Julie Baars Kaczynski for promptly processing purchase orders for me, and for all the interesting conversations on a variety of non engineering topics. It was fun working with her.

Diane Brancazio, for designing the furnace shell. It was a pleasure working with her.

David Brancazio and James Serdy, for being ever ready to help me.

Mark Belanger, for making all my visits to the LMP machine shop fun experiences, and for being a good friend. I'd also like to thank Gerry Wentworth for helping me in the machine shop.

Peter Morley of MIT Central Machine Shop, for expediting all my job orders.

Yin- Lin Xie of Material Science, for helping me section, polish and photograph infiltrated parts.

I would also like to thank the following folks for making my stay at the 3D printing lab a memorable one: Andreas Straube, Ben Polito, Berndt Heid, Bjorn DeBear, Costas Hadjiloucas, David Ables, David Guo, Diana Buttz, Enrico Vezzetti, Garth Grover, Huaijun Wu, Markus Werner, Olaf Dambon, Patrick Saxton, Sang-bum Hong, Xiaorong Xu and Zubin Irani. Special thanks to David Guo for being a great friend.

Finally, I would like to thank my parents, C.V. Avadhani and C. Prasanna, for all their love and encouragement, without which this work would not have been possible.

Table of Contents

List of Figures

Chapter 1

Chapter 2

Chapter 3

Chapter 4

Chapter 5

Chapter 6

Chapter 7

List of Tables

Chapter 2

Chapter 5

1 Introduction

1.1 Three Dimensional Printing

Three dimensional printing (3DP) is a rapid prototyping process that forms parts directly from a computer model by joining powdered material with a binder. A thin layer of powder is spread and is selectively joined by a binder deposited using ink jet printing technology. The powder bed is then lowered, another powder layer is spread and binder is deposited to print the next cross section. This process is repeated until the whole part is generated. Figure 1.1 shows the steps involved in 3DP. The part thus obtained is called a green part. 3DP is fast and flexible, allowing the use of different material and binder systems.

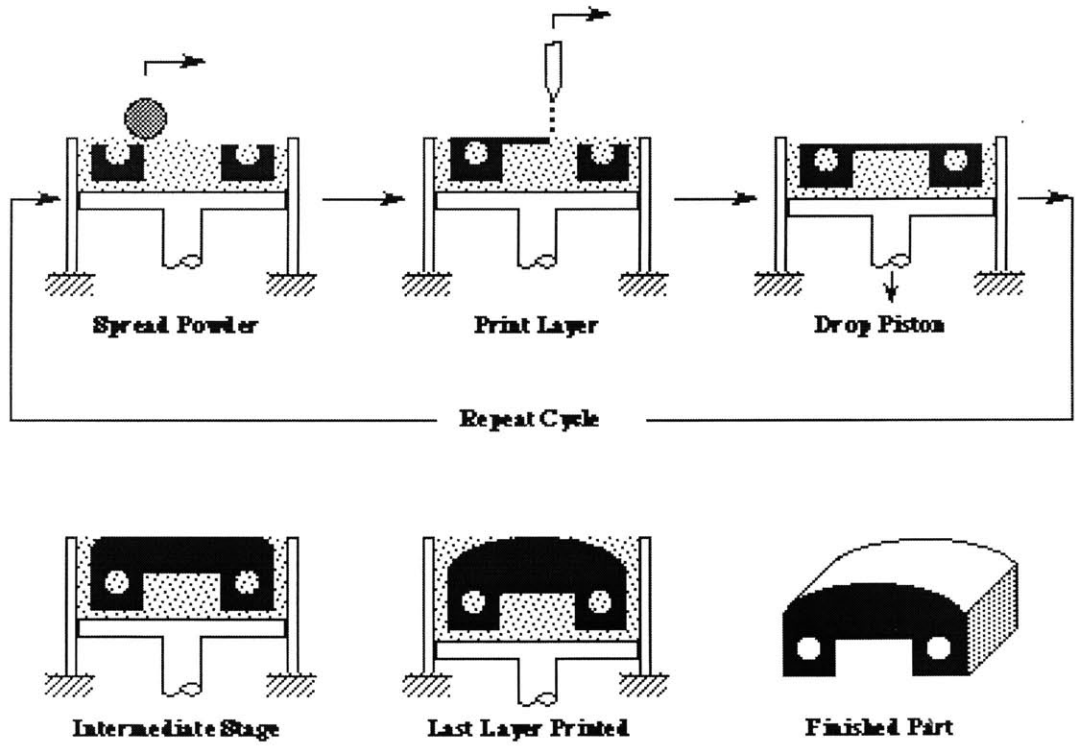

Figure 1.1: Schematic showing steps involved in the Three Dimensional Printing process.

The green part is delicate and must undergo further processing before it can be used. The green part has 60% metal powder by volume, and the rest is void space. The binder is burned out in a furnace where the part also undergoes light sintering. The part is then sintered and infiltrated with a low melting point alloy to fill the porosity. Figure 1.2 shows the post processing steps.

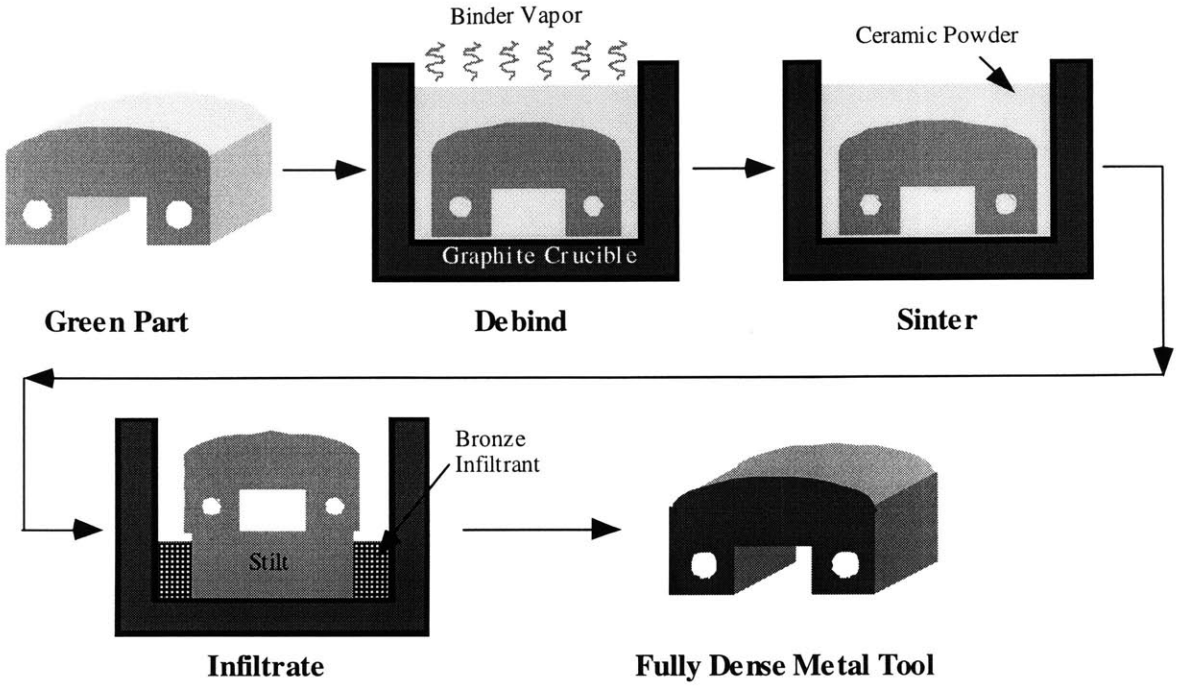

Figure 1.2: Schematic showing the post processing steps carried out on a green part.

1.2 Motivation and objective

Existing furnaces such as the MRF furnace currently being used to post process 3D printed parts at MIT are expensive. The MRF furnace is capable of holding a vacuum and running in a pure hydrogen atmosphere. Scaling up this furnace would be very expensive since the cost of components such as heating elements, heat shields, vacuum pumps, and shell wall capable of withstanding vacuum increase rapidly with size.

The primary focus of this research is on developing a post-processing furnace that can be scaled up economically.

Interconnected porosity in 3D printed parts is a phenomenon that needs to be understood and eventually eliminated. Porosity that is connected is not desirable since it causes cooling channels in 3D printed injection molding tooling to leak. It is believed that porosity occurs due to solidification shrinkage, trapped gases and evolution of gases from the infiltrant melt during solidification. Previous work has tried to investigate some of these issues: however, to date, leak free molds have not been obtained. Lack of a custom furnace has impeded a comprehensive investigation of the porosity issue. One of the objectives of this work is to develop a custom furnace and equip it with features needed to conduct experiments to identify and control

parameters affecting porosity. Experiments include gated infiltration and directional solidification. Gated infiltration refers to separating the molten infiltrant from the sintered skeleton until a gate is opened. Directional solidification involves inducing a temperature gradient in a cooling part such that infiltrant in different zones of the part solidifies at different points in time.

Currently, MIT uses two separate MRF furnaces for post processing: one for debinding the green part and the other for sintering and infiltrating it. The furnace used for debinding gets contaminated with condensed vapors of the polymeric binder thus making it unsuitable to be used for sintering or infiltration. Hence, a separate furnace is needed for sintering and infiltration. Great savings in capital cost could be achieved if one furnace could be used for all three post-processing steps. This work also develops a method by which the same furnace can be used for all the post processing steps.

1.3 Previous work

Previous work on scalable furnace processing was done at the MIT 3D printing lab by Adam Lorenz [4]. Lorenz built and tested a series of experimental furnaces in order to come up with a design for an economical furnace. The design consisted of a gas tight outer shell, Alumina insulation and metallic-heating elements embedded in ceramic heater plates. It used a forming gas atmosphere instead of pure Hydrogen or a vacuum in order to achieve significant cost savings. MIT then hired a furnace manufacturing company, C.I. Hayes of Providence, RI, to build a large scale furnace. However, this furnace failed to provide a proper atmosphere for sintering (resulting in oxidized parts), necessitating a review of some of the design elements. The furnace built by Hayes used 3" of Alumina board as insulation. It was found that the board released water vapor even when the furnace was at 1200 C. This was because insulation away from the shell did not get hot enough to expel moisture even when the inside of the furnace was at 1200 C. Moreover, the board had silica-based binder that decomposed and contaminated the furnace atmosphere at high temperatures. As part of a revised design, the board was replaced by high Alumina content (95%) blanket insulation. In order to expel moisture out of the insulation more effectively, it was decided that the shell might need to be heated from the outside. In order for the outside heating to be effective, the shell material was changed from SS to Aluminum, a

better thermal conductor. These design changes were incorporated in a small scale prototype furnace consisting of an aluminum shell, alumina insulation and Kanthal heaters (Figure 1.3).

Figure 1.3: Small scale furnace built at MIT.

This research is aimed at optimizing the small scale furnace to yield good quality parts, and using the parameters thus obtained to build and test a large scale furnace, which in addition to demonstrating scalability could be used to conduct experiments on porosity.

1.4 Organization of this work

This work is organized into seven chapters. The second chapter deals with experiments conducted on Alumina insulation to understand its moisture release properties as a function of temperature. It also explains how the small scale furnace was optimized to obtain oxide free parts. Chapter three explains the design of a debinding mechanism that was successfully built and tested in the small scale furnace. Chapter four describes experiments on directional solidification conducted mainly on the SS420-Bronze material system using the small scale furnace. Chapter five deals with the mechanical and thermal system design of the large scale furnace. A lot of the design parameters used were obtained experimentally. Chapter six deals with the electrical, gas and safety systems of the large scale furnace. It gives a detailed description of the control and wiring scheme of the furnace. Chapter seven describes furnace testing and optimization. Finally, chapter eight summarizes this work and lays ground for future work using the furnace built in this work.

2 Insulation Experiments

This chapter describes how a previously developed small scale furnace was optimized to yield oxide free parts. Doing this involved a series of experiments conducted to study the moisture content inside the furnace as a function of temperature.

2.1 Small scale furnace

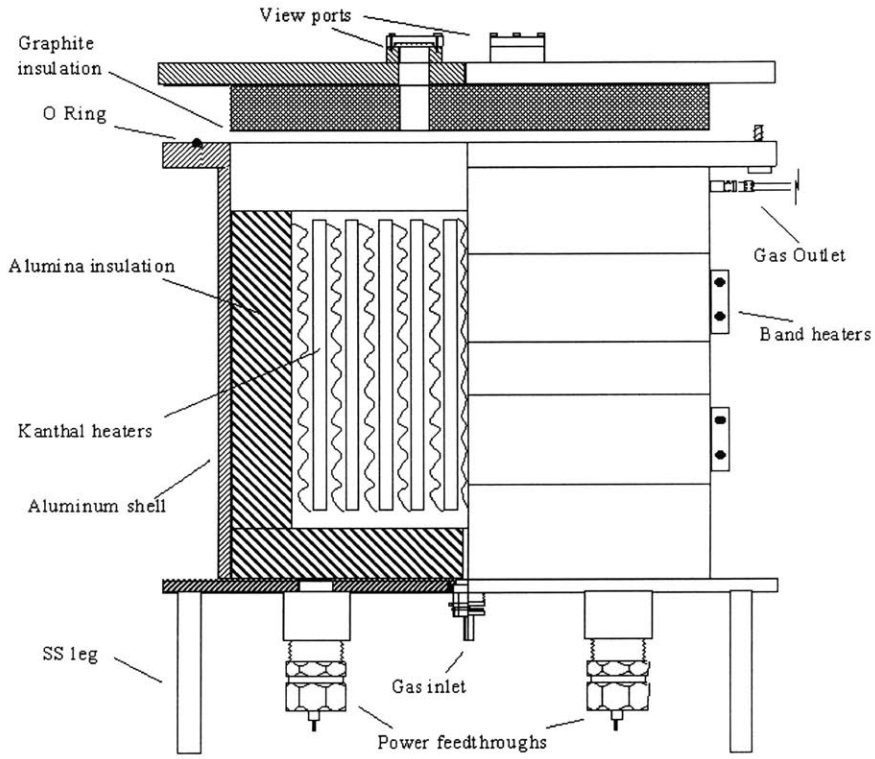

Figure 2.1: Schematic of the small scale furnace showing various features.

The small scale furnace (Figures 2.1 and 2.2) was designed to have an operating temperature of 1200 C on the inside and a shell temperature of 200 C in steady state. An inch of high purity (95%) Alumina insulation was used to achieve this. The furnace would run in Forming gas (95% Argon and 5% Hydrogen) and a volume flow rate of five volume changes an hour was considered enough to prevent oxidation of stainless steel (SS) parts.

A typical sintering run involves soaking the SS part at 1200 C for an hour. When the furnace was ramped to 1200 C at 5 C/min starting at room temperature, it was found that the parts got oxidized during sintering.

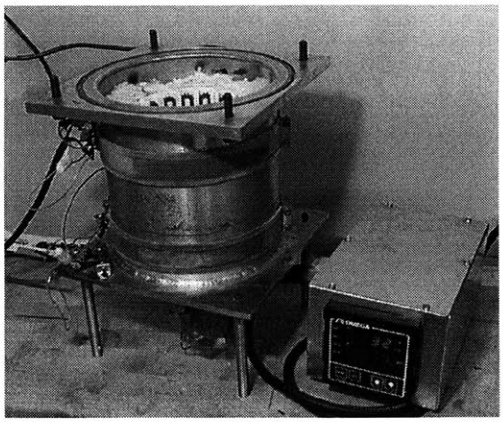

Figure 2.2: Picture of the small scale furnace developed at MIT.

This was because moisture was being released from the hygroscopic Alumina insulation even when the furnace was at 1200 C, at which temperature SS was most susceptible to oxidation. In order to overcome this problem, the furnace was purged at room temperature for two hours before ramp up until the dew point reached a sufficiently low value (-25 C). However, as soon as ramp up started, the dew point shot up to high levels (Figure 2.3). Clearly, moisture was being expelled out of the insulation as the insulation got heated up. Also, the outer parts of the insulation did not reach 100 C or above until the inside was around 1000 C. Thus water was continued to be expelled even when the furnace temperature was in a region where steel was most susceptible to oxidation (the reactivity follows an Arrhenius temperature dependence). No doubt, the part was oxidized (Figure 2.6a). In order to overcome this problem, two band heaters were mounted around the shell of the furnace. These were provided with thermostats to control the shell temperature at 200 C. The idea was to turn the internal heaters and the external heaters on at a set point of 200 C and purge the furnace with forming gas at five volume changes an hour until the dew point got to –25 C. This would ensure that all the insulation soaked at 200 C and thus any water in the insulation would be expelled before the ramp to 1200 C started.

This method worked and produced a part that was much cleaner than that produced in the previous run (Figure 2.6b). Figure 2.4 shows the dew point as a function of time in one such run. It is interesting to note that the dew point starts going up when the ramp begins and peaks when the furnace is at around 480 C before starting to down again. Another interesting fact is that the dew point begins to rise as the furnace temperature goes past 900 C. This behavior can also be seen in figure 2.3. Since the entire vapor from the Alumina insulation had been expelled by this time, some other phenomenon was taking place at furnace temperatures above 900 C.

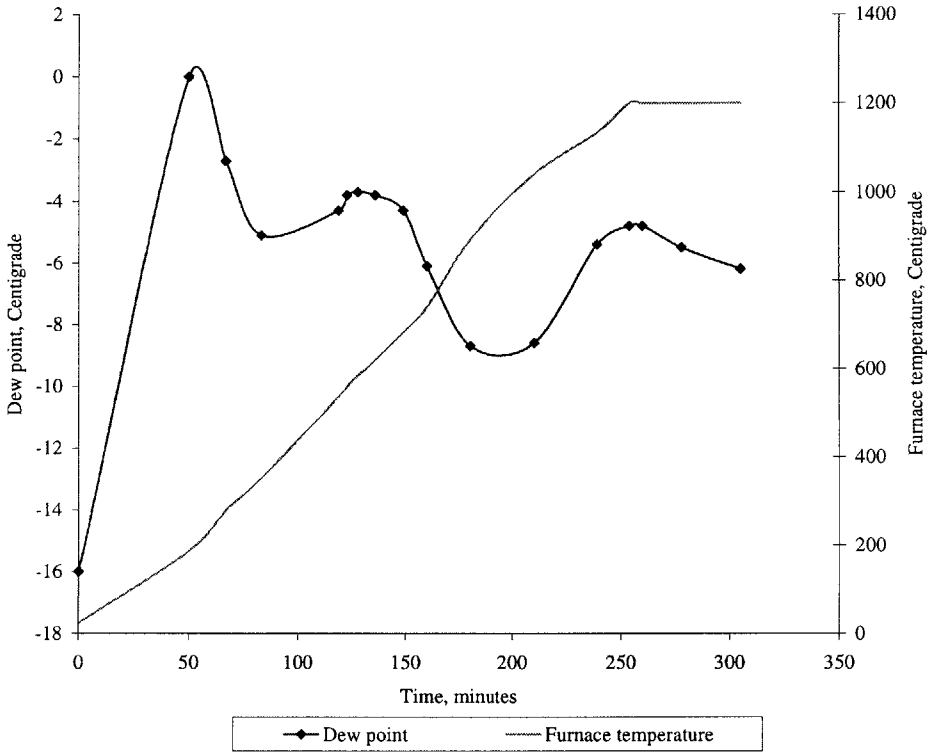

Figure 2.3: Dew point vs. time: purge at room temperature for two hours followed by a ramp to 1200 C.

2.2 Effect of Silica in the heater plates

Clearly, a chemical reaction was taking place at temperatures above 900 C. A closer look at the heater plate composition showed that the plates had 33% Silica. It was hypothesized that a possible cause of the water vapor could be the reduction of this Silica by Hydrogen present in the Forming gas. In order to test this hypothesis, a run was carried out in which the atmosphere was switched from Forming gas to Argon. This switch was done at 600 C so that at a ramp rate of 5 C/min and a flow rate of 5 volume changes an hour, the entire furnace would be purged of

Hydrogen by the time the furnace got to 900 C. If a chemical reaction involving Hydrogen was causing a rise in dew point (and oxidation of the part) at temperatures above 900 C, then, the switch to Argon should yield a clean part (since there would be no Hydrogen to reduce the Silica and produce water vapor). Indeed, the part quality obtained (Figure 2.6c) was much better than

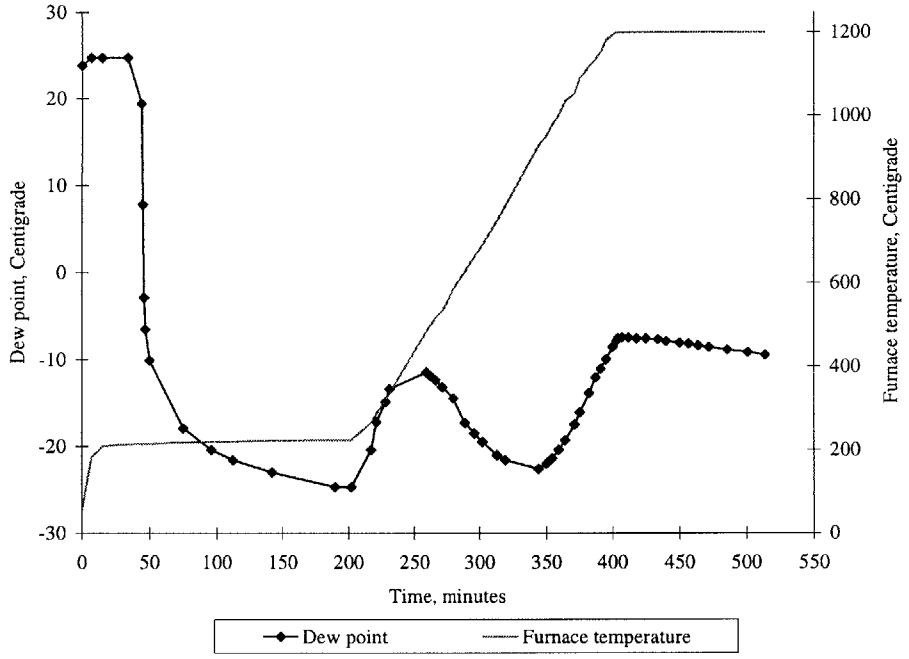

Figure 2.4: Dew point vs. time: soak at 200 C until dew point goes to -25 C, then ramp to 1200 C.

that obtained in the run without the switch.

With sufficient reason to believe that Silica in the heaters was responsible for the rise in dew point level at furnace temperatures above 900 C, a set of new heaters having 93% Alumina and just 7% Silica as opposed to the 33% in the previous heaters was installed in the furnace. Figure 2.5 compares the variation of dew point with time when the furnace was run with the low Alumina heaters and the high Alumina heaters respectively. It can be seen that the rise in dew point when the furnace temperature is around 900 C is negligible with the high Alumina heaters as compared to that seen with the low Alumina heaters. Also, the part obtained had no oxidation when the high Alumina heaters were used (Figure 2.6d). This can be explained by the fact that

the heaters had low Silica content and thus water vapor released by the reduction of Silica was minimal.

Thus, it was established that the reduction of Silica present in the heater plates was indeed responsible for the increase in the amount of water vapor in the furnace at high temperatures. Also, it was found that as the furnace was run in Forming gas, over time, the Silica got continuously depleted and the rise in dew point at high furnace temperatures was no longer seen.

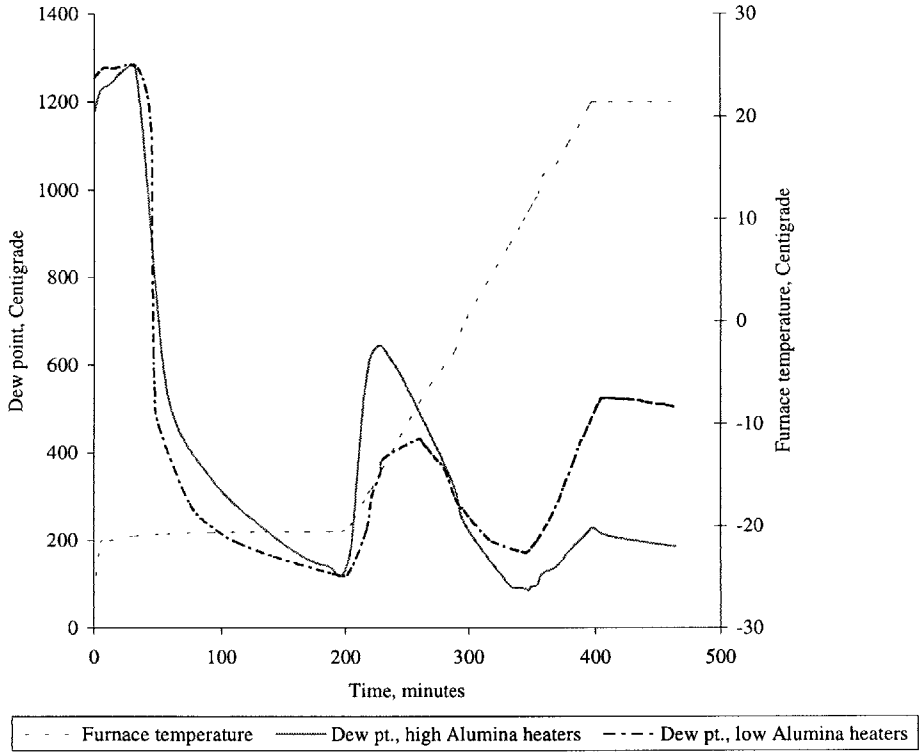

Figure 2.5: Comparison of moisture release at temperatures above 900 C: low vs. high Alumina heaters.

2.3 Other considerations

In order to ensure that the parts sintered in the furnace were oxide free, a moisture trap was used in the gas flow line. Also, high purity Forming gas having less than 10 PPM of water vapor was used as opposed to the previously used industrial grade Forming gas that had up to 30 PPM of moisture. It was decided to replace the Alumina insulation on the top door of the furnace with Graphite. Graphite would act as a gettering agent by reacting with and removing any water

vapor in the furnace. If the dew point inside the furnace is relatively high over several runs (as a result of say, not purging the furnace long enough at 200 C before ramping up to 1200 C), a

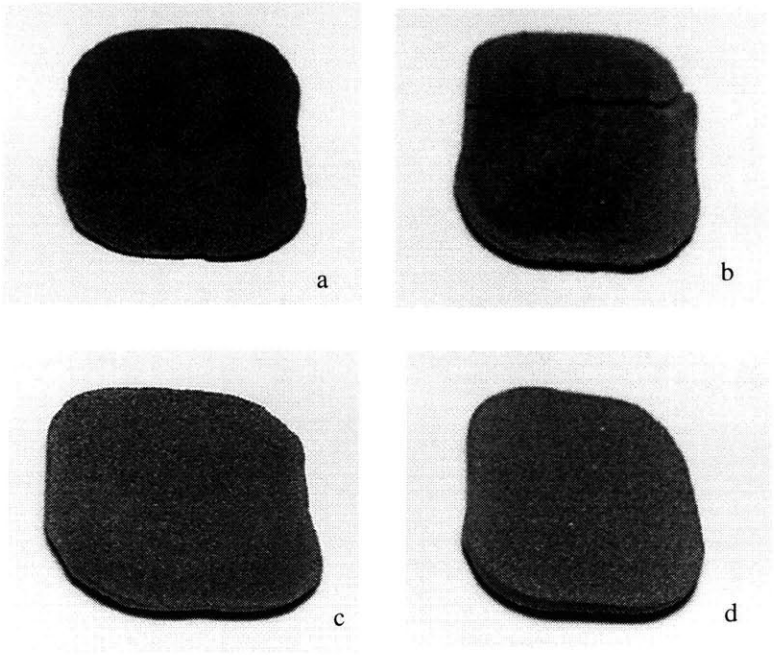

Figure 2.6: Parts sintered in the small scale furnace: (a) with no band heaters, ramp to 1200 C, Forming gas atmosphere, low Alumina heaters (b) with band heaters, soak at 200 C, then ramp to 1200 C, Forming gas atmosphere, low Alumina heaters (c) same as 2.6b, except that atmosphere is switched from Forming gas to Argon at 600 C (d) same as 2.6b, except that the heaters in the furnace have a high Alumina content.

visible change can be seen in the Graphite, indicating loss of material by oxidation. The chapter on the assembly of the large scale furnace discusses the issue of Graphite vs. Alumina in greater detail.

A vacuum test was performed on the furnace to get an idea of the size of any leaks that existed in the furnace. Figure 2.7 shows a schematic of the set up for the vacuum test. The idea was to seal all the furnace openings, pull a vacuum inside the furnace and observe the rate of pressure rise inside the furnace. This could then be used to compute the average gas flow rate into the furnace through the leaks. In order to dilute the effect of inflow through the leaks, purging gas a twenty times the leak flow rate could be made to flow through the furnace. It is important to note that this method is extremely conservative since the leak rate into the furnace when it is running with positive pressure inside will be much less than the leak rate when there is

a vacuum inside. All openings in the furnace were sealed off and a vacuum was pulled inside the furnace. The pump was shut off and the pressure rise in the furnace was recorded as a function of time. Table 2.1 shows the rise in furnace pressure as a function of time (t = 0 is when the vacuum is pulled).

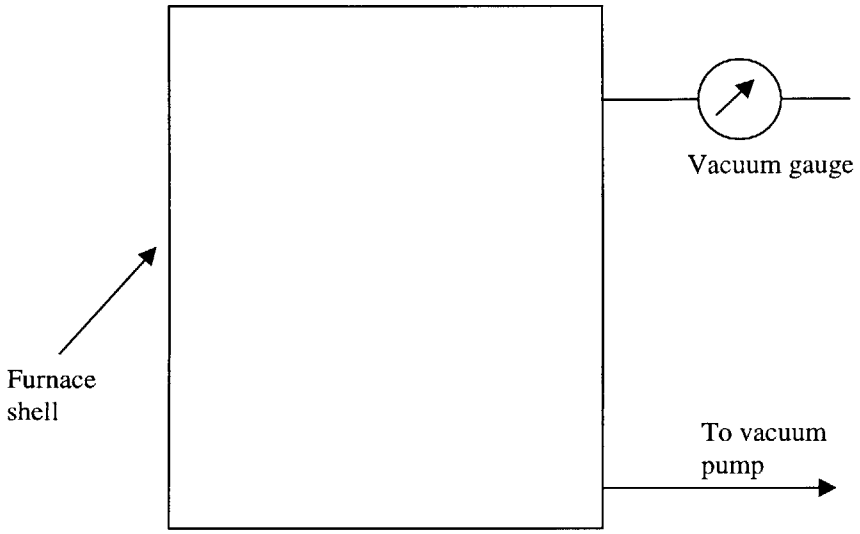

Figure 2.7: Schematic of the set up for the vacuum test carried out using the small scale furnace.

The volume inside the furnace, neglecting that of the tubes going to the pump and the gauge is V = 0.006613 cubic meters. The air in the room was at a temperature T = 24 C. A pressure change inside the furnace, Δp= 5 Torr corresponds to a difference in density $\Delta\rho = \Delta p/RT$, where R is the gas constant. The mass of air that leaked in is $\Delta m = \Delta\rho * V$, which comes to $5.17*10^{-5}$ kg. The average flow rate of air can be calculated from the times in the table to be about $5*10^{-7}$ kg/sec. That gives a ball park value of the air leakage that can be expected. In order to dilute this

Time, seconds	Pressure, Torr
0	10
105	15
220	20
330	25

Table 2.1: Furnace pressure vs. time. A vacuum was pulled into a "sealed" furnace and the pressure rise as a function of time was used to quantify leaks into the furnace.

leakage, we may want the flow rate of forming gas to be 20 times this value, i.e. around $1*10^{-5}$ kg/sec. The molecular weight of forming gas, which is 95% Argon and 5% hydrogen by volume is 0.95*40+0.05*2 = 38.1 g/mole. This means that the gas constant for Forming gas is 8314/38.1 = 218.2 kJ/kg K (8314 J/kg K is the universal gas constant). The density of forming gas is p/RT= 10^5 /(218.2*298) = 1.54 kg/cubic meter. Thus a mass flow of $1*10^{-5}$ kg/sec corresponds to a flow rate of $1*10^{-5}$ /1.54 = $0.64*10^{-5}$ cubic meter/sec. This is about 4 volume changes an hour. Thus, the flow rate of five volume changes an hour used in the experiments described in this chapter is a good flow rate.

2.4 Summary

It was found from experiments that the following were needed to obtain good quality, and unoxidized sintered parts in the small scale furnace:

- external heaters to keep the aluminum shell at 200 C
- high alumina heater plates
- graphite on the door to act as a gettering agent
- high purity forming gas at a flow rate of at least 5 volume changes an hour
- a purge with the furnace soaking at 200 C until the dew point was –25 C

This information was used in the design of the large scale furnace, which is described in Chapter 5.

3 Design of a Debinding Apparatus

Currently, two furnaces are needed for complete post processing of 3D printed parts. The first to debind green parts, which involves binder burn off and the second to sinter and infiltrate the debound parts. In addition to the additional capital investment the second furnace entails, debinding the green part in a separate furnace is more time consuming since it involves an additional ramp up and cool down.

This chapter describes the design, fabrication and testing of a debinding apparatus for use in the small scale furnace. The developed design is easily scalable and thus can also be used in the large scale furnace.

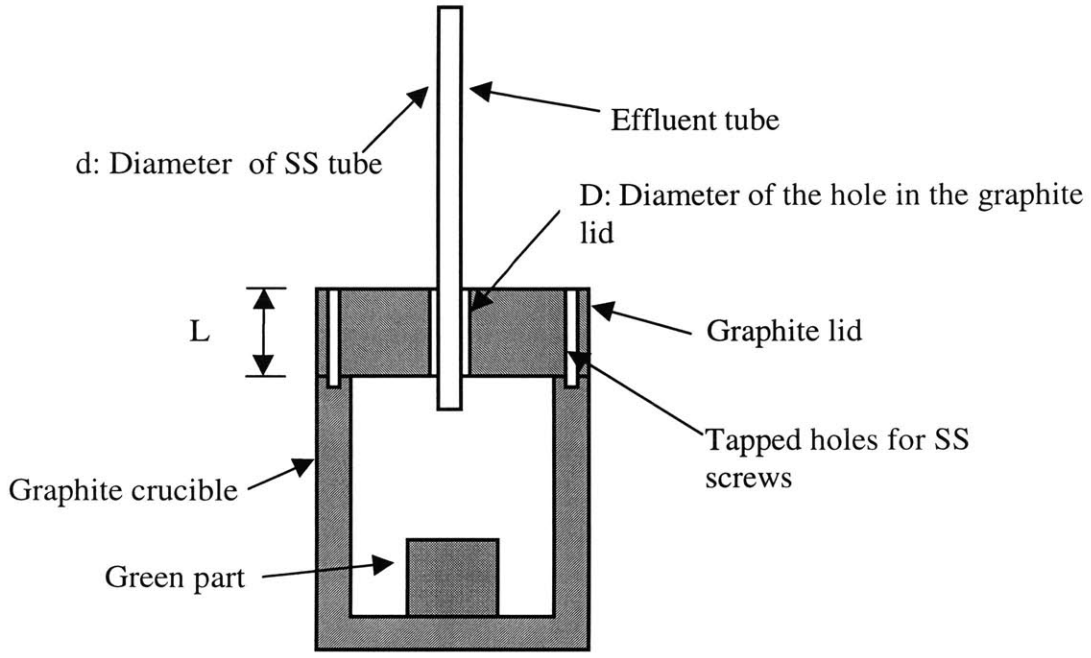

Figure 3.1: Schematic showing the concept of a debinding chamber. Note that the annular clearance between the effluent tube and the hole in the Graphite lid, t =1/2(D-d).

3.1 Current practice

A 3D printed green part consists of powder that is held together by binder, which is typically a polymer such as Acrysol. This polymer is burnt off at around 500 C at which temperature the part undergoes light sintering, giving the part structural integrity. Binder burnout releases hydrocarbons that tend to deposit on the walls of the furnace. This makes the furnace unusable for sintering or infiltration, both of which require a contaminant free environment.

To get around this problem, the current practice is to use two separate furnaces, one for debinding and the other for sintering and infiltration. This involves an additional capital expenditure on a second furnace and increases the post processing time. Also, it requires that the debound part (that is not structurally strong) be physically transferred from one furnace to the other. Clearly, it would be ideal to have debinding and sintering take place in a single run in the

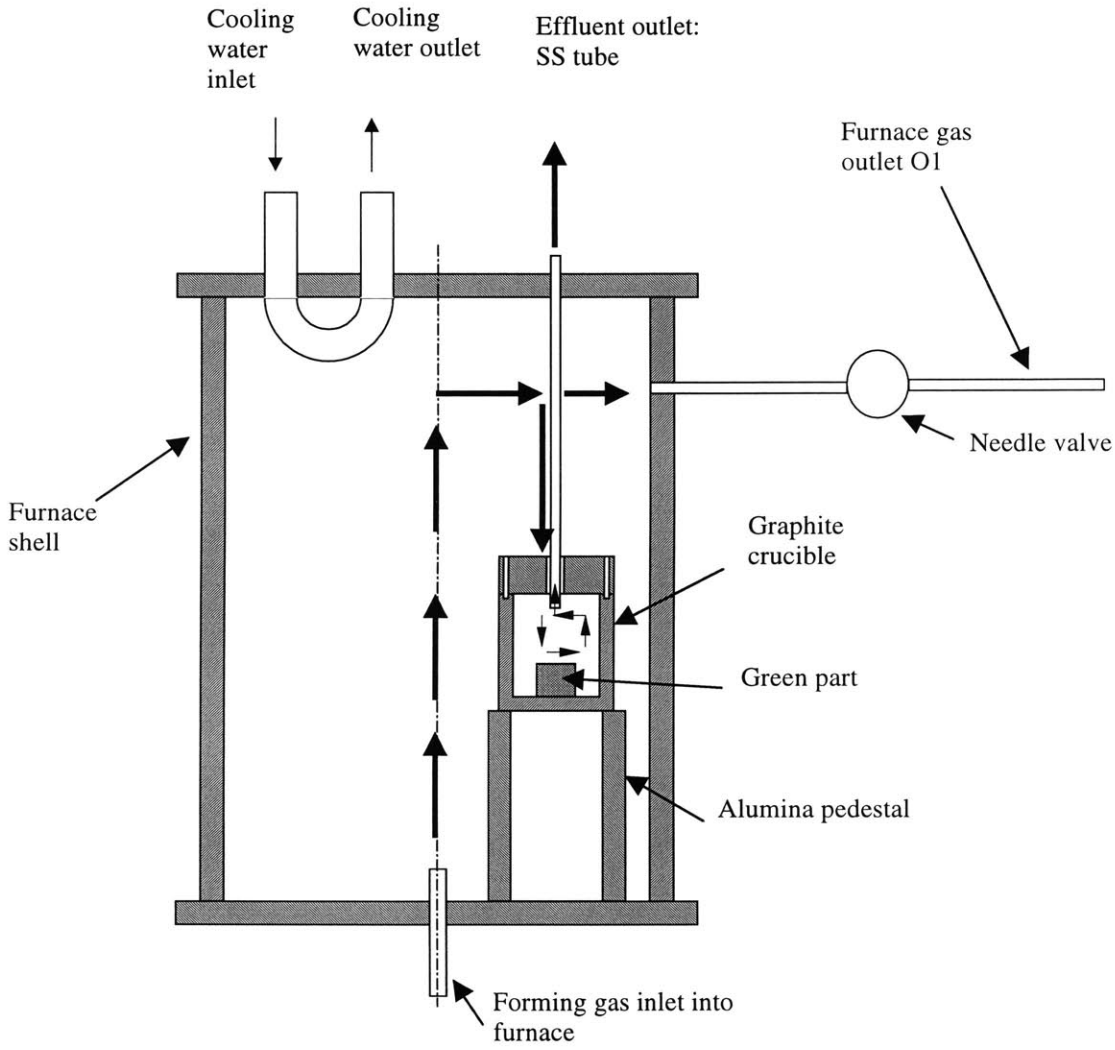

Figure 3.2: Schematic showing gas flow into the furnace and two possible exit paths for outgoing gas: one through the annular gap and out through the effluent tube and the other through the regular outlet O1.

same furnace.

3.2 Design of a debinding apparatus

In order to prevent contamination of the furnace due to binder burnout, the green part was housed in a graphite crucible with a graphite lid. The lid had a through hole in its center and was screwed on to the crucible by means of two SS screws (Figure 3.1). It should be noted that SS is not the best material to be used for the screws, since it reacts with the graphite to form cast iron. For future applications, use of Alumina screws is recommended. A SS tube passing through this hole carried the effluent generated inside the crucible out of the furnace. In order to keep the effluent generated by binder burnout from leaking out into the furnace through the annular gap between the tube and the hole, the pressure outside the crucible must be maintained higher than the pressure inside it. Forming gas entering the furnace through the bottom can get out of the furnace through the regular outlet O1, whose opening is controlled by a needle valve or through the annular gap into the graphite crucible and out of the SS effluent tube (Figure 3.2). The fraction of inlet gas going out of the furnace through the regular outlet and the effluent tube depends on the resistance the two openings offer to its flow. Let p1 denote the pressure inside the graphite crucible and p2 that in the furnace (outside the crucible). The effluent tube vents out into the atmosphere and is roughly 2m long. The gas flowing though it cools down to room temperature very soon after it leaves the furnace and can thus be assumed to be at room temperature for purposes of calculation. Pressure drop for flow through the effluent tube is given by

$$p1-pa = 8Q\mu L/(\pi R^4) \quad \ldots\ldots(1)$$

where pa is atmospheric pressure, Q is the flow through the tube, μ is the viscosity of the Forming gas, L is the length of the effluent tube and R is the inside radius of the effluent tube. Equation 1 assumes fully developed flow in the tube. If all the Forming gas entering the furnace were to leave it through the effluent tube (worst case), then $Q = 8.7*10^{-6}$ m^3/s. Also, at room temperature, $\mu = 2.2*10^{-5}$ kg m/s. Using L = 2 m and R = 0.085" in equation 1 gives a pressure drop of 0.2" of water over the length of the tube. Thus, for all practical purposes, the pressure inside the graphite crucible is atmospheric.

During furnace use, it is desired to maintain a pressure difference p2-p1 equal to 4" of water. The problem at hand was to determine the annular clearance, t, such that a reasonable amount of flow would pass through the annulus for the given pressure difference of 4" of water.

3.2.1 Determination of the annular clearance

The viscous pressure drop during flow through the annulus can be approximated by using the Poiseuille equation. For flow between two plates of width w and separated by a distance h, the flow rate, Q is given by

$Q/w = h^3/12\mu^* (-dp/dx)$.....(2)

where x is in the direction of flow.

In the case of the annulus (see Figure 3.1),

$w = \pi^*(D+d)/2$.....(2a)

$H = t$.....(2b)

$-dp/dx = (p2-p1)/L$.....(2c)

Thus, in this case, using equations 2a and 2b, the Bernoulli pressure drop ($=1/2\rho v^2$) is $1/2\rho(Q/wt)^2$ and the viscous pressure drop is $12Q\mu L/(w\ t^3)$. Neglecting Bernoulli pressure drop, which is found to be negligible compared to the viscous term, the drop p2-p1 is given by

$p2-p1 = 12Q\mu L/(w\ t^3)$.....(3)

Now, Q, the flow through the annulus is a fraction of Q', the flow into the furnace. At temperatures above room temperature, Q' is related to Q_{rt} , the flow at room temperature, by

$Q' = Q_{rt}\rho_s/\rho$.....(4)

where ρ_s is the density of forming gas at room temperature and ρ is the density of the gas at the furnace temperature.

Also, let

$Q = nQ'$ .....(5)

where n is the fraction of incoming gas that leaves the furnace through the annular gap.

Plugging equations (3) and (4) into (2) gives

$\Delta p = 12\mu L(n\ Q_{rt}\rho_s/\rho)/(wt^3)$ .....(6)

The annular clearance t was estimated by assuming a pressure difference of 4" of water and that 30% of the flow went through the annulus (n = 0.3) at room temperature. At room temperature, $\mu = 2.2*10^{-5}$ kg m/s, $\rho = \rho_s = 1.546$ kg/m^3, $Q_{rt} = 8.7*10^{-6}$ m^3/s (=5 volume changes an hour for an 8" diameter by 8" height furnace). Choosing a diameter of ¼" for the SS tube fixes w (see equation 2a). L, the thickness of the crucible's graphite cover is chosen to be ¾". Plugging these in equation 6 gives t = 3.5/1000".

3.2.2 Testing the design

When it came to drilling the hole in the Graphite lid, the diameter of the SS tube was measured to be 0.242" and thus the hole was reamed to a diameter of 0.249". The first test that was done with the setup (at room temperature) involved closing outlet O1 such that all the flow entering the furnace went out through the annular gap. It was found that the pressure build up in the furnace was 2" as opposed to 12" which is predicted by equation 6 for n=1. This can be explained by the fact that the SS effluent tube is not concentric with the hole in the lid. (Figure 3.3). Clearly, as figure 3.3 shows, the effective annular gap for a non-concentric case is larger than t and thus resistance to flow is lesser, which results in a lower pressure build up for a given flow. A trial and error method was used to find the gap that would yield a pressure difference of 2" in the case when all the flow entering the furnace went out through the annular gap. It was found that using a value equal to 1.83t in equation 6 for the annular gap yielded a pressure difference of 2". Thus the effective annular clearance is 1.83t. This makes sense, for, as figure 3.3 shows, going clockwise, the annular gap starts off at zero where the tube touches the hole in the graphite top and reaches a maximum of 2t before going back to zero. If this value of 1.83t

were correct, then the theoretically predicted and experimentally observed pressure in the furnace would agree at 500 C. To test this, when the furnace was at 500C, outlet O1 was closed and the pressure inside the furnace was noted to be 10" of water. At 500 C, the theoretical pressure difference assuming that all the flow goes out of the furnace through the annular gap (= 1.83t) can be predicted using equation 6. At 500 C, $\mu = 4.63*10^{-5}$ kg m/s, $\rho = 0.58$ kg/m^3 and the annular gap shrinks a little since the thermal expansion of SS is greater than that of Graphite. ($\alpha_{graphite} = 6*10^{-6}$ and $\alpha_{steel} = 12*10^{-6}$). Plugging these values in equation 6 yields a pressure difference of 11.3" of water that is close to the observed value of 10" of water. Thus, the assumption that the effective annular gap is 1.83t is a good one.

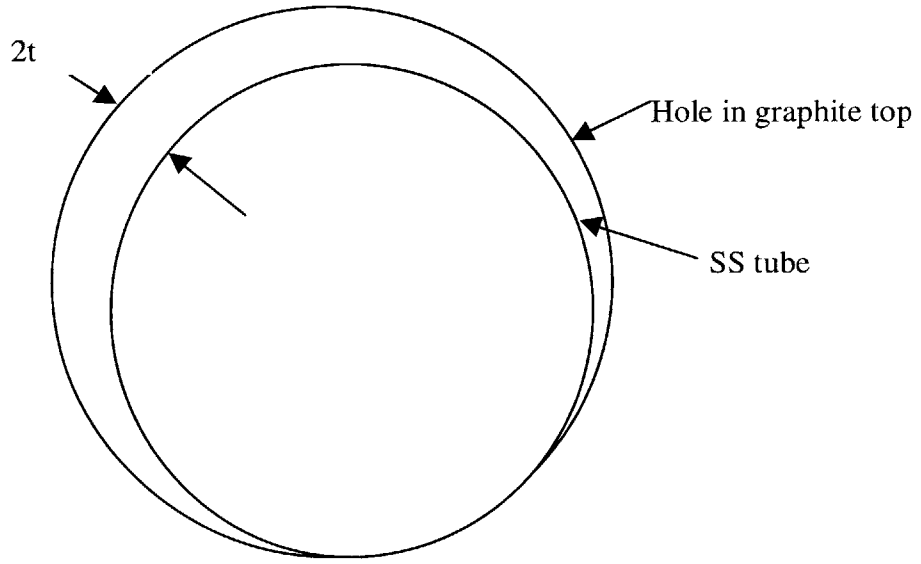

Figure 3.3: Schematic showing an increase in the effective annular gap between the tube and the hole due to misalignment.

It is important to note that the annular gap will vary every time the debinding mechanism is assembled before a furnace run. The annular gap could be t all around (perfectly concentric case) or could vary from zero to 2t as shown in figure 3.3 (perfectly non-concentric case) or could be somewhere between the two extreme cases. Irrespective of what the alignment is like, the following scheme can be used during any furnace run. At room temperature, Outlet O1 can be opened enough to get a furnace pressure of around 2" of water and to have enough flow through O1 to take dew point measurements. As the furnace ramps up, the pressure inside the furnace would rise, and O1 would need to be opened as required to keep the furnace pressure at 4" of water. Equation 6 can be used to see that at 500 C, when outlet O1 has been opened enough

to get the furnace pressure to 4" of water, around 35% of the gas flowing into the furnace leaves via the annular gap. At 1200 C, using, $\mu = 7*10^{-5}$ kg m/s, $\rho = 0.324$ kg/m^3 in equation 6 it is seen that around 13% of the flow leaves the furnace via the annular gap when O1 has been opened enough to keep the furnace pressure at 4" of water.

The next step was to debind and sinter a green part using the set up. In order to ensure that the mechanism was working and no binder from the green part leaked out into the furnace, a U tube was mounted inside the furnace (Figure 3.2). This tube carried a continuous flow of water, and thus served as a cold finger. If any polymer leaked out into the furnace, it would condense on the finger and would thus be visible after the test.

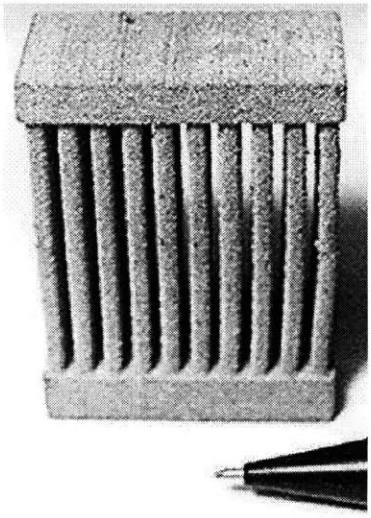

Figure 3.4: Picture of a SS truss that was successfully debound and sintered using the described set up.

A green part was placed in the graphite crucible and the cover was tightened onto the crucible using two SS screws. Boron nitride paint was smeared on to the part of the SS effluent tube that was inside the Graphite lid in order to prevent any reaction between the SS tube and the Graphite. Before the flow of cooling water was started, the furnace was purged for half an hour with forming gas at 10 volume changes an hour. Once the dew point in the furnace was below the temperature of the cooling water, cooling water flow was started. Had the flow been started earlier, water vapor inside the furnace would have condensed on the cooling tube. The furnace was then ramped up and outlet O1 was opened according to the previously described scheme.

Debinding was carried out at 500 C for one hour after which the furnace was ramped to 1200 C. Upon completion of the run, the U tube was examined and no condensate was found on the tube. This showed that there was no leakage of effluent gas out of the crucible. Figure 3.4 shows a part that was sintered and debound successfully using this setup.

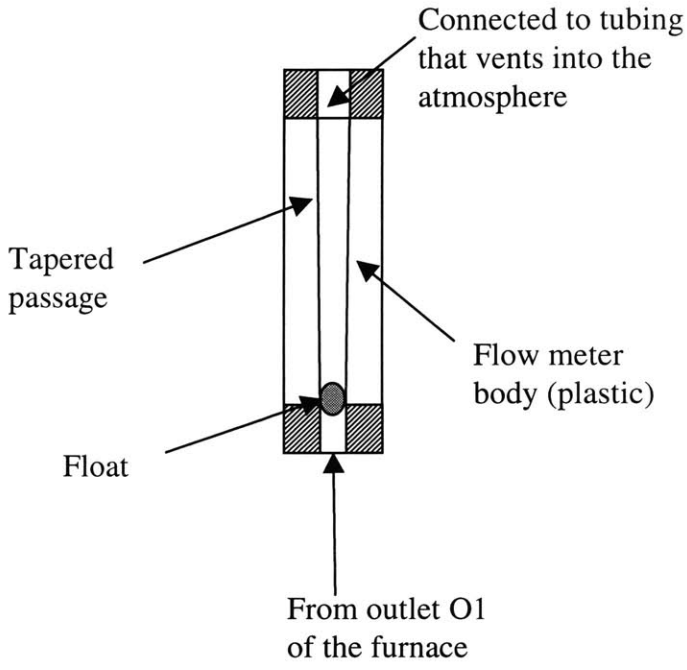

Figure 3.5: Simplified schematic of a modified flow meter. Such a flow meter, when mounted at outlet O1 of the furnace can be used to maintain constant pressure inside the furnace during the entire furnace cycle without user intervention.

3.3 Improved design

The design described in the previous section works well. However, as the furnace heats up, furnace pressure begins to rise and the needle valve at outlet O1 needs to be opened in order to keep the furnace pressure at 4" of water. This needs to be done frequently as the furnace heats up, and, needless to say, is inconvenient. Figure 3.5 shows a simplified schematic of an alternative to using a needle valve at outlet O1. The idea is to use a variable area flow meter instead. The flow meter has a varying cross section passage (slightly tapered) and a float that sits over an orifice that serves as the gas inlet. The float stays in equilibrium under the influence of its own weight and the force of the gas underneath. The idea is to find the weight of the float (by trial and error) that will cause it to not rise above the orifice until the pressure of the gas is 4" of

water or more. The float weight can be altered by changing the material of the float. If this flow meter is fitted at outlet O1 of the furnace, then, as long as the pressure inside the furnace is below 4" of water, all the forming gas entering the furnace will leave it through the effluent outlet. However, as soon as the furnace pressure starts to rise above 4" of water as a result of furnace ramp up, the float will rise, causing part of the gas to exit the furnace out of outlet O1. This method will ensure that the pressure inside the furnace stays below 4" of water during the entire furnace run without user intervention.

3.4 Summary

This chapter described the design and successful application of a debinding apparatus that can be used to debind and sinter a green part in a single run without contaminating the furnace. An improved design that involves using a modified flow meter to maintain constant pressure inside the furnace without user intervention is also presented. The debinding apparatus presented in this chapter can easily be scaled up for use in the large scale furnace.

4 Directional Solidification

Interconnected porosity in 3D printed parts causes leakage in injection molding tooling and thus needs to be eliminated. It is believed that porosity is caused due to solidification shrinkage, trapped gas or evolution of dissolved gas when the liquid melt solidifies. Having optimized the small scale furnace to deliver oxide free sintered parts, the next step was to conduct experiments using this furnace to study the issue of porosity.

4.1. Porosity

4.1.1. Problems associated with porosity

The infiltrant has a lower melting point than the matrix material and gets wicked up the sintered part by capillary action. For successful infiltration, good wetting must occur between the infiltrant and the sintered skeleton. After infiltration, the resulting structure should be fully dense: however, this is almost never the case. Usually, there is porosity in infiltrated parts. Pores are undesirable since they act as crack nucleation sites, thus making the part more susceptible to failure. Interconnected porosity is worse, since it causes cooling channels in 3D printed injection molds to leak, rendering the molds unusable.

4.1.2. Causes of porosity

It is believed that the following mechanisms contribute to porosity:

- If a region in the sintered part is oxidized or contaminated, infiltrant will not wet it and thus there will be residual porosity.
- Porosity can also arise if a gas pocket is enveloped by the infiltrant melt inside the part.
- Metals shrink on solidification and this may lead to the formation of shrinkage voids. For instance, bronze, which is used to infiltrate SS skeletons shrinks 4 to 5 volume % on

solidification. If liquid is not available to feed this void, it remains unfilled and becomes a pore.

- Hydrogen is soluble in molten copper alloys. However, its solubility in solid metal is far less. Thus, on cooling, hydrogen is released, and it gets trapped, forming a pore.

4.1.3. Experiments to study and minimize porosity

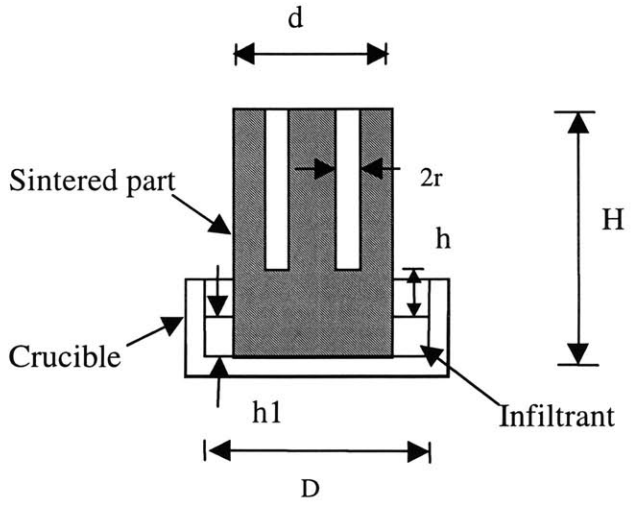

Figure 4.1: Schematic showing important dimensions of the test part.

Ensuring that the sintered part has no contaminants and is not oxidized eliminates the issue of porosity due to infiltrant not reaching a given region in the part. Argon has very low solubility in molten copper alloys. Thus, switching from Forming gas to Argon near the solidus of the alloy will eliminate porosity caused by the evolution of dissolved hydrogen from the melt on cooling. This leaves the issues of enveloped gas and shrinkage porosity. Of these two it is thought that shrinkage porosity is more predominant. A series of experiments was conducted in the small scale furnace to study this issue.

4.2. Design of experiment

4.2.1. Hypothesis

Figure 4.1 shows a schematic of a part being infiltrated. When the part cools, it undergoes considerable shrinkage (~ 4 to 5 volume % in SS- Bronze systems). This shrinkage manifests itself in the form of voids. If it were somehow possible to supply additional liquid to the shrinking regions, cavities would not result. In order to achieve this, it was decided to induce a temperature gradient in the cooling part. The idea was to keep the bottom hotter than the top. Then, the top would solidify before the bottom. Any shrinkage occurring in the top would be filled by liquid metal from the bottom melt. This would considerably reduce, if not eliminate shrinkage cavities.

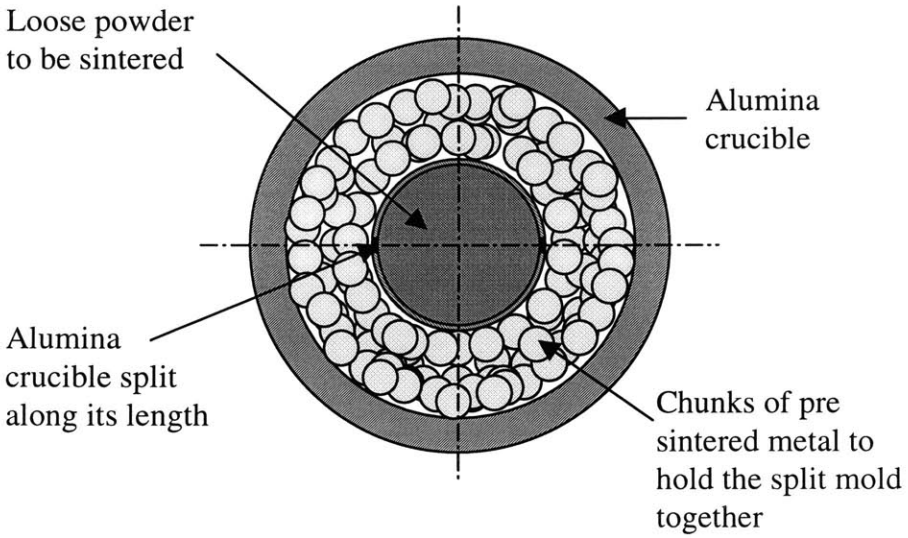

Figure 4.2: Illustration of the split mold concept: pre sintered metal chunks on the outside hold the two halves of the mold together.

4.2.2. Experimental set up

A split mold was made by sawing an Alumina tube into two along its length. This was done in order to facilitate easy removal of the sintered part from the mold. The two halves of the mold were held together by already sintered chunks of metal on the outside. Figure 4.2 shows a schematic of the top view of the split mold filled with loose powder and surrounded by chunks of

sintered metal. The diameter of the part being sintered was limited by the size of the small scale furnace. Before being put inside the furnace, the mold was tapped to obtain good packing of the powder. After sintering, sixteen holes were drilled into the part (Figure 4.3b). The idea was to have as many holes as possible, so that it would be easier to detect interconnected porosity (by pressurizing the holes one by one and looking for leaks through the others, when the part was immersed in water). The depth to which the holes could be drilled was limited by the fact that capillary rise of the infiltrant into the holes was not desired.

In figure 4.1, let h denote the vertical distance from the free surface of the infiltrant melt to the bottom of the drilled hole, and r, the radius of the drilled hole. In order that the infiltrant does not rise up into the holes,

$$h \geq 2\sigma \cos\theta / (\rho r g) \quad \text{.....(1)}$$

where θ is the wetting angle. For the SS-Bronze and Molybdenum-Copper systems with good wetting, $\theta \sim 0$ is a good approximation. Using $\sigma = 1$ N/m, r = 0.11 inch, and $\rho = 8.99$ g/cc gives h ~ 0.315". Next, the height h1 of the free surface of the melt from the bottom of the sintered part was calculated. Refer to figure 4.1 for notation. Define the following:

M_s : Mass of sintered part

M_I : Mass of infiltrant required

ρ_s: Density of matrix material

ρ_I: Density of infiltrant

V_s : Volume of the sintered part: calculated by dividing the part's mass by its density

V_I: Volume of infiltrant

Then,

$$V_s = M_S/\rho_s$$

$$V_I = 0.4\ V_S/0.6 \text{ *safety factor} \quad \text{.....(2)}$$

M_S is obtained by weighing the sintered part. The 0.4/0.6 factor comes from the fact that the sintered part is only 60% dense. The safety factor denotes the amount of excess infiltrant that goes into the crucible with the sintered part and is typically 1.25 to 1.50. Assuming a factor of 1.50 in equation 2 gives

$$V_I = V_S \quad \text{.....(3)}$$

Referring to figure 4.1, it can be seen that conservation of volume gives

$$V_I = [0.4\pi/4d^2 + \pi/4(D^2 - d^2)]\ h1 \quad \text{.....(4)}$$

For d = 2", D =3.5" and $V_I = 4.93\ in^3$, h1 comes to 0.64". Using the previously calculated value of h=0.315" from equation 1, h+h1 comes to 0.955", which shows that drilling a hole that ends 1" above the melt will ensure that the melt does not rise into the holes. Thus 2" deep holes was drilled into a 3" tall sintered part (see Figure 4.3a).

4.2.3. Determination of cooling gas flow rate

In order to induce a temperature gradient in a part cooling inside the small scale furnace, it was decided to set up a jet of Argon to strike the top of the part. The jet would be started at the end of the infiltration cycle, when the furnace was ready to begin cooling down. Figure 4.3a shows a schematic of the setup. It was decided that the end of the tube carrying the Argon would be at a distance of ½" from the top of the part. In order to compute the mass flow rate of Argon that would be needed to induce a certain temperature gradient in the part, a one dimensional heat transfer model was used. It was assumed that the part lost a major part of its heat only in the x direction (see Figure 4.4). This is a reasonable assumption when the furnace heaters are on, since heat loss from the part in the radial direction is minimal.

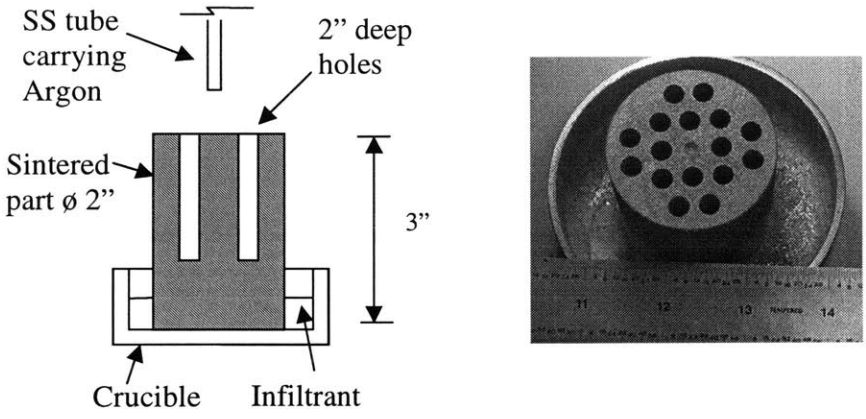

Figure 4.3: (a) Schematic showing dimensions chosen for the test part (left) and, (b) picture of the test part (right).

Define the following notation:

M_{Ar}: Mass flow rate of Argon

Cp_{Ar}: Specific heat capacity of Argon at 1200 C

ΔT: Temperature rise of the Argon gas from furnace inlet to outlet

k: Thermal conductivity of the part

A: Area of cross section of the part

If the temperature gradient induced inside the part in the x direction is taken to be dT/dx, then, energy balance in the x direction gives:

$$k\ A\ dT/dx = M_{Ar}\ Cp_{Ar}\ \Delta T \quad \text{.....(5)}$$

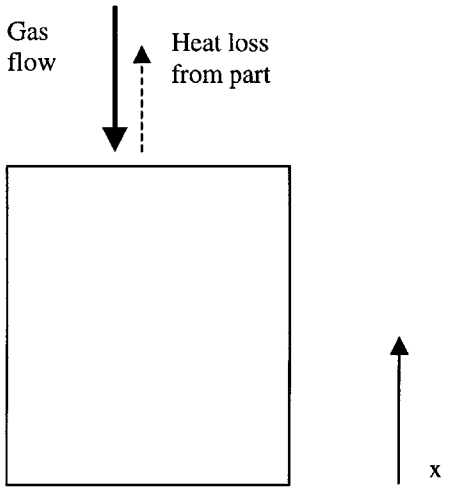

Figure 4.4: Heat and gas flow directions, assuming one dimensional heat transfer.

This equation assumes that the gas heats up from room temperature to the furnace temperature only when it contacts the top of the part that is being infiltrated. In reality, though, the gas starts heating up from room temperature right from the moment it enters the furnace. Thus, by the time it strikes the part, it is already much hotter than room temperature. Also, equation 5 assumes that the gas heats up to 1200 C when it comes in contact with the part. This is not necessarily true. Hence, equation 5 is only approximate. However, it can be used to get an estimate of the mass flow rate of Argon needed to induce a desired temperature gradient in the part. A heat transfer analysis is presented later in this section to get an idea of the maximum amount of heat that can be transferred from the part to the gas. The material system used for initial testing had Molybdenum as the matrix material and Copper as the infiltrant. The sintered part had a height H of 3" and a diameter d of 2" (Figure 4.3a). Ignoring the area of cross section of the holes drilled out, the area A is $\pi/4d^2$, which comes to $2.03*10^{-3}$ m^2. The thermal conductivity of Molybdenum is around 90 W/mK at 1200 C. The specific heat of Argon, Cp_{Ar} is 520 J/kg K. The rise in temperature of the Argon can be assumed to be around 1180 C (1200 minus room temperature,

which is 20 C). Assuming that a temperature gradient of 10 C/cm is desired in the part, equation 5 gives, $M_{Ar} = 2.93*10^{-4}$ kg/s. At room temperature, the density of Argon is ρ_{Ar} 1.622 kg/ m^3. Thus, the flow rate needed at room temperature is M_{Ar}/ρ_{Ar} = 23 standard cubic feet per hour (scfh). As the Argon gets heated up, its density goes down to 0.324 kg/ m^3 and thus the flow rate increases. A calculation was thought to be necessary to compare the velocity of the Argon issuing out of the tube to the speed of sound at 1200 C. For a ¼" diameter tube with 0.035" thick walls, the area of cross section is $1.64* 10^{-5}$ m^2. A flow of 23 cfh at 1200 C would be 23*1.622/0.324 = 115 cfh. The velocity at the tube outlet would thus be 55 m/s. The speed of sound in Argon at 1200 C is given by

$$V_{sound} = (\gamma RT)^{1/2} \quad \text{.....(6)}$$

For Argon, substituting $\gamma = 1.66$, R = 208 J/kgK gives V_{sound} = 713 m/s. Thus the velocity of the issuing jet is far below sonic and a flow rate of 23 scfh was chosen for the cooling gas.

A simple heat transfer model was used to check if the heat loss from the part to the Argon jet, given by $M_{Ar}\, Cp_{Ar}\, \Delta T$ in equation 5 was a reasonable value. For purposes of heat transfer, the part being infiltrated was taken as a flat plate, with Argon flowing over it. The length of the plate was taken to be equal to the diameter of the part being infiltrated (L~50 mm). The velocity of the Argon flowing over the plate was taken to be equal to the velocity of the Argon jet striking the part on its top (v = 55 m/s). For purposes of calculation, properties of Argon were taken at 600 C, which is roughly the average of room temperature and 1200 C, the furnace temperature. At 600 C, $\mu = 5*10^{-5}$ kg m/s and $\rho = 0.515$ kg/m^3 for Argon. The Reynolds number for this flow is $Re = \rho vL/\mu$= 28321, implying that the flow is laminar. The Prandtl number of Argon at 600 C is 0.661(from gas tables). For Laminar flow, the Nusselt number $Nu = 0.664\ Re^{0.5}Pr^{0.33}$, which comes to 97.3. But, by definition, $Nu = hL/k_{Ar}$, where k_{Ar} = conductivity of Argon at 600 C =0.047 W/mK. Thus, using Nu = 97.3 gives h, the heat transfer coefficient = 91.5 W/m^2K. The heat transferred from the part to the gas by convection is given by $Q = hA(T_{plate}-T_{gas})$. Using A = the area of the top of the part, which is circular with a diameter of 2", T_{plate} = 1200 C and T_{gas} = (1200+25)/2 = 612.5 C, gives $Q_{convection}$= 105.4 W. In equation 5, it was assumed that an amount of heat equal to $M_{Ar}\, Cp_{Ar}\, \Delta T$ = 175.2 W would be transferred to the gas from the part. Given that $Q_{convection}$= 105.4 W, 175.2 W seems to be an overestimate.

4.3. Directional solidification experiments

4.3.1. Initial efforts

The first experiments were conducted on small Molybdenum parts infiltrated with Copper. These parts were 1.4" in diameter, 2" tall, and had nine 1" deep blind holes drilled into them (note that since these parts had a smaller area than that assumed while calculating the flow rate of Argon in equation 5, a temperature gradient higher than 10 C/cm is expected). When these parts were infiltrated without any cooling gas, leaks were found. Then, in the next run, cooling gas was turned on at the end of the infiltration at 1200 C, when the internal heaters were turned off. This flow was continued until the melt was solid, which occurred when the furnace temperature was around 870 C. The part was then leak tested by pressurizing the holes one by one and testing for leaks through the other holes. It was found that none of the holes leaked. Inspired by this success, the part dimensions were increased to those shown in figure 4.3 for the next run. It was found that these parts did not leak either. In order to confirm that the absence of leakage was indeed due to the cooling gas, the next run was carried out without any cooling gas. Surprisingly, it was found that the parts still did not leak. This was unexpected. A little thought into the issue showed that there was a temperature gradient within the furnace, with the temperature dropping off towards the top in the zone where the part was present. Thus, it was hypothesized that although this effect was not noticeable for small parts, since they were effectively in a uniform temperature zone, the taller parts were experiencing directional solidification, even without the use of cooling gas.

4.3.2. Reverse directional solidification

In order to examine the effect of introducing a temperature gradient in a cooling part on porosity, it was decided to compare porosity in two cases, one where the cooling gas hit the part at the top and the other where the cooling gas hit the liquid melt from the bottom. The first case is directional solidification (ds), in which the top is cooler than the bottom, and the second case is reverse directional solidification (rds), where the bottom is cooler than the top. Since the bottom

cools before the top in rds, shrinkage cavities in the top cannot be fed with liquid melt and thus we expect much greater porosity in the part than in the ds case. In order to ensure that the majority of heat loss is in the x direction (as opposed to the radial direction), cooling was done at 2-degrees/min from 1200 C to 800 C (solidus of 90-10 Cu-Sn bronze is 870 C). Also, both these runs were done with a SS-Bronze system using only 25% excess melt as opposed to the 50% used in the initial trials with the Molybdenum parts. Cutting the excess melt from 50% to 25% reduced its thermal mass and made rds more effective, thus improving the contrast between porosity in parts cooled using ds and rds.

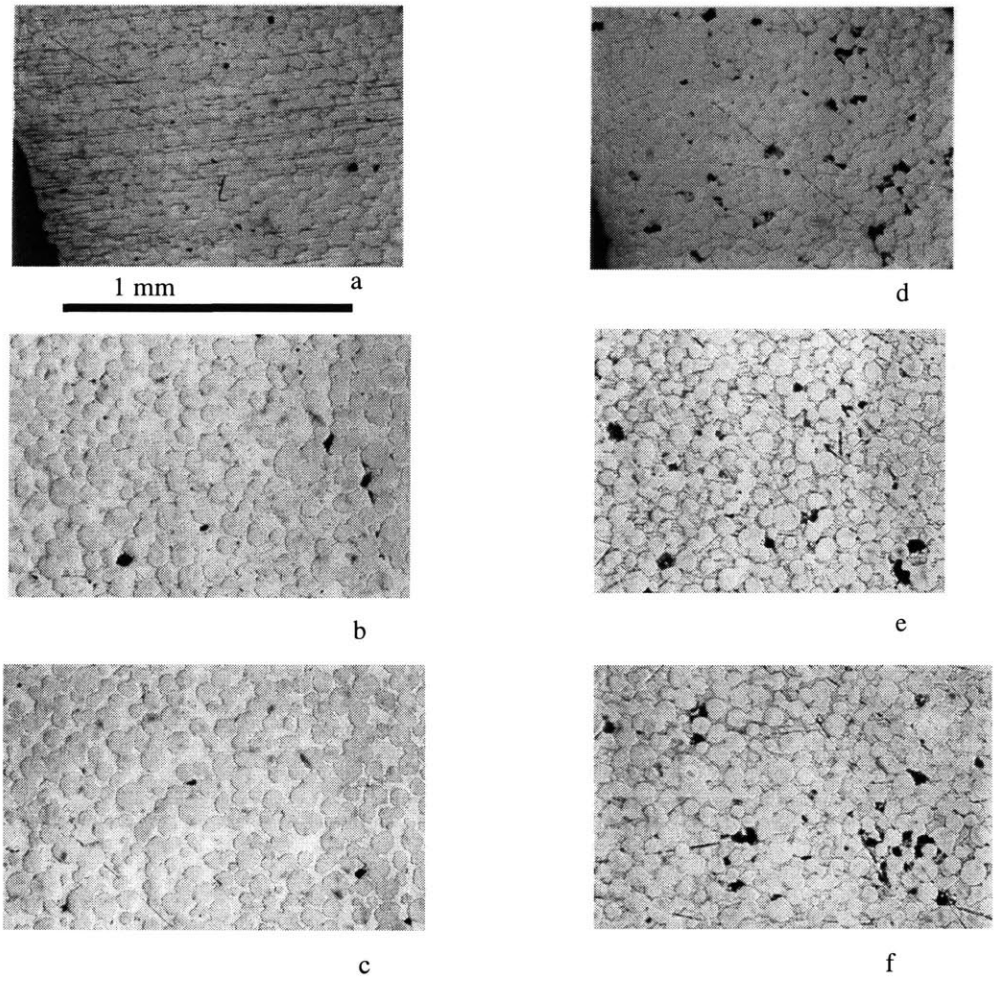

Figure 4.5: Pictures a, b and c are from the cross section of a directionally solidified part. Pictured d, e and f are from a part that was solidified using reverse directional solidification. The particles are SS, and the filler is Bronze. Pores are seen as black spots.

Figure 4.5 shows cross-sections at the same height from the bottom of parts cooled using ds and rds respectively. It is evident that porosity in the rds case in much greater than that in the ds case. It was also noted that the porosity in the part cooled by ds decreased as one went from the top of the part to the bottom. This is consistent with the theory that porosity is caused by shrinkage cavities: the farther a section is from the melt, the less likely it is for liquid melt from the bottom to fill up a shrinkage cavity there.

4.3.3. Modeling surface porosity

Often, porosity occurs at the surface of a part. An attempt was made to investigate if this could be caused by shrinkage cavities within the part. Figure 4.6 shows a schematic of what powder at the surface of the part may look like. Let us assume that a shrinkage cavity forms at the location shown in the figure. Then, liquid metal from the melt rushes up through the matrix to fill the cavity. This flow up the matrix causes a pressure drop. If the pressure difference is large enough, a vacuum could be created inside the cavity. This would cause the pressure difference across the surface infiltrant film to be one atmosphere. If the film cannot sustain this pressure, it could rupture causing a surface pore. A simple way to model this situation would be to assume that flow of liquid metal to a shrinkage cavity takes place through a pipe of uniform diameter ϕ. If d_p is the diameter of the powder constituting the matrix, then, the cross section available for flow between 4 adjacent powder particles is $d_p^2 - \pi d_p^2/4$ (Figure 4.7). The diameter d_c of a circular cross section having the same area is given by

$$\pi d_c^2/4 = (d_p^2 - \pi d_p^2/4) \quad \text{.....(7)}$$

For d_p = 30 micron, d_c turns out to be 15.6 micron. From figure 4.1, the height of the part above the melt is (H-h1), where H is the height of the part and h1 is the distance from the bottom of the part to the top of the melt. The volume of a porous cylinder with diameter d_c extending to the top of the part is $\pi d_c^2/4$ (H-h1). Copper shrinks 5.2% on solidification. Thus the volume sucked up through the porous cylinder in order to fill the shrinkage cavity is $0.052*\pi d_c^2/4$ (H-h1). Copper freezes at 1080 C. During an infiltration run (with the Moly.-Copper system), it was observed

that the liquid melt solidified when the furnace was at 1015 C, time t = 3.5 minutes after the top froze, giving the liquid melt time t to fill up any shrinkage cavities. Thus, the average flow rate of the metal that fills up the shrinkage cavity is $Q = 0.052*\pi\ d_c^2/4\ (H-h1)/t$.

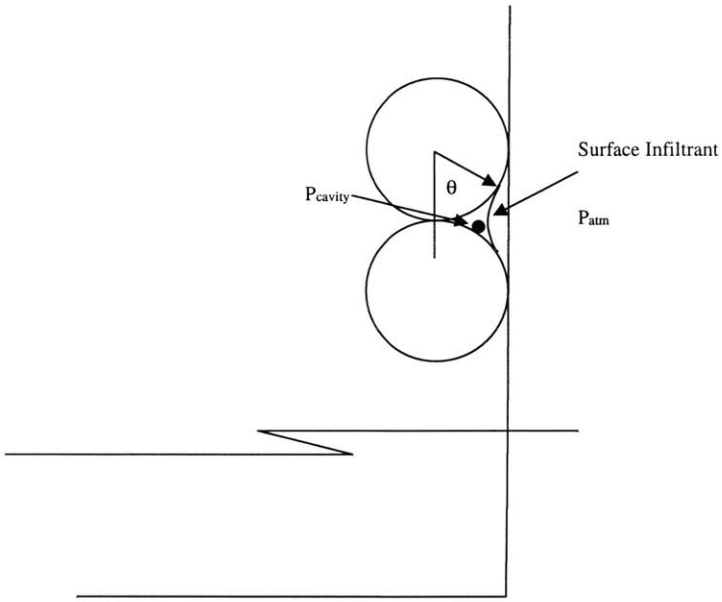

Figure 4.6: Schematic showing a shrinkage cavity formed near the surface of a cooling part. If the pressure difference across the infiltrant film at the surface is too high, the film might rupture giving rise to surface porosity.

The pressure drop due to this flow rate can be found from the equation for flow through a pipe. It

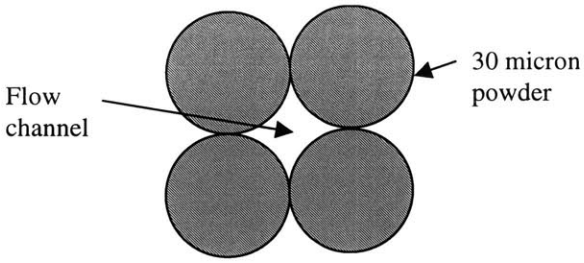

Figure 4.7: Approximation showing the cross section of a channel that the liquid infiltrant could flow through to reach a shrinkage cavity and fill it.

is given by:

$\Delta p = 128Q\mu L/\pi D^4$.....(8)

where L is the length of the channel and D is the channel diameter. Substituting L = H-h1, D = d_c and Q = $0.052*\pi\ d_c^2/4\ (H-h1)/t$ in equation 8 gives,

$\Delta p = 0.416\ \mu\ (H-h1)^2/(t\ d_c^2/4)$.....(9)

where μ is the viscosity of liquid copper =$3.24*10^{-3}$ Pa sec between 1100 to 1200 C. Using H-h1 = 2.36", $\mu = 3.25*10^{-3}$ Pa sec, and an observed value of t = 3.5 minutes in equation 8 gives Δp = 410 N/m^2. The pressure difference across the surface infiltrant is maintained by surface tension. If good wetting is assumed between the powder and the infiltrant and R is the radius of the power particles, then the pressure difference that can be supported across the interface is given by:

$\Delta p = 2\ \sigma/R$.....(10)

In the equations above, σ is the interfacial surface tension = 1.35 N/m and R is the radius of the spherical powder particles = 15 microns. Substituting these in equation 10 gives $\Delta p = 1.8*10^5$ N/m^2. Clearly, a pressure difference of 410 N/m^2 caused by flow of the liquid melt can easily be supported by the infiltrant. In fact, there is plenty of room for safety since there is a three orders of magnitude difference between the two values. Thus, even if the liquid got sucked up at 100 times the rate assumed in equation 9, the pressure difference caused across the film would be 0.41 atmospheres, around 4.5 times less than the 1.8 atmospheres that can be supported. A much more severe case would be the creation of a vacuum due to shrinkage right at the surface of the part. This would cause a pressure difference of 1 atmosphere across the infiltrant. Clearly, even this can be supported across the infiltrant without rupture. Thus, surface porosity is not caused due to rupture of the infiltrant film at the surface of the part.

4.3.4. Temperature profiles

In order to be certain that the flow of cooling gas was indeed causing the predicted temperature gradient in the part, the temperature inside the part was recorded as a function of the depth from the top. To do this, two 2" deep holes were drilled into a sintered SS part (Figure 4.8). The x coordinate was measured from the bottom of the hole (x = 0). Measurements were made for x = 0.25" to x = 1.5". Temperature was not measured at the very top of the hole since it

would not be a true representation of the temperature of the part (due to convection heat loss from the thermocouple to the cooling gas).

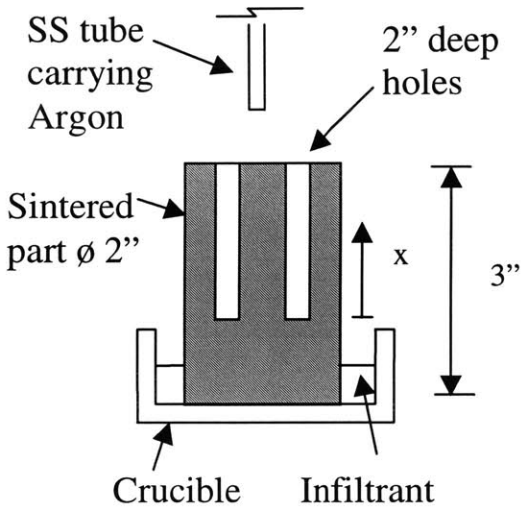

Figure 4.8: Schematic showing the two holes that were drilled into a part to do temperature profiling inside the part.

Temperatures were recorded using a bare wire thermocouple that was sheathed in a dual hole Mullite sheath. The thermocouples were of type K and had a wire diameter of 0.02". The Mullite sheath had an outer diameter of 1/8". Figure 4.9 shows a cross section of the sheath. The Mullite sheathed thermocouples were let into the furnace through fittings on the furnace cover. The fittings were Aluminum pieces with a slight clearance hole for the Mullite sheaths to pass through. Friction between the sheaths and the holes was enough to keep the sheaths at a given height and prevent them from sliding down. Figure 4.10 shows a picture of the setup used.

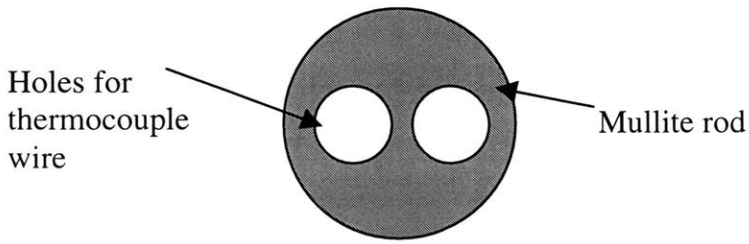

Figure 4.9: Cross section of Mullite sheath used for the type K profiling thermocouple.

The first profile was obtained when the furnace was at 1200 C and in steady state with no cooling gas. Figure 4.11 shows the variation of temperature in the part with height. A gradient of 2.2 C/cm exists in the part even when the cooling gas is not cooling the part. The other profile in the figure was obtained after cooling gas was turned on and steady state was reached at 1200 C. In order to avoid errors due to differences among thermocouples, the same thermocouple was used to get both the profiles shown in the figure.

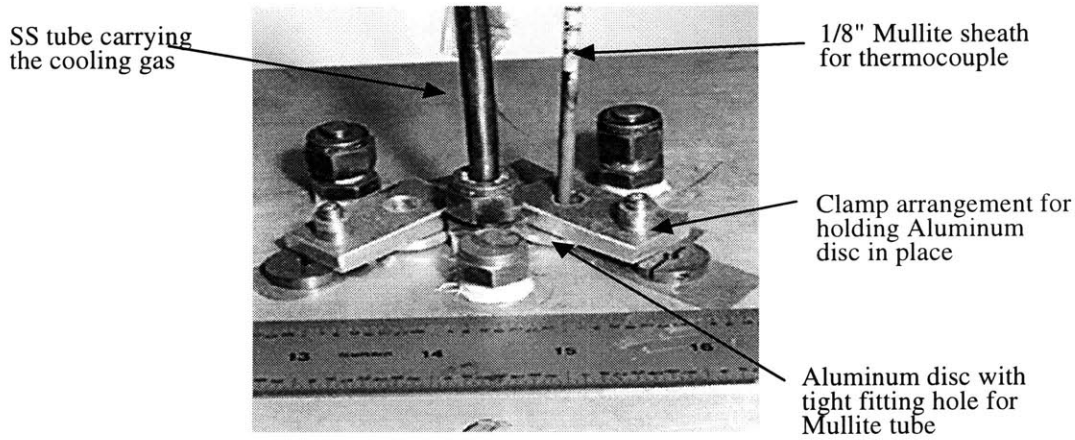

Figure 4.10: Picture of the set up used for temperature profiling. Note the Mullite sheath and the Aluminum clamps.

It can be seen that the gradient in the part increases to 7.24 C/cm when the cooling gas is turned on. Thus, the cooling gas has induced an additional gradient of 7.24-2.2 = 5.04 C/cm. This is just 50.4% of the theoretically estimated value of 10 C/cm that should have been induced inside the part. This can be explained by looking at the heat transfer analysis in section 4.2.3. While calculating the mass of Argon required, it was assumed that $M_{Ar}\ Cp_{Ar}\ \Delta T$ = 175.2 W was removed from the part by the cooling gas. However, the heat transfer calculation in section 4.2.3 shows that convection can remove just 105.4 W form the part. If this were true, then the gradient would be 105.4/175.2*10 C/cm = 6 C/cm, which is close observed value of 5 C/cm. Thus, what is probably happening is that convection heat transfer is limiting the amount of heat withdrawn from the part, thus causing a lower than expected temperature gradient in the part.

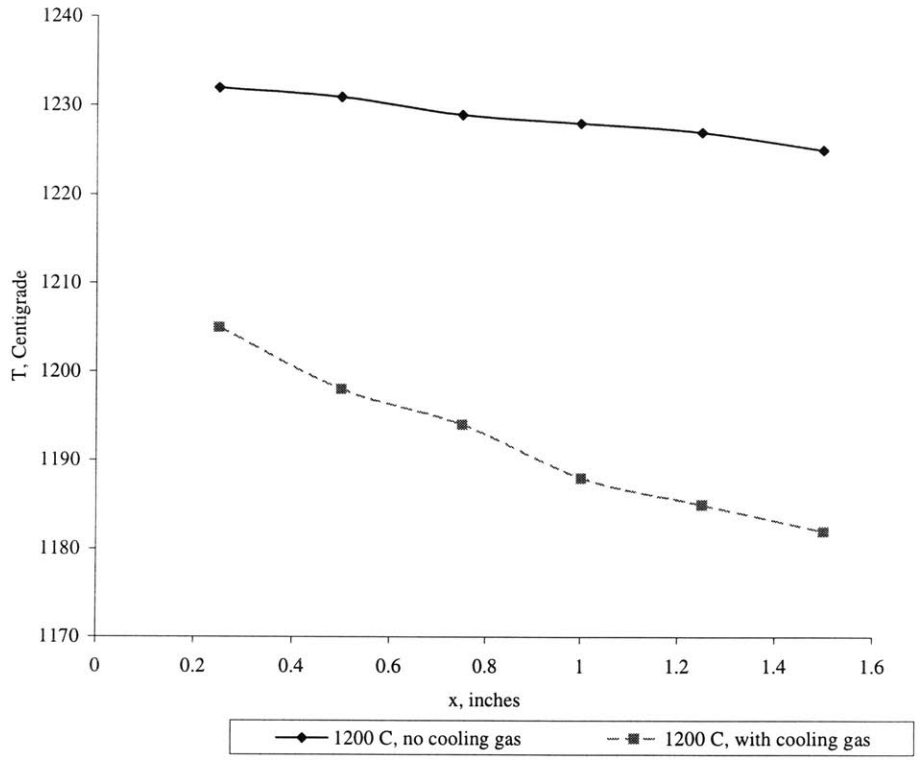

Figure 4.11: Graph showing the variation of temperature inside an infiltrated part with and without cooling gas. The cooling gas induces a gradient of around 5 C/cm in the part. The 1200 C in the legend indicates the furnace thermocouple reading in steady state.

Once it was established that the cooling gas did induce a temperature gradient, profiling was done inside a cooling part. At the end of the infiltration cycle at 1200 C, the heaters inside the furnace were turned off and cooling gas was started. Since the temperature in the part needed to be measured continuously with time, two thermocouples were used. They were placed at different heights (x = ¼" and x =1 1/2") in the two holes drilled into the part. In steady state, without gas flow, the temperature recorded by the bottom thermocouple was 1228 C and that by the top one was 1214 C. The difference in temperatures between top and bottom previously recorded using the same thermocouple was 7 C. Hence, any difference in temperature recorded by the two thermocouples was reduced by 7 C. Figure 4.12 shows the temperature gradient along the height of the part as a function of time. Also shown is the temperature recorded by the control thermocouple of the furnace. Cooling gas flow was turned on 15 seconds before t = 0. This caused the temperature gradient inside the part to begin increasing sharply from the 2.2 C/cm that existed before the cooling gas was turned on. The sharp increase in temperature gradient that can

be seen at t = 0 is a manifestation of this. The temperature gradient stabilized at around 13 C/cm around 2 minutes after gas flow was started. Around 75 minutes after turning on the gas flow, it was turned off. A steep drop in the temperature gradient inside the part is clearly seen in the figure.

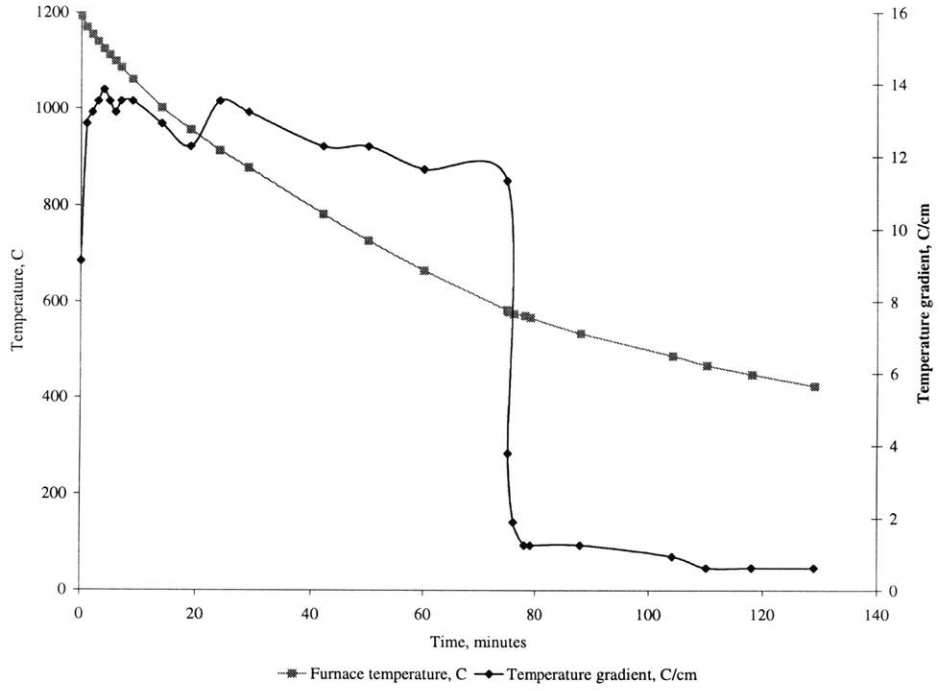

Figure 4.12: Temperature profile measured in a cooling part. A positive gradient indicates that the top is cooler than the bottom. Note the effect the cooling gas flow has on the gradient. The sharply increasing temperature gradient seen at t=0 is a transient caused by turning the cooling gas on 15 sec before t=0. Also shown in the graph is the furnace temperature.

As long as the cooling gas was on, the average temperature gradient in the cooling part was around 13 C/cm, a good value.

4.4. Summary

This chapter described experiments that were conducted to study the issue of porosity that occurs in parts during infiltration. It was shown that inducing a temperature gradient in a cooling part reduces porosity. Temperature profiling was done in order to study the temperature gradient in a cooling part. A possible mechanism for the occurrence of surface porosity was investigated.

5 Design and Fabrication of the Large Scale Furnace

This chapter describes the design and various features of the large scale furnace. A lot of its features were scaled up from the small scale furnace. However, some of the problems encountered while designing the large scale furnace were not seen during the design of the small scale furnace. Solutions to these design problems were obtained by experimenting with various alternatives. This chapter describes issues relating to the thermal and mechanical design of the large scale furnace.

5.1. Thermal design

Any furnace needs power for two reasons: to ramp up to the operating temperature and to overcome steady state heat losses at that temperature. A simple approach was used to estimate the power requirement of the large scale furnace. Steady state heat loss was experimentally determined for the small scale furnace and was scaled up based on surface area to estimate steady state heat loss for the large scale furnace. The power required to ramp up was estimated by considering all the thermal mass that would go into the furnace. The following sub sections describe the process.

5.1.1. Estimating steady state heat losses

The small scale furnace has two semi cylindrical internal heaters, each rated to run off 115V AC. The resistance of each heater plate was measured to be 16 ohms. Thus, the total power of the two heaters combined is $2V^2/R=2(115)^2/16=1.8$ kW. When the small scale furnace was at 1200 C, with the external band heaters turned off, the controller output in steady state was noted to be 53.5%. Thus, the steady state heat loss was 0.535*1.8kW~1kW. Figure 5.1 shows a schematic of the hot faces of the Alumina insulation that goes into the small scale furnace. Figure 5.2 is a schematic of the resistance to heat loss from the hot face of the insulation that is at 1200 C to the ambient atmosphere. Assuming that the convective heat transfer resistance for heat loss from the furnace wall to the atmosphere is independent of the furnace size, the steady state heat loss from the large scale furnace will simply scale as the area of the insulation exposed to

1200 C. The surface area of the insulation exposed to 1200 C was calculated to be around 340 square inches for the small scale furnace.

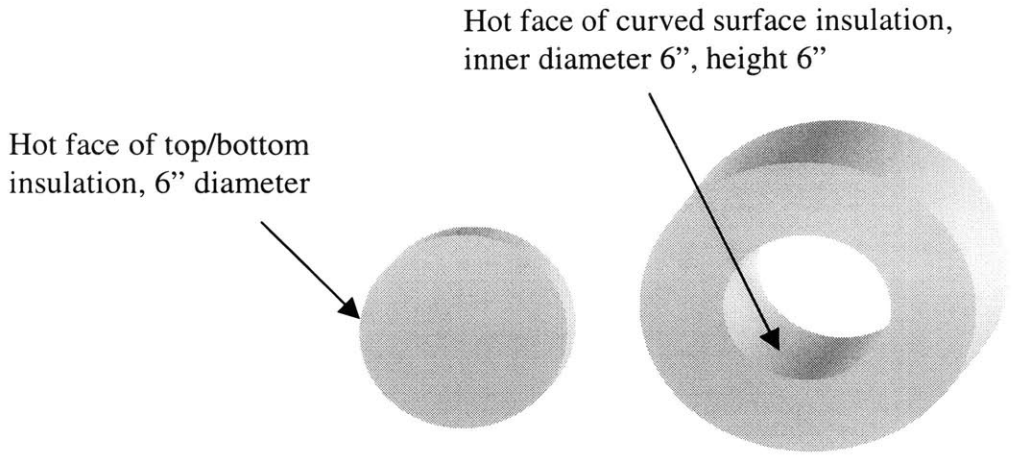

Figure 5.1: Schematic showing dimensions of the hot faces of the insulation that goes into the small scale furnace. These dimensions were used to calculate the area of the hot zone of the furnace.

The interior dimensions of the large scale furnace were estimated by using the fact that the part piston that would go into the furnace would have dimensions of 7" by 9" by 13". The maximum size of the part that can be printed into the part piston is 6" by 8" by 12". Thus, this would also be the maximum size of a part that would be post processed in the furnace. To account for temperature non uniformity near the furnace walls due to heat loss from the walls to the outside, it was decided to have a dead zone on all sides between the part and the insulation (see Figure 5.3). Adam Lorenz's [4] experience with profiling temperature in C. I. Hayes's furnace showed that a dead space of 3" was a good value to use.

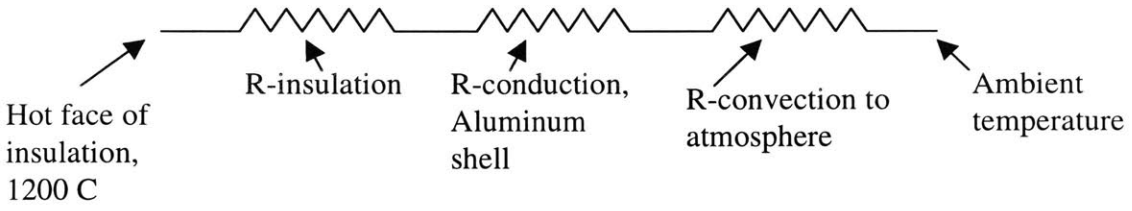

Figure 5.2: Resistance to heat transfer from the hot zone that is at 1200 C to the ambient atmosphere. Heat transfer involves conduction through the insulation, conduction through the Aluminum shell and convection to the atmosphere.

Based on specifications from a heater manufacturer's catalog, it was inferred that heater plates mounted on the sidewalls would be at the most an inch thick. Thus, the width of the heated zone was estimated to be 7" (piston width) +2*3" (dead space) +2*1" (space for two heaters) = 15". The height of the heated zone was estimated to be 9" (piston height) + 2*3" (dead space) =

15". While estimating the depth of the heated zone, a 3" dead space was assumed in front of the piston and a 5" space was taken behind the piston, in order to accommodate an infiltrant crucible that might be used during a gated infiltration. Part of the infiltrant crucible would be located in a non uniform temperature zone: however, this was not an issue as long as all the infiltrant melted. Thus, the depth of the heated furnace zone comes to 21". The dimensions of the interior heated space of the large scale furnace were thus estimated to be 15" by 15" by 21". The corresponding surface area of the insulation exposed to the interior heated space is thus 1710 square inches. Scaling up from the small scale furnace according to surface area, the steady state heat loss form the large scale furnace comes to 1 kW*(1710/340)=5.1 kW.

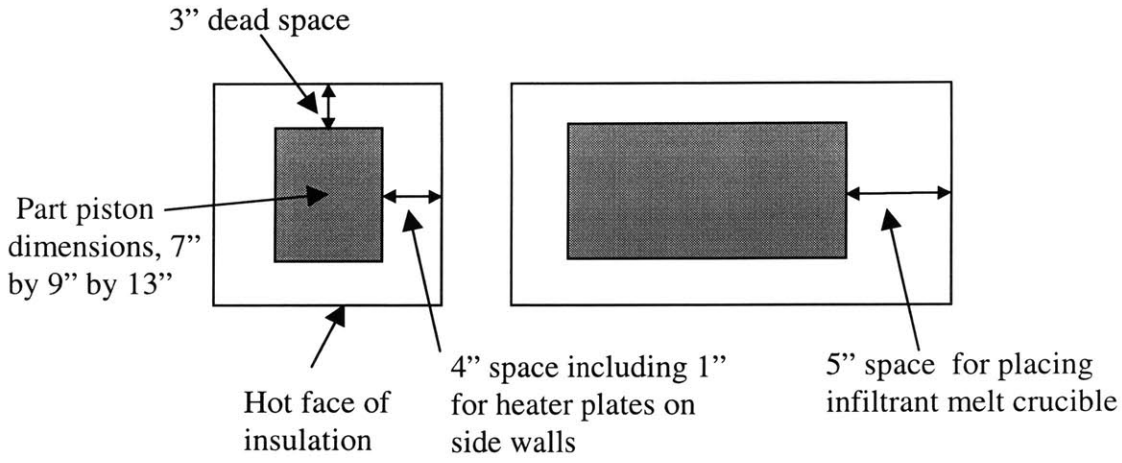

Figure 5.3: Schematic showing dead space between the part piston and the insulation. Dimensions of the insulation were estimated by assuming values for the dead space between the piston and the hot face of the insulation. The dimensions thus obtained were used to determine steady state heat losses by scaling up those from the small scale furnace based on the area of insulation exposed to 1200 C.

5.1.2. Estimating ramp up and total power requirement

The ramp up power requirement of a furnace depends on the thermal mass inside it. Thermal mass is the product of the mass of a given entity and its specific heat capacity and has units of J/K. In order to obtain a rough estimate of the thermal mass of the furnace, assumptions were made about the size of the shell, weight of the heater plates that would go into it, etc. Table 5.1 shows a computation of the thermal masses of various parts of the furnace. In this table, it is important to note that if external strip heaters are not used, the Aluminum shell only heats up to 200 C when the furnace heats to 1200 C, and thus its thermal mass is effectively $1/6^{th}$ of the

theoretical value. However, since the normal practice would be to maintain the shell at 200 C using external strip heaters, the thermal mass of the shell would not really contribute to the thermal load of the internal heaters during ramp up. If the external strip heaters are on, then the Alumina insulation in contact with the shell is maintained at 200 C throughout the furnace cycle, while the insulation facing the internal heated area of the furnace ramps to 1200 C from 200 C. If a linear temperature gradient is assumed to exist inside the insulation, then the effective thermal mass of the insulation is roughly half the theoretical value. While determining the mass of the infiltrant, it was assumed that the part was 40% porous and that 30% extra infiltrant would be used. The net thermal mass of the furnace comes to around 71.5 kJ/K, including the effective thermal mass of the Aluminum shell. For a ramp rate of 5 K/min, the power required is mcdT/dt = 71.5*5/60 kW =5.96 kW.

S. No.	Part name	Material	Dimensions	Mass	Spec. ht. capacity	Thermal mass
				kg	kJ/kgK	kJ/K
1	Part piston	Graphite	7"*9"*13" outer dim.	8.84	0.709	6.30
			1/2" wall thickness			
2	Aluminum shell	Aluminum	22*18.5"*24.5" outer	86.5	0.903	13.02
			dim., 3/4" thick			
	Note: 13.02 kJ/K is 1/6 th of the obtained value and is to be used if external heaters are not on.					
	If external heaters are used, do not consider shell's thermal mass.					
3	Heater plates	Alumina	Estimated from sample	12.96	0.765	9.91
4	Part for sintering	SS	6"*12"*8", 60%dense	44.2	0.48	21.22
5	Infiltrant	Bronze	40% dense part and	44	0.355	15.62
			30% extra infiltrant			
6	Hearth plate	Graphite	14"*8"*1"	2.3	0.709	1.63
7	Infiltrant crucible	Graphite	3.75"*7"*9" outer dim.,	3.8	0.709	2.69
			1/2" walls			
8	Insulation	Alumina	Inner dimensions of	1.5	0.765	0.57
Note: see text for discussion			shell, and 1" thick			
			insulation			
9	Catch tray	SS	Estimated mass	1	0.48	0.48
					TOTAL	71.45

Table 5.1: Estimation of the thermal mass of a fully loaded furnace.

Having estimated the ramp up power requirement, the next step was to calculate other heat losses from the furnace. Power would be supplied to the internal heaters using a brass tube

brazed to the heater leads (Figure 5.9 and Figure 5.16). Heat is lost from the inside of the furnace to the outside by conduction along the heater lead and the brass tube. The heater lead has a lower conductivity than brass. An upper bound estimate of the heat loss can be obtained by assuming that the conductivity of the heater lead is equal to that of the brass tube. The brass tube has an outer diameter of 0.125" and a wall thickness of 0.015" which gives it an area of cross section of $A = 2.9*10^{-6}$ m^2. As a worst case analysis for estimating heat loss, it can be assumed that the temperature drop of $\Delta T = 1000$ K occurs entirely along a length L = 1" of the insulation. The corresponding heat loss by conduction is kA $\Delta T/L$, where k is the thermal conductivity of brass = 111 W/mK (@room temperature, worst case scenario). This heat loss comes to around 13W. For 24 feedthroughs, the total heat loss by conduction comes to 312 W. To account for heat loss through other fittings in the furnace by conduction, the total heat loss by conduction can be taken to be around 1kW.

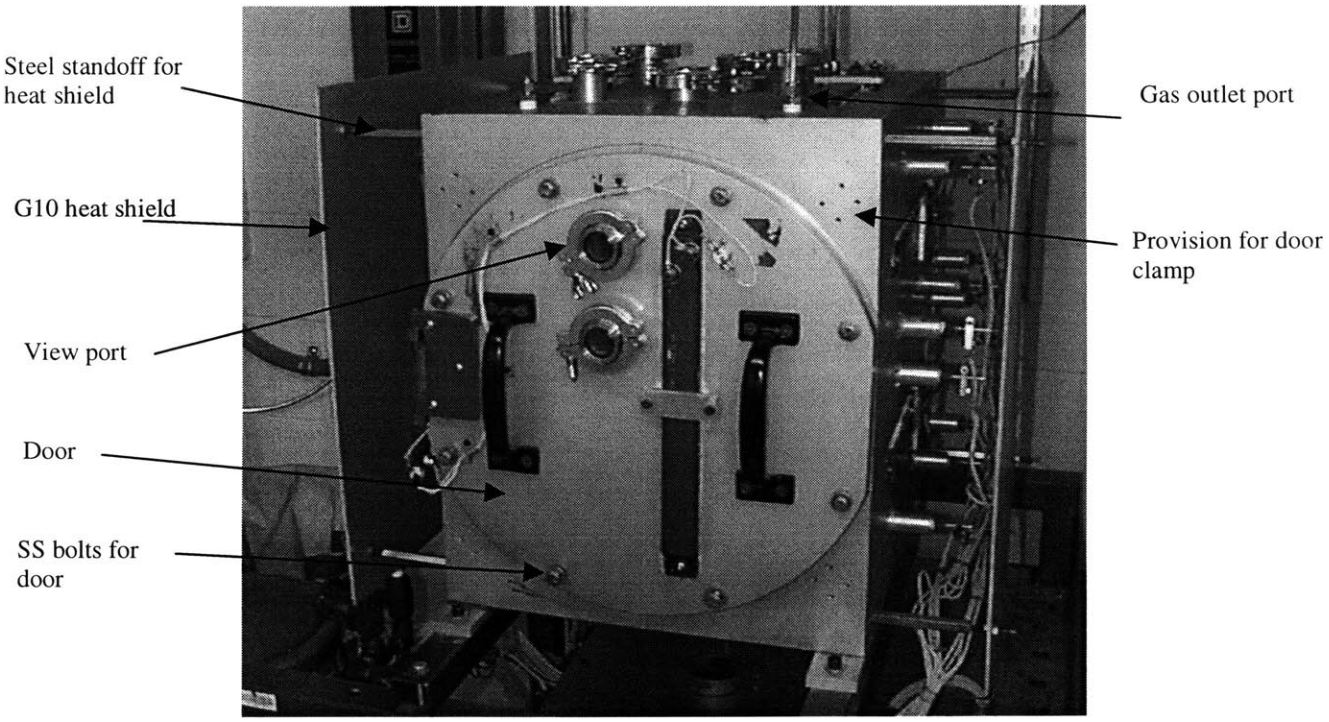

Figure 5.4: Picture of the large scale furnace. Note the strip heater and the view ports on the front door.

Thus, the power requirement for the furnace is 5.1 kW (steady state heat loss at 1200 C) + 5.96 kW (ramp up power requirement at 5 K/min) + 1 kW (loss through power feedthroughs etc.) = 12.06 kW.

5.1.3. Selection of internal heaters

Thermcraft Inc., of Winston-Salem, NC was chosen to provide heaters for the furnace. The heaters had Fe-Cr-Al, "super Kanthal" resistance wire (able to reach 1350 C) embedded in Alumina plates and were of a similar kind as the ones used in the small scale furnace. Due to considerations of size and watt density, the heater plates chosen gave a maximum power of 850 W. Twelve such heaters were ordered, giving a total power of 10.2 kW. At first glance, this power seems lower than the required 12.06 kW. While arriving at the 12.06 kW, it was assumed that the charge inside the furnace would be the maximum possible that could be accommodated by the piston. However, this is almost never the case, and thus the ramp power requirement will be less than the calculated 5.96 kW. Also, the steady state requirement of 5.1 kW is when the furnace is at 1200 C: at lower temperatures, the power requirement to offset heat loss is lower and thus more heat is available to ramp up. Moreover, as discussed earlier, with the external strip heaters on, the thermal mass of the Aluminum shell shall not be heated by the internal heaters. This will reduce the ramp up power requirement by 1.1 kW. Thus, it was decided to stick with the twelve 850 W heaters.

5.2. Furnace shell and external features

Aluminum was retained as the shell material. This was because of its excellent thermal conductivity that would enable the shell to attain uniform temperature when heated by external strip heaters. Since the shell would attain a temperature of around 200 C when the furnace was running, it was important for the shell material to exhibit good strength at this temperature. Three potential candidates: Aluminum 5052, 5083 and 6061 were examined for suitability for use as shell material. At 200 C, the yield strengths of Aluminum 5052, 5083 and 6061 are 75 MPa, 117 MPa and 103 MPa respectively. At 260 C, these numbers become 52 MPa, 75 MPa, and 35 MPa respectively. Clearly, Aluminum 5083 is superior to the others in terms of strength. This, together with the fact that it exhibits good corrosion resistance made it an ideal candidate for shell material.

As mentioned previously, shell dimensions were chosen keeping in mind the fact that an entire part piston having dimensions of 7" by 9" by 13" would need to be fired in the furnace. Also, dead space was provided around the periphery of the part where the temperature would not be uniform due to greater heat loss at the ends. An inch of Alumina insulation was used just as in the small scale furnace. These guidelines were given to a consulting engineer, Diane Brancazio, who was staffed on this project in order for her to design a rectangular cross section shell.

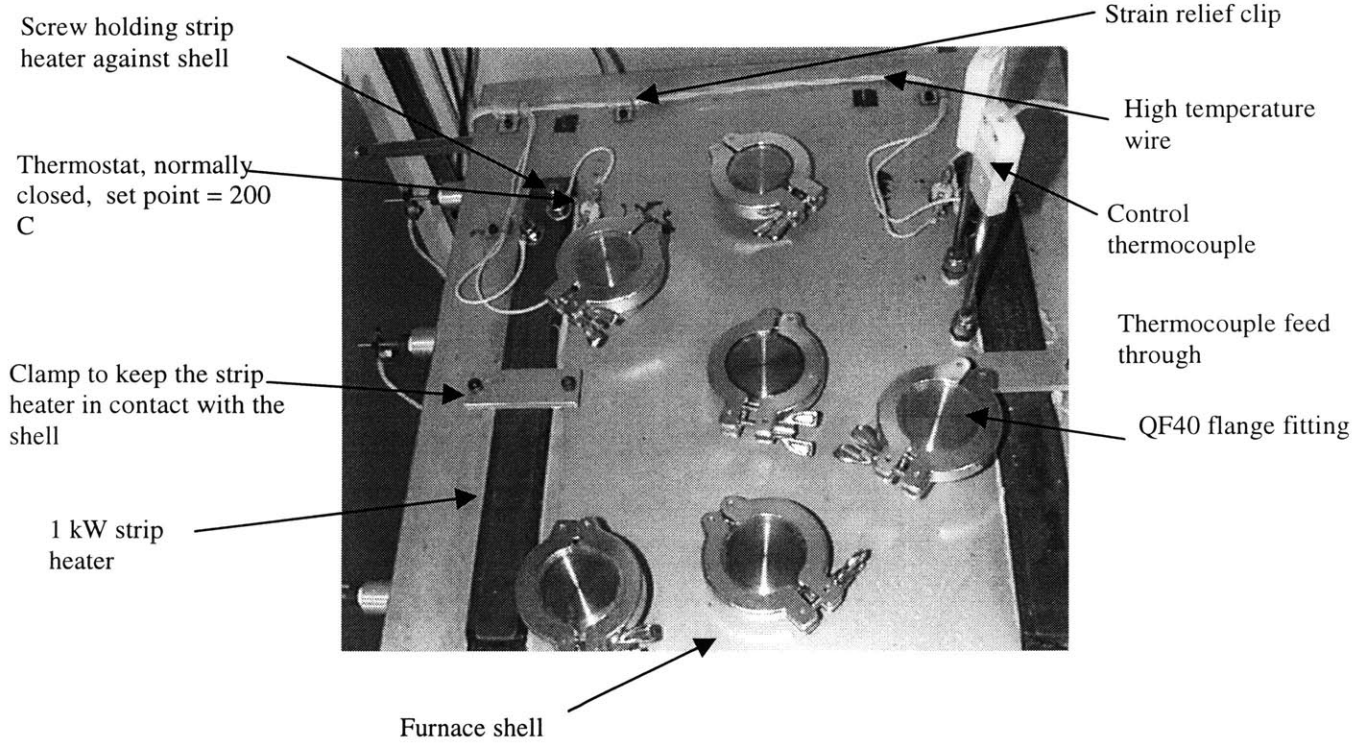

Figure 5.5: Picture showing a top view of the furnace shell. Note the QF40 fittings and the thermocouple feedthroughs.

A shell thickness of ¾" was chosen and the shell was designed using Solidworks, a CAD software. Features such as standoffs on the furnace sidewalls for power feedthroughs, flange fittings, gas ports, and mounts for internal heaters were incorporated into the shell. Design parameters for features on the shell were determined as the design progressed and parts such as heaters, thermostats, burst disc etc. chosen to go into the furnace were finalized. Figure 5.4 shows a picture of the shell. The outside dimensions of the shell are 18.5" by 22" by 24". The shell was fabricated by NU Vacuum Systems Inc., a Massachusetts based vacuum chamber manufacturing company. The shell was welded to be leak tight and was vacuum tested by the manufacturer. Detailed engineering drawings of the furnace and its subassembly are included in

Appendix 2 of this document. The sections below briefly describe the internal and external features of the furnace.

5.2.1. External strip heaters

Figure 5.5 shows a top view of the furnace shell. Two strip heaters (1 kW each) can be seen on the top face. There are two such heaters on each face of the furnace, except on the door that has only one heater, due to space considerations. Each strip heater runs off 240 V AC and is controlled by its own normally closed thermostat which opens at 200 C. The strip heaters are held against the shell by screws at the ends and a clamp in the middle (Figure 5.5). Heat transfer paste (see list of vendors in Appendix 1 for details) between the strip heaters and the Aluminum shell ensures good heat transfer between the two. High temperature wires (rated for use at 400 C, see list of vendors in Appendix 1 for details) carry current to the strip heaters and run along the furnace shell. Strain relief clips have been provided on the shell at regular intervals to relieve these wires.

5.2.2. Fittings on the shell

Also seen in Figure 5.5 are six QF40 flange fittings on the top face. The bottom face has two similar fittings, one of which is fitted with a burst disc designed to rupture at 4.5 psig. The QF40 fittings can be used for various purposes such as: a passage for a linear feeding mechanism to be used for gated infiltration, for the effluent tube of a debinding apparatus, or as ports for additional thermocouples. The figure also shows two type K thermocouples: the front one is the control thermocouple. The thermocouples go into the furnace through standard ¼" NPT compression fittings. A gas outlet port can be seen in Figure 5.4 on the top face of the furnace. Four such ports have been provided, two on the top face and two on the rear face for use as gas inlet or outlet ports. Gas tubing goes into the furnace through 3/8" NPT compression fittings.

5.2.3. Furnace Doors and heat shields

Figure 5.6 shows a comparison of the two doors that can be used with the furnace. Both doors are fastened on to the shell using eight SS bolts. A provision was made at four locations on the front face of the furnace shell for mounting door clamps to clamp the door to the shell (Figure 5.4). However, it was found that the clamps interfered with the opening of the door and were thus not used. In Figure 5.6, the door on the right has two view ports and is meant for use during regular operation of the furnace. The door shown on the left has six ports for thermocouples that can be used to measure temperature profiles inside the furnace. This door is to be used whenever the temperature inside the furnace needs to be measured and adjusted along the depth of the furnace by using trim potentiometers (more on this in Chapter 7). Figure 5.7 is a picture of the furnace fitted with this door.

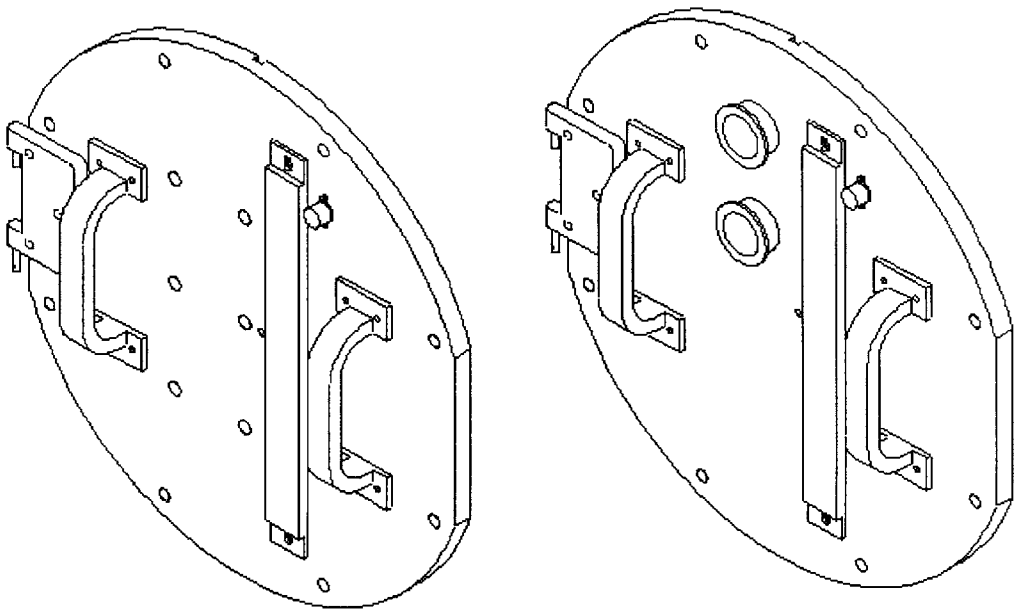

Figure 5.6: Comparison of the two kinds of doors that can be used with the furnace. The left door is for use during temperature profiling and the right door with the viewports is for use during regular furnace runs.

Figure 5.4 shows two G-10 heat shields, one on each side of the furnace. G-10 is a woven glass fabric laminated with epoxy resin, can operate continuously at 140 C, and is a superior electrical insulator. The purpose of the G-10 shields is to prevent radiation from the hot furnace wall (at 200 C) from reaching the surrounding furnace electrical control box and gas tanks. These

shields are held on to the furnace wall by means of steel standoffs that screw into blind threaded holes in the furnace wall.

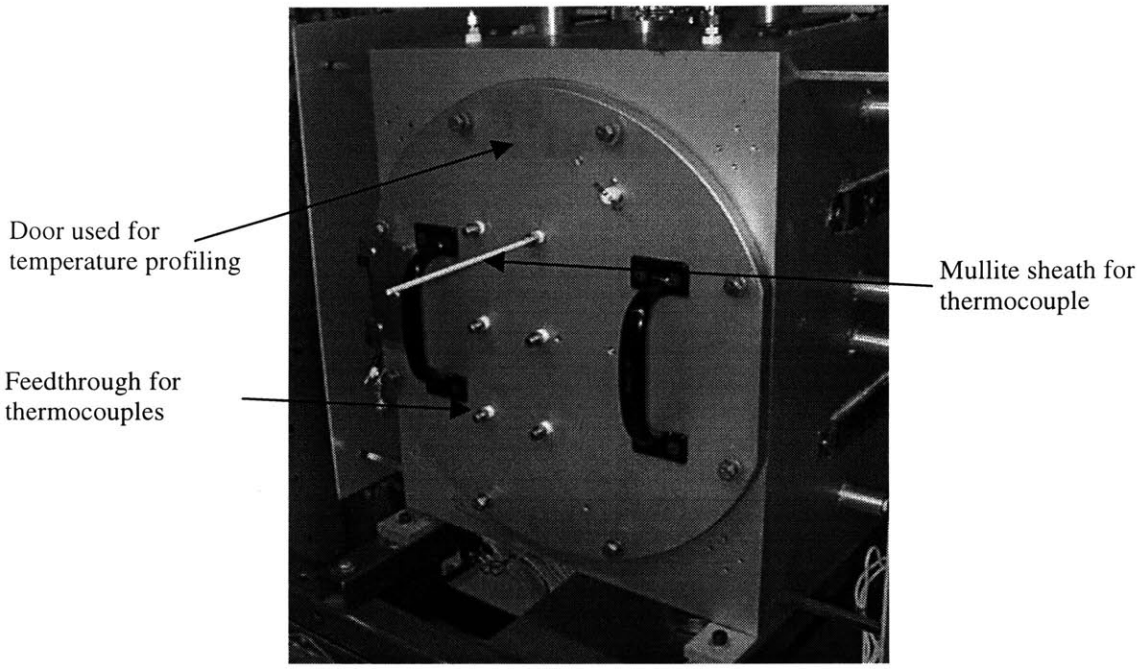

Figure 5.7: Picture of the furnace fitted with a door used for temperature profiling. The door has six ports for inserting thermocouples into the furnace. The thermocouples can be used to measure the temperature inside the furnace as a function of the distance from the door.

5.2.4. Power connections to internal heaters

There are twelve internal heaters, six on each side wall of the furnace. These heaters need to be connected to power leads from the SCRs. The heater leads were brazed (leak tight joint) to 1/8" outer diameter Brass tubes using a Copper-Silver eutectic alloy (see Figure 5.8 and Figure 5.9). An important issue was to bring the Brass tubes out of the furnace while maintaining a leak proof seal. Conventional methods such as using a Swagelok compression fitting and a Teflon sealant did not work. This was because the Teflon crept under the influence of the high shell temperature and the force of the compression fitting. Figure 5.10 shows the Swagelok fitting-Teflon sleeve assembly that was used to test if this assembly would work at 200 C. As will be explained later in the chapter, as part of preliminary testing, a single heater was mounted into the furnace and an enclosure was created around it in order to test if the heater could heat the enclosure up to 1200 C. When this test was done, Swagelok assemblies like the ones shown in

Figure 5.10 were used to create leak proof feedthroughs. Figure 5.11 shows the resulting creep in the Teflon sleeve of one such assembly. A second series of tests involved tightening assemblies like the one shown in Figure 5.10 and placing them in an oven at 200 C for a few hours and examining the behavior of the Teflon sleeve. Creep was observed in the sleeves.

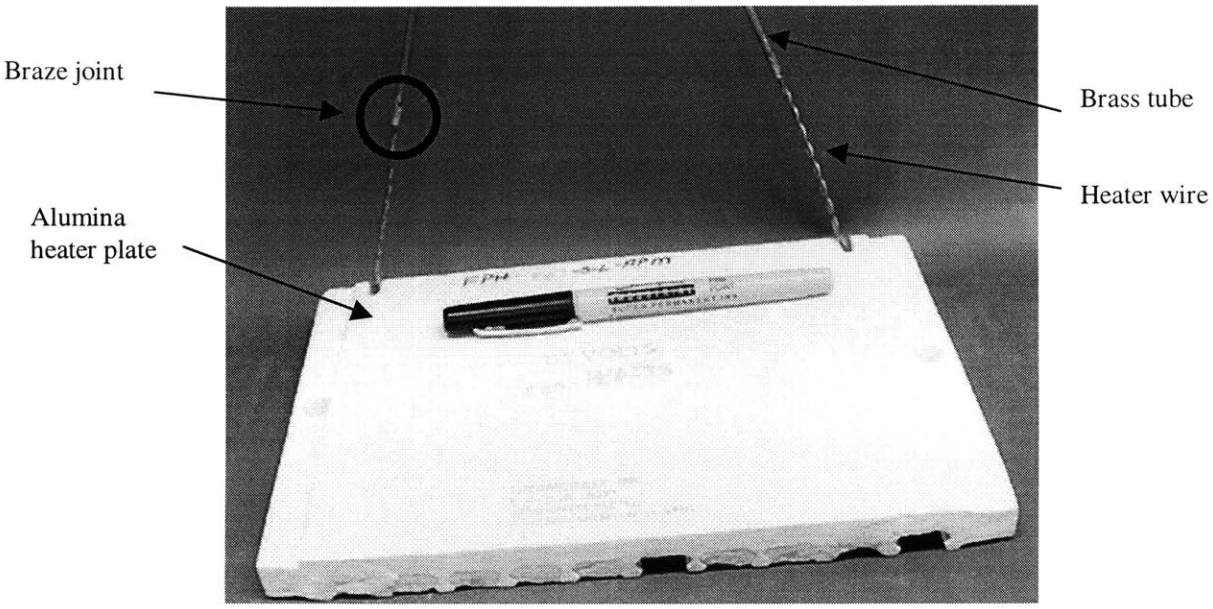

Figure 5.8: Picture showing an internal heater with its leads braze joined to Brass tubes. The heater leads stick ½" into the Brass tubes. The braze is a Silver-Copper eutectic.

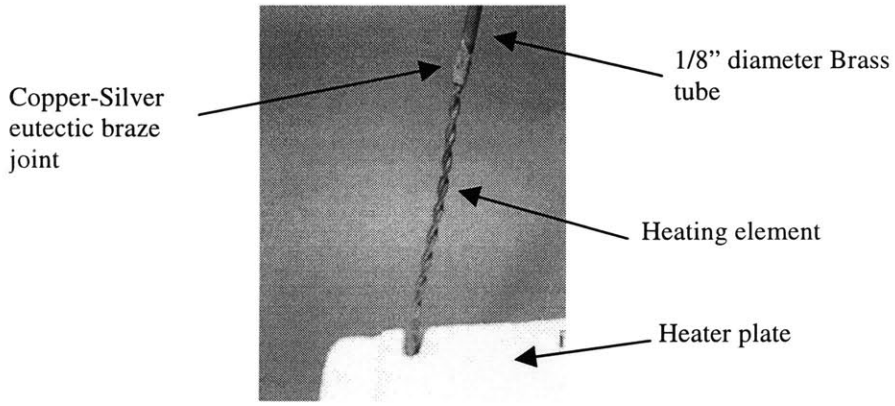

Figure 5.9: Picture showing the braze joint between the heating element and the Brass tube. Once outside the heater plate, the heating element is double twisted to reduce resistive heating. This keeps the braze joint cool.

To overcome this problem, fittings shown in Figure 5.12 were machined out of Ultem. Ultem is a plastic that has excellent machinability, mechanical strength, and dimensional stability. Moreover, it is electrically insulating and can withstand temperatures up to 170 C. As can be

seen in Figure 5.12 and Figure 5.13, the fitting has ¼" NPT male threads on one end, a small projection on the other, and a through hole that is slightly bigger than 1/8" in diameter (0.128"). The Brass tube slides into the fitting through this hole. A detailed engineering drawing (drawing # FUR025) of the Ultem fitting is included in Appendix 2. A Silicone rubber tube

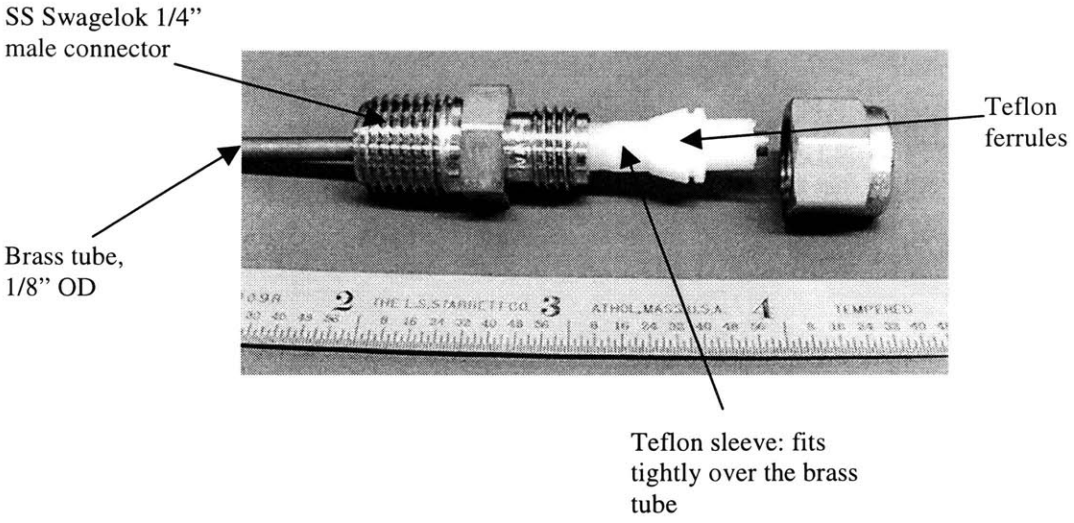

Figure 5.10: Picture showing the Swagelok fitting and Teflon sleeve assembly that was tested as a possible candidate for use as a power feedthrough.

having an ID of 3/32" and an OD of 5/32" is slid over the Brass tube and on to the projection on the Ultem part to form a leak proof seal (Figure 5.13).

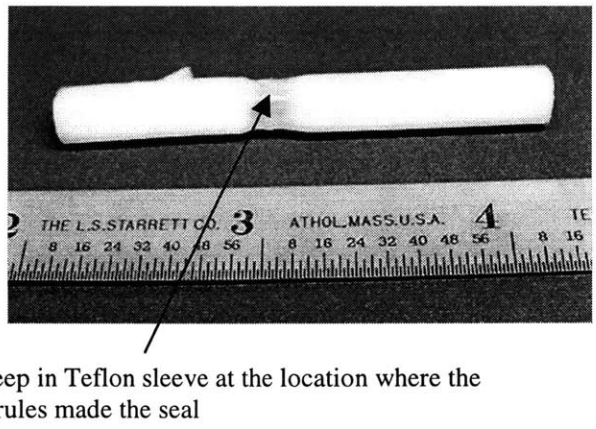

Figure 5.11: Picture showing creep in the Teflon sleeve that was used in a Swagelok fitting and maintained at 200 C for a few hours.

The seal formed by the Silicone tube and the Brass tube was tested for leaks under positive pressure and was found to not leak even at 15 psig. Moreover, this seal will perform very well when the furnace is run under vacuum, since atmospheric pressure outside will force the Silicone sleeve against the brass tube, resulting in a more secure seal. Figure 5.14 shows how a current

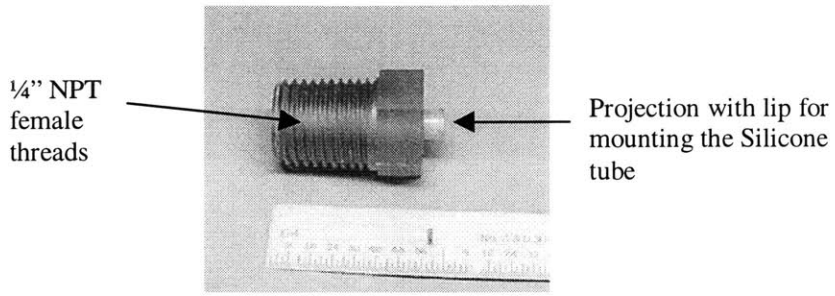

Figure 5.12: Ultem fitting which was used as a power feedthrough for heater wires.

carrying wire from an SCR is connected to the Brass tube using a Brass connector. Figure 5.15 shows a drawing of the brass connector. Note the slit in the middle. Force from a clamping screw decreases the slit spacing and clamps the connector firmly on to the brass tube. Figure 5.14 shows the how the Ultem fitting threads into an Aluminum standoff welded on to the furnace shell. There are twelve such standoffs each on the left and the right faces of the furnace shell, some of which can be seen in Figure 5.4. Figure 5.16 shows a schematic of a cross section of the standoff. The Mullite tube inside the standoff is to prevent the heater wire from accidentally coming in contact with the Aluminum shell.

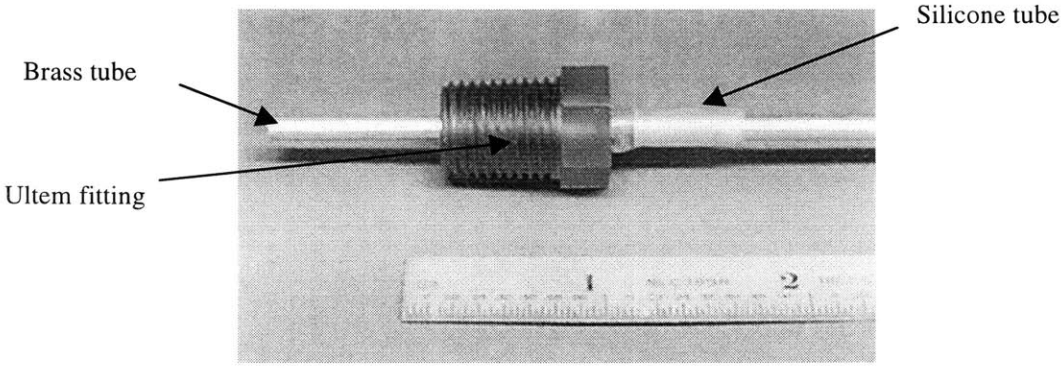

Figure 5.13: Picture demonstrating how a Silicone tube can be used to achieve a leak proof joint at the Ultem fitting-Brass tube interface.

5.3. Insulation

5.3.1. Initial efforts

The small scale furnace used an inch of Alumina as insulation. Mounting the Alumina insulation into the small scale furnace was relatively easy since most of the insulation was well secured and did not have to be held against its weight. However, attempts to mount Alumina

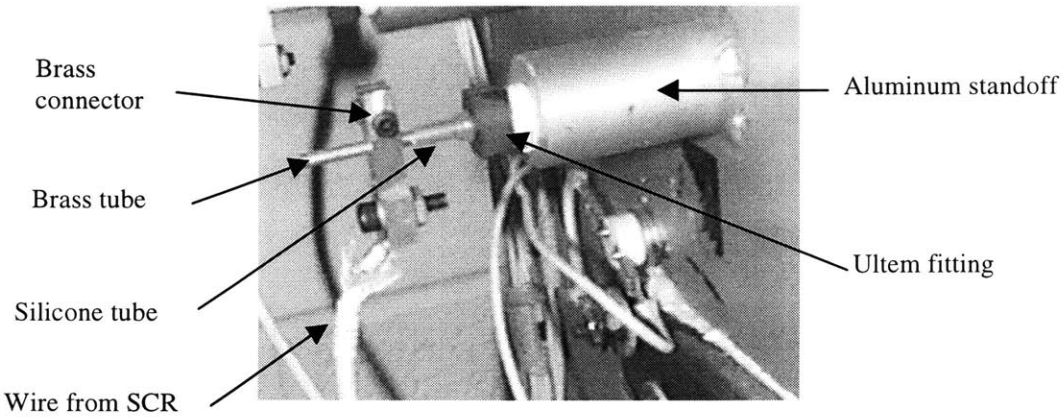

Figure 5.14: Picture showing the power feedthrough assembly. The wire from the SCR is connected to the Brass tube by a Brass connector. The Ultem fitting is screwed into the Aluminum standoff.

insulation into the large scale furnace proved difficult. This was especially true of the insulation on the top, back and front faces of the furnace that had to be held against its own weight.

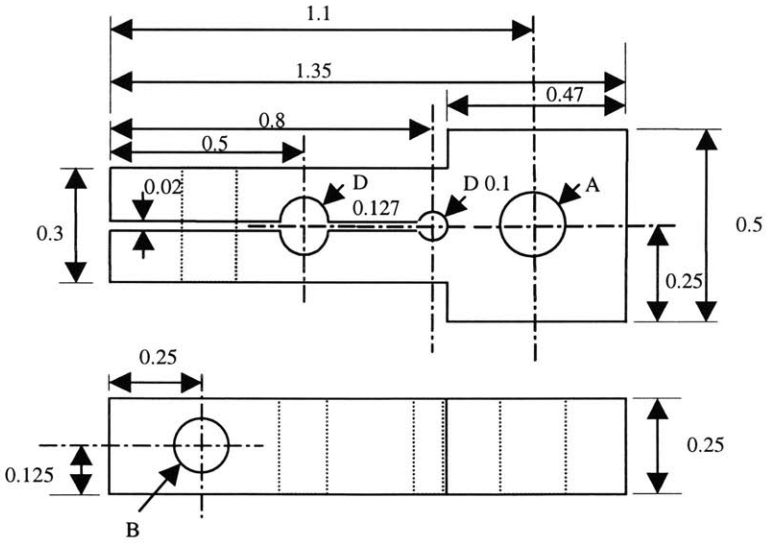

Figure 5.15: Drawing of the Brass connector used to connect a wire from the SCR to a Brass tube that is brazed to a heater lead. Holes A and B in the drawing are clearance holes for 8-32 and 6-32 screws respectively.

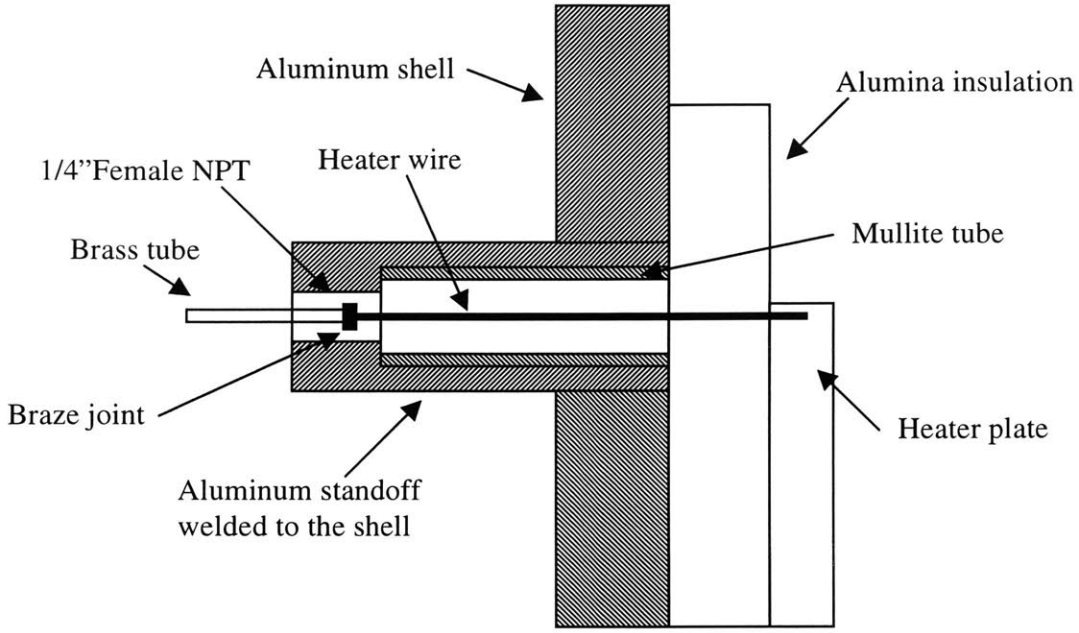

Figure 5.16: Schematic showing a section through an Aluminum standoff on the furnace wall. The Mullite tube inside the standoff is to prevent the heater wire from touching the Aluminum shell.

The problem was that the 1" thick Alumina blanket from which insulation was cut was actually composed of many thin sheets of Alumina that were stitched to each other by fine thread. When insulation of the desired size was cut from a roll of Alumina blanket, the fine threads that held the sheets together got cut and thus the insulation got ripped off easily. When this insulation was mounted into the furnace, it did not retain structural integrity. Insulation on the top, front and back faces sagged and peeled off. Peeling was not an issue for insulation on the sides, since the heaters held it against the Aluminum shell of the furnace. Clearly, peeling was an issue that had to be addressed.

5.3.2. Polymer spray

There were two requirements: one, the insulation had to be stiff at room temperature so that mounting would be easy and two, the insulation needed to be held in place even when the furnace was at 1200 C. In order to attain stiffness at room temperature, it was decided to spray the face of the insulation that would be exposed to the hot zone with polymer. The polymer

would disintegrate at high temperatures and the insulation would be free from the polymer after the first furnace run. The cold face of the insulation was not sprayed with polymer since it would not get hotter than 200 C, at which temperature the polymer would not disintegrate. The important thing was to search for a polymer that would disintegrate at 1200 C without leaving a trace. Three polymeric binders were tried: Rhoplex, Polyethylene Glycol (PEG) and Polyacrylic Acid (PAA).

In order to compare these binders, the hot face of the top insulation of the small furnace was sprayed with an 11 weight % binder solution and fired to 1200 C. This process was repeated with fresh insulation for all three binders. In Figure 5.17, the black coating on the insulation on the left was obtained when it was sprayed with Rhoplex and ramped up to 1200 C at 5 C/min. This might have occurred since the Rhoplex did not have sufficient time to decompose at lower temperatures. In subsequent runs, the furnace run involved a 90-minute soak at 500 C before ramping to 1200 C at 5 C/min and staying there for 60 min. The idea was to give the binder sufficient time to decompose at 500 C before ramping up to 1200 C. The insulation on the right in Figure 5.17 shows the result of this treatment on Rhoplex sprayed insulation. As can be seen, there is binder residue on the insulation and this is unacceptable. When a similar experiment was carried out using PEG, there was no residue on the hot side of the insulation. However, polymer vapors did condense on the cold face of the Aluminum top door. This too was unacceptable. PAA on the other hand, worked well and left no visible trace in the furnace. Thus it was decided to spray the insulation that went into the large scale furnace with an 11 weight percent solution of PAA (See list of vendors in Appendix 1 for details of the PAA solution).

5.3.3. Nextel thread and Inconel mesh

The PAA coating on the insulation took care of structural integrity issues at room temperature and made mounting the insulation into the furnace an easy task. However, as mentioned earlier, the insulation also needs to retain structural integrity at high temperatures, after polymer burn off. 3M manufactures a product called Nextel, which is a high temperature ceramic capable of continuous operation at 1371 C (see list of vendors in Appendix 1 for details). The two most common grades of Nextel are types 312 and 440. Nextel 440 was chosen

over Nextel 312 for use in the furnace since it has a higher Alumina content (70% vs. 62%) and because its filament tensile strength is higher (2000 MPa vs. 1700 MPa). Nextel 440 thread and

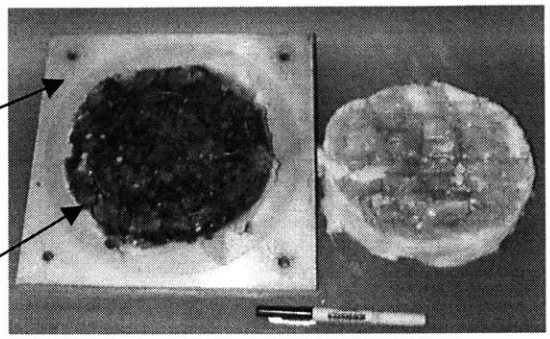

Figure 5.17: Picture of the results of firing insulation sprayed with Rhoplex to 1200 C. The insulation on the left was ramped to 1200 C at 5 C/min starting at room temp., while that on the right was held in the furnace at 500 C for an hour before ramping to 1200 C at 5 C/min. The idea was to give time for complete polymer burnout at 500 C before ramping to 1200 C. Both these results were unacceptable.

cloth are available in two varieties: with sizing and without sizing. Sizing is a chemical coating that makes the Nextel thread easy to handle while sewing. The sizing burns off at around 300 C. However, sized thread could not be used to sew the insulation since parts of it away from the hot zone of the furnace (i.e. facing the Aluminum shell) would not get hot enough to burn off the sizing. Hence, it was decided to use unsized thread to sew the periphery of the insulation in order to prevent it from delaminating (Figure 5.18). Unsized Nextel sleeve was sown on the insulation on the front face of the furnace. This was done to protect it from tearing apart while loading and unloading parts in and out of the furnace. In addition to sewing the insulation, Inconel wire mesh was used on the back, front and top faces to hold the insulation in place (Figure 5.19). Refer to the list of vendors in Appendix 1 for details on the mesh.

5.3.4. Initial testing

As seen in section 5.1, the installed capacity of the internal heaters was a little less than the theoretical power estimate (10.2 kW vs. 12.06 kW). Hence, it was decided to conduct experiments to determine if extra insulation would be required in order for the furnace to reach

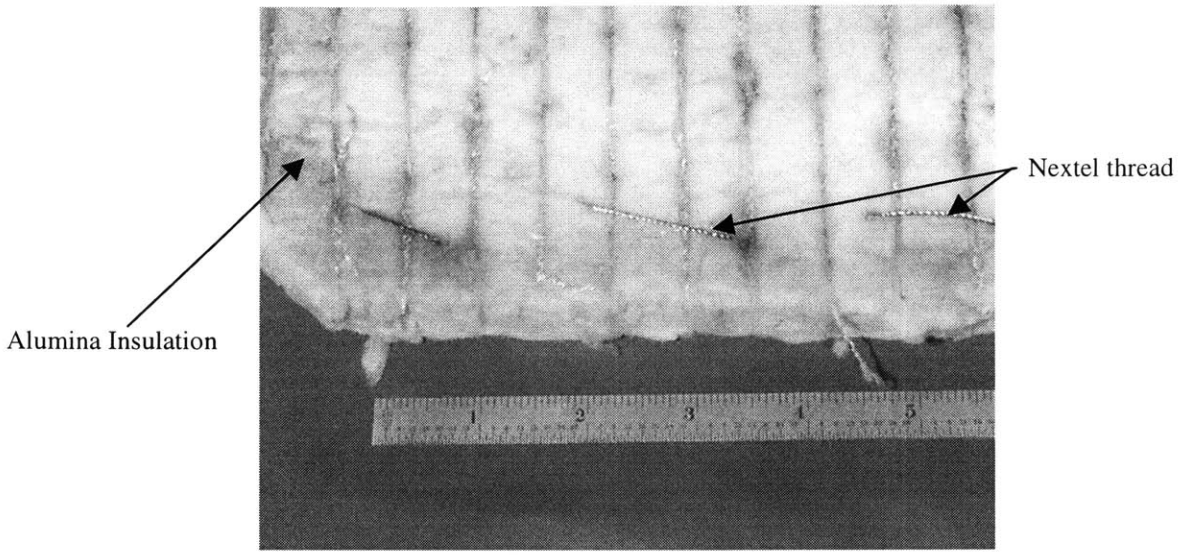

Figure 5.18: Picture showing Alumina insulation sewn together along the periphery using Nextel thread.

1200 C. When all twelve heaters are mounted into the furnace, the area heated by them is composed of the top, bottom, front and back faces of the furnace insulation. The heated zone has dimensions of 13" by 19" by 20", and thus the area heated by the twelve heaters comes to 2(13* 19 +13* 20)=1014 square inches. The area per heater is thus 1014/12=84.5 square inches. A single heater was mounted into the lower left corner of the furnace and a box was built around it using 1" Alumina insulation, such that the area heated by the heater would be close to 84.5 square inches. Figure 5.20 shows a schematic of the enclosure.

A simple calculation shows that the area of the insulation exposed to the heater is 99 square inches. The heater was run off a variac and it was found that 133 V needed to be applied across the heater in order to attain 1200 C inside the enclosure. This was $(133^2/115^2-1)*100$ ~34% extra power over the rated 850 W. The extra power requirement could have been due to the fact that the heater was heating 99 square inches as opposed to the 84.5 square inches it would heat when all twelve heaters were running. Also, there were gaps at the interfaces between the insulation through which heat loss could have been occurring. However, to be on the safe side, it was decided that extra insulation (in addition to the 1" of Alumina already in the furnace) would need to be added to the furnace to make sure that it would reach 1200 C when all twelve heaters were installed.

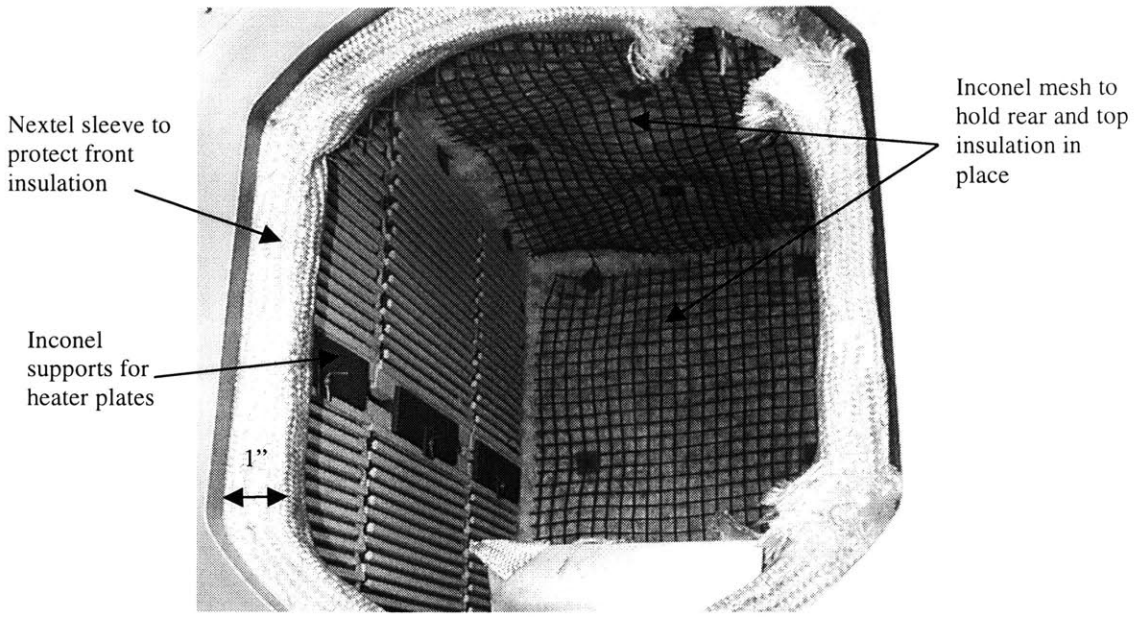

Figure 5.19: Interior of furnace. Inconel wire mesh supports the insulation on the top, back, and front faces of the furnace. Nextel sleeve on the periphery of the front insulation protects it from being damaged when the furnace is being loaded/unloaded. Also note how the heaters are mounted on the Inconel supports.

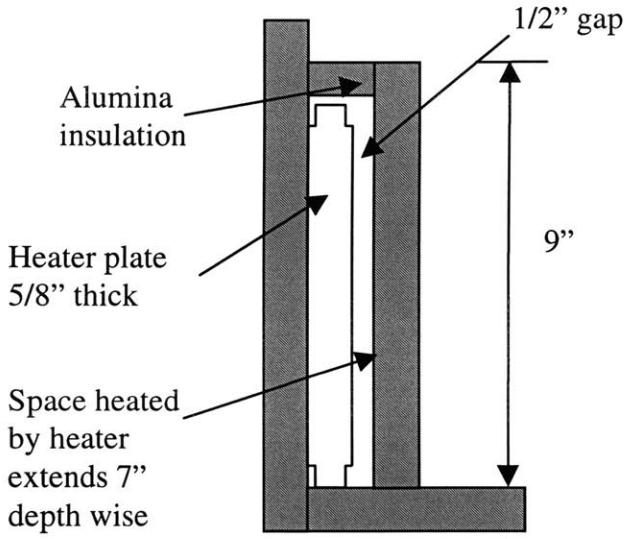

Figure 5.20: Schematic showing a section through the enclosure that was built around a single heater. This heater was powered by a variac and the voltage required to attain a steady state temperature of 1200 C inside the enclosure was found as a function of the quantity of insulation on the 9" by 7" face opposite the heater plate.

5.3.5. Choice of extra insulation material

Choice of material for the extra insulation was critical since adding extra insulation meant adding extra moisture that needed to be purged before a furnace run. Two candidates were considered: Alumina and Graphite. Fiber Materials Inc. of Biddeford, ME offers two kinds of Graphite insulation to choose from: CH grade Carbon felt that has a thermal conductivity of 0.053 W/mK (at 50 C) and GH grade Graphite felt with a thermal conductivity of 0.068 W/mK (at 50 C). Although Carbon felt is better than Graphite felt in terms of thermal conductivity, it has a lower percentage of Carbon (94% vs. 99.7%) and absorbs a higher amount of water vapor when exposed to the atmosphere (5% vs. 2% of weight) than the Graphite felt. Thus, GH grade Graphite felt was chosen over CH grade Carbon felt. The next step was to compare the Graphite felt with Alumina. In order to compare their insulating properties, first, a second layer of 1" Alumina was added behind the already existing 9" by 7" Alumina insulation on the face of the enclosure around a single heater (described in section 5.3.4). It was found that 115 V was required to attain an enclosure temperature of 1200 C. Next, an inch of Graphite was added instead of the Alumina, and it was found that 115 V supplied to the heaters resulted in an enclosure temperate of only 1086 C. This data pointed to the fact that, at 1200 C, Alumina has better insulating properties than Graphite.

Another important criterion was the moisture absorptivity of Alumina vs. Graphite. In order to compare the two, the idea was to heat chunks of each type of insulation in a furnace and observe moisture release by monitoring the dew point inside the furnace. A tube furnace, consisting of a Mullite tube and SS heat shields at both ends was used to fire the insulation. SS heat shields were used instead of the standard ceramic heat shields in order to avoid corruption of test data due to moisture release from the ceramic shields. Also, an Argon atmosphere was used in these tests in order to prevent any chemical reaction between the insulation and the process gas.

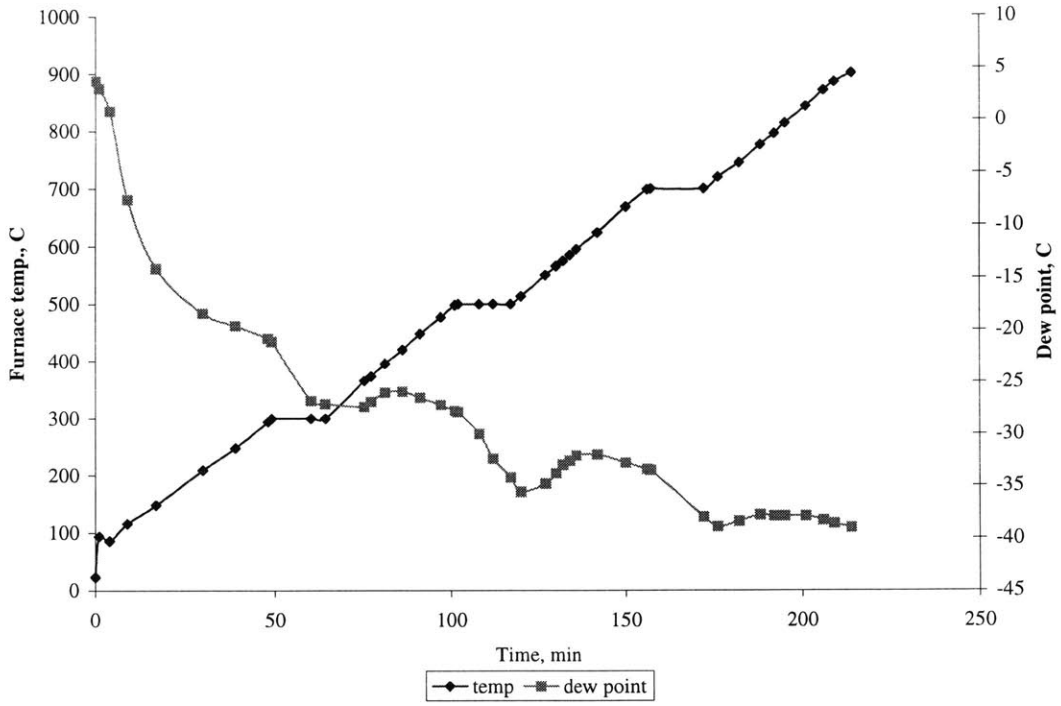

Figure 5.21: Dew point inside the furnace vs. time for a sample of Alumina insulation fired in the tube furnace. Note the humps in dew point when the furnace temp. is 400 and 600 C.

First, the empty tube furnace was heated at 5 C/min to 1200 C and cooled down. Then, the furnace was opened for exactly 5 minutes and a sample of Alumina insulation was placed in it. This 5-minute opening time was used whenever the furnace was opened between runs in order to ensure that the same amount of moisture diffused into the furnace from the atmosphere each time it was opened. Also, all the runs were done in a 24-hour period to minimize the effect of changes in ambient humidity conditions on the outcome of the runs. The furnace was then ramped up at 5 C/min and held for 15 minutes each at 300 C, 500 C, 700 C and 900 C before ramping down to room temperature. The hold at various temperatures was done to ensure that all the moisture that could be expelled at the given temperature was expelled before the ramp continued. Figure 5.21 shows the dew point as a function of time with Alumina inside the furnace. After this run, the furnace was again opened for 5 minutes and the Alumina was taken out. Next, as a control run, the empty furnace was subjected to the same cycle. Figure 5.22 shows the dew point curve for the empty furnace. The next run was done with the same volume of Graphite insulation as Alumina used in the first run. Figure 5.23 shows the dew point curve for the run with Graphite.

It can be seen from figure 5.22 that for the run with the empty furnace, the dew point keeps falling with time. However, in the run with the Alumina insulation (figure 5.21), humps corresponding to moisture release can be noticed, with peaks in dew point at furnace temperatures of around 400 C and 600 C. In the case of Graphite (figure 5.23), no such humps are seen. Moreover, the average dew point level is much lower than in the case with the Alumina insulation. These tests established that Graphite absorbed less moisture than Alumina.

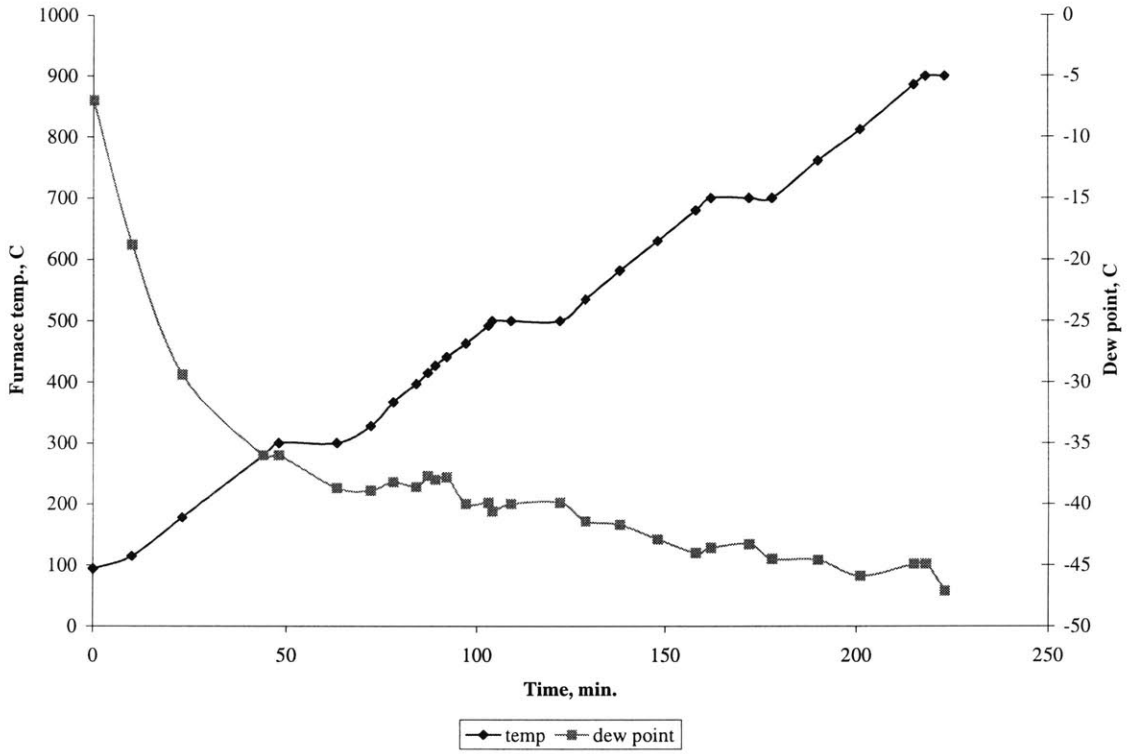

Figure 5.22: Dew pt. vs. time for the empty furnace. This is a control run. Note the absence of humps in dew point unlike in Figure 5.21.

It was decided to use Graphite for the extra insulation despite the fact that Graphite was a poorer insulator than Alumina. This was because of the fact that it absorbed lesser moisture than Alumina when exposed to the atmosphere. Before Graphite was used, though, another issue needed to be investigated. The heaters used in the furnace need to be fired in air at 1200 C for a few hours the first time they are used. Thus, if Graphite insulation were to be used behind the (already existing) 1" of Alumina insulation, then oxidation could be an issue. The plan was to use ¼" of Graphite insulation behind the 1" of Alumina insulation. Thus, if the furnace were at 1200 C and the shell were at 200 C, assuming roughly similar conductivities for Graphite and Alumina, the temperature of the Graphite-Alumina interface would be 400 C. A chunk of

Graphite insulation kept in an oven at 500 C for 5 hours showed less than 0.2% weight loss, while a similar piece

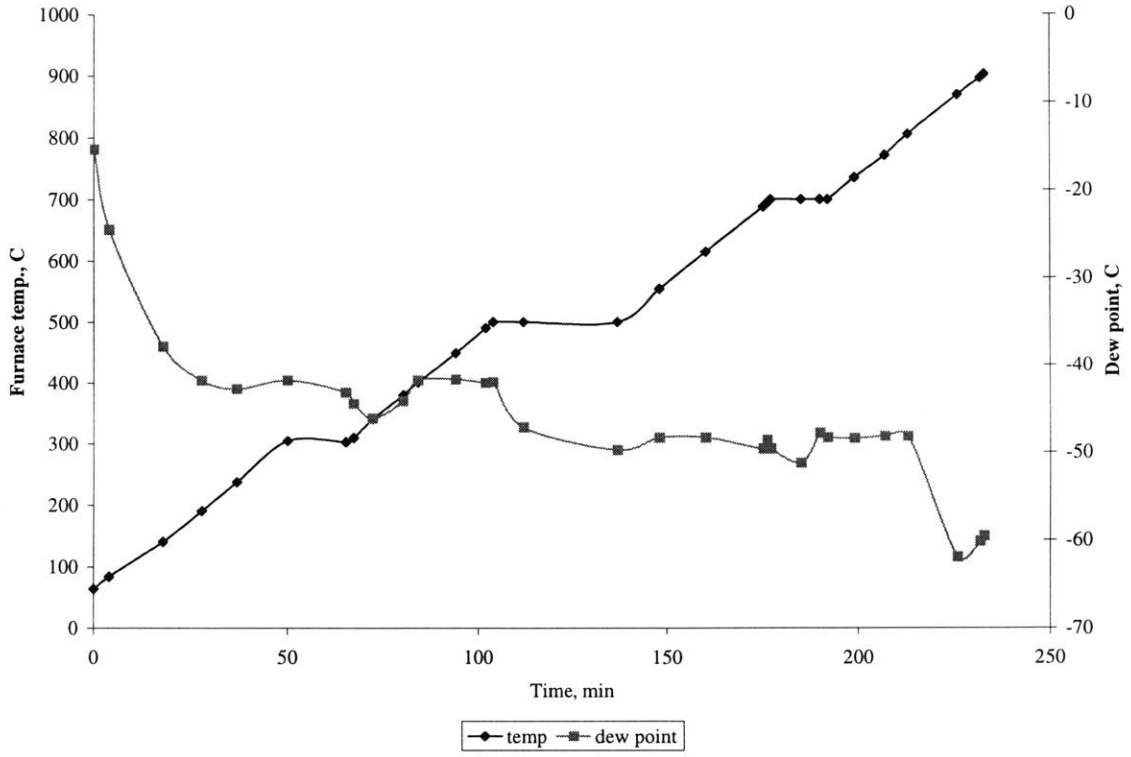

Figure 5.23: Dew pt. vs. time for a run with Graphite inside the furnace. Note that the average dew point level is far less than that for Alumina (Figure 5.21). Also, humps in dew point are not as prominent as in Figure 5.21.

kept at 600 C for 5 hours lost 18% weight. Thus, being exposed to 400C in air during heater burn in would do no harm to the Graphite.

Thus, a decision was made to use ¼" of Graphite insulation behind the 1" of Alumina insulation on all faces of the furnace. To facilitate ease of mounting, the two pieces of insulation were sown together before mounting. On the sidewalls, in order to avoid shorting, 1.5" holes were cut out of the Graphite insulation at the locations where electrical leads passed through the walls. Figure 5.24 shows a picture of the Graphite and Alumina insulation on the front door. In case there is a leak between the insulation on the front door and the Nextel sleeved insulation on the furnace front face, hot gases from inside the furnace can reach the door and damage it. In order to prevent this from happening, ¼" thick Graphite insulation which is larger than the Alumina insulation has been mounted on the door (Figure 5.24). This Graphite also serves as a

gettering agent and removes moisture from the furnace by reacting with it (See Chapter 2 for an explanation of gettering action.)

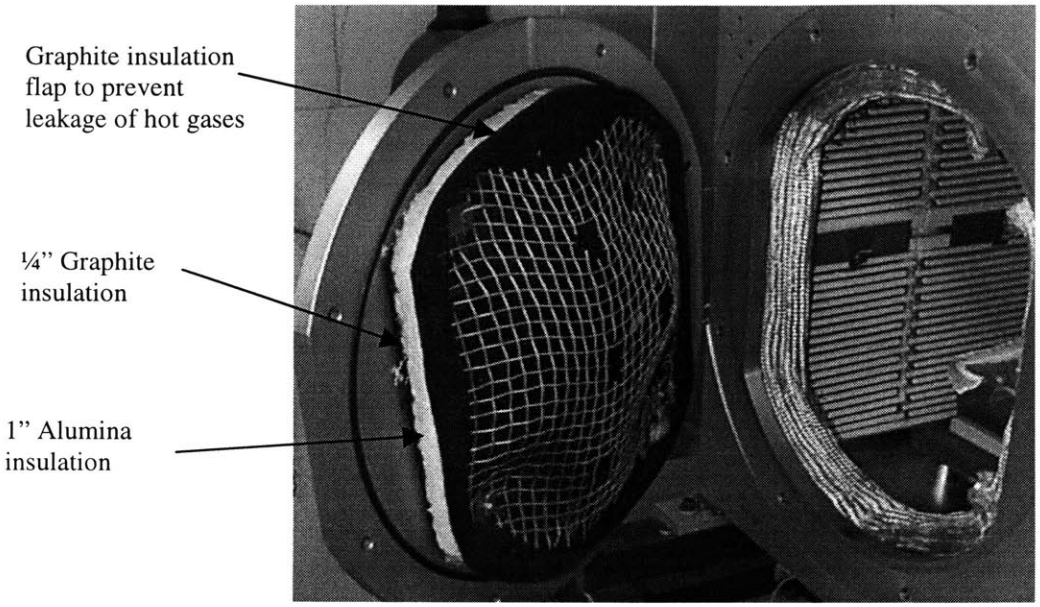

Figure 5.24: Picture showing the ¼" Graphite insulation that goes behind the 1" Alumina insulation. Also seen in front of the Alumina insulation on the door is a second layer of ¼" Graphite insulation, whose purpose is to prevent any leaking hot gas from reaching the Aluminum shell and to act as a gettering agent.

5.4. Summary

This chapter looks at the thermal design of the furnace, which involved estimating the power requirement of the large scale furnace. In addition, mechanical design of the furnace shell and some of the features on it are described. Various experiments conducted on insulation that went into the furnace are also presented. The next chapter describes the electrical, gas and safety systems of the furnace.

6 Electrical, Gas and Safety Systems

This chapter describes the electrical, gas and safety systems of the furnace. Equipment such as controllers, relays, solenoids and alarms used with the furnace were salvaged from the C.I. Hayes furnace that was talked about in Chapter 1.

6.1 Electrical systems

The large scale furnace runs in closed loop mode and has a controller that compares the desired set point with the process variable (furnace temperature), and accordingly adjusts the power supplied to the internal heaters through SCRs. The furnace controller has events that, through relays can be used to control solenoids, external heaters, internal heaters etc. In addition, the furnace has an over temperature alarm, pressure switches and a low gas flow alarm. The following sub sections describe the electrical features of the furnace. Figure 6.1 shows the convention used to represent wiring in all wiring diagrams. Most of the wires used in the furnace were salvaged form the wiring of the C I Hayes furnace that was talked about in Chapter 1. For the sake of convenience, most wire numbers (examples: 141-3, I:001 etc.) have been retained from the Hayes wiring.

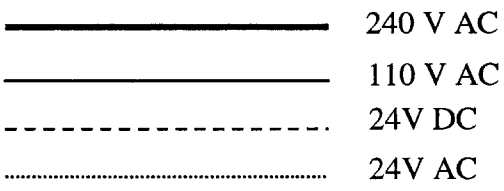

Figure 6.1: Convention used for representing wires in all wiring diagrams in this chapter.

6.1.1 Power supply

The furnace obtains its power from a 240 V AC wall power source capable of providing a maximum of 80 A. There is a manually operated safety switch on the wall that separates the furnace from the power supply. The external and the internal heaters run off this 240 V AC power supply. The furnace controls, on the other hand, operate off of 120 V AC. A transformer is used to step down the 240 V supply voltage to the 120 V required to operate the controls. The

right half of Figure 6.2 shows the wiring scheme from the transformer to the 120 V AC bus. Turning manually operated switch 157 SS operates two switches, physically located one behind the other, both of which are spring loaded 3 position switches that operate in tandem (The front switch is denoted by 157SS-F and the rear switch by 157SS-R.). To turn control power on, switch 157SS is turned to the "on" position momentarily, after which it returns to the middle position due to spring action. This causes wire 141-3 to be connected to 157-2 via 157-1. This energizes relay 157CR, which connects 141-3 to 157-1 (terminals 1 and 3). Since 157-1 coming out of terminal 3 of relay 157CR is connected back to switch 157SS-R, and since the middle and "on" terminals of switch 157SS-R are connected together, relay 157CR remains energized even when switch 157CR returns to its middle position. To turn power off, switch 157SS is turned to the "off" position. This causes switch 157SS-R to turn to the off position, cutting off power to 157-2. This de-energizes the relay, cutting off power to the furnace controls.

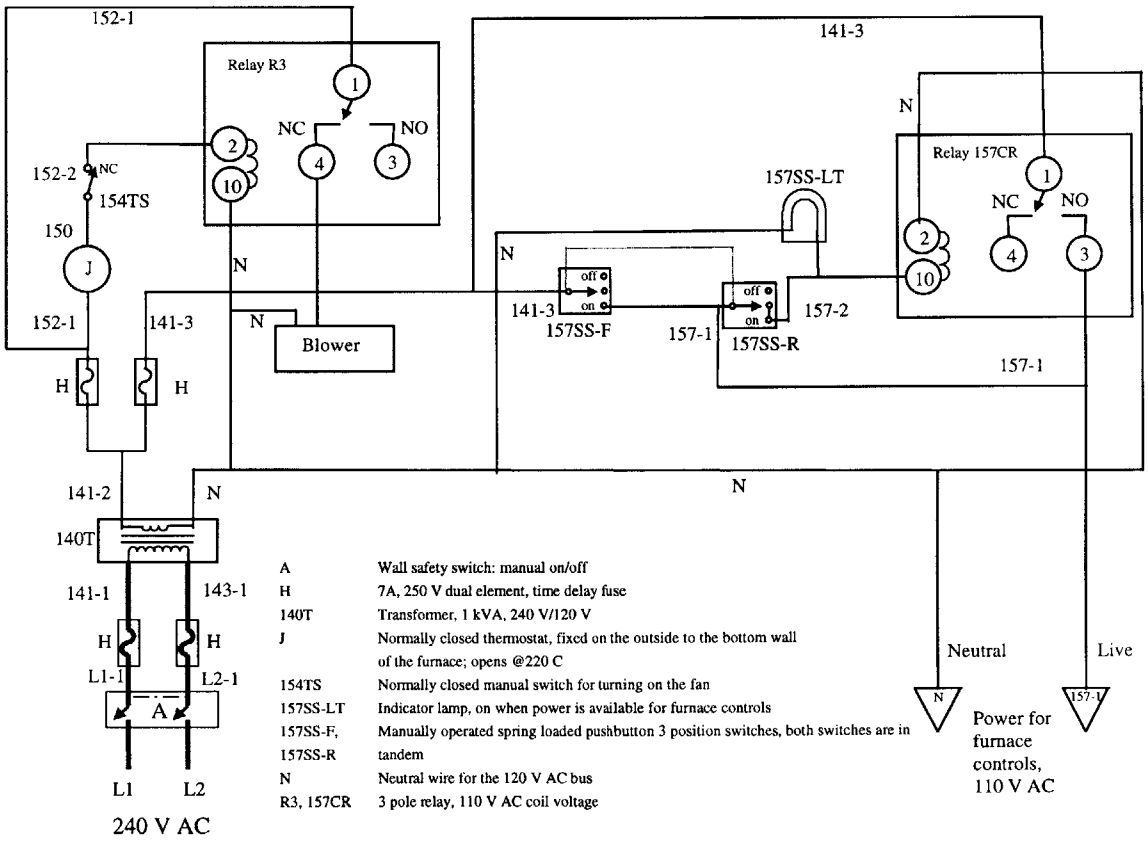

Figure 6.2: Schematic showing wiring from the 240 V AC source to the 120 V AC bus used to power the controls of the furnace. Also shown in the figure is the wiring of the blower that shall be discussed in section 6.1.5.

The furnace also has a 24 V DC power supply that is powered by the 120 V AC bus. Figure 6.3 shows the wiring scheme of the 24 V DC source. The 24 V DC signal is required to trigger events from the furnace controller (a Honeywell DCP552 digital control programmer). In addition, there are two 240 V AC to 24 V AC transformers, T1 and T2, that provide power to the SCR firing cards. The wiring diagram for these is shown in Figure 6.4.

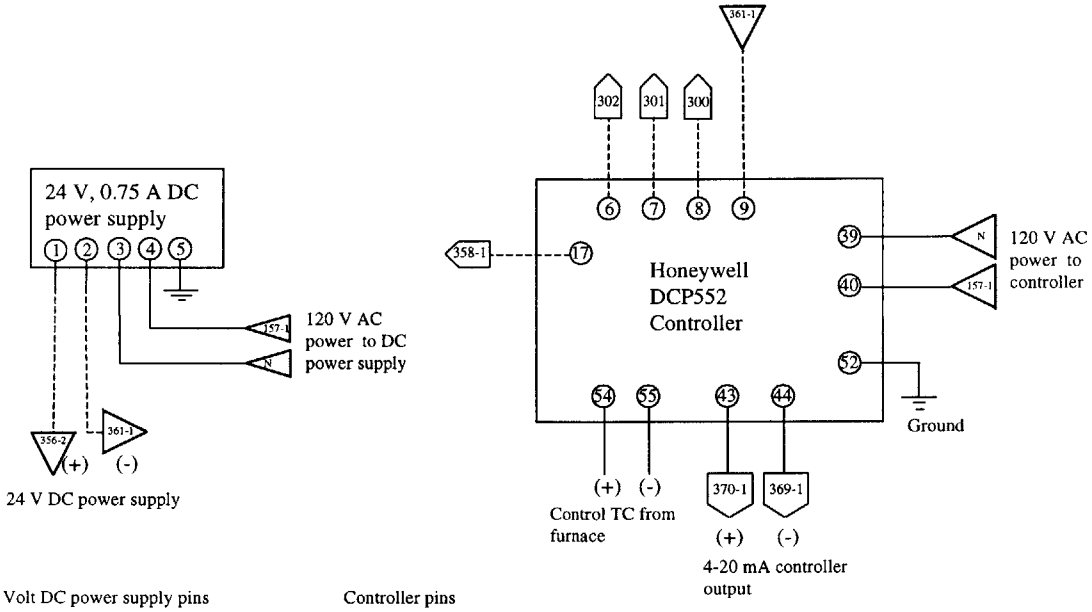

24 Volt DC power supply pins

1	Positive terminal of 24 V DC
2	Negative terminal of 24 V DC
3,4	120 V AC power supply for unit
5	Ground

Controller pins

6	Event 2 output
7	Event 3 output
8	Event 4 output
9	Connected to -ve terminal of 24 VDC power supply
17	Event 5 output
39, 40	120 V AC power supply for unit
43,44	Controller channel 1 output, 4-20 mA
52	Ground
54,55	Furnace control thermocouple

Figure 6.3: Figure showing wiring of the 24 V DC power supply (on the left). Also shown in the figure on the right is a schematic of the controller pins, to be discussed later.

6.1.2 Wiring scheme for external heaters

As explained in the previous section, the 240 V AC wall power source is capable of providing a maximum of 80 A. As stated in Chapter 5, the external heaters are each rated to supply 1 kW @240 V AC. Thus, the total current drawn when all eleven are running is 46.2 A. There are twelve internal heaters, each rated at 850 W, 120 V AC. These are connected in pairs in series across 240 V AC. Thus, the total maximum current drawn by all the internal heaters is 42.5 A. If both the internal heaters and the external heaters were to run simultaneously, then the

maximum current drawn by all the heaters would be 46.2+ 42.5= 87.7 A, which exceeds the 80 A that the wall can supply. In order to overcome this problem, it was decided to adopt the following scheme. At the beginning of a furnace run, all eleven external heaters would be turned

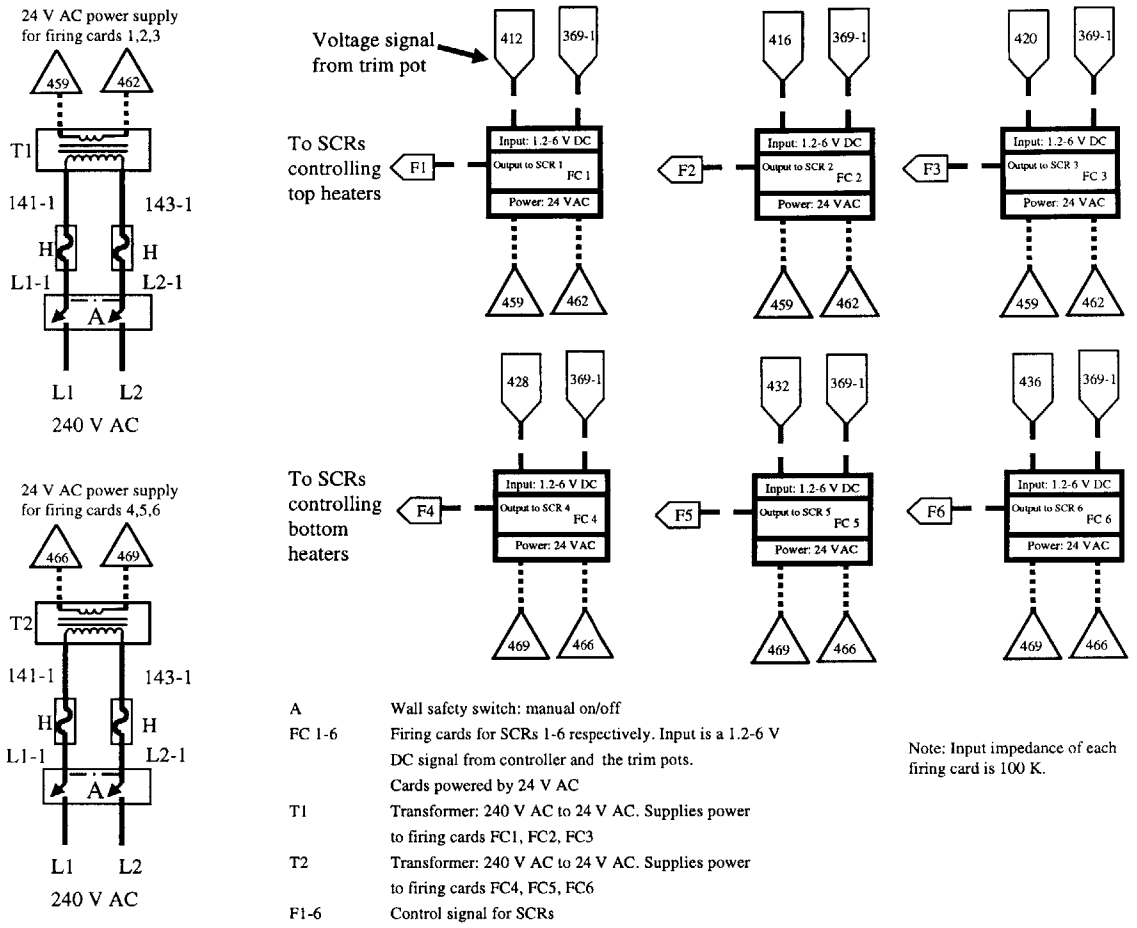

Figure 6.4: Wiring diagram for the 24 V AC power supplies that are used to power the SCR firing cards, whose wiring schematic is shown on the right. The firing cards are physically mounted on to the SCRs.

on and the furnace wall would be maintained at 200 C until the dew point inside the furnace dropped to around –15 C (the internal heaters would remain off during this stage). At this point, six of the external heaters would be turned off and the internal heaters would be turned on. The internal heaters would maintain the inside of the furnace at 200 C until the dew point dropped to –25 C at which point the ramp to 1200 C would start. Under this scheme, the maximum current that can be drawn is 45.2 A (for the internal heaters) + 21 A (for the 5 external heaters), a total of 66.2 A, which is well below the maximum of 80 A.

Thus, it was decided to divide the eleven external heaters into two banks, each one controlled separately by its own relay. As seen when facing the furnace front door, Bank 1 consists of the right heater on the top face, top heater on the left face, left heater on the bottom face, bottom heater on the right face and the top heater on the back face. Bank 2 consists of the remaining heaters, including the single heater on the door. The staggering of heaters between the two banks was done in order to ensure temperature uniformity of the shell even when only one bank was turned on and the other was turned off. When carrying out a furnace run, the idea was to switch off bank 2 of the external heaters when the dew point reached –25 C, and turn the internal heaters on right after that.

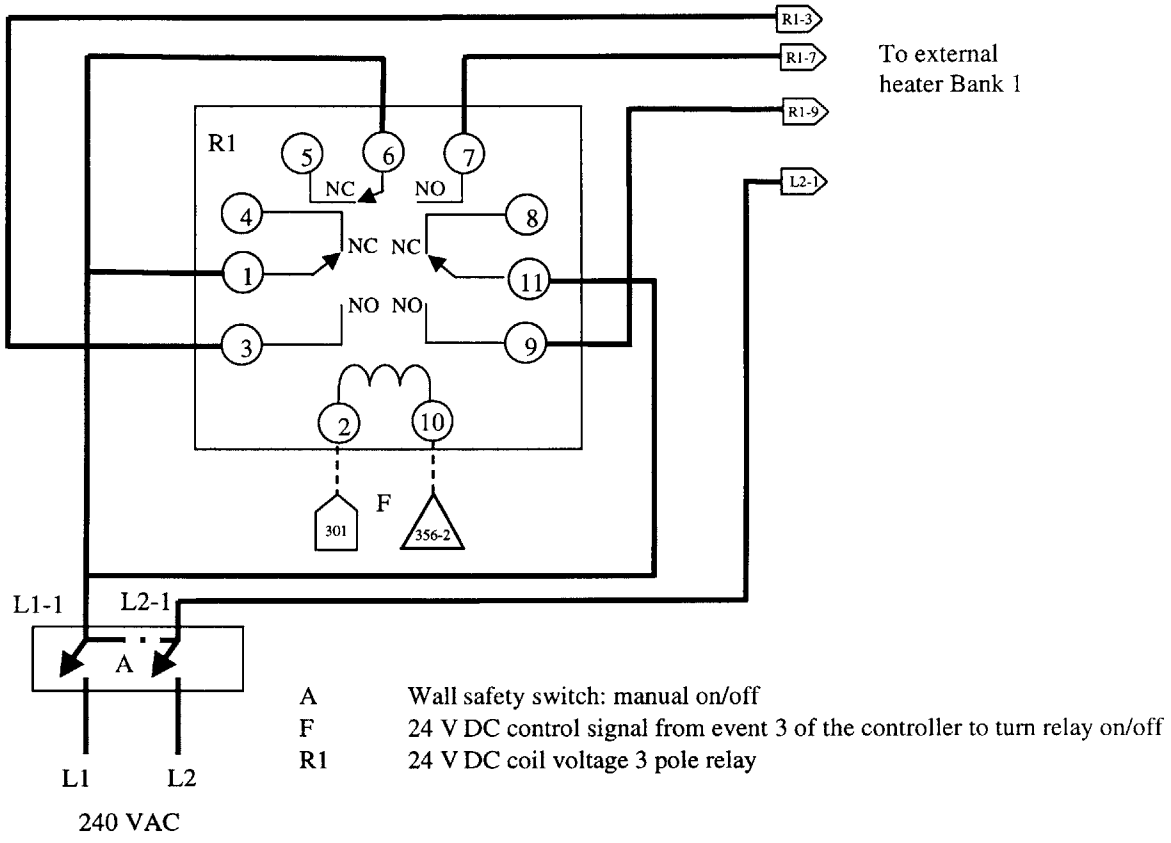

Figure 6.5: Wiring diagram for relay R1 that turns bank 1 of external heaters on/off. Also see Figure 6.7.

Figure 6.5, Figure 6.6 and Figure 6.7 show a schematic of the wiring of the external heaters. Heaters of Bank 1 are hooked to the 240 V AC power supply through relay R1, while those of Bank 2 are hooked to the power supply through relay R2. The closing and opening of relays R1 and R2 is controlled by 24 V DC signals from events 3 and 4 respectively of the controller. To understand the working of the external heaters, consider external heaters 1 and 2,

labeled EH1 and EH 2 in Figure 6.7. When event 3 of the controller is active during a segment of a furnace run, the voltage across terminals 2 and 10 of relay R1 (Figure 6.5) is 24 V DC. This energizes relay R1, closing the switch between terminals 1 and 3. If the thermostats T1 and T2 (Figure 6.7) are closed (which will be the case if the shell is cooler than 200 C), contact between terminals 1 and 3 causes power to be supplied to heaters EH1 and EH2.

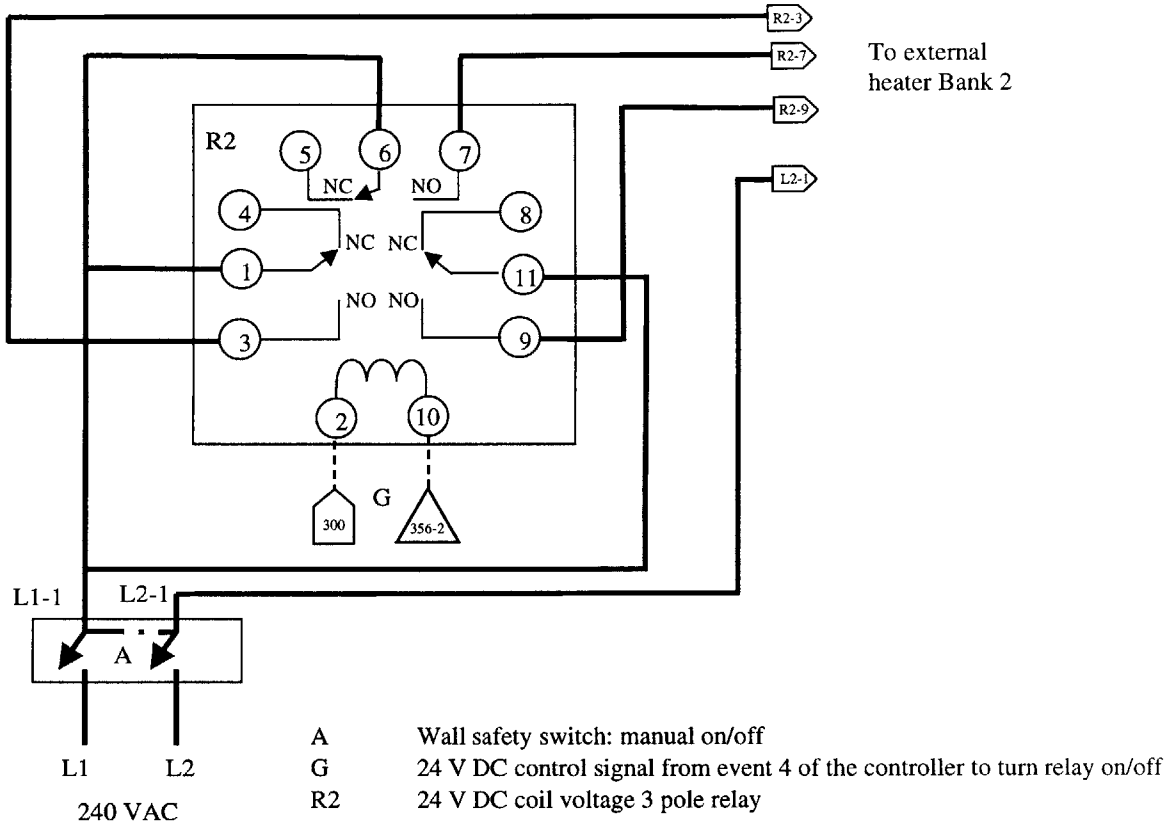

Figure 6.6: Wiring diagram for relay R2 that turns bank 2 of external heaters on/off. Also see Figure 6.7.

6.1.3 Controller

The controller that is used to control the furnace cycle is a Honeywell DCP 552 that is powered by the 120 V AC bus of the furnace (see list of vendors in Appendix 1 for details on the controller). The controller has two independent channels, each of which is capable of accepting its own input signal from its thermocouple and putting out a 4-20 mA output. Thus, in theory, channel 1 of the controller could be used to control the top internal heaters of the furnace while channel 2 could be used to control the bottom internal heaters. This would make it easy to turn off one zone while keeping the other one on for doing directional solidification. However, two

channels were not used to control the two heater zones, and only one channel was used instead. Details on why the two channel scheme was not used are given in Chapter 7 on furnace testing.

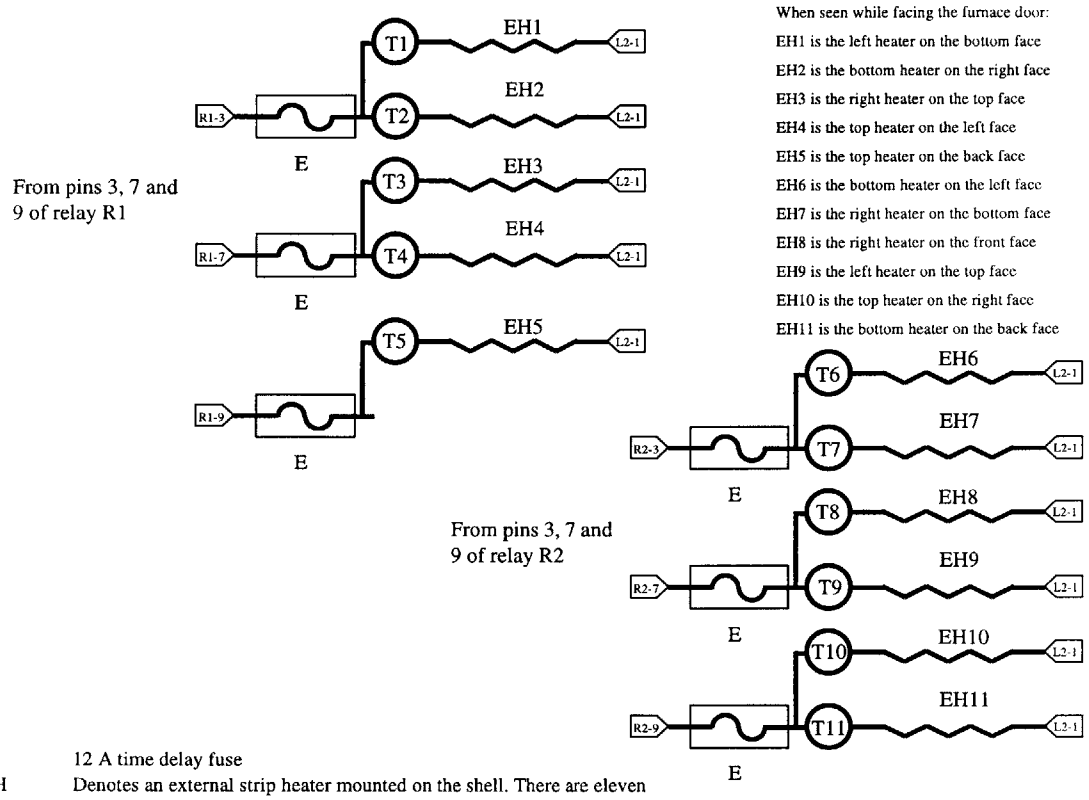

E 12 A time delay fuse

EH Denotes an external strip heater mounted on the shell. There are eleven such heaters, EH 1-11. Each has a power rating of 1 kW @240 V AC

T 1-11 Denotes a normally closed ceramic thermostat mounted on the furnace shell near each external heater. The thermostat opens at 200 C

Figure 6.7: Wiring diagram for the eleven external heaters. Also see Figure 6.5 and Figure 6.6.

Section 6.1.4 gives details on how the top and bottom heater zones have been wired to be controlled by the output of channel 1 of the controller. Figure 6.3 shows a pin diagram of the controller. The controller's 4-20 mA channel 1 output is between pins 43 and 44.

The controller has sixteen events, each of which can be triggered during any segment of a furnace cycle. These events can be time based or process variable (furnace temperature) based. Of the 16 events, only 15 events, event #'s 2 to 16 are functional. Event 1 is damaged. Four controller events have been set up for use with the furnace. Event 2 (pin 6) turns the flow of purging gas (Argon) into the furnace off (on) and simultaneously turns the flow of Forming gas on (off). Events 3 and 4 (pins 7 and 8 respectively) are used to turn banks 1 and 2 of external heaters respectively on/off. Event 5 (pin 17) is used to turn the top internal heaters off for

directional solidification. Details of various circuits controlled by the controller events are presented in later sections.

In addition to the process controller, the furnace also has a Honeywell UDC 2000 limit controller which is used as an over temperature alarm. Details of the overtemp. circuit are given in section 6.3 on safety systems.

6.1.4 Internal heaters

As mentioned in section 6.1.2, the furnace has 12 internal heaters, each rated to deliver 850 W @ 120 V AC. Figure 6.8 shows a schematic of the heater hook up. When seen facing the front of the furnace, heater plates facing each other are connected in series. The heaters can be divided into two zones: a top zone consisting of heaters 1, 2, 3, 4, 5 and 6 and a bottom zone consisting of heaters 7, 8, 9, 10, 11 and 12. In the top zone, heaters 1 and 2 are controlled by SCR1, 3 and 4 by SCR2, 5 and 6 by SCR3. In the bottom zone, heaters 7 and 8 are controlled by SCR4, 9 and 10 by SCR5 and 11 and 12 by SCR6 (Figure 6.9).

Figure 6.10 shows a schematic of the wiring that goes into the SCR inputs. As can be seen in the figure, between the 240 V AC wall power supply and the wires going into the SCRs, there is a manual safety switch followed by a contactor, which is turned on by a 120 V AC control signal. The contactor turns on only when there is sufficient pressure in the purge and process gas tanks, the flow rate of gas through the furnace is above a preset minimum level, the furnace temperature is not above the limit set in the overtemp. controller and a manual switch is on. Details of this set up are given in section 6.3 on safety systems.

The SCRs control the power going into the internal heaters according to the control signal they receive from their firing cards (Figure 6.9). A firing card sends an output (0-100%) to its SCR according to the voltage input (1.2-6 V DC) it receives (Figure 6.4). Since the output of the controller is a 4-20 mA current, it needs to be converted into a voltage that can be fed into a firing card. Another requirement is to be able to control the power put out by heater pairs in the front, middle and rear sections (both top and bottom) of the furnace independently. Since there is greater heat loss from the furnace from near the front and rear walls as compared to the middle

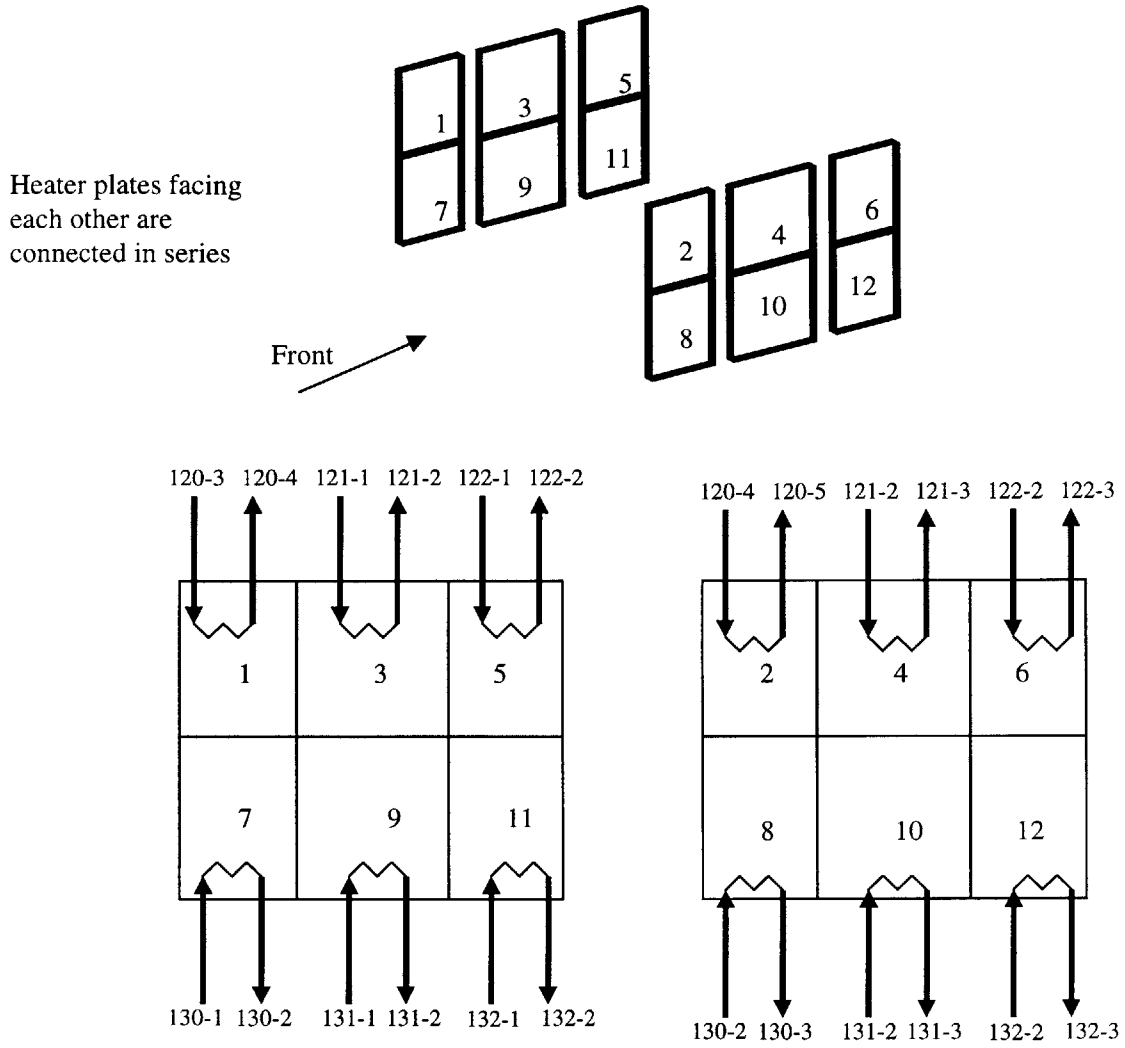

Figure 6.8: Schematic showing relative positions of the internal heater plates and power connections to each plate. See Figure 6.9 for details on how the heaters are hooked to the SCRs.

section, the temperature profile inside the furnace may be non uniform. Hence the ability to control power going into heaters in different zones independently can be used to adjust the temperature profile to be as uniform as possible.

Figure 6.11 illustrates the scheme used to independently vary the control signal going into the SCRs. The figure shows a resistor, R, put across the output of the controller in order to convert the 4-20 mA signal into a 1.2-6 V signal. The calculation of R shall be explained in detail later. The resulting voltage signal is fed directly into three 10 K potentiometers, whose output goes to the firing cards of the SCRs hooked to the bottom heaters. The voltage signal from

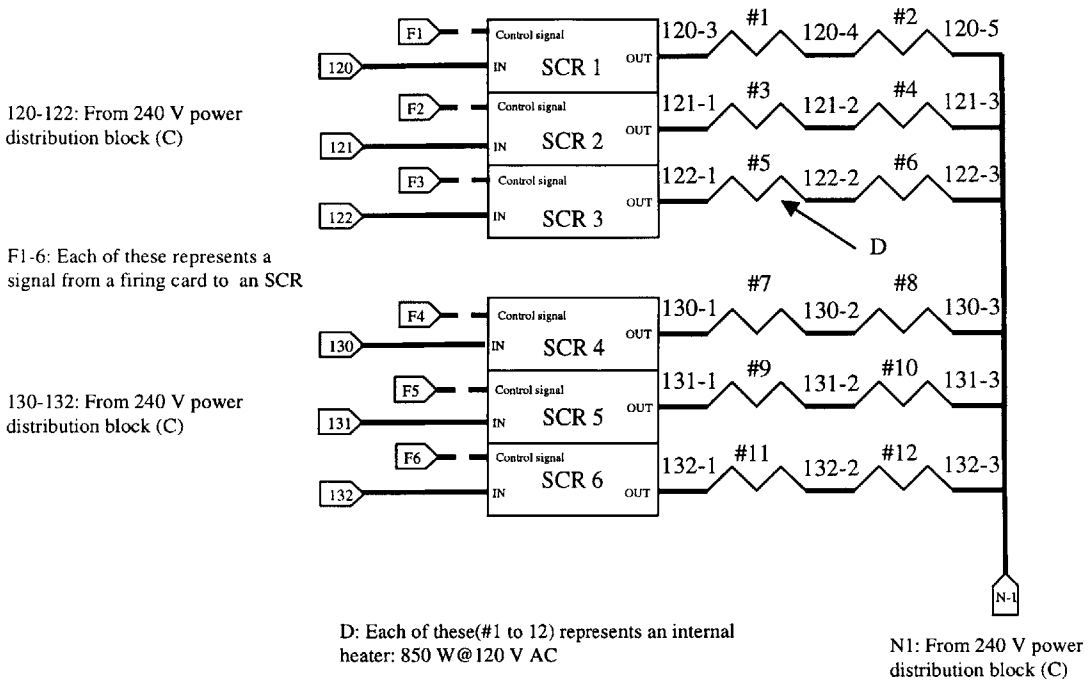

Figure 6.9: Schematic of wiring between the SCRs and the heaters. Also seen in the figure are the control signals to the SCRs. See Figure 6.10 for schematic of wiring from 240 V AC supply to SCRs.

the output of the controller is also fed through a relay into three additional potentiometers whose output goes to the firing cards of the SCRs hooked to the top heaters. This relay, 358CR (seen in the figure) is controlled by event 5 of the controller and can be used to cut off the control signal to the top heaters, if necessary. This feature can be used to perform directional solidification by turning off the top heaters at the end of an infiltration cycle.

The value of R was estimated by considering effect of loading due to the six 10 K potentiometers, and the six firing cards, each having an input impedance of 100 K. Figure 6.12 shows a schematic of all the resistances in parallel with R across the output of the controller. Since the potentiometer resistances in series with the firing cards will be close to 10 K even after they have been adjusted to get a uniform temperature profile inside the furnace, the equivalent resistance of each pot.-firing card combination is 10K ||100K =9.09K. Since there are six such pairs in parallel, their equivalent resistance is 9.09/6=1.515K. This, in || with R should give 300 ohm such that a 4-20 mA current output from the controller corresponds to 1.2-6 V across R. Solving 1.515 K||R=0.3 K gives R= 374 ohm. However, a 374 ohm resistor across the output did not exactly give a 1.2-6 V voltage range for a controller output of 4-20 mA. By trial and error, the right value of R was found to be 379 ohm.

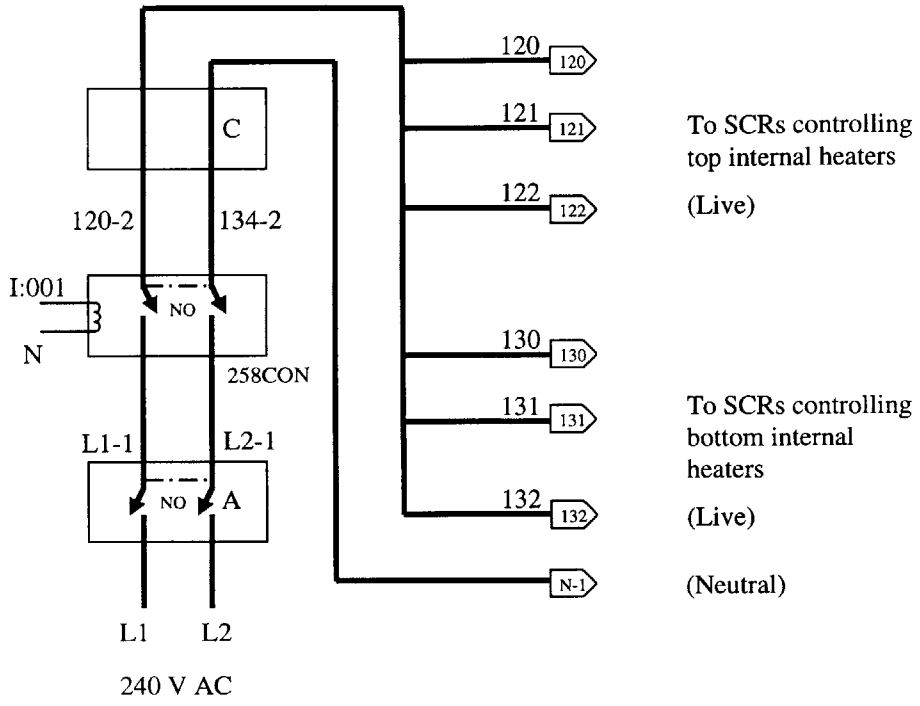

A Wall safety switch: manual on/off
258CON Contactor: Turns on/off by 120 V AC control signal, wire I:001
C Power distribution block

Figure 6.10: Wiring from the 240 V AC supply to the SCRs. The contactor is turned on/off by a 120 V AC signal.

6.1.5 Blower

When the furnace reached its steady state operating temperature of 1200 C, it was found that some places on the outside of the bottom face of the shell reached around 260 C. This is bad from a strength point of view (the yield strength of Aluminum 5083 drops from 117 MPa at 200 C to 75 MPa at 260 C). In order to prevent the furnace shell from heating way above the design temperature of 200 C, a blower was installed on the furnace frame below the bottom face of the furnace shell (see list of vendors in Appendix 1 for details). The blower was hooked to the 120 V furnace power supply through a NC ceramic thermostat which opens at 220 C. The left half of Figure 6.2 shows the wiring diagram for the blower. Relay R3 was needed since the thermostat was NC as opposed to being NO. If blower operation is required even when the shell is cooler than 220 C, manual switch 154TS which is NC, can be flipped open to turn the blower on.

6.1.6 Gas solenoids

Event 2 of the controller is used to open/close gas solenoid valves. When event 2 is on, it energizes relay 356CR, which closes the NO valve on the Argon line while simultaneously opening the NC valve on the Forming gas line (Figure 6.13). Indicator lamp 267LT lights up when the Argon solenoid valve is open, while indicator lamp 261LT lights up when the Forming gas valve is open.

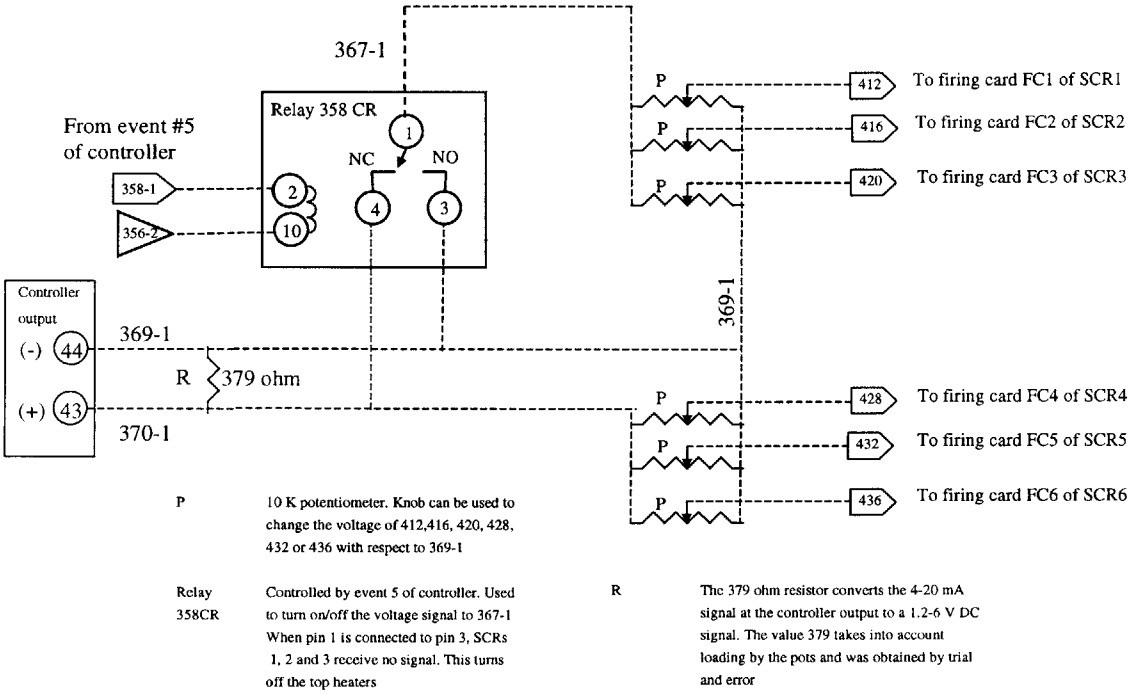

Figure 6.11: Schematic of the wiring of the potentiometers that can be used to trim the voltage signal going to the SCRs. The controller gives a 4-20 mA signal that is converted to a voltage signal using the resistor R.

6.2 Gas systems

The furnace is intended to operate under a Forming gas atmosphere for the most part, especially at higher temperatures (>900 C). However, during the soaking period at 200 C, Argon can be used to purge the furnace of water vapor. Thus, a system capable of dealing with and switching between the two gases was put in place. Figure 6.14 and Figure 6.15 show a schematic of the gas system of the furnace. The pressure regulator being used with the Forming gas tank is set to step the gas pressure down from the tank pressure to around 40 psi. A lot of this pressure drops in the moisture trap, which, due to the presence of numerous desiccant beads in it,

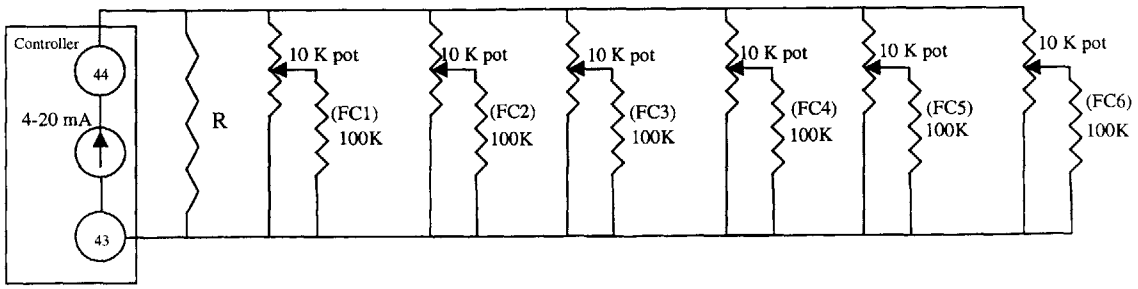

should be equivalent to

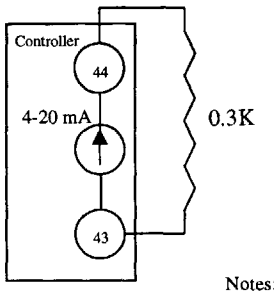

Notes:

1. The controller is assumed to be equivalent to a current source.

2. Each firing card has a 100K input impedance.

3. R in parallel with all the other resistances should be 300 ohm in order to give a 1.2 -6 V output across itself when the controller gives a current output of 4-20 mA.

Figure 6.12: Schematic of all the resistances in parallel with each other as seen from the controller's output terminals 43 and 44. The idea is to determine R that will cause the equivalent resistance across pins 43 and 44 to be 0.3 K.

offers high resistance to gas flow. The low pressure regulator then drops the pressure down to 4 psi. The value 4 psi was chosen since the burst disc that is attached to the furnace is rated to burst at 4.5 psi, and in the event of the furnace outlet getting blocked, pressure buildup inside the furnace would not burst the disc. The low pressure regulator has good flow characteristics and consequently no droop can be observed in the outlet pressure when the flow rate through it is increased from 0 to 13 scfh (~3 volume changes an hour). The Argon gas tank on the other hand has a pressure regulator whose outlet pressure drops by around 1 psi when the flow through it is increased from 0 to 13 scfh. Although this is not too good, it is acceptable.

Both the Argon line and the Forming gas line have NO spring loaded pressure switches that close when the line pressure is >2 psig. These switches are connected in series with other switches that turn the control signal to the contactor for the internal heaters on/off. More details about this are given in section 6.3 on safety systems. The Argon line has a NO solenoid valve on

it and the Forming gas line has a NC solenoid valve on it. As explained in section 6.1.6, the opening and closing of these valves is controlled by event 2 of the controller.

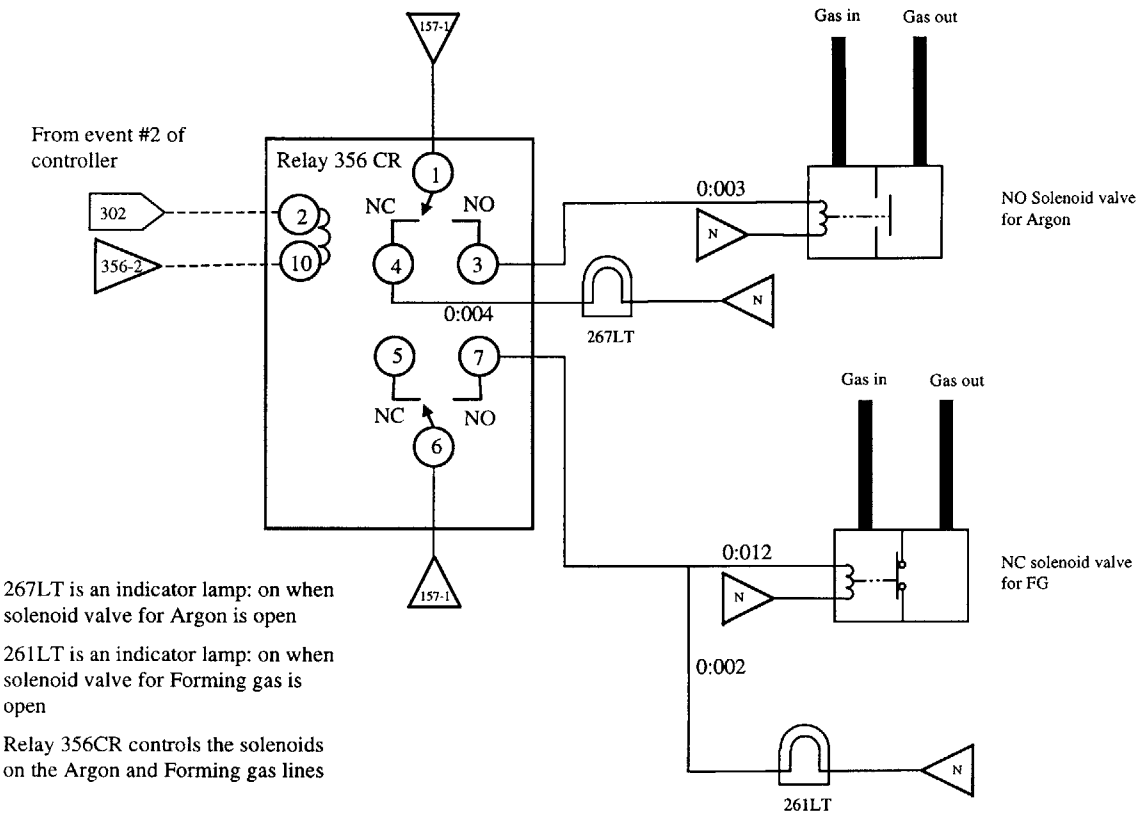

Figure 6.13: Wiring diagram for relay 356CR which is used to close (open) the NO Argon solenoid while simultaneously opening (closing) the NC Forming gas solenoid.

The idea is to be able to automate events such as switching from Argon to Forming gas after the purge phase of the furnace run and switching from Forming gas to Argon before the melting point of the infiltrant (to avoid dissolution of Hydrogen in the infiltrant melt) to occur through a furnace program. The wiring of the solenoid valves in Figure 6.13 ensures that both Argon and Forming gas can never be turned on simultaneously. If this were to happen, excess flow would occur through the flow meter (range of operation: 0-30 scfh) and damage it.

The two needle valves seen in Figure 6.14 can be preset at different openings so as to pass different flow rates of gas through each (flow rate of Argon, which is used for purging, will typically be lesser than that of Forming gas used during the rest of the process). The idea of having check valves after the pressure regulators is to prevent one gas from filling up the tank of the other in case the solenoid valves fail.

Figure 6.15 shows the gas line coming out of the furnace shell. Positive pressure (~ 4-5" of water) is maintained inside the furnace using the modified flow meter shown in the figure. The device is a flow meter with no needle valve. The weight of the float inside the flow meter was changed (by changing the material of the float), until the weight was such that a furnace

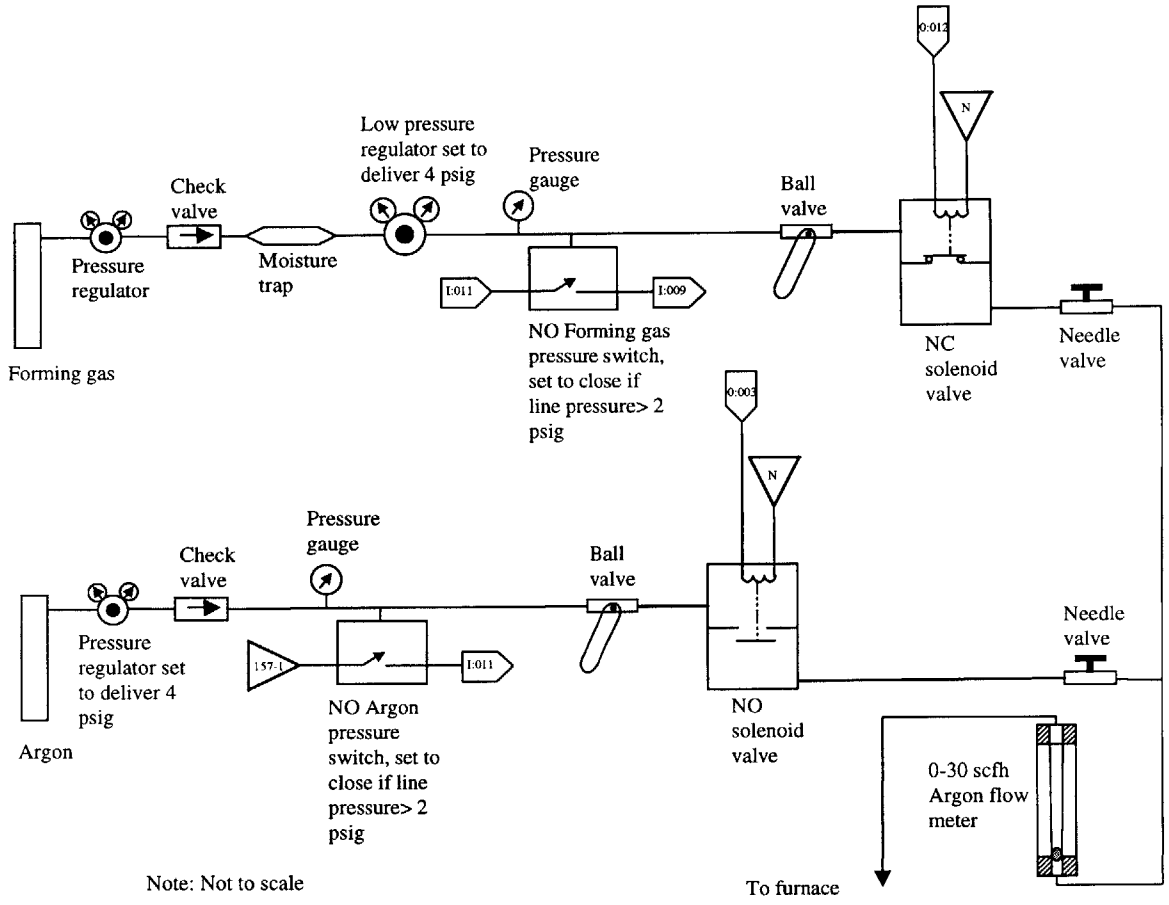

Figure 6.14: Schematic of the gas system used in the furnace. There are two possible atmospheres the furnace has been set up to run in: Argon and Forming gas.

pressure of around 4" of water was developed with 13 scfh flowing through the furnace. The advantage of this set up over using a needle valve is that there is a lower chance of the outlet getting clogged, as the float floats high above the gas inlet of the modified flow meter. Also, since the flow meter is transparent, a quick indication of normal flow through the furnace can be obtained by just looking to see if the float is floating in the tube.

There is a dew point sensor on the line after the modified flow meter. This is followed by tubing to an exhaust vent. This tubing is long enough (>1m) to prevent diffusion of air from the atmosphere from affecting dew point readings.

6.3 Safety systems

The idea behind the safety systems is to protect the furnace and the parts being processed in it in the event of things going wrong. As a first step, the furnace shell has an overpressure burst disc, is grounded and has fuses at appropriate places. The furnace has been provided with a

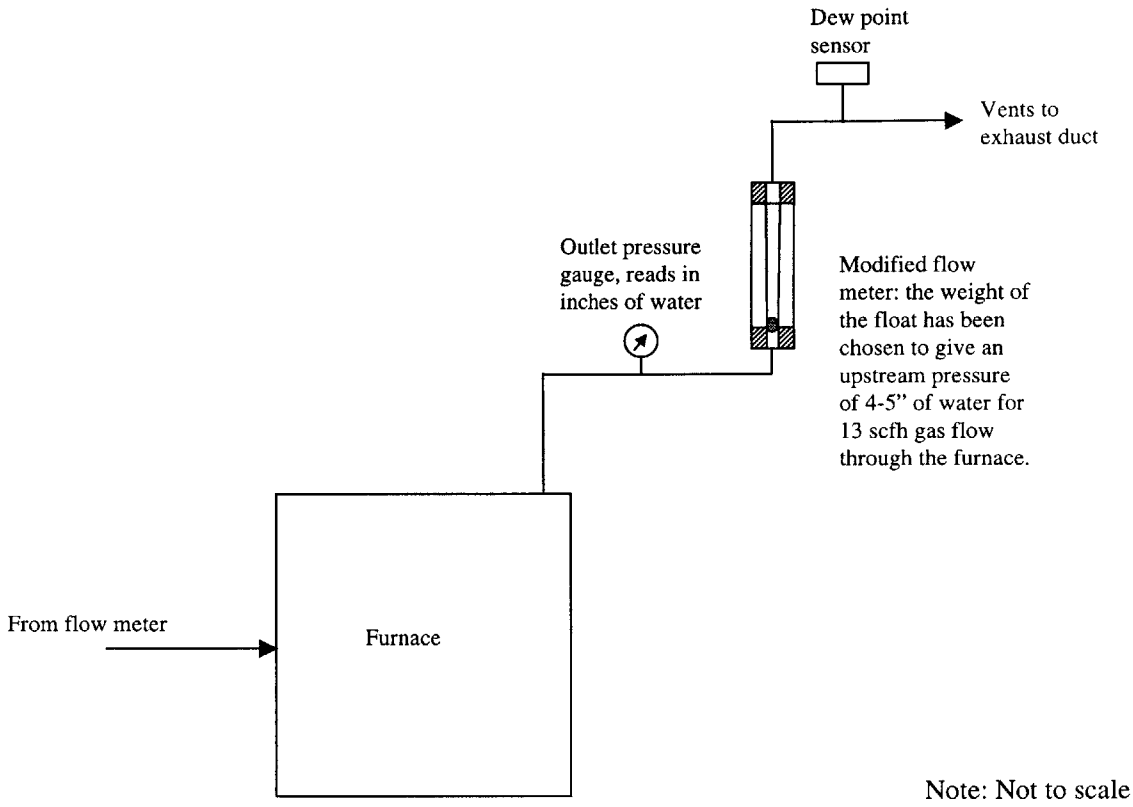

Figure 6.15: Schematic of the gas flow line from the furnace outlet to the exhaust duct.

Honeywell overtemp. controller (details in list of vendors in Appendix 1) which is set to cut off power to the internal heaters (and thus prevent a furnace meltdown) if the temperature inside the furnace exceeds 1250 C. This overtemp. controller gets its temperature input from an over temperature thermocouple mounted into the furnace through a fitting on the rear wall. The furnace also has a thermocouple that measures the temperature of the bottom heater zone, and displays it on Channel 2 of the furnace controller. Thus, the furnace has three thermocouples in all, including the control thermocouple that is connected to channel 1 of the controller. The Argon and Forming gas lines have been provided with pressure switches that cut off power to the internal heaters if the pressure in either line goes below 2 psi (Figure 6.14). In addition to this, the furnace has a low flow alarm that cuts off power to the internal heaters if the flow of gas

through the furnace is below a set limit. These features ensure that the furnace will never run without gas, and thus protect the quality of the parts being processed in the furnace.

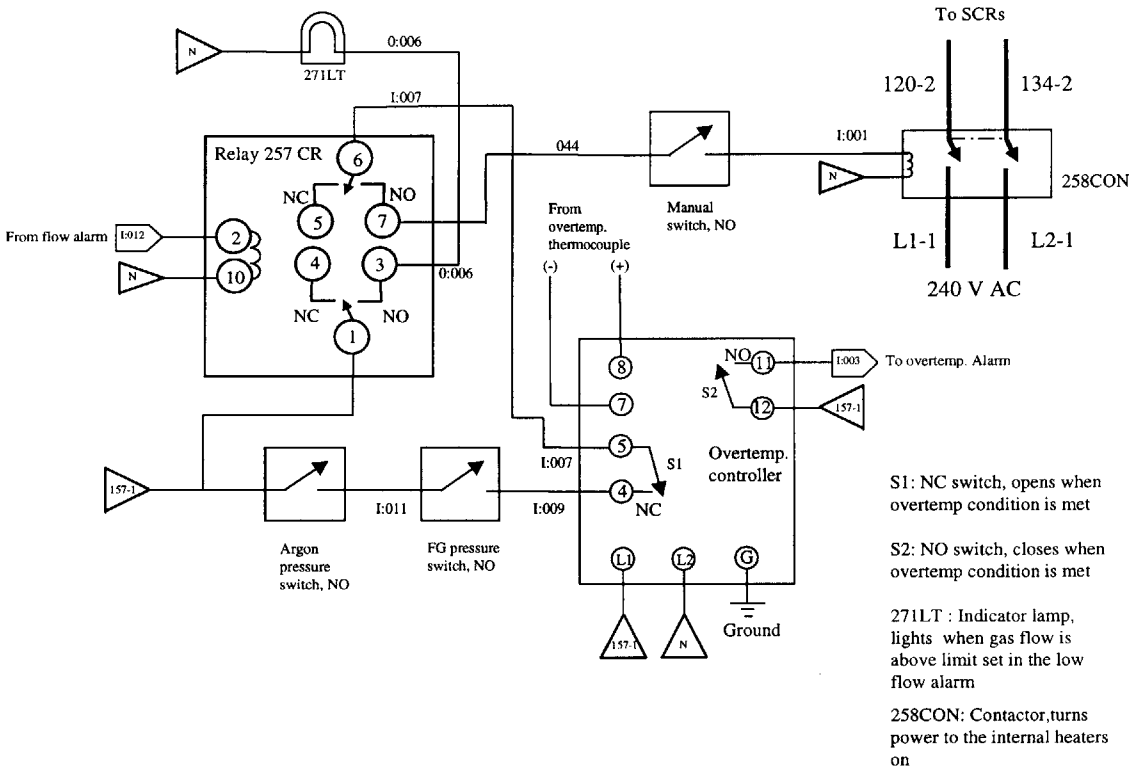

Figure 6.16: Schematic of the wiring of safety switches in series. The switches carry the 120 V AC control signal to the contactor, 258CON, that turns on power to the internal heaters.

Figure 6.16 shows a schematic of the safety switches wired in series. They carry the 120 V AC signal from 157-1 to I:001 that turns the contactor (258CON) for the internal heaters on. The flow alarm circuit board's terminals are shown in Figure 6.17. The flow alarm sensor body is mounted on to the flow meter, and the circuit board is mounted on the furnace frame. Switch S2 of the overtemp. controller is NO and is hooked to a buzzer. The wiring for the buzzer is shown in Figure 6.18. When the overtemp. condition is met, I:003 gets live and energizes relay 279CR. This connects wire 157-1 to 190-1, which being connected to 190-2, activates the buzzer. 194PB is a spring loaded pushbutton switch (NO) that is used to silence the alarm buzzer. Pushing it causes a momentary contact between 194-1 and 190-1. This energizes relay 194CR, which cuts off contacts 1 and 4, silencing the alarm. Lamp 194PBLT remains on as long as the overtemp. alarm condition is on.

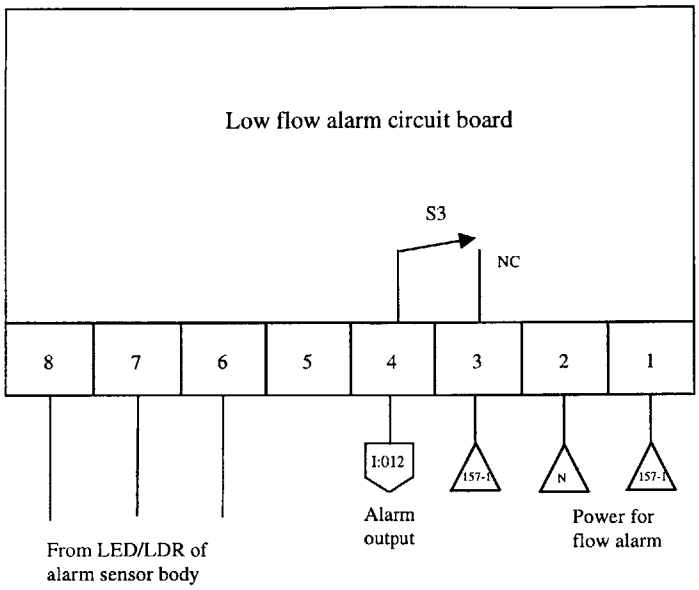

Figure 6.17: Schematic of the flow alarm's pins. Switch S3 is normally closed. The flow alarm sensor body is mounted on the flow meter, while the circuit board is mounted on the furnace frame.

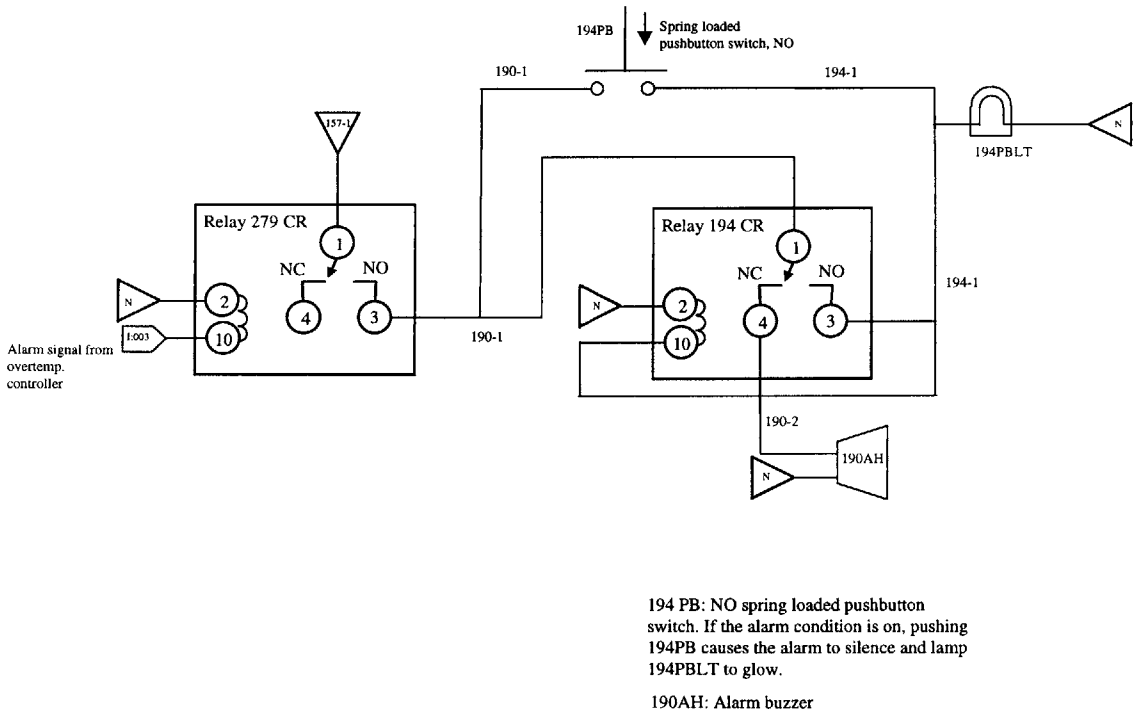

Figure 6.18: Wiring diagram for the overtemp. buzzer alarm which gets activated by an alarm signal from the overtemp. controller. The spring loaded pushbutton, when pressed, silences the alarm.

6.4 Conclusion

This chapter presented the electrical, gas and safety systems of the furnace. Detailed wiring diagrams were provided for all the circuits in the furnace. Details of the furnace gas system were also presented. The next chapter describes furnace testing and the procedure that was used to obtain optimal quality parts using the furnace. It also describes the results of temperature profiling experiments that were carried out inside the furnace.

7 Furnace Testing

This chapter describes the steps leading to the successful firing of the furnace to obtain oxide free parts. It also describes temperature profiling experiments aimed at obtaining a uniform temperature profile along the furnace depth by independently adjusting the power going into the front, middle and rear heaters using trim potentiometers, if necessary.

7.1 Initial furnace runs

The first time the furnace was fired, the controller was operated in manual mode and the ramp to 1200 C was carried out with 100% power going to all the heaters. This procedure, of ramping to 1200 C at full power is recommended by the heater manufacturer, and is required to "transform" the APM wire of the heaters. As the furnace temperature approached 1200 C, the power going to the heaters was turned down by trial and error to a value (~78%) that could maintain 1200 C in steady state. The furnace was then held at 1200 C for four hours to complete the "transformation" of the APM wire. Air flow through the furnace was maintained at 2 volume changes an hour (9 scfh) throughout this process. This was done for two reasons: first, the "transformation" of the APM wire needs to happen in air, and second, the presence of air would ensure complete burning off of the polymer that was sprayed on to the Alumina insulation to make its mounting into the furnace easy (see Chapter 5). When the furnace was opened after this run, the Inconel pins, mounts and mesh inside were found to be oxidized since the furnace had been run in air. However, this oxide got reduced in subsequent runs that were carried out in a Forming gas (5% Hydrogen, 95% Argon) atmosphere.

The next furnace run involved auto tuning the furnace controller at three temperatures in order for it to determine the right PID variables for optimal control at these temperatures (procedure is described on page 9-6 of the controller programming manual). The three temperatures chosen for auto tuning were 500 C, 1000 C and 1200 C, and the corresponding PID parameters were automatically written by the controller into PID constants PID1, PID2 and PID 3 respectively. Thus, while programming any furnace cycle, PID1 should be chosen for segments with set points (SP's)<=500 C, PID2 for those segments with 500< SP <=1000 C and PID3 for those segments with 1000< SP<=1200.

Two tests were conducted to test if the controller was indeed doing a good job controlling the furnace. These involved looking at the response of the furnace to a step change in set point. In the first experiment, the furnace was allowed to reach steady state at 1180 C, after which the furnace set point was programmed to ramp up to 1200 C in 1 second. Figure 7.1 shows the response of the furnace to this step change. In the next test, the furnace temperature was allowed to reach steady state at 800 C before bumping the set point down to 780 C in 1 second. Figure 7.2 shows the furnace response to this step change. The absence of any major overshoot in furnace temperature in either case illustrates good control by the controller.

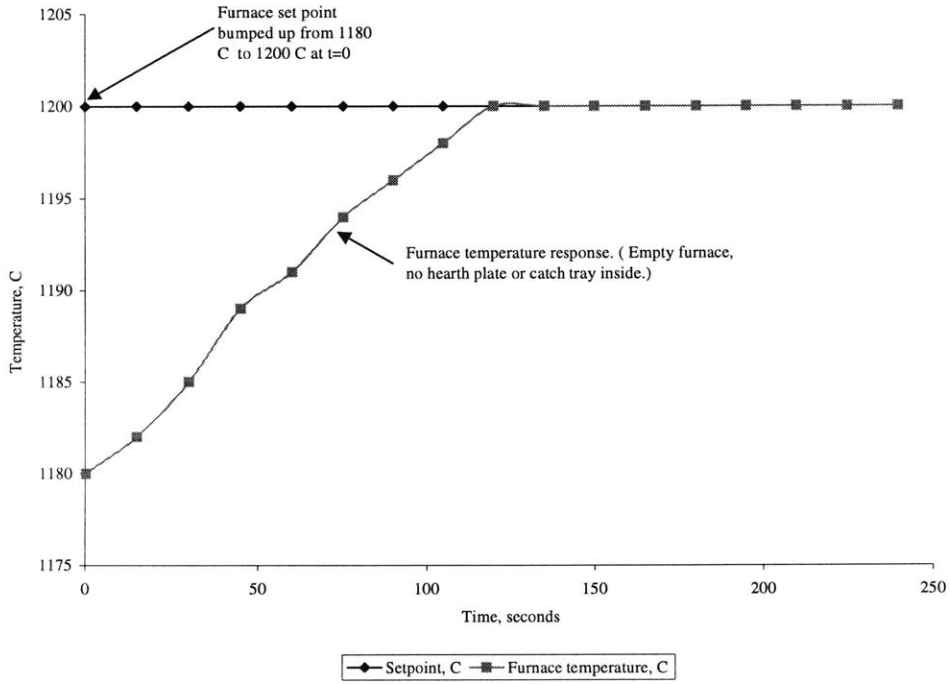

Figure 7.1: Graph showing the response of the furnace to a step change in set point from 1180 C to 1200 C. The absence of any significant overshoot in the response shows good controller action.

7.2 Determining an optimal furnace run

This section describes experiments that were conducted in order to determine a furnace ramp scheme that would yield oxide free parts in the shortest possible furnace cycle.

7.2.1 Furnace runs for obtaining oxide free parts

Having auto tuned the controller, the next step was to sinter SS420 powder in the furnace and obtain an oxide free sintered part. As can be recalled from Chapter 2, the procedure followed while running the small scale furnace was to let the furnace soak at 200 C (with the internal and external heaters both set at 200 C) until the dew point inside got below –25 C, and then ramp the furnace to 1200 C.

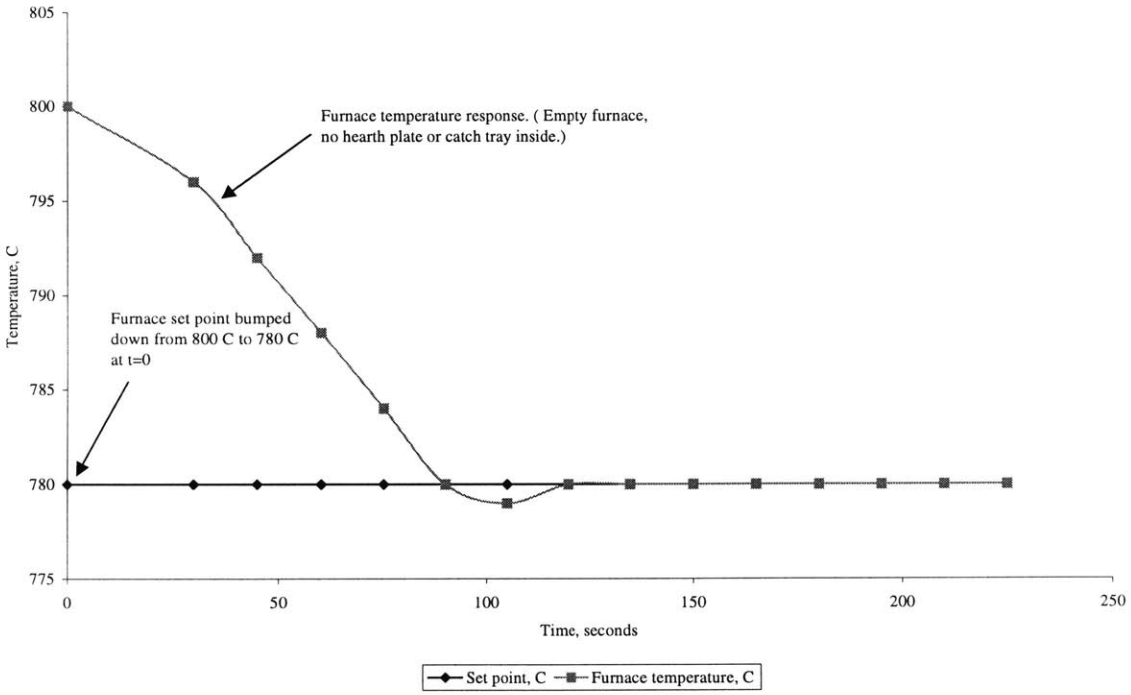

Figure 7.2: Graph showing the response of the furnace to a step change in set point from 800 C to 780 C. The absence of any significant overshoot in the response shows good controller action.

A similar procedure was followed with the large scale furnace. As was explained in Chapter 6, due to a limit on the amount of current that can be drawn from the wall (maximum of 80A), all the external heaters cannot be run simultaneously along with the internal heaters, unlike in the small scale furnace where this could be done. Hence, the following procedure was used. All eleven band heaters were turned on (with the internal heaters kept off), and the furnace was purged with Forming gas at 3 volume changes an hour (13-14 scfh) until the dew point inside the furnace dropped to around –10 C to –15 C. Then, six of the external heaters were turned off (using a controller event) and the internal heaters were turned on. The controller set point was set

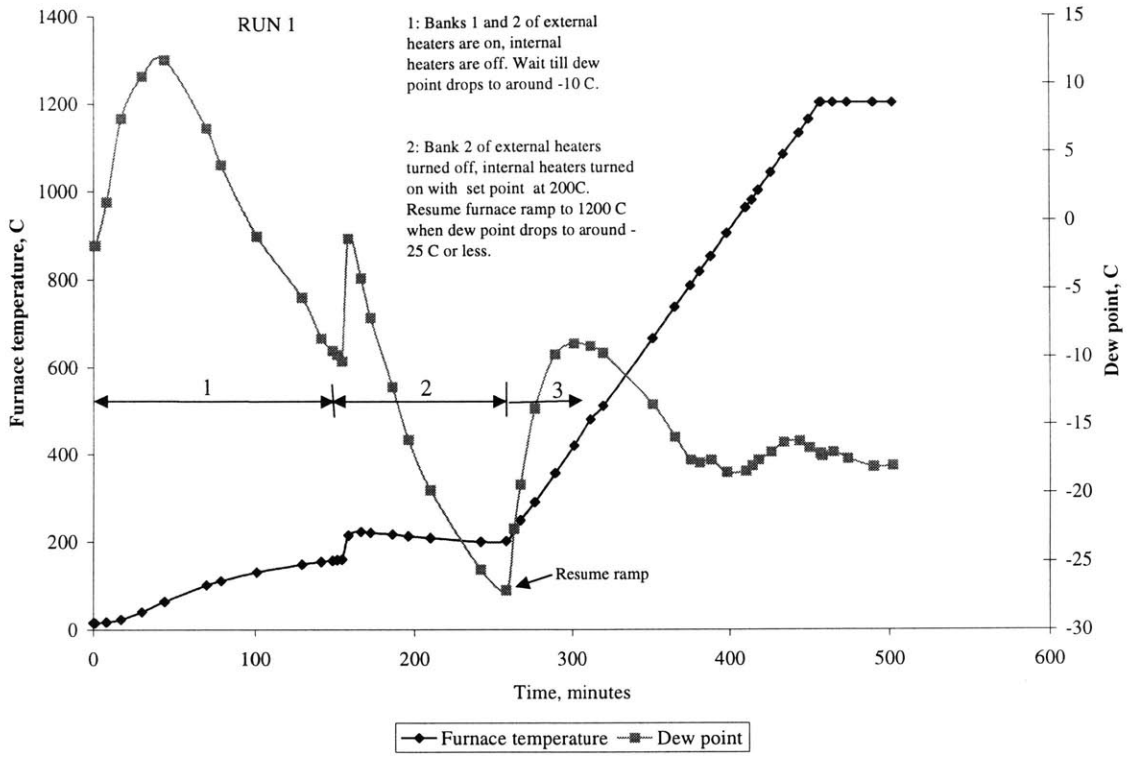

Figure 7.3: Dew point curve for a furnace run (run 1) conducted using the scheme described in the text. Note that the purging time (regions 1 and 2) is around 4 hours. Compare this with run 2 in Figure 7.5, where the purge time is 3 hours.

at 200 C, and the furnace was allowed to soak at 200 C until the dew point got down to –25 C. At this point, the furnace was ramped up to 1200 C at 5 C/min. Figure 7.3 shows the dew point curve that was obtained the first time the furnace was run according to the above mentioned scheme (call this run 1). It can be seen that the nature of the dew point curve in region 3 is similar to that seen in runs with the small scale furnace (see Chapter 2). The external strip heaters were turned off at the end of this run. Run 1 yielded an oxide free sintered SS part (Figure 7.4). It is worth noting that clean parts were obtained using just 3 volume changes an hour of Forming gas as opposed to the 5 volume changes an hour used in the small scale furnace. After the furnace cooled down to room temperature at the end of the run, it was opened for 40 minutes, loaded with another SS420 sample and the previous run was repeated (call this run 2). Figure 7.5 shows the dew point curve for run 2. Two things can be noted by comparing Figure 7.3 with Figure 7.5. First, in run 2, it took just 185 minutes before the dew point was low enough to start the ramp to 1200 C as opposed to the 242 minutes taken in run 1. This is a saving of almost 1

hour in purging time. The second difference between the two runs is that the dew point levels in run 2 are lower

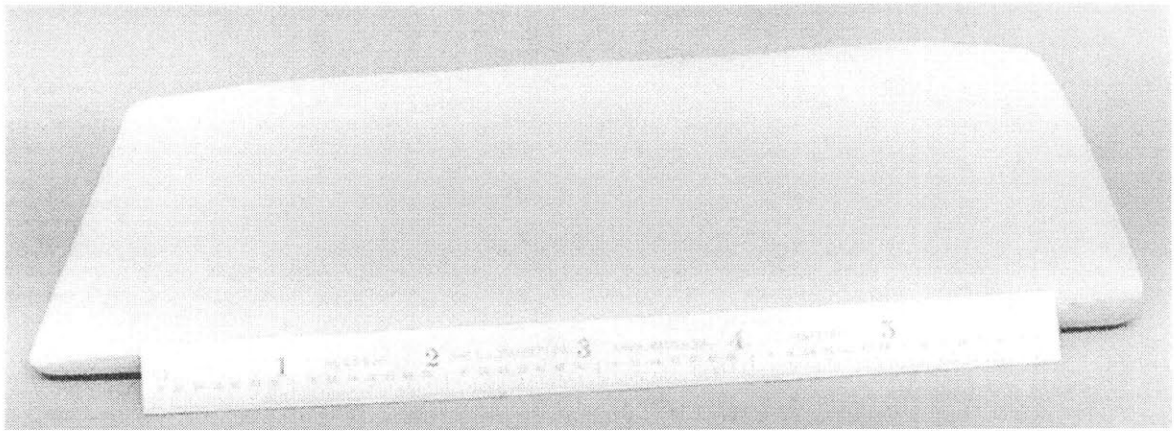

Figure 7.4: Picture of the SS420 part that was successfully sintered in the furnace using the scheme described in section 7.2.1. The dew point curve for this run is shown in Figure 7.3.

than those in run 1. The difference in the dew point curves could be due to the fact that the insulation did not have enough time to soak up water vapor from the atmosphere, as the furnace was opened for just 40 minutes between the runs.

To get an idea of how many volume changes of ambient air would be needed to saturate the furnace insulation, the following calculation was performed. The total mass of Alumina insulation inside the furnace was calculated to be ~3 kg , while that of the Graphite insulation was estimated to be ~ 0.75 kg. Alumina absorbs 5% moisture by weight and Graphite absorbs 2% moisture by weight. Hence, the total moisture that would be needed to saturate the insulation inside the furnace with moisture is 165 gram. Under normal room conditions (25 C, 50% RH), a psychrometric chart shows that 1 gram of water vapor is contained in 0.77 cubic meter of air. Thus, the volume of air that would contain enough water vapor to saturate the insulation is 13 cubic meter. The volume of the furnace is 4.5 cubic feet, which is roughly 0.127 cubic meter. Thus more than 100 volume changes of air would be needed to saturate the insulation. This points to the fact that if the furnace is opened for a limited amount of time between runs, not much moisture will be absorbed by the insulation. In addition, if the strip heaters of the furnace are kept on all the time, then the insulation will be at around 200 C all the time and this will further reduce the amount of water vapor absorbed from the atmosphere each time the furnace is opened. To test this assumption, two back to back runs (call them run 3 and run 4 respectively) were conducted in the furnace. The furnace was left sitting open for five hours after a previous run that had been performed just before run 3. The purge time (time from beginning of run to the

point when the dew point first reaches –25 C) during run 3 was found to be 243 minutes. Unlike in other runs, the strip heaters were not turned off at the end of run 3, but were left on while the

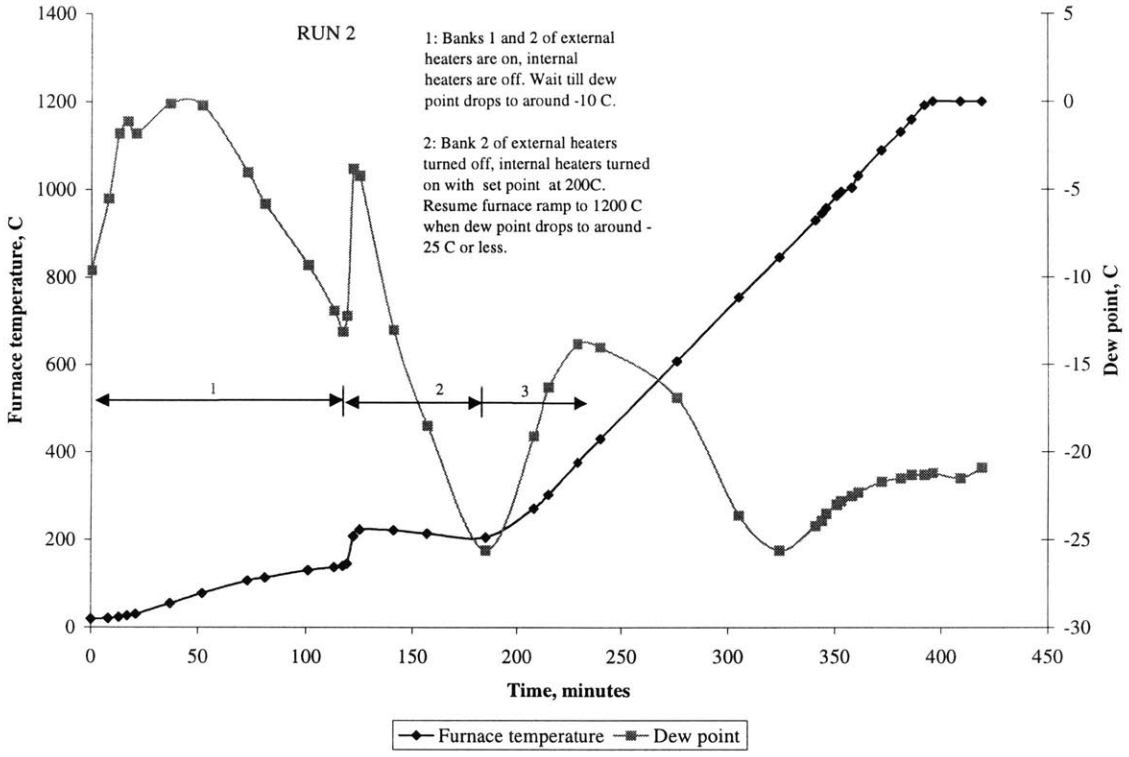

Figure 7.5: Dew point curve for run 2, conducted right after run 1 whose dew point curve is shown in Figure 7.3. The furnace was opened for 40 minutes after it cooled down to room temperature at the end of run 1, before starting run 2. Note that the purging time for this run is around 3 hours as opposed to 4 hours for run 1.

furnace cooled. When the furnace cooled down to 195 C (steady state internal temperature reached with all eleven external heaters on), it was opened (the strip heaters were left on) for exactly 10 minutes and then closed again for performing run 4. For this run, the purge time was found to be just 124 minutes. This represents almost a 50% reduction in purge time over that in run 3.

7.2.2 Other ramp schemes

Looking at Figure 7.3 and Figure 7.5, it can be seen that part of the reason it takes a long time ~ 4 hours for the dew point inside the furnace to reach –25 C is that the inside of the furnace heats up very slowly (at about 1 C/min) when the internal heaters are off and only the external heaters are heating the furnace. The furnace heats up slowly because heat from the external

heaters has to travel through the furnace insulation and heat up the significant thermal mass of the furnace, including that of the internal heater plates. Ideally, one would want to turn both the

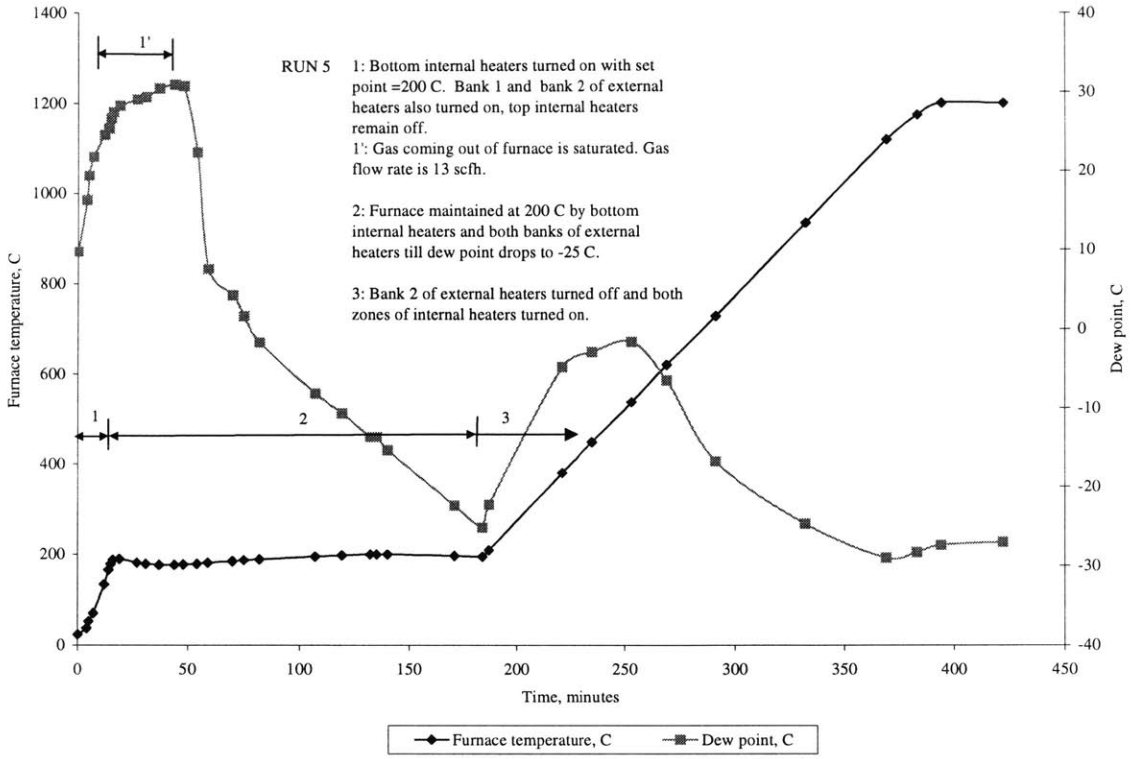

Figure 7.6: Dew point curve for run 5. The bottom zone of internal heaters was kept on with a set point of 200 C during the purge in order to quickly heat up the inside and speed up the moisture removal process.

top and bottom internal heater zones (with a set point of 200 C) and the external heaters on simultaneously, to get the fastest expulsion of moisture. However, this cannot be done due to a restriction on the amount of current that can be drawn from the wall. Hence, a run was carried out (call it run 5), during the purging phase of which the bottom internal heaters were turned on with a set point of 200 C, all eleven external heaters were turned on and the top internal heaters were kept off (see appendix 3 for details of a furnace program similar to one used in this run). The maximum current drawn under this scheme was 67.5 A, well below the 80 A limit imposed by the wall power supply. The top heaters were conveniently turned off using event 5 of the controller. Figure 7.6 shows the dew point curve obtained during run 5. It can be seen that the purge time is around 184 minutes, a significant reduction from the 242 minutes in run 1, performed without turning on any internal heaters during the purge (Figure 7.3). One thing that can be noted from Figure 7.6 is that the Forming gas coming out of the furnace is saturated

during the period marked 1'. This shows that the limitation on the rate of moisture removal from the furnace is posed by the gas flow rate. Clearly, 13 scfh is not enough to remove moisture from the furnace fast enough to avoid saturation. A possible solution to this problem is to use a higher

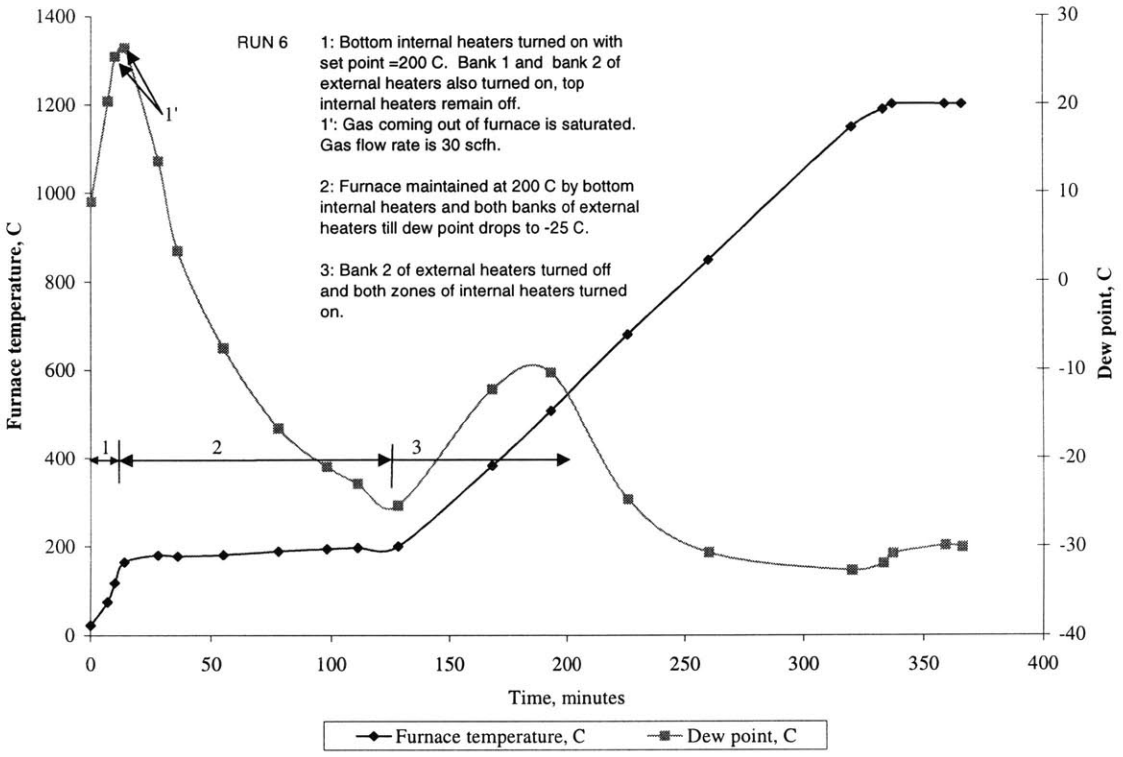

Figure 7.7: Dew point curve for run 6. The gas flow rate in this run was 30 scfh as opposed to the 13 scfh used in run 5. Note that the purge time in this run is 122 minutes, more than 60 minutes lower than that in run 5, whose dew point curve is shown in Figure 7.6.

gas flow rate. As noted in Chapter 6, the maximum gas flow rate that the furnace's flow meter can handle is 30 scfh. Thus, in the next furnace run (call it run 6), the flow rate of Forming gas was set at 30 scfh and the same furnace cycle as that used in run 5 was followed. Figure 7.7 shows the dew point behavior for this run. It can be seen that the purge time is just a little over 120 minutes, more than a 60 minute reduction over the 184 minutes seen in run 5, that used 13 scfh of Forming gas. Also, the overall dew point levels in run 6 are lower than those in run 5. Figure 7.8 is the picture of a part that was successfully infiltrated in this furnace run.

Thus, it can be seen that turning on the bottom internal heaters during the purge phase and increasing the flow rate to 30 scfh helps in significantly lowering the purge time compared to the scheme followed in section 7.2.1. Even greater reduction in purge time may be obtained if, in addition, the furnace shell is always maintained at 200 C by keeping the external heaters on

between runs and the furnace door is mostly kept closed except while loading/unloading parts in and out of the furnace.

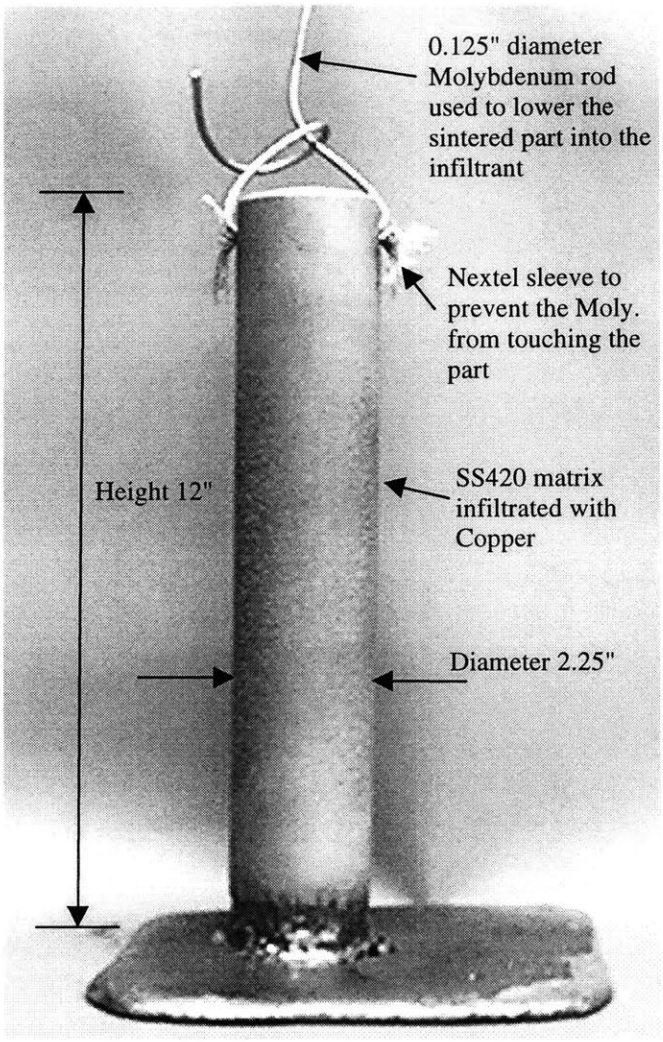

Figure 7.8: Picture of a SS 420- Copper part that was infiltrated successfully during run 6. The dew point curve of the cycle used in run 6 is shown in Figure 7.7. The part was suspended inside the furnace using the 1/8" diameter Moly. rod seen in the picture, and dipped into the copper melt only after all the copper had melted and steady state had been attained at 1200 C.

7.2.3 Dew point sensing

As can be gathered from Chapter 2 and sections 7.2.1 and 7.2.2 of this chapter, sensing the dew point inside the furnace is a critical part of every run. The method currently being used is to "hold" the furnace run when it is in the purging segment, and wait for the dew point to get to -25 C before manually resuming the ramp to 1200 C. This method is cumbersome since it

requires the furnace operator to monitor the dew point at regular intervals of time. Also, the dew point sensor currently being used is very basic and only has a digital readout (see list of vendors in Appendix 1 for details on the dew point sensor).

There are two ways of getting around the problem of having to monitor dew point manually. The first is to simply assume that a 3 hour purge at 200 C will be sufficient to attain a dew point of -25 C inside the furnace, and program the furnace accordingly. The other solution is to automate the entire run/hold process. A few general comments which might be helpful while designing such a scheme follow. A feature of the furnace controller that could be used is the fact that the "hold" and "run" functions of the controller can be operated using momentarily applied external switch inputs (see pages 9-8 and 9-9 of the controller manual for details). The "hold" switch could be closed momentarily at the arrival of the "hold at 200 C" segment of the furnace run, indicated by, say, a short furnace time based event. Using a dew point sensor that gives a 4-20 mA output corresponding to a given dew point range, and a current sensing relay with a set threshold current, a dew point of -25 C can be detected. The current sensing relay could then be used to close the "run" switch which just needs momentary contact. Once this has been done, even when the dew point rises above -25 C as the furnace ramps up and the current sensing relay switch opens, it will not have any effect on the "run" condition, which can only be overridden by a hold signal.

7.3 Two zone control scheme and temperature profiling

7.3.1 Experiments with two zone control

As explained in Chapter 6, the furnace controller has two independent channels that can accept inputs from separate thermocouples and give out separate 4-20 mA outputs. During initial stages of furnace testing, SCRs controlling the top heaters of the furnace were wired to receive their input from channel 1 of the controller while SCRs controlling the bottom heaters received their input from channel 2. The idea was that this would make it easy to shut off the top heaters in order to perform directional solidification, as it would simply involve programming channel 1

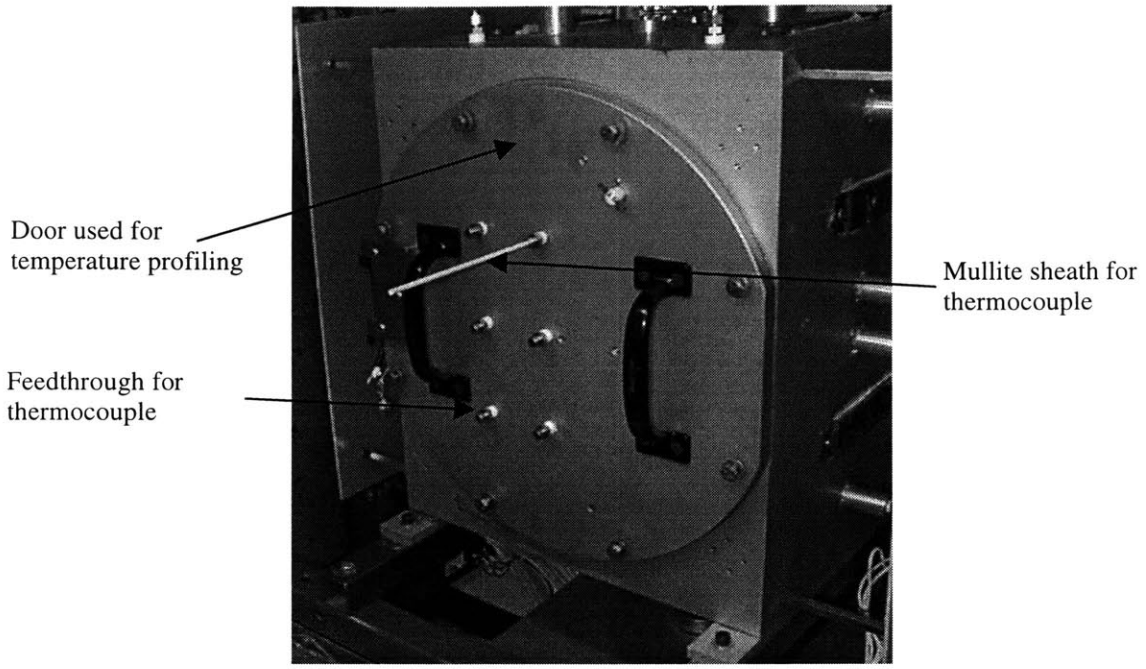

Figure 7.9: Picture of the furnace fitted with the door used for temperature profiling.

and channel 2 of the controller separately. This method was tried out, by hooking channel 1's input to a thermocouple located in the top heater zone and channel 2's input to a thermocouple located in the bottom heater zone. However, when the furnace was fired, it was found that when steady state was attained at 1200 C, the top thermocouple read 1200 C, while the bottom one read 1193 C. This was not surprising since the tolerance of type K thermocouples at 1200 C is +/-9 C. However, what was of concern was the fact that the bottom heaters were running at 100% power while the top heaters while running at only 53% power. Clearly, channel 2 of the controller, which controlled the bottom zone, was trying its best to get the temperature read by its thermocouple to 1200 C by making the bottom heaters put out 100% power (in fact the bottom zone of the furnace was measured to be at 1211 C (+/-9 C) using independent profiling thermocouples through the front door. Moreover, when the bottom thermocouple was raised to the same height as the top one, it was found to read 1194 C while the top one read 1200 C. All this points towards the advantage of using a low error, custom thermocouple calibrated for use at 1200 C to control the furnace.). Since the furnace heating zones are highly coupled (each location in the hot zone has a good radiation view factor with respect to the other), the bottom heaters putting out 100% power caused the top heaters to cut back their power to 53%. (If this happens over an extended period of time, it will result in a difference between the lives of the top and bottom heaters.)

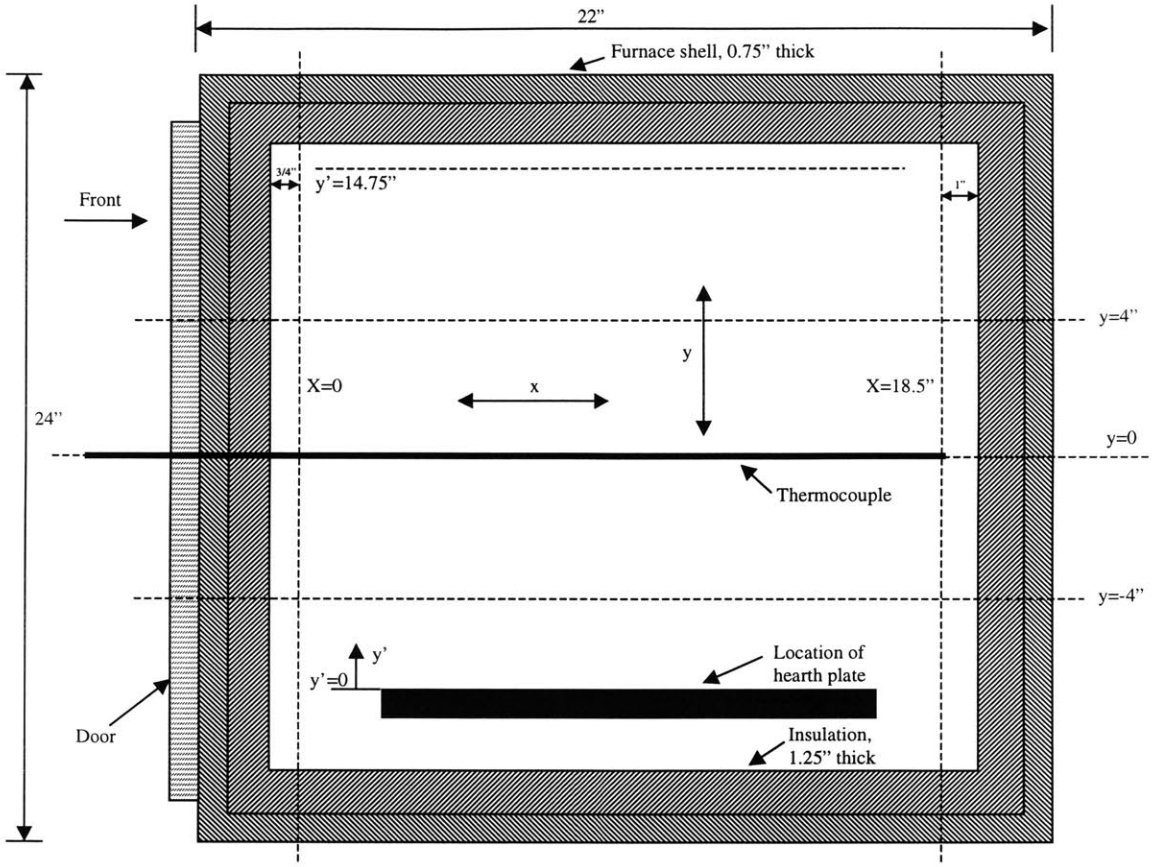

Figure 7.10: Schematic of a section through the furnace, as seen from the side. Profiling was done for x=0 to x=18.5" along the furnace depth at each of the six ports shown in Figure 7.9. The front, middle and rear heater plates are respectively 6", 8" and 6" long and roughly extend from the front insulation to the rear insulation.

To verify the fact that the top and bottom heater zones were indeed coupled, the furnace control was changed to manual at 1200 C and the following pairs of power output going to the top and bottom heater zones were tried out: (53%,100%), (63%,90%), (68%,85%) and (73%,80%). The idea was to keep the total power going into both zones combined roughly constant, and only vary the its distribution between the top and bottom heaters. In a highly coupled system, this should not have an effect on the temperature recorded by either the top or the bottom thermocouple. At each power setting, temperatures read by the two thermocouples were recorded after steady state was attained. The following values were recorded by the top and bottom thermocouples respectively, corresponding to the power output % pairs given above: (1200,1193), (1195,1184), (1195,1181) and (1198,1181). Clearly, the difference between the readings of the two thermocouples is not significant, if the +/-9 C tolerance of each thermocouple is taken into account (A point worth mentioning is that the two channels of the controller were

found to read different temperature values when connected to the same thermocouple, probably due to a difference in their A/D converters. This further adds to the argument against using two zone control.).

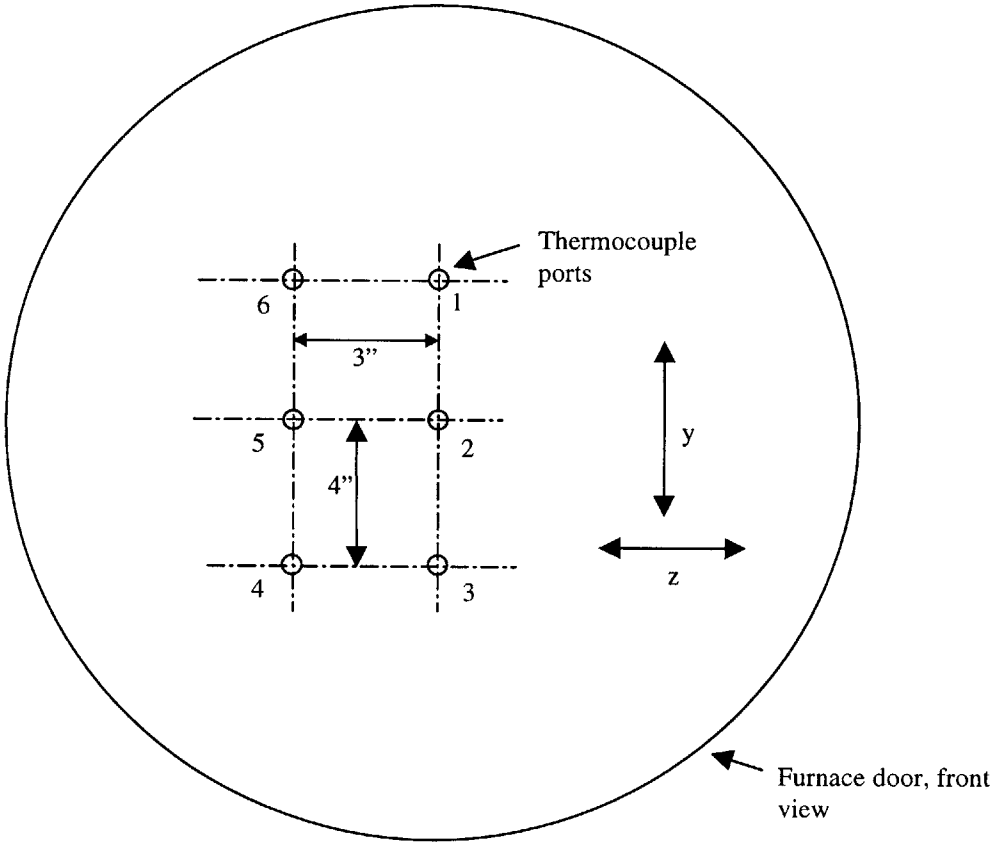

Figure 7.11: Schematic showing the relative location of the thermocouple ports on the front door.

This proved beyond doubt that two zone control was not worth it, since the top and bottom zones of the furnace are highly coupled. Hence, a single controller channel, channel 1 was used to control both heater zones using the thermocouple in the top heater zone. (The wiring for this scheme is explained in detail in Chapter 6.)

7.3.2 Temperature profiling

As mentioned in Chapter 5, the furnace has a door that can be used for temperature profiling. Figure 7.9 shows a picture of the furnace fitted with the profiling door. Six thermocouple feedthroughs can be seen on the door. These are 3/16" bored through pipe fittings whose bore was drilled to a diameter of 0.205". This was done to prevent jamming of the 0.1875" outer diameter Mullite thermocouple sheath inside the fitting due to thermal expansion.

The Mullite sheath is 24" long and has two holes in it, each of which has a diameter of 0.060". Each wire of the type K thermocouple that passes through the sheath has a diameter of 0.032". To prevent inaccuracies resulting from differences in different thermocouples of the same type,

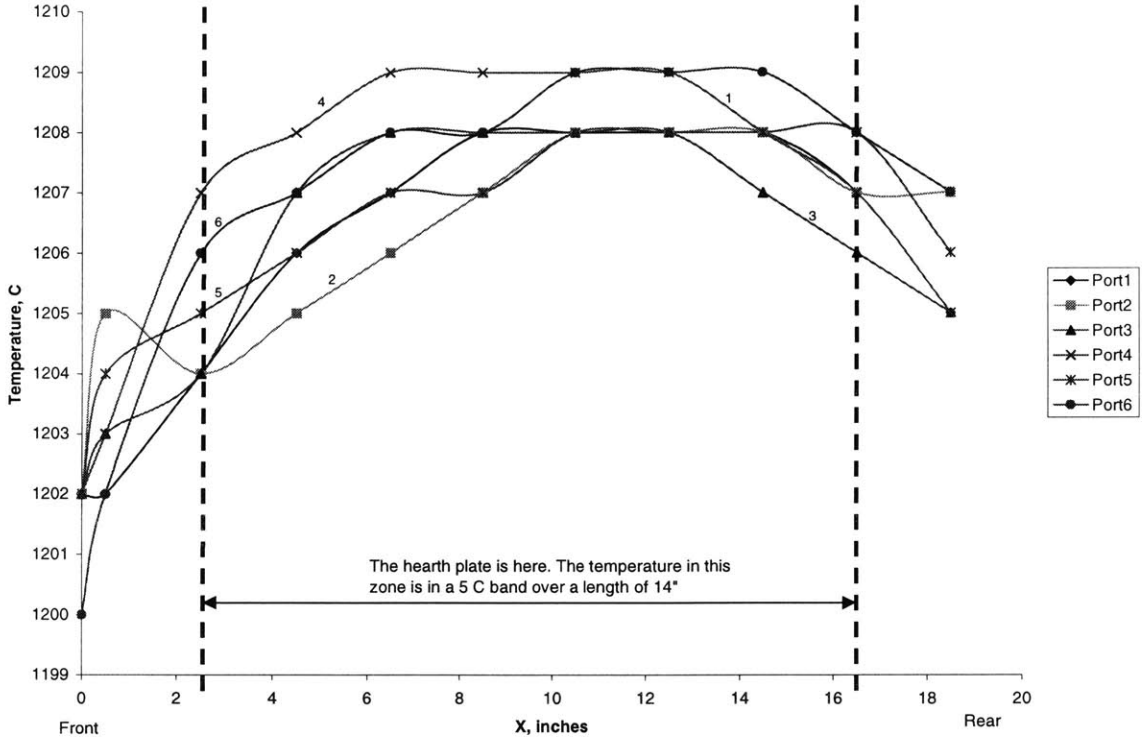

Figure 7.12: Temperature profiles obtained along the depth of the furnace at each of the six ports shown in Figure 7.11. Note that the temperature is in a 5 C band over the length of the hearth plate.

the same thermocouple was used to profile the furnace depth at all six locations in the door. Figure 7.10 shows a schematic of a section of the furnace looking from the side. Figure 7.11 is a schematic showing the relative locations of the thermocouple ports (numbered 1 to 6) on the profiling door as seen from the front. Temperature profiling was carried out at each of the six ports. At each port, temperature was recorded at 11 locations along the furnace depth, from x=0 to x=18.5". When the thermocouple is at x=18.5", due to the clearance between the sheath, (which has a diameter 0.1875") and the 0.205" diameter hole in the fitting in the door, the tip of the thermocouple describes a circle of radius 0.5". This introduces a slight uncertainty in the exact location at which temperature is measured. Figure 7.12 is a graph showing the temperature profile along the depth of the furnace at each of the six ports, 1 to 6. It is important to note that the standard type K thermocouples used for profiling have an accuracy of +/-0.75%, which

translates to an accuracy of +/9C when measuring a temperature of 1200 C. The hearth plate extends form x=2.5" to x=16.5". It can be seen that the temperature in this zone is in a 5 C band. This represent very good temperature uniformity in the furnace hot zone.

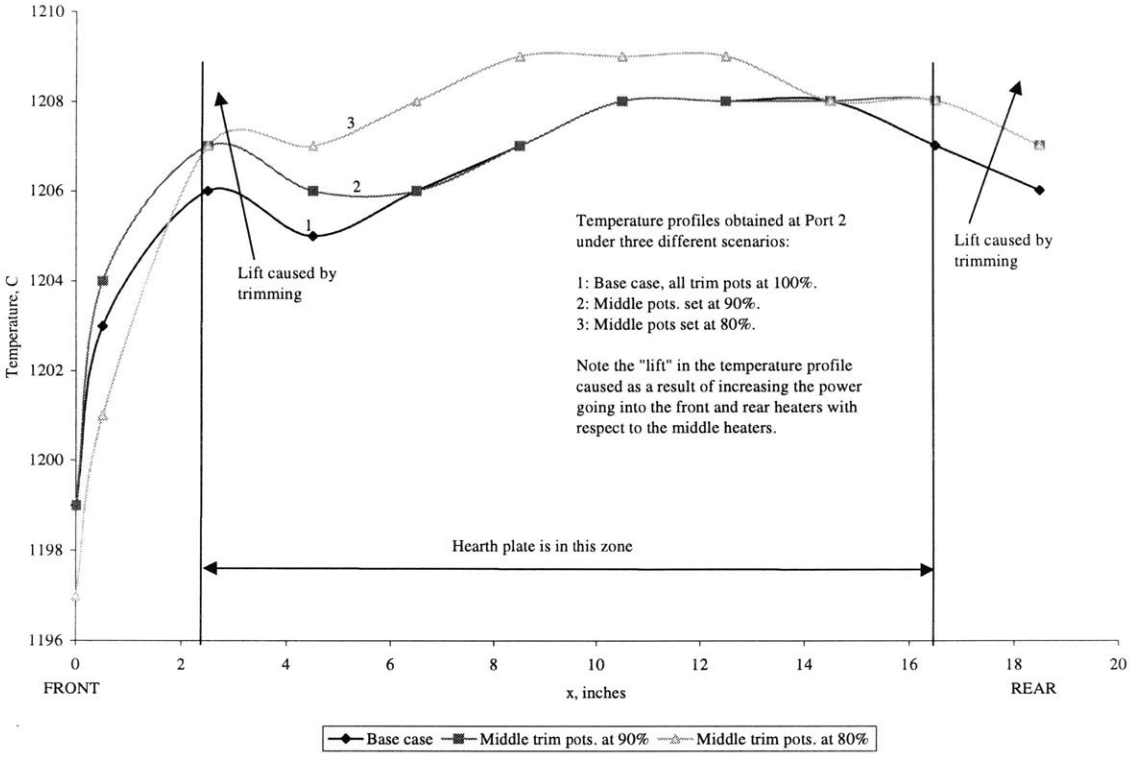

Figure 7.13: Temperature profiles obtained at port 2 as part of the trimming experiment carried out to try and smooth out the temperature profile inside the furnace.

Although this was not very crucial, (in view of the excellent temperature uniformity already existing in the furnace) a few experiments were conducted to try and adjust the power going into the front, middle and rear heater zones in such a way as to smoothen the profiles shown in Figure 7.12. As discussed in Chapter 6, potentiometers were wired to the controller output to independently vary the control signal (and thus the power) going to the top and bottom heaters of the front, middle and rear zones, and thus control the relative temperature profile inside the furnace.

In steady state, with all potentiometer knobs turned to 100%, the controller put out 77% power to all the heaters. The temperature profile along the furnace depth at port 2 for this setting is shown in Figure 7.13 (call this the base case, labeled 1 in the figure). Note that the temperature between x=2.5" and x=16.5", the hearth plate zone, is in a 3 C band. Also note that the temperature drops off rapidly towards the front of the furnace (x=0). It also drops a little towards

the rear of the furnace (x=18.5"). In order to "lift" the profile at the front and the rear, the potentiometers controlling the middle heaters were adjusted to the 90% setting. This would raise

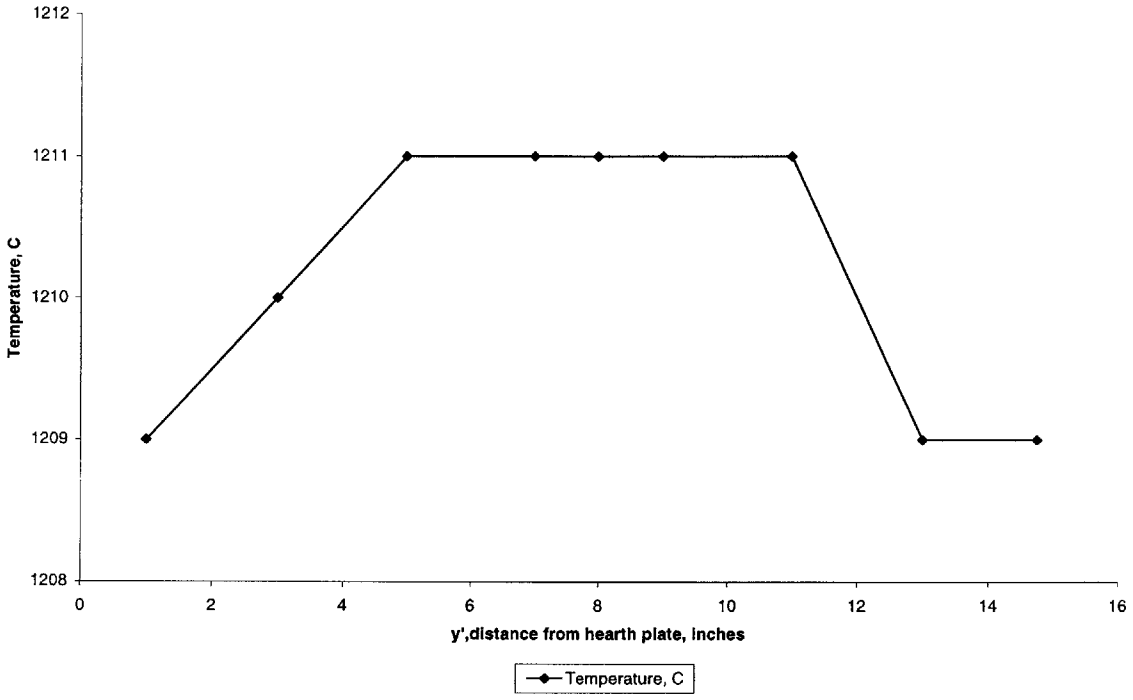

Figure 7.14: Temperature profile along the height of the furnace, measured using a port in the middle of the top face of the furnace. Note the tight 2 C band the temperature is in over a 14" height.

the power going to the end heaters relative to the middle ones. In steady state under this setting, the controller output went up to 80.5% and the resulting temperature profile is labeled 2 in Figure 7.13. In this case, the power going to the front and rear heaters is 80.5% and that going to the middle heaters is 0.9* 80.5% = 72.45%. Note the rise in temperature in the front and rear zones over the base case. Also, the overall variation in temperature over the hearth plate zone (x=2.5" to x=16.5") reduced to 2 C from 3 C in the base case. However, the steep fall in temperature as x tends to 0 still exists. To try and rectify this, the potentiometer knobs of the middle heaters were turned down further from 90% to 80%. In steady state, the controller output went up to 83%. In this case, the power going to the front and rear heaters is 83% and that going to the middle heaters is 0.8* 83% = 66.4%. The resulting temperature profile is labeled 3 in Figure 7.13. Note that the overall temperature in the hearth plate zone goes up a couple of degrees. Interestingly enough, the temperature as x tends to 0 actually decreases as compared to

the previous cases. Somehow, the extra power going into the front heaters ends up heating up the middle zone of the furnace instead of the front zone.

These experiments showed that trimming did have a small impact on the relative temperature profiles in the sense that it tightened the band over which the temperature varied over the length of the hearth plate from 3 C to 2 C. Having said this, however, it should also be noted that the temperature profile obtained inside the furnace with all the trim pots set at 100% is also very acceptable for processing parts without distortion.

The next experiment involved obtaining a vertical temperature profile inside the furnace. Temperature was recorded starting at y'=1" (see Figure 7.10 for details of coordinate system) from the hearth plate to y'=14.75", which is 1" below the top insulation. This profile was obtained using the QF40 fitting in the middle of the top face of the furnace. Figure 7.14 shows the temperature profile obtained. Note that the temperature is in a tight 2 C band over a height of around 15" starting at the hearth plate. This is excellent temperature uniformity.

In order to get a sense of the vertical temperature gradient that could be induced inside the furnace for performing directional solidification, the furnace was switched to manual mode when steady state was attained at 1200 C. Then, the top heaters were shut off and the bottom ones were given 100% power. The furnace started to cool, and in steady state (bottom thermocouple reading 1013 C), a temperature difference of 23 C was recorded between thermocouples in the top and bottom zones, which were separated vertically by about 7" (a temperature gradient of a little more than 3 C/inch). This further demonstrates the fact that the top and bottom zones of the furnace are highly coupled (a point made in section 7.3.1.) and that large temperature gradients cannot be obtained inside the furnace. However, is should be noted that the presence of a large part inside the furnace shall decrease cross radiation from the bottom heaters on one face to the top corner of the opposite face, possibly giving rise to a higher temperature difference between the top and the bottom zones of the furnace.

7.4 Summary

If the furnace power supply has a high enough current capacity (~90 A) to permit running all the internal and external heaters simultaneously, then it is recommended that the furnace be purged with the internal heaters set at 200 C, and all the external heaters turned on. Otherwise,

the schemes identified in this chapter can be used to purge the large scale furnace in order to obtain oxide free parts.

It was shown in this chapter that excellent temperature uniformity exists inside the furnace, both from top to bottom and along the depth in the region where the hearth plate is located. Reasons for not using two zone control in the furnace were discussed. The results of some experiments examining the effect of trimming the power going into heaters in different zones on the furnace temperature profile were also discussed. The next chapter, which is the final chapter of this thesis gives a summary of the achievements of this work, and recommendations for future work using the large scale furnace.

8 Conclusion and Future Work

This chapter summarizes the achievements of this work and talks about future work that can be carried out using the large scale furnace that was successfully built and tested as part of this work.

8.1 Summary of achievements

As mentioned in Chapter 1, the primary motivation behind this work was to develop a post processing furnace for 3D printed parts that could be scaled up economically. As a first step, the small scale furnace previously developed at MIT was optimized to yield good quality, oxide free sintered and infiltrated parts. The important thing learnt from the small scale furnace was that it in order to get oxide free parts, it was necessary to heat the furnace shell from the outside and allow the furnace to soak at 200 C until the dew point inside got to a low value like –25 C, before ramping the furnace to 1200 C.

Having learnt about the process and obtained design parameters from the small scale furnace, a large scale furnace was constructed. This furnace has a rectangular cross section and is more than 20 times bigger in volume than the small scale furnace, which had a circular cross section. This furnace has an Aluminum shell, uses Alumina and Graphite insulation and uses Kanthal heating elements embedded in high Alumina content heater plates to heat the inside of the furnace (12 internal heaters for a total of 10.2 kW). It is designed to operate in a Forming gas or Argon atmosphere. In addition to the internal heaters, it has eleven strip heaters on the shell (a total power of 11 kW) to expel moisture from the insulation during the purging phase of a furnace run. The furnace has a Honeywell controller that uses PID control to ensure the desired operation of the furnace. The controller has events that are used to control the switching of the strip heaters and gas solenoid valves.

SS420 parts were successfully sintered and infiltrated in this furnace using a furnace cycle similar to that used in the small scale furnace. In fact, clean parts were obtained in the large scale furnace using just 3 volume changes an hour of Forming gas as opposed to the 5 volume changes an hour flow rate used in the small scale furnace. Temperature profiling done inside the furnace showed excellent temperature uniformity inside. It was found that the temperature along the depth of the furnace was in a 5 C band over the 14" length of the hearth plate. Also, the

temperature was found to be in a 2 C band over a height of 15 inches going upward from the hearth plate.

The successful scaling up and operation of this furnace proves the concept of economical scalability. However, one of the major problems with the large scale furnace design as it stands is that of assembly of internal heaters into the furnace. As may be recalled from Chapter 5, the furnace had originally been designed to have 1" of insulation on all faces. However, an additional 0.25" of Graphite was used on all faces to decrease heat loss from the furnace, and an Inconel mesh was used on the front, top and rear faces to prevent the insulation from falling apart. The presence of extra insulation and Inconel mesh on the top face of the furnace made mounting the top heaters onto the furnace side walls very difficult since there was very little room at the top for maneuvering the heaters into their Inconel supports. Reaching into the interior of the furnace through the front door in order to mount the four heaters located towards the furnace rear was also found to be hard. Similarly, mounting insulation onto the top face of the furnace was found to be difficult since it was not easy to reach the Inconel supporting pins located towards the rear of the furnace.

If the existing design of the large scale furnace is scaled up, it will be even harder to mount insulation and heaters into the furnace, primarily because of difficulty accessing the innards of the furnace through the front door. To overcome this problem, it is suggested that a SS cage housing the insulation and heaters be assembled outside the furnace and then be mounted into the furnace as a single unit.

A second issue that was studied as part of this work was the effect of directional solidification on porosity in infiltrated parts. The small scale furnace was used to conduct directional solidification experiments on SS420 parts infiltrated with Bronze. These involved inducing a temperature gradient in a part (using a jet of Argon striking the part on the top) at the end of an infiltration cycle. By comparing two extreme cases, directional solidification, in which the top of a solidifying part is kept cooler than the bottom, with reverse directional solidification, in which the bottom of the part is kept cooler than the top as it solidifies, it was established that directional solidification reduces porosity in parts. A switch that is controlled by a furnace controller event has been provided in the large scale furnace to shut off the top heaters in order to conduct directional solidification in cooling parts.

The economics of requiring two separate furnaces for post processing, one for debinding and the other for sintering was addressed in Chapter 1. An apparatus for carrying out debinding and sintering in the same furnace run without contaminating the furnace was designed and successfully tested in the small scale furnace. This apparatus can be scaled up for use in the large scale furnace, and will eliminate the need for using two separate furnaces for post processing, resulting in a halving of capital cost.

8.2 Recommendations for future work

As mentioned in the previous section, the large scale furnace has a switch that can be used to cut off power to the top heaters. This feature can be used to perform directional solidification at the end of an infiltration, just before cool down. The effect of directional solidification on porosity that was identified during experiments conducted in the small scale furnace can be tested using the large scale furnace.

The furnace has a number of QF40 flange fittings on the top face. One of these can be used as a passage for the actuator of a gating mechanism that can be used to perform gated infiltrations. These experiments can be carried out to learn more about the effect of gated infiltration on porosity in infiltrated 3D printed parts. In addition, the debinding apparatus that was successfully tested in the small scale furnace can be scaled up and be used to debind and sinter green parts in a single run in the large scale furnace.

Appendix 1: List of Vendors

S.no.	Item name	Item specifications	Vendor
1	Alumina insulation	Alumina blanket type AB, 95% Alumina content	Zircar Products Inc. 110 North Main Street PO BOX 458 Florida, New York 10921-0458 Phone: 914 651 4481
2	Brass Connector	Connectors to connect wires from SCR to the Brass tubes coming out of the furnace	MIT Central Machine Shop See part drawing in Appendix 2
3	Braze alloy	Eutectic alloy: Ag 72% Cu 28% 0.062" diameter SB72 wire	Prince/ Izant Company 12333 Plaza Drive Cleveland, OH 44130 Phone: 216 362 7000
4	Braze Flux	Ultra black flux	
5	Burst disc	Part # 1MA1X2X5X72 2" Graphite disc, burst pr. 5psig@ 22 C and ~4.5 psig @ 200 C	Zook Enterprises, LLC 16809 Park Rd., Chagrin Falls OH, 44022 Phone: 440 543 1010
6	Ceramic tubes	Mullite tubes for hearth plate supports, heater location and electrical insulators, see part drawings in Appendix 2	East Coast Sales Co. Inc. 554 North State Road Briarcliff Manor, NY 10510 Phone: 914 923 5000
7	Contactor	Turns power to internal heaters on/off Is controlled by a 120 V AC signal from the controller Part# AB 100 A60 ON D3 Max current : 60 A @ 240 V AC	Allen Bradley 1201 South Second Street Milwaukee, WI 53204 Phone: 414 382 2000 Local retailer, Boston area: Eagle Electric Phone: 781 302 2000
8	Controller	DCP 552 Digital Control Programmer Two Channel Model HW DCP 552 E20 200	Honeywell Inc. Industrial Controls Div. 1100 Virginia Dr., Ft. Washington, PA 19034-3260 Phone: 215 641 3000 Customer Service: 800 423 9883
9	Dew point sensor	Part# E-37450-04F Thermohygrometer with dew point	Cole Parmer Instrument Co. E. Bunker Court, Vernon Hills IL 60061 Phone: 800 323 4340

10	Flow meter	Waukee flow meter, type MPX-2, 0-30 CFH Argon, 5psig	Waukee Engineering Co. Inc. 5600 West Florida Avenue Milwaukee, WI 53218 Phone: 414 462 8200
11	Flow alarm	Waukee flow alarm, model ML	
12	Furnace shell	Welded Aluminum box with various fittings. See part drawings in Appendix 2	NU VACUUM SYSTEMS INC. 23 Joseph Street Kingston, MA 02364 Phone: 781 585 4371
13	Fuses	External heaters: BUSS MDL 12, 12 A, 250 V time delay fuses Before/after transformer : BUSS FRNR-7, 7A, 250V dual element, time delay fuses	Newark Electronics 59 Composite Way, Lowell MA, 01851-5150 Phone: 978 551 4300
14	Hearth plate	Graphite ISO 63 grade, see drawing in Appendix 2	Graphite Engg. & Sales Co. 712 Industrial Park Drive PO Box 637 Greenville MI 48838-9984 Phone: 800-472-3483
15	G-10 heat shields	Garolite G-10 sheet 1/8" thick, 2' by 2'	Mc Master Carr PO Box 440 New Brunswick, NJ 08903-0440 Phone: 732 329 3200
16	Graphite insulation	Graphite felt, GH grade, 1/4" thick	Fiber Materials Inc. 5 Morin Street Biddeford, ME 04005-4497 Phone: 207 282 5911
17	High temp. wiring	For wiring external heaters. Model #: HTMG-1CU318S/C 18 AWG Mica glass insulated ultra high temp. wire rated for use at 450 C	Omega Engineering Inc. One Omega Drive PO Box 4047 Stamford, CT 06907-0047 Phone: 800-TC-OMEGA
18	Inconel pins,mounts, washers	For mounting insulation and heaters inside the furnace. See part drawings in Appendix 2	Axis Technologies 27 Industrial Avenue Chelmsford, MA 01824 Phone: 978 250 9909
19	Inconel mesh	Part # : Inco 601, 0.063" wire diameter 2 mesh	Alliant Metals Inc. 134B, Route 111, Hampstead, NH 03841 Phone: 800 543 1453

20	Internal heaters	FPH207-S-L-APM heaters as per drawings in Appendix 2	Thermcraft Inc. PO Box 12037 Winston-Salem, NC 27117 Phone: 336 784 4800
21	Moisture trap	Model # : 8012-4	BOC Gases PO BOX 3053 Edison, NJ 08818-9869 Phone: 800 892 7706
22	Pressure regulator	Part# ADS-SSC-5, low pressure regulator, 1.1-5 psig outlet pressure	Airgas Northeast 17 Northwestern Drive PO Box 1647 Salem, NH 03079 Phone: 603 890 4600
23	Nextel	Nextel 440 BF20 fabric Nextel 440 BT30 thread heat cleaned (sizing removed)	Thermal Ceramics 2730 INDL PKWY Elkhart, IN 46516-5401 Phone: 330 562 8890
24	Overtemp. Controller	Universal digital controller, limit control model Model# HW CD200H-2-000-100000OT*	Honeywell Inc. Industrial Controls Div. 1100 Virginia Dr., Ft. Washington, PA 19034-3260 Phone: 215 641 3000 Customer Service: 800 423 9883
25	Polymer spray	Poly Acrylic Acid, 35 wt% solution in water. Average Mol. Wt. 250000 Catalog # : 41600-2	Aldrich Chemical Company Inc. PO Box 335 Milwaukee WI 53201 0335 Phone: 414 273 3850
26	Power supply	Part# B24G75 24 V DC power supply, 0.75A	Acopian Technical Co. PO Box 638 Easton, PA 18044 Phone: 800 523 9478
27	Pressure switch	Model # : 4NN-K4-N4-B1A-MM Range: 2-25psi	SOR Inc. 14685 W. 105th St. Lenexa, KS 66215 2003 Phone: 913 888 2630
28	Relay: plug/socket	Socket: Part# 7170K18 120V coil voltage plug: Part# 7170K14 24 V coil voltage plug: Part# 7170K12	Mc Master Carr PO Box 440 New Brunswick, NJ 08903-0440 Phone: 732 329 3200
29	SCR Power Controller	Firing card model# : 1021A Unit part# : 1651-24-20 20A, 240V, 1PH, 3 PAK SCR controller	Control Concepts 7870 Park Drive Chanhassen, MN 55317

			Phone: 800 765 2799
30	Solenoid valve	Nomally open, part# : 8210G34 Normally closed, part# : 8210G94 Control voltage: 120 V AC 3/4" NPT female fittings	ASCO: Automatic switch Co. 50 Hanover Rd., Florham Park, NJ 07932 Phone: 800 937 ASCO
31	Strip heaters	Model# : OT-1505W 1kW strip htr. with Chrome steel sheath	Chromalox Leo Pelkus Inc. 170 Worcester St., PO Box 349 Wellesly Hills, MA 02181 Phone: 617 235 8040
32	Swagelok fittings	Pipe fittings: Connectors, adapters, reducing unions etc.	Cambridge Valve and Fitting Inc. 50 Manning Road, Billerica, MA 01821 Phone: 781 272 8270
33	Thermal paste	Omegatherm thermally conductive heat. transfer paste Part# : OT-201	Omega Engineering Inc. One Omega Drive PO Box 4047 Stamford, CT 06907-0047 Phone: 800-TC-OMEGA
34	Thermocouple wire, Mullite sheath	Type K thermocouple wire, 0.032" dia. Part# : A-13-21 Double bore Mullite thermocouple ID 0.060" insulator, part# : A-14-2 Used for temperature profiling	Nanmac Corporation 9, Mayhew Street Framingham, MA 01702 Phone: 800 758 3932
35	Process, overtemp. thermocouples	Part# : KQIN-14G, type K with Inconel sheath	Omega Engineering Inc. One Omega Drive PO Box 4047 Stamford, CT 06907-0047 Phone: 800-TC-OMEGA
36	Thermostat	Part# : OA C 606, Ceramic thermostat Type H, 250 V AC 5A max, NC, opens at 200 C	Selco Products Co. 709 N. Poplar St. Orange, CA 92868-1013 Phone: 714 712 6200
37	Transformer	1 kVA 240 V/120 V Model# : TA-2-81217	Acme Electric Corp. 4815 W. 5th Street Lumberton, NC 28358 Phone: 800 334 5214
38	Silicone tubing	Part# : LU- 06411-63 3/32" ID, 5/32" OD Silicone tubing to make seal at the Ultem-brass interface of the power feedthrough	Cole Parmer Instrument Co. E. Bunker Court, Vernon Hills IL 60061 Phone: 800 323 4340

39	Ultem fitting	Ultem stock purchased from Mc Master Carr. Fittings machined according to drawing in Appendix 2	Central Machine Shop, MIT
40	Viewport	Part# : 450043 Model # : KVP-150 W 0.9" view diameter ports for use on furnace door	MDC Vacuum Products Corp. 23842 Cabot Blvd. Hayward, CA 94545 Phone: 510 265 3500

Appendix 2: Furnace Part Drawings

Laboratory Vacuum Furnace
Lab for Manufacturing and Productivity, 3DP Project
revised 5/25/99, D. Brancazio

Table 1 (summary)			Totals Furnace Box	Door 1	Door 2
A	1/4" NPT		3	6	
B	3/8" NPT		7		
C	4-40 UNC-2B, .20 deep	steel insert	20	2	2
D	1/4-20 UNC-2B, .38 deep	steel insert	59	7	7
E	8-32 UNC-2B, .25 deep	steel insert	16		
F	QF-40 Flange fitting		8		2
G	3/8-16 UNC-2B, .50 deep	steel insert	8		
H	f .255 +.005, - .000, .50 deep	flat bottom	24		
J	standoffs, 1" OD, 1/4" NPT end (detail F)		24		
K	Welded cups, 1.25 OD, .80 ID (detail H)		6		
L	** fitting TBD		1		
M	1/4-20 UNC-2B, .38 dp	steel insert		8	8
N	f .4062 thru			8	8
	welded pockets, dwg FUR003		31	4	4

Complete List of Features

Furnace Box

	31	welded pockets, dwg FUR003		welded pockets for heaters, insulation
J	24	welded standoffs, 1" OD		power feedthroughs
L	1	** fitting TBD		pressure relief fitting
B	1	3/8" NPT		pressure relief fitting
H	24	f .255 +.005, - .000, .50 deep	flat bottom	heater plate locators
K	6	Welded cups, 1.25 OD, .80 ID		hearth plate locators
B	6	3/8" NPT		gas ports
A	3	1/4" NPT		thermocouples
F	2	QF-40 Flange fitting		piston up/down
F	1	QF-40 Flange fitting		debind outlet
F	1	QF-40 Flange fitting		part thermocoouples
F	1	QF-40 Flange fitting		infiltrant gate
F	1	QF-40 Flange fitting		vacuum port
F	2	QF-40 Flange fitting		extras
C	20	4-40 UNC-2B, .20 deep	steel insert	thermostats
D	40	1/4-20 UNC-2B, .38 deep	steel insert	strip heaters
D	8	1/4-20 UNC-2B, .38 deep	steel insert	Guard mounts
D	3	1/4-20 UNC-2B, .38 deep	steel insert	hinge mount
D	8	1/4-20 UNC-2B, .38 deep	steel insert	Mounting Bar mounts
G	8	3/8-16 UNC-2B, .50 deep	steel insert	Door bolts
E	16	8-32 UNC-2B, .25 deep	steel insert	clamps for door

Door 1 (with thermocouples)

	4	welded pockets		insulation
A	6	1/4" NPT		thermocouples
M	8	1/4-20 UNC-2B, .38 dp	steel insert	handles
D	4	1/4-20 UNC-2B, .38 deep	steel insert	strip heaters
C	2	4-40 UNC-2B, .25 deep	steel insert	thermostats
D	3	1/4-20 UNC-2B, .38 deep	steel insert	hinge mount
N	8	f .4062 thru		bolt holes

Door 2 (with viewports)

	4	welded pockets		insulation
F	2	QF-40 Flange fitting		viewports
M	8	1/4-20 UNC-2B, .38 dp	steel insert	handles
D	4	1/4-20 UNC-2B, .38 deep	steel insert	strip heaters
C	2	4-40 UNC-2B, .25 deep	steel insert	thermostats
D	3	1/4-20 UNC-2B, .38 deep	steel insert	hinge mount
N	8	f .4062 thru		bolt holes

Laboratory Vacuum Furnace - **Feature Size and Location Tables**

Lab for Manufacturing and Productivity, 3DP Project

revised 4/29/99, D. Brancazio

TABLE 2	**(FRONT, FUR001 Sheet 1)**	
X, Y location tolerances: +/- .010		
	X	Y
E1	0.824	18.825
E2	1.425	19.426
E3	1.531	18.118
E4	2.132	18.719
E5	17.075	19.426
E6	17.676	18.825
E7	16.368	18.719
E8	16.969	18.118
E9	16.969	3.882
E10	17.676	3.175
E11	16.368	3.281
E12	17.075	2.574
E13	0.824	3.175
E14	1.531	3.882
E15	1.425	2.574
E16	2.132	3.281
G1	0.935	14.444
G2	5.806	19.315
G3	12.694	19.315
G4	17.565	14.444
G5	17.565	7.556
G6	12.694	2.685
G7	5.806	2.685
G8	0.935	7.556

TABLE 3	**(RIGHT SIDE, FUR001 Sheet 1)**	
X, Y location tolerances: +/- .010		
	X	Y
C1	17.536	16.9
C2	18.5	16.9
C3	17.536	5.25
C4	18.5	5.25
D1	4.75	15.65
D2	19	15.65
D3	4.75	6.5
D4	19	6.5
D5	11.875	16.9
D6	11.875	14.4
D7	11.875	7.75
D8	11.875	5.25
D9	1.75	21
D10	22.25	21
D11	1.75	1
D12	22.25	1
J1	7.31	19.21
J2	15.56	19.21
J3	21.56	19.21
J4	7.31	12.21
J5	15.56	12.21
J6	21.56	12.21
J7	7.31	10.06
J8	15.56	10.06
J9	21.56	10.06
J10	7.31	3.06
J11	15.56	3.06
J12	21.56	3.06

TABLE 4 (TOP VIEW, FUR001 Sheet 4)			
X, Y location tolerances: +/- .010			
	X	Y	
A1	14.25	13.25	
A2	14.25	15.25	
B1	3.75	2.5	
B2	14.75	2.5	
C1	4.25	18.5	
C2	4.25	17.536	
C3	14.25	18.5	
C4	14.25	17.536	
D1	3	4.75	
D2	3	19	
D3	15.5	4.75	
D4	15.5	19	
D5	1.75	11.875	
D6	4.25	11.875	
D7	14.25	11.875	
D8	16.75	11.875	
F1	5.25	6	
F2	5.25	15	
F3	9.25	7	
F4	9.25	12	
F5	9.25	18.5	
F6	13.25	10	

TABLE 5 (BACK, FUR001 Sheet 6)		
X, Y location tolerances: +/- .010		
	X	Y
B1	3.75	19.75
B2	14.75	19.75
B3	3.75	2.75
B4	14.75	2.75
C1	14.911	15.25
C2	15.875	15.25
C3	14.911	6.25
C4	15.875	6.25
D1	2.125	16.5
D2	16.375	16.5
D3	2.125	5
D4	16.375	5
D5	9.25	17.75
D6	9.25	15.25
D7	9.25	6.25
D8	9.25	3.75
L1	9.25	11.75

TABLE 6 (LEFT SIDE, FUR001 Sheet 6)		
X, Y location tolerances: +/- .010		
	X	Y
C1	17.536	16.9
C2	18.5	16.9
C3	17.536	5.25
C4	18.5	5.25
D1	4.75	15.65
D2	19	15.65
D3	4.75	6.5
D4	19	6.5
D5	11.875	16.9
D6	11.875	14.4
D7	11.875	7.75
D8	11.875	5.25
D9	1.75	21
D10	22.25	21
D11	1.75	1
D12	22.25	1
D13	1.17	12.75
D14	1.17	11
D15	1.17	9.25
J1	7.31	19.21
J2	15.56	19.21
J3	21.56	19.21
J4	7.31	12.21
J5	15.56	12.21
J6	21.56	12.21
J7	7.31	10.06
J8	15.56	10.06
J9	21.56	10.06
J10	7.31	3.06
J11	15.56	3.06
J12	21.56	3.06

TABLE 7 (SECTION E-E, FUR001 Sheet 7)				TABLE 8 (BOTTOM, FUR001 Sheet 7)			
X, Y location tolerances: +/- .010				X, Y location tolerances: +/- .010			
	X	Y			X	Y	
H1	2.08	3.25		A1	4.25	13.25	
H2	2.08	6.25		B1	9.25	16.75	
H3	2.08	10.375		C1	13	3.786	
H4	2.08	13.375		C2	13	4.75	
H5	2.08	17.5		C3	5.5	3.786	
H6	2.08	20.5		C4	5.5	4.75	
H7	16.42	3.25		D1	14.25	4.75	
H8	16.42	6.25		D2	4.25	4.75	
H9	16.42	10.375		D3	14.25	19	
H10	16.42	13.375		D4	4.25	19	
H11	16.42	17.5		D5	15.5	11.875	
H12	16.42	20.5		D6	13	11.875	
H13	2.58	3.75		D7	5.5	11.875	
H14	2.58	5.75		D8	3	11.875	
H15	2.58	9.875		D9	17.25	1.5	
H16	2.58	13.875		D10	17.25	2.5	
H17	2.58	18		D11	17.25	21.5	
H18	2.58	20		D12	17.25	22.5	
H19	15.92	3.75		D13	1.25	1.5	
H20	15.92	5.75		D14	1.25	2.5	
H21	15.92	9.875		D15	1.25	21.5	
H22	15.92	13.875		D16	1.25	22.5	
H23	15.92	18		F1	9.25	21	
H24	15.92	20		F2	9.25	12	
				K1	12	7	
				K2	6.5	7	
				K3	12	13	
				K4	6.5	13	
				K5	12	19	
				K6	6.5	19	

TABLE 9 (FRONT, FUR002 Sheet 1)		
X, Y location tolerances: +/- .010		
	X	Y
A1	-3.00	4.00
A2	0.00	4.00
A3	-3.00	0.00
A4	0.00	0.00
A5	-3.00	-4.00
A6	0.00	-4.00
C1	3.5	6.482
C2	3.5	5.518
D1	2.00	7.125
D2	2.00	-7.125
D3	0.75	0.00
D4	3.25	0.00
D5	-8.715	2.375
D6	-7.465	0.625
D7	-8.715	-1.125
M1	-6.00	3.25
M2	-4.625	3.25
M3	4.625	3.25
M4	6.00	3.25
M5	-6.00	-3.25
M6	-4.625	-3.25
M7	4.625	-3.25
M8	6.00	-3.25
N1	8.315	3.444
N2	3.444	8.315
N3	-3.444	8.315
N4	-8.315	3.444
N5	-8.315	-3.444
N6	-3.444	-8.315
N7	3.444	-8.315
N8	8.315	-3.444

TABLE 10 (FRONT, FUR010 Sheet1)								
X, Y location tolerances: +/- .010								
	X	Y						
C1	3.5	6.482						
C2	3.5	5.518						
D1	2	7.125						
D2	2	-7.125						
D3	0.75	0						
D4	3.25	0						
D5	-8.715	2.375						
D6	-7.465	0.625						
D7	-8.715	-1.125						
F1	-1	2.5						
F2	-1	6.25						
M1	-6	3.25						
M2	-4.625	3.25						
M3	4.625	3.25						
M4	6	3.25						
M5	-6	-3.25						
M6	-4.625	-3.25						
M7	4.625	-3.25						
M8	6	-3.25						
N1	8.315	3.444						
N2	3.444	8.315						
N3	-3.444	8.315						
N4	-8.315	3.444						
N5	-8.315	-3.444						
N6	-3.444	-8.315						
N7	3.444	-8.315						
N8	8.315	-3.444						

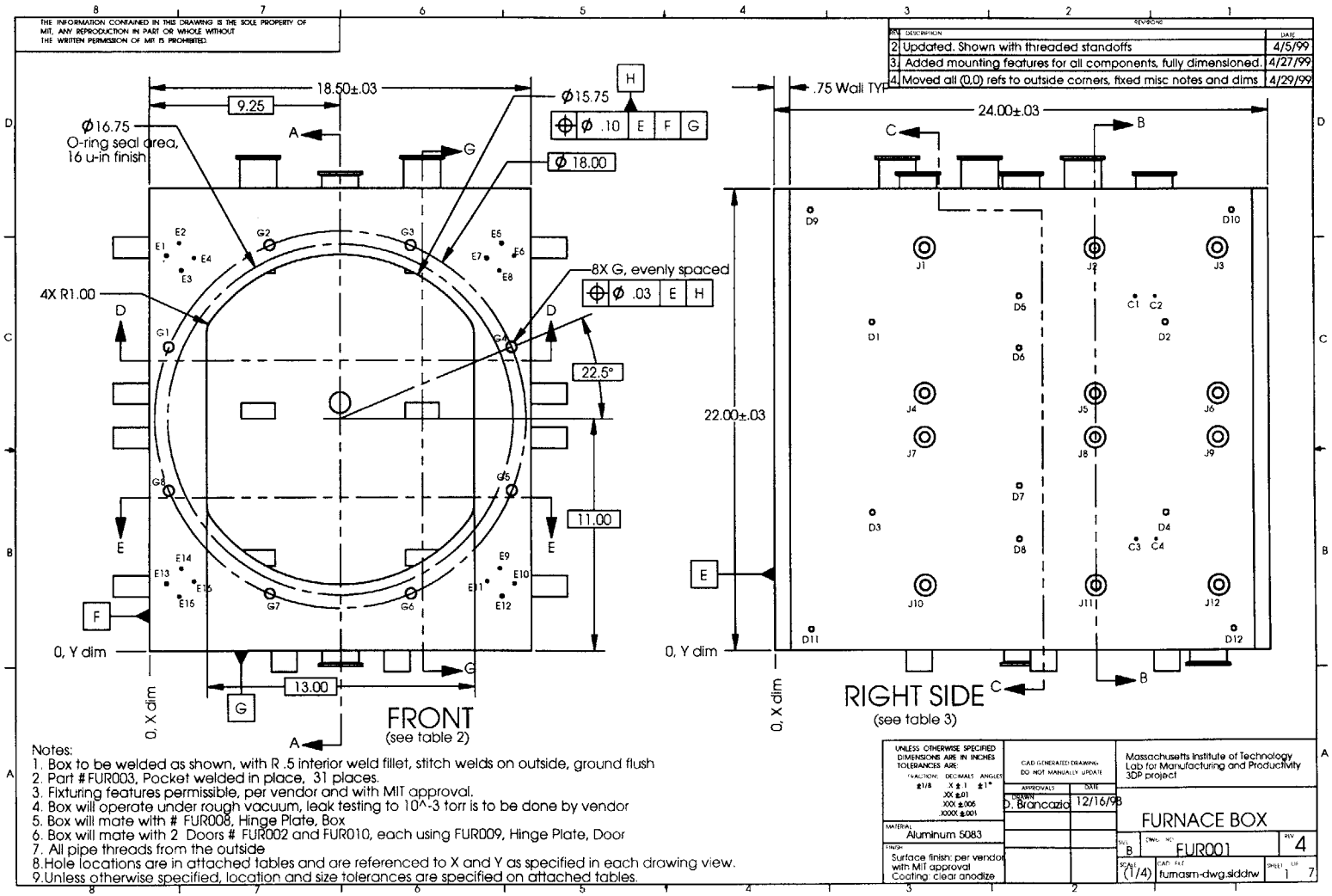
THE INFORMATION CONTAINED IN THIS DRAWING IS THE SOLE PROPERTY OF MIT. ANY REPRODUCTION IN PART OR WHOLE WITHOUT THE WRITTEN PERMISSION OF MIT IS PROHIBITED.
REVISIONS
DESCRIPTION
DATE
2 Updated. Shown with threaded standoffs 4/5/99
3 Added mounting features for all components, fully dimensioned. 4/27/99
4 Moved all (0,0) refs to outside corners, fixed misc notes and dims 4/29/99
18.50±.03
9.25
Ø16.75
O-ring seal area,
16 u-in finish
Ø15.75
Ø .10 E F G
Ø 18.00
8X G, evenly spaced
Ø .03 E H
4X R1.00
22.5°
11.00
13.00
0, Y dim
0, X dim
FRONT
(see table 2)
.75 Wall TYP
24.00±.03
22.00±.03
RIGHT SIDE
(see table 3)
Notes:
1. Box to be welded as shown, with R .5 interior weld fillet, stitch welds on outside, ground flush
2. Part # FUR003, Pocket welded in place, 31 places.
3. Fixturing features permissible, per vendor and with MIT approval.
4. Box will operate under rough vacuum, leak testing to 10^-3 torr is to be done by vendor
5. Box will mate with # FUR008, Hinge Plate, Box
6. Box will mate with 2 Doors # FUR002 and FUR010, each using FUR009, Hinge Plate, Door
7. All pipe threads from the outside
8. Hole locations are in attached tables and are referenced to X and Y as specified in each drawing view.
9. Unless otherwise specified, location and size tolerances are specified on attached tables.
UNLESS OTHERWISE SPECIFIED DIMENSIONS ARE IN INCHES
TOLERANCES ARE:
FRACTIONS DECIMALS ANGLES
±1/8 X ±.1 ±1°
XX ±.01
XXX ±.005
XXXX ±.001
CAD GENERATED DRAWING DO NOT MANUALLY UPDATE
APPROVALS DATE
DRAWN D. Brancazio 12/16/98
MATERIAL Aluminum 5083
FINISH Surface finish: per vendor with MIT approval Coating: clear anodize
Massachusetts Institute of Technology
Lab for Manufacturing and Productivity
3DP project
FURNACE BOX
SIZE B
DWG. NO. FUR001
REV 4
SCALE (1/4)
CAD FILE furnasm-dwg.slddrw
SHEET 1 OF 7

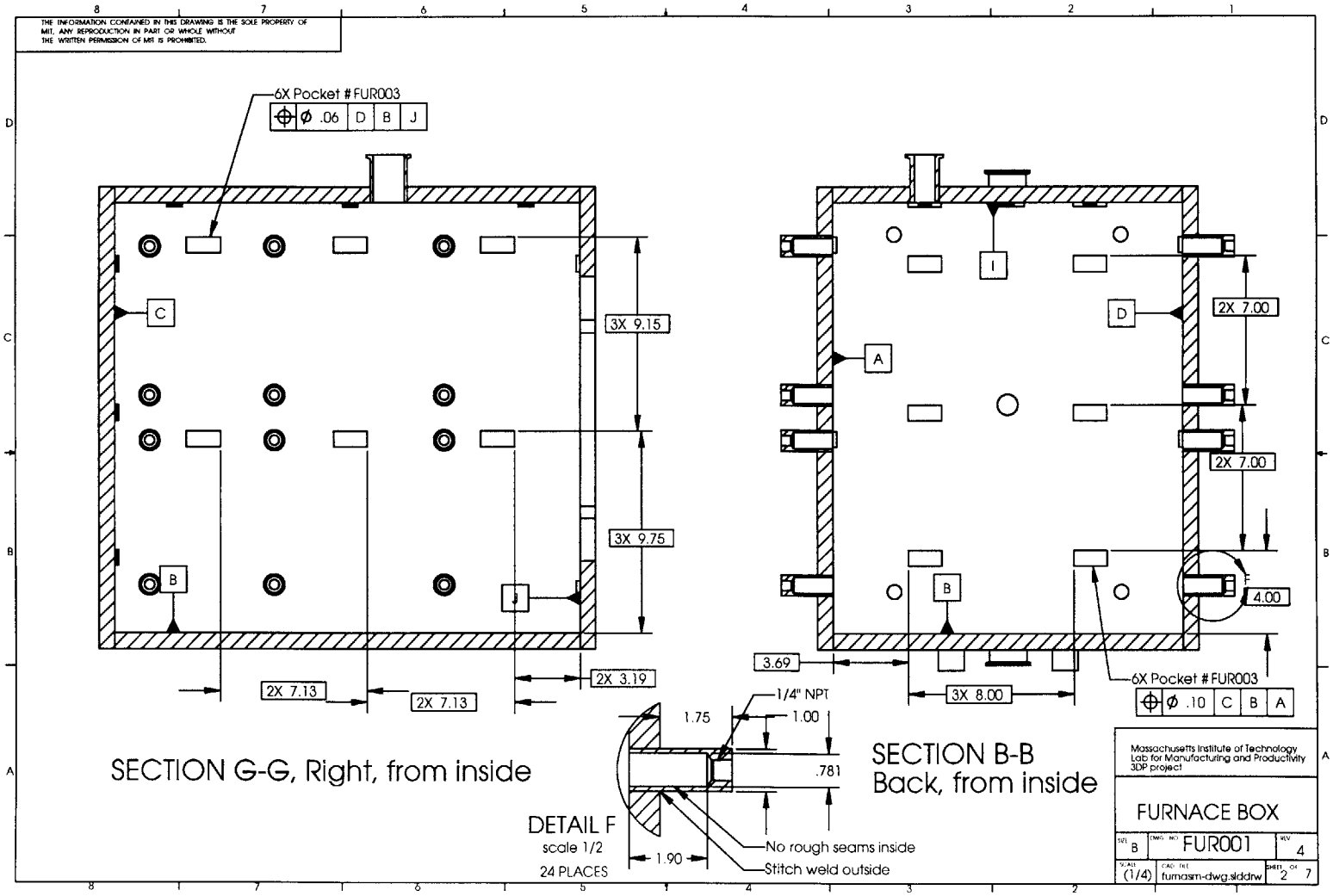
THE INFORMATION CONTAINED IN THIS DRAWING IS THE SOLE PROPERTY OF MIT. ANY REPRODUCTION IN PART OR WHOLE WITHOUT THE WRITTEN PERMISSION OF MIT IS PROHIBITED.
6X Pocket # FUR003
Ø .06 D B J
C
B
J
3X 9.15
3X 9.75
2X 7.13
2X 7.13
2X 3.19
SECTION G-G, Right, from inside
I
D
A
B
2X 7.00
2X 7.00
4.00
3.69
3X 8.00
6X Pocket # FUR003
Ø .10 C B A
SECTION B-B
Back, from inside
1.75
1/4" NPT
1.00
.781
DETAIL F
scale 1/2
24 PLACES
1.90
No rough seams inside
Stitch weld outside
Massachusetts Institute of Technology
Lab for Manufacturing and Productivity
3DP project
FURNACE BOX
SIZE B
DWG. NO. FUR001
REV 4
SCALE (1/4)
CAD FILE furnasm-dwg.slddrw
SHEET 2 OF 7

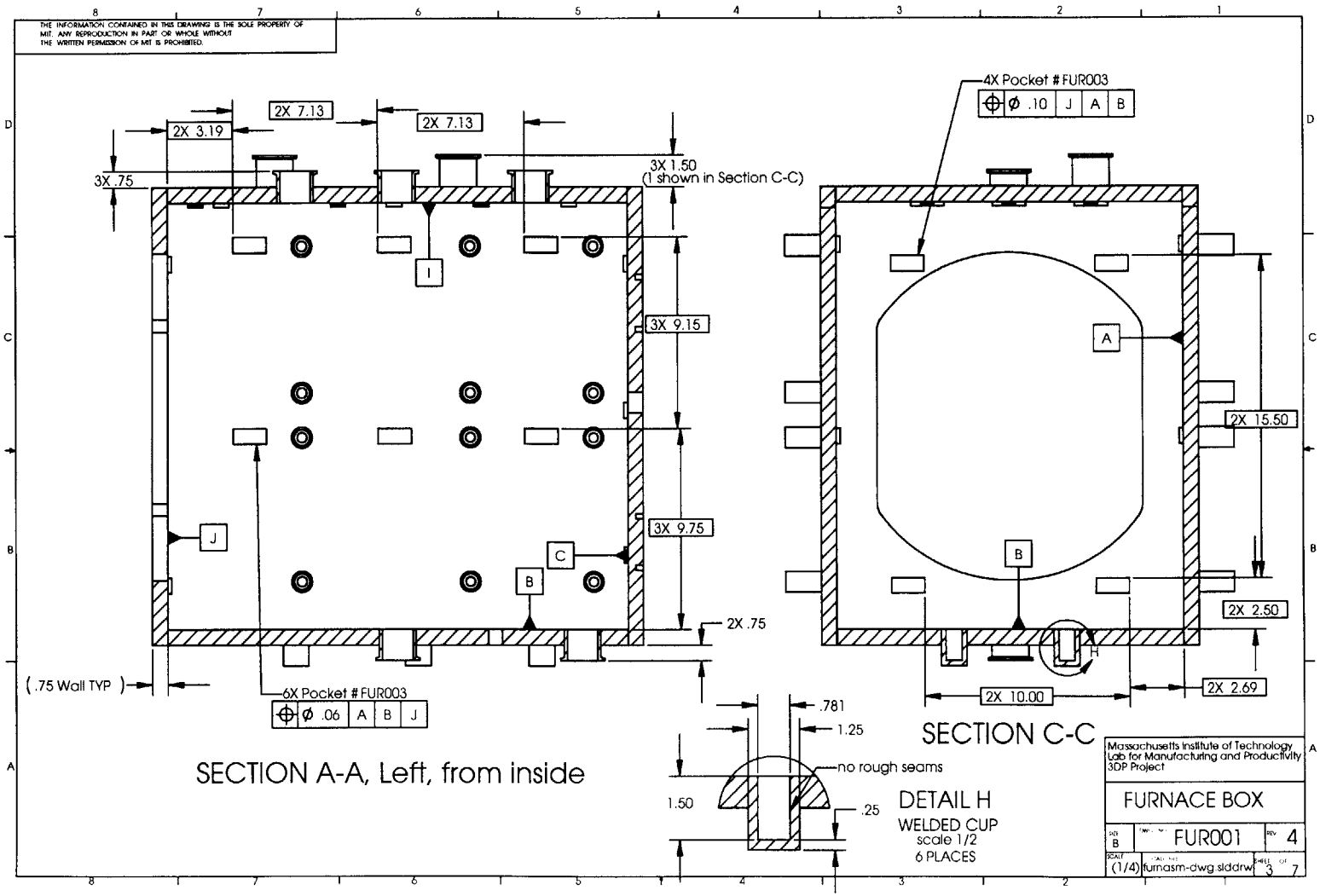
THE INFORMATION CONTAINED IN THIS DRAWING IS THE SOLE PROPERTY OF MIT. ANY REPRODUCTION IN PART OR WHOLE WITHOUT THE WRITTEN PERMISSION OF MIT IS PROHIBITED.
2X 7.13
2X 7.13
2X 3.19
3X .75
3X 1.50
(1 shown in Section C-C)
3X 9.15
3X 9.75
2X .75
(.75 Wall TYP)
6X Pocket # FUR003
Ø .06 A B J
SECTION A-A, Left, from inside
4X Pocket # FUR003
Ø .10 J A B
2X 15.50
2X 2.50
2X 10.00
2X 2.69
SECTION C-C
.781
1.25
no rough seams
1.50
.25
DETAIL H
WELDED CUP
scale 1/2
6 PLACES
Massachusetts Institute of Technology
Lab for Manufacturing and Productivity
3DP Project
FURNACE BOX
FUR001
4
(1/4) furnasm-dwg.slddrw
3 7

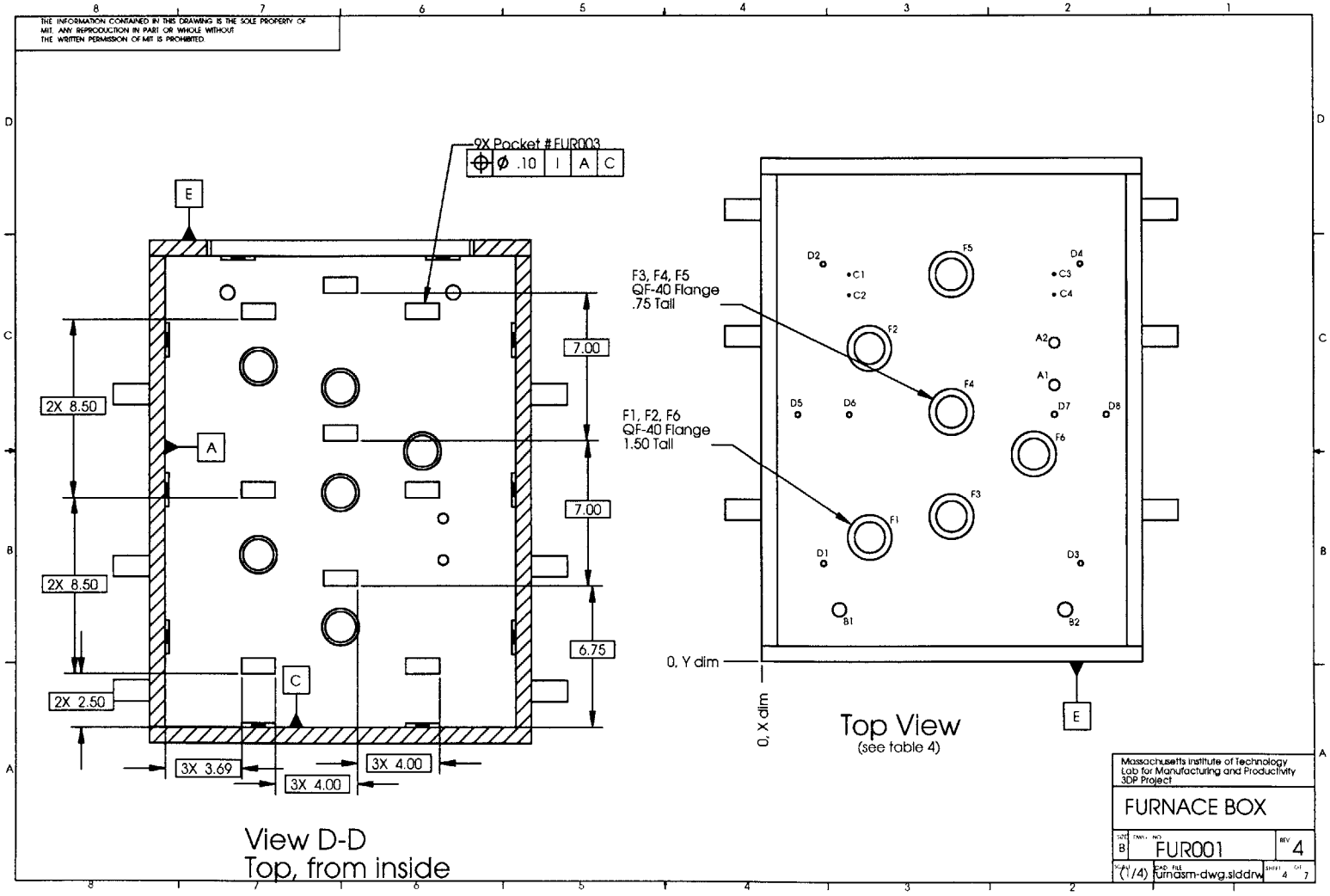
THE INFORMATION CONTAINED IN THIS DRAWING IS THE SOLE PROPERTY OF MIT. ANY REPRODUCTION IN PART OR WHOLE WITHOUT THE WRITTEN PERMISSION OF MIT IS PROHIBITED.
9X Pocket # FUR003
Ø .10 I A C
E
A
C
2X 8.50
2X 8.50
2X 2.50
7.00
7.00
6.75
3X 3.69
3X 4.00
3X 4.00
View D-D
Top, from inside
F3, F4, F5
QF-40 Flange
.75 Tall
F1, F2, F6
QF-40 Flange
1.50 Tall
0, Y dim
0, X dim
Top View
(see table 4)
Massachusetts Institute of Technology
Lab for Manufacturing and Productivity
3DP Project
FURNACE BOX
B
FUR001
4
(1/4)
furnasm-dwg.slddrw

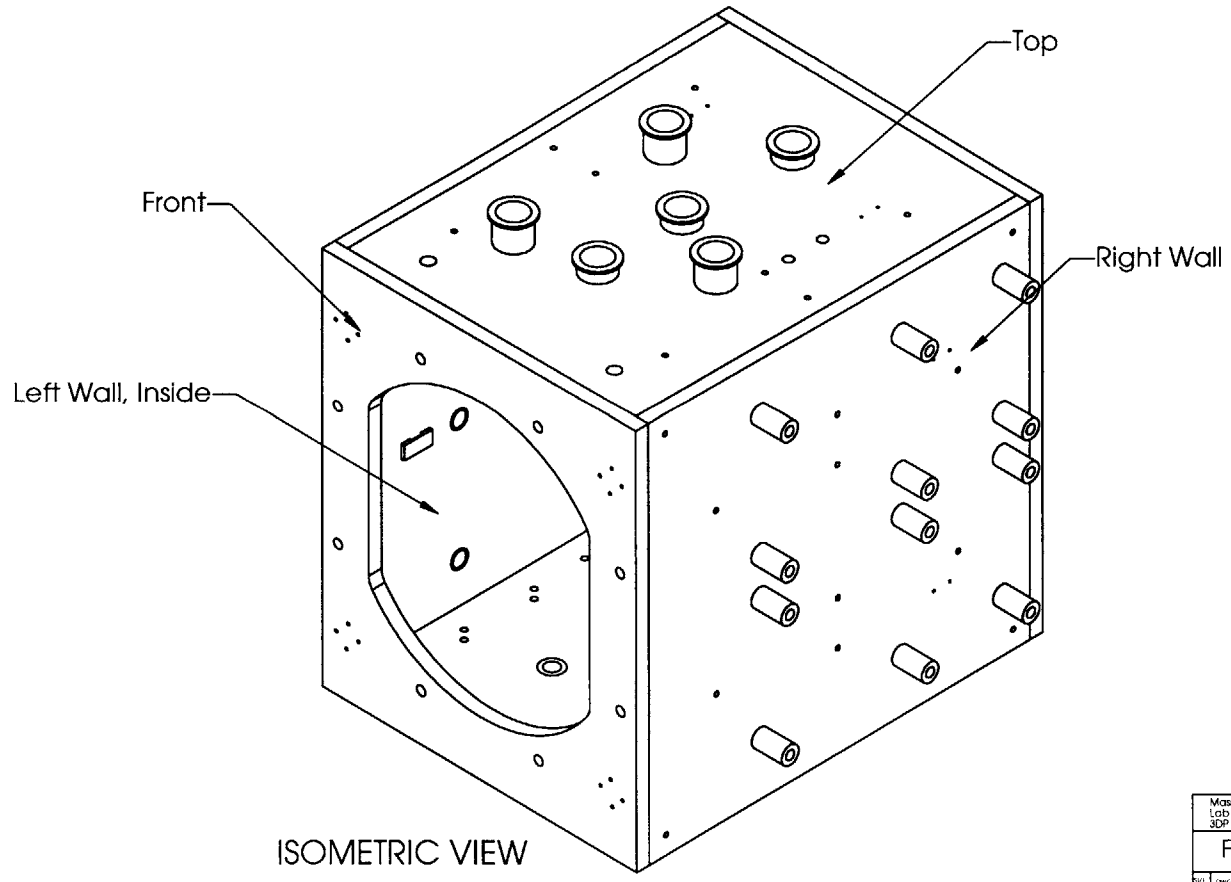

ISOMETRIC VIEW

Massachusetts Institute of Technology
Lab for Manufacturing and Productivity
3DP Project

FURNACE BOX

SIZE	DWG. NO.	REV
B	FUR001	4
SCALE	CAD FILE	SHEET 5 OF 7
(1/4)	furnasm-dwg.siddrw	

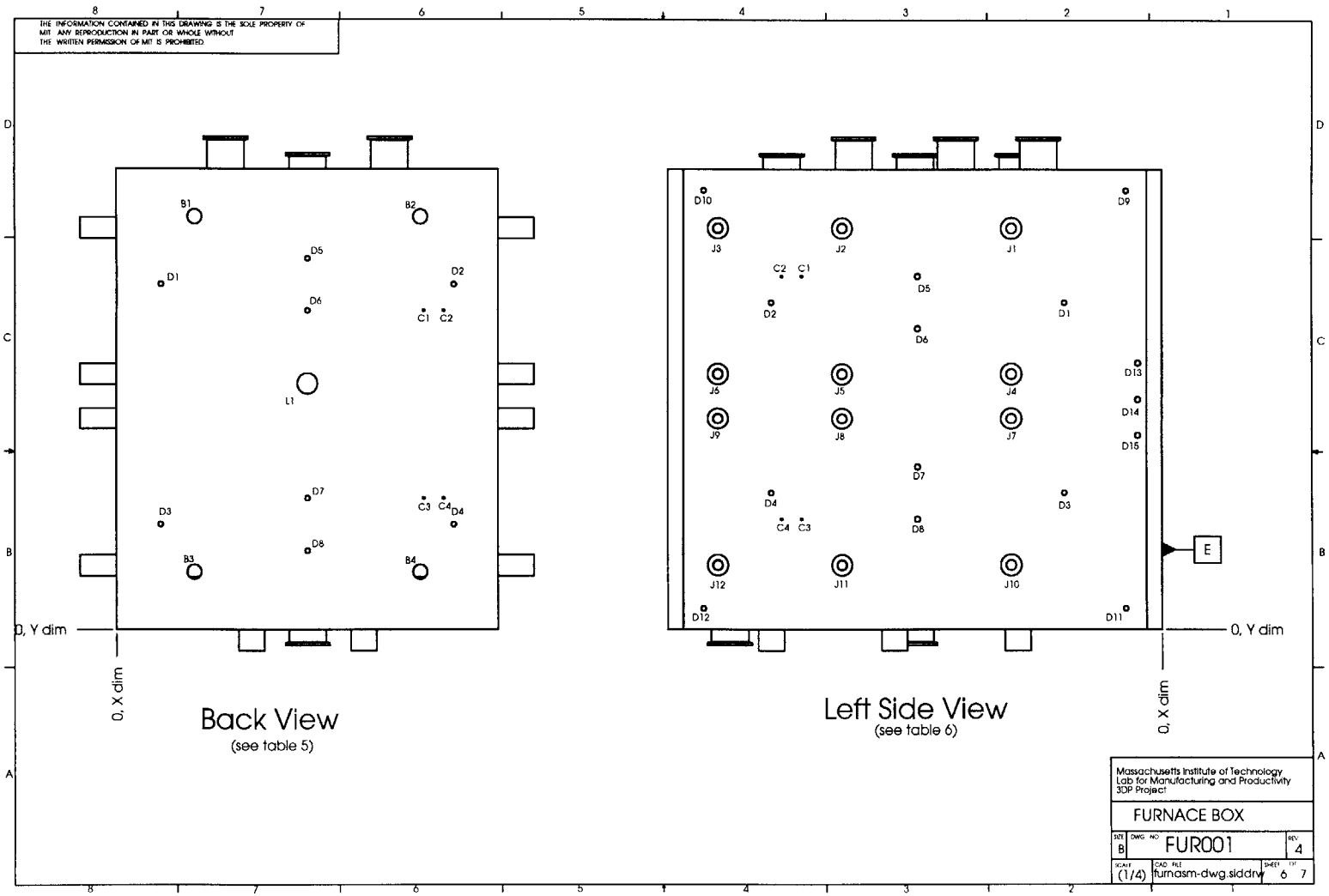

Massachusetts Institute of Technology
Lab for Manufacturing and Productivity
3DP Project

FURNACE BOX

SIZE	DWG NO	REV
B	FUR001	4

SCALE	CAD FILE	SHEET
(1/4)	furnasm-dwg.slddrw	6 7

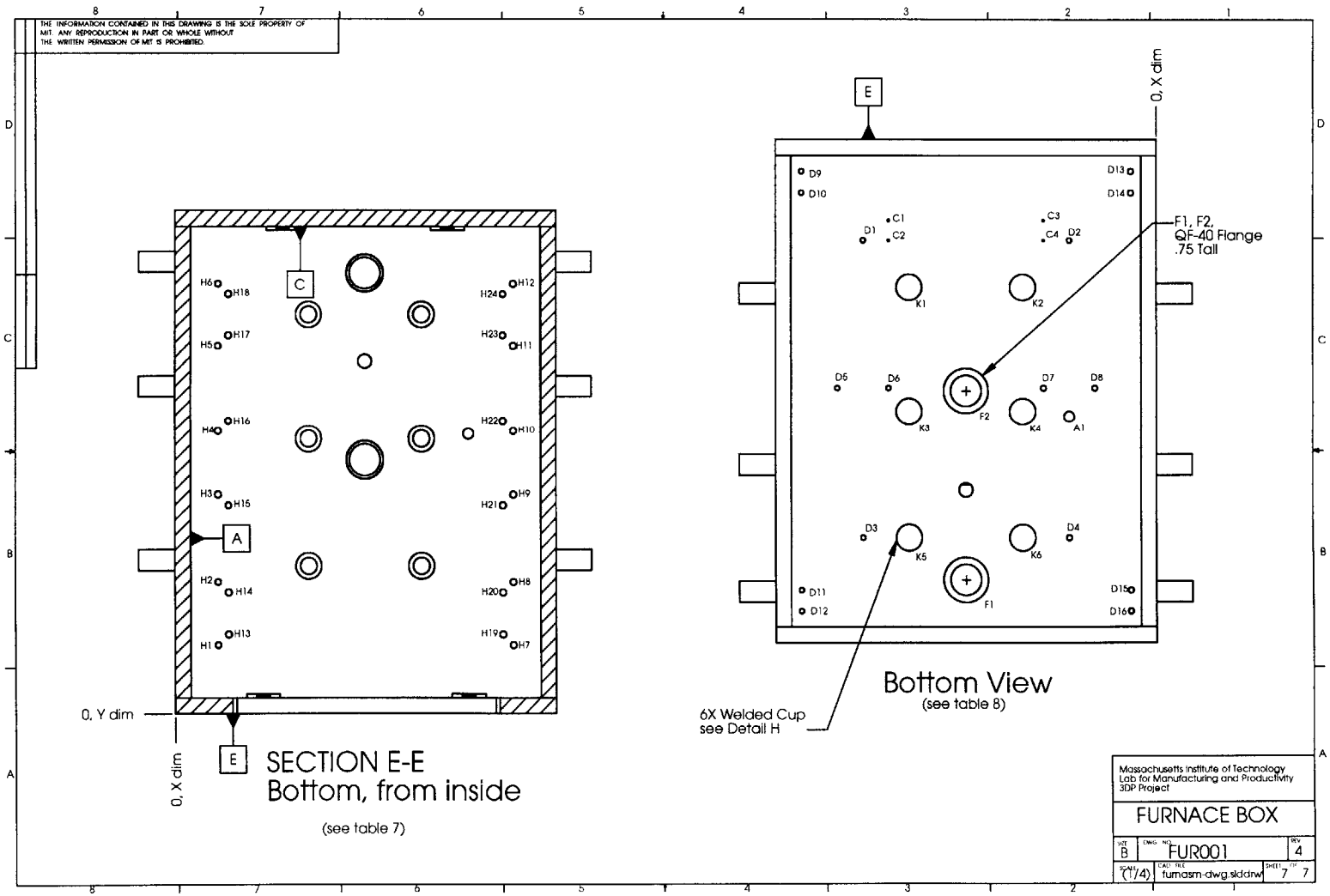
THE INFORMATION CONTAINED IN THIS DRAWING IS THE SOLE PROPERTY OF MIT. ANY REPRODUCTION IN PART OR WHOLE WITHOUT THE WRITTEN PERMISSION OF MIT IS PROHIBITED.
0, X dim
E
F1, F2,
QF-40 Flange
.75 Tall
D9
D10
D13
D14
C1
C2
C3
C4
D1
D2
K1
K2
D5
D6
D7
D8
K3
F2
K4
A1
D3
D4
K5
K6
F1
D11
D12
D15
D16
Bottom View
(see table 8)
6X Welded Cup
see Detail H
H6
H18
H12
H24
H5
H17
H23
H11
H4
H16
H22
H10
H3
H15
H21
H9
H2
H14
H20
H8
H1
H13
H19
H7
C
A
0, Y dim
0, X dim
E
SECTION E-E
Bottom, from inside
(see table 7)
Massachusetts Institute of Technology
Lab for Manufacturing and Productivity
3DP Project
FURNACE BOX
SIZE B
DWG. NO. FUR001
REV 4
SCALE (1/4)
CAD FILE furnasm-dwg.slddrw
SHEET 7 OF 7

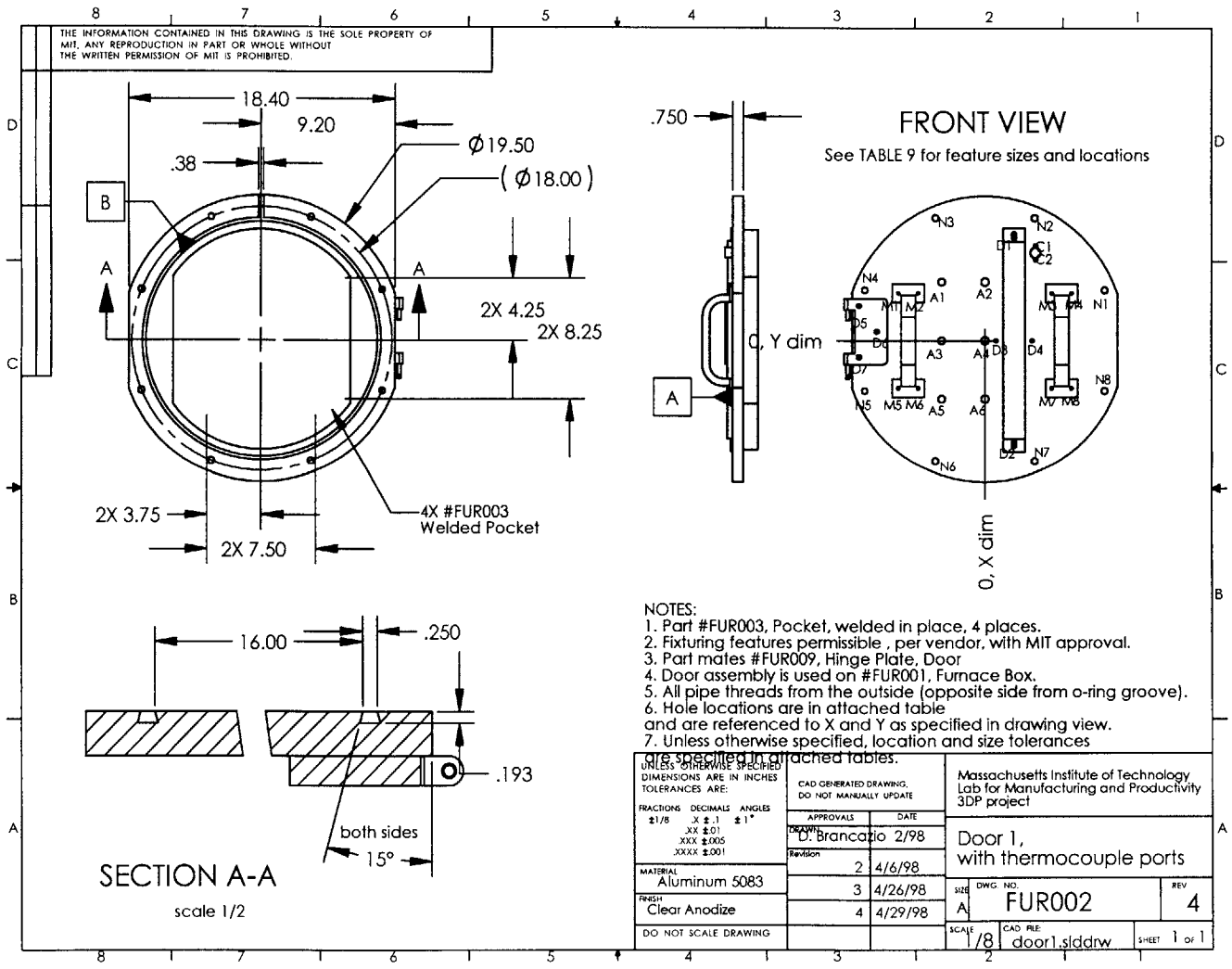
THE INFORMATION CONTAINED IN THIS DRAWING IS THE SOLE PROPERTY OF MIT. ANY REPRODUCTION IN PART OR WHOLE WITHOUT THE WRITTEN PERMISSION OF MIT IS PROHIBITED.
18.40
9.20
.38
Ø19.50
(Ø18.00)
B
A
A
2X 4.25
2X 8.25
2X 3.75
2X 7.50
4X #FUR003
Welded Pocket
.750
C, Y dim
A
FRONT VIEW
See TABLE 9 for feature sizes and locations
N3
N2
D1
C1
C2
N4
A1
A2
N1
M1 M2
M3 M4
D5
D6
A3
A4
D3
D4
D7
N8
N5
M5 M6
A5
A6
M7 M8
D2
N7
N6
0, X dim
16.00
.250
.193
both sides
15°
SECTION A-A
scale 1/2
NOTES:
1. Part #FUR003, Pocket, welded in place, 4 places.
2. Fixturing features permissible , per vendor, with MIT approval.
3. Part mates #FUR009, Hinge Plate, Door
4. Door assembly is used on #FUR001, Furnace Box.
5. All pipe threads from the outside (opposite side from o-ring groove).
6. Hole locations are in attached table
and are referenced to X and Y as specified in drawing view.
7. Unless otherwise specified, location and size tolerances
are specified in attached tables.
UNLESS OTHERWISE SPECIFIED DIMENSIONS ARE IN INCHES TOLERANCES ARE:
FRACTIONS DECIMALS ANGLES
±1/8 .X ±.1 ±1°
.XX ±.01
.XXX ±.005
.XXXX ±.001
CAD GENERATED DRAWING, DO NOT MANUALLY UPDATE
APPROVALS DATE
DRAWN D. Brancazio 2/98
Revision
2 4/6/98
3 4/26/98
4 4/29/98
MATERIAL Aluminum 5083
FINISH Clear Anodize
DO NOT SCALE DRAWING
Massachusetts Institute of Technology
Lab for Manufacturing and Productivity
3DP project
Door 1,
with thermocouple ports
SIZE A
DWG. NO. FUR002
REV 4
SCALE 1/8
CAD FILE: door1.slddrw
SHEET 1 OF 1

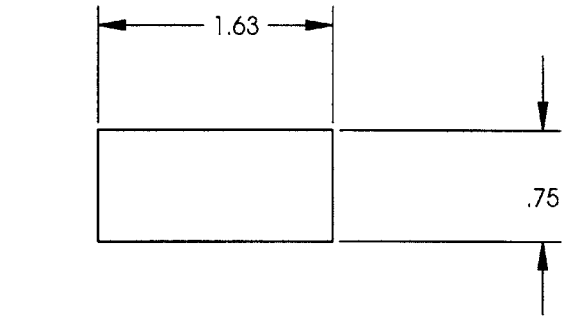

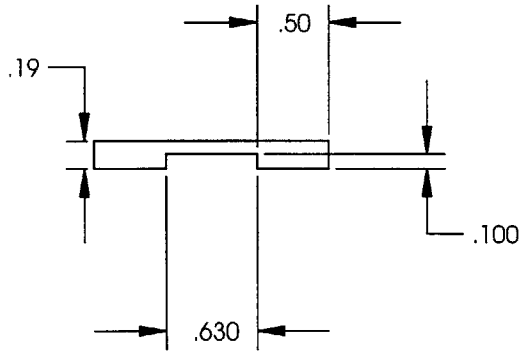

Notes:
1. Used on Part # FUR001, Furnace Box, 31 places, part # FUR002, Door 1, 4 places, and part # FUR010, Door 2, 4 places (Total 39)

UNLESS OTHERWISE SPECIFIED DIMENSIONS ARE IN INCHES TOLERANCES ARE: FRACTIONS ±1/8 DECIMALS .X ±.1 .XX ±.01 .XXX ±.005 .XXXX ±.001 ANGLES ±1°	CAD GENERATED DRAWING. DO NOT MANUALLY UPDATE	Massachusetts Institute of Technology Lab for Manufacturing and Productivity 3DP project
	APPROVALS / DATE	
	DRAWN D. Brancazio 12/15/98	POCKET
	REVISION 2 4/26/99	
MATERIAL Aluminum 6061-T6	3 4/29/99	SIZE A DWG. NO. FUR003 REV 3
FINISH --		
DO NOT SCALE DRAWING		SCALE 1/1 CAD FILE pocket.slddrw SHEET 1 OF 1

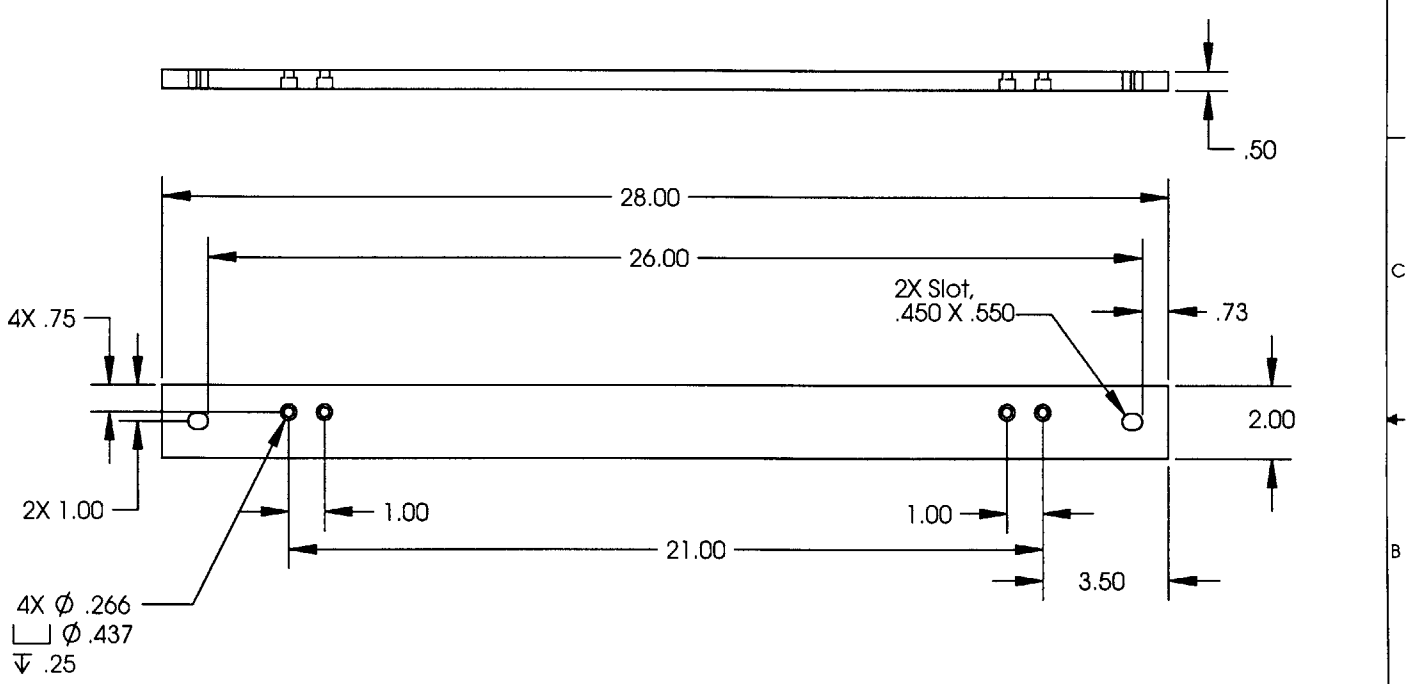

Notes:
1. Used on # FUR001, Furnace Box, 2 Places.

UNLESS OTHERWISE SPECIFIED DIMENSIONS ARE IN INCHES TOLERANCES ARE: FRACTIONS ±1/8 DECIMALS .X ±.1 .XX ±.01 .XXX ±.005 .XXXX ±.001 ANGLES ±1°	CAD GENERATED DRAWING. DO NOT MANUALLY UPDATE	Massachusetts Institute of Technology Lab for Manufacturing and Productivity 3DP project
	APPROVALS / DATE	Mounting Bar, Box
	DRAWN D. Brancazio 4/27/99	
	APPROVED	
MATERIAL Aluminum 6061-T6	REVISION	SIZE A / DWG NO. FUR004 / REV. 1
FINISH --		SCALE 1/4 / CAD FILE / SHEET 1 OF 1
DO NOT SCALE DRAWING		

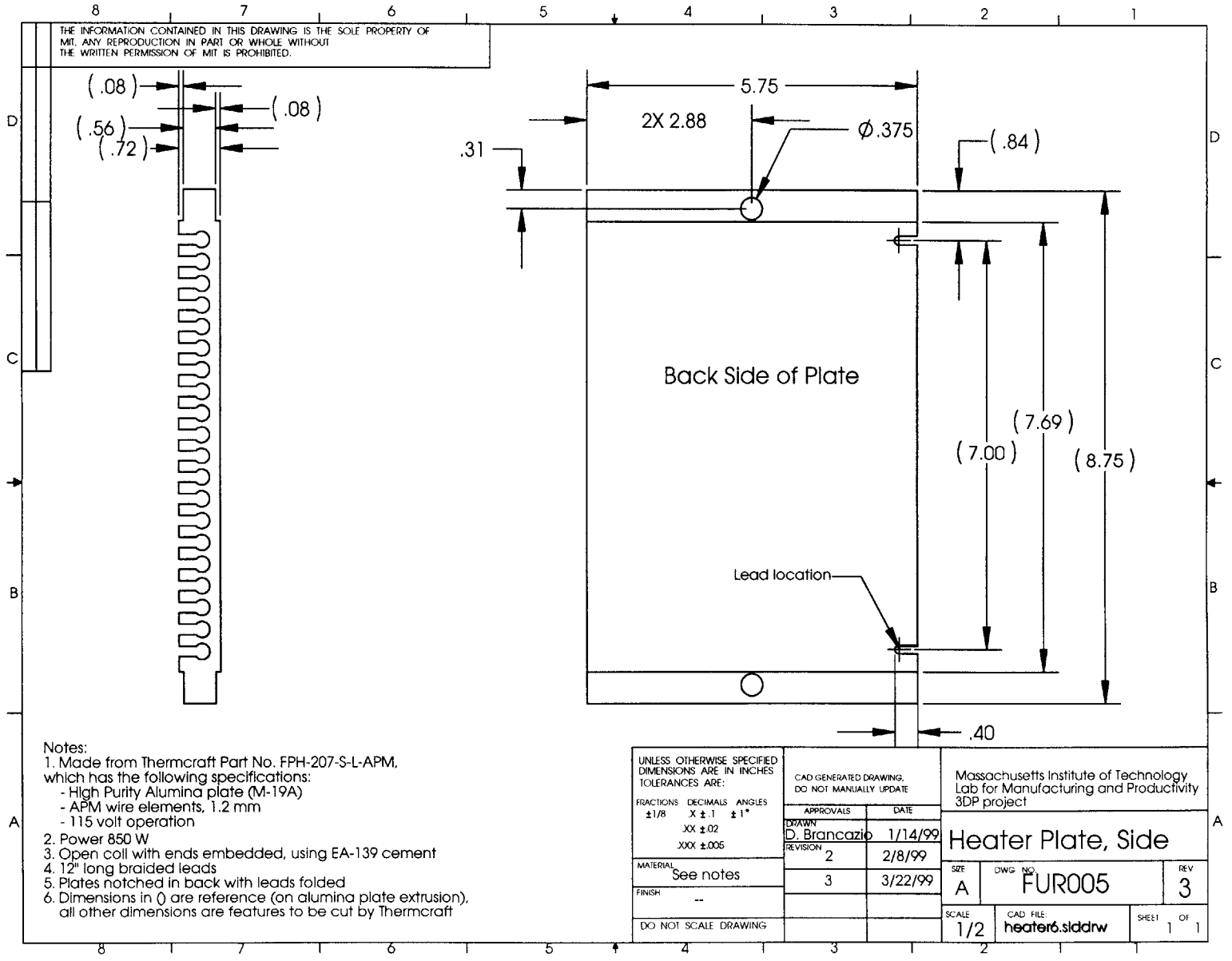
THE INFORMATION CONTAINED IN THIS DRAWING IS THE SOLE PROPERTY OF MIT. ANY REPRODUCTION IN PART OR WHOLE WITHOUT THE WRITTEN PERMISSION OF MIT IS PROHIBITED.
(.08)
(.08)
(.56)
(.72)
5.75
2X 2.88
Ø.375
.31
(.84)
Back Side of Plate
(7.69)
(7.00)
(8.75)
Lead location
.40
Notes:
1. Made from Thermcraft Part No. FPH-207-S-L-APM, which has the following specifications:
- High Purity Alumina plate (M-19A)
- APM wire elements, 1.2 mm
- 115 volt operation
2. Power 850 W
3. Open coil with ends embedded, using EA-139 cement
4. 12" long braided leads
5. Plates notched in back with leads folded
6. Dimensions in () are reference (on alumina plate extrusion), all other dimensions are features to be cut by Thermcraft
UNLESS OTHERWISE SPECIFIED DIMENSIONS ARE IN INCHES
TOLERANCES ARE:
FRACTIONS ±1/8 DECIMALS .X ±.1 ANGLES ±1°
.XX ±.02
.XXX ±.005
MATERIAL See notes
FINISH --
DO NOT SCALE DRAWING
CAD GENERATED DRAWING, DO NOT MANUALLY UPDATE
APPROVALS DATE
DRAWN D. Brancazio 1/14/99
REVISION 2 2/8/99
3 3/22/99
Massachusetts Institute of Technology
Lab for Manufacturing and Productivity
3DP project
Heater Plate, Side
SIZE A
DWG NO FUR005
REV 3
SCALE 1/2
CAD FILE: heater6.slddrw
SHEET 1 OF 1

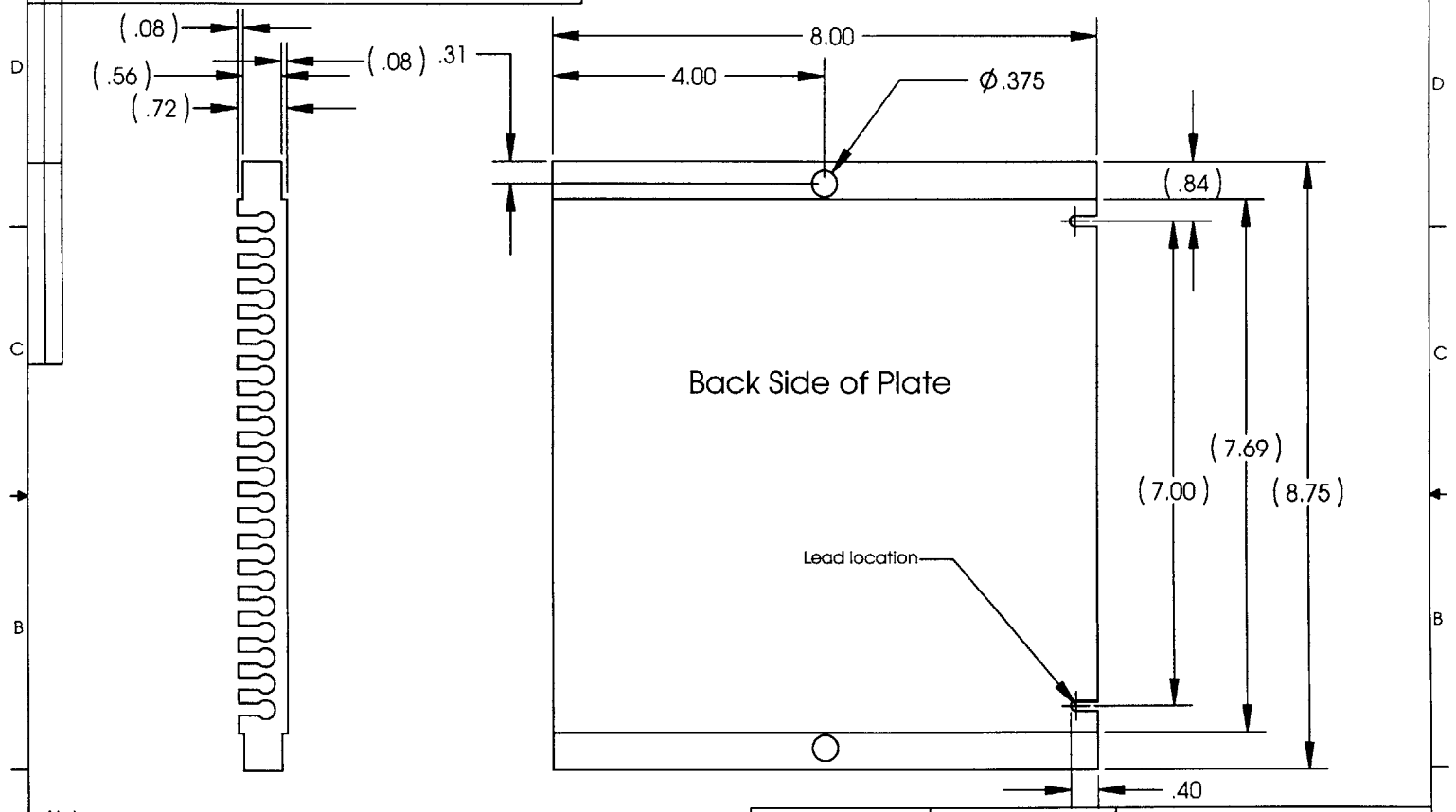

Notes:
1. Made from Thermcraft Part No. FPH-207-S-L-APM, which has the following specifications:
   - High Purity Alumina plate (M-19A)
   - APM wire elements
   - 230 volt operation
2. Power: 1050 W
3. Open coil with ends embedded, using EA-139 cement
4. 12" long braided leads
5. Plates notched in back with leads folded
6. Dimensions in () are reference (on alumina plate extrusion), all other dimensions are features to be cut by Thermcraft

UNLESS OTHERWISE SPECIFIED DIMENSIONS ARE IN INCHES TOLERANCES ARE: FRACTIONS ±1/8 DECIMALS .X ±.1 .XX ±.02 .XXX ±.005 ANGLES ±1°	CAD GENERATED DRAWING. DO NOT MANUALLY UPDATE	Massachusetts Institute of Technology Lab for Manufacturing and Productivity 3DP project
	APPROVALS / DATE	
	DRAWN D. Brancazio 1/14/99	Heater Plate, Middle
	REVISION 2 2/8/99	
MATERIAL See notes	3 3/22/99	SIZE A · DWG NO. FUR006 · REV 3
FINISH --		SCALE 1/2 · CAD FILE: heater8.slddrw · SHEET 1 OF 1
DO NOT SCALE DRAWING		

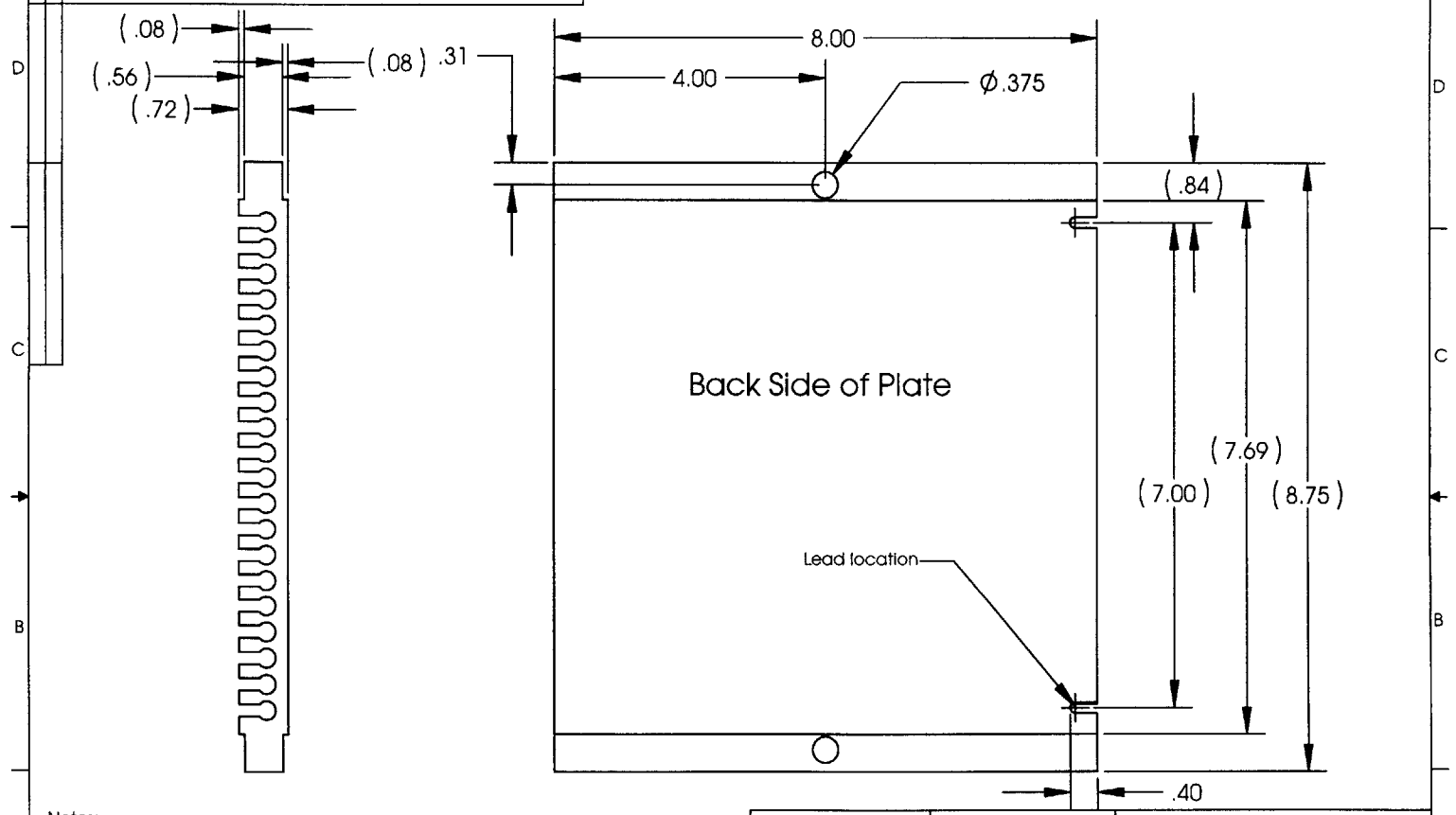

Notes:
1. Made from Thermcraft Part No. FPH-207-S-L-APM, which has the following specifications:
   - High Purity Alumina plate (M-19A)
   - APM wire elements, 1.2 mm
   -115 volt operation
2. Power: 850 W
3. Open coil with ends embedded, using EA-139 cement
4. 12" long braided leads
5. Plates notched in back with leads folded
6. Dimensions in () are reference (on alumina plate extrusion), all other dimensions are features to be cut by Thermcraft

UNLESS OTHERWISE SPECIFIED DIMENSIONS ARE IN INCHES TOLERANCES ARE: FRACTIONS ±1/8 DECIMALS .X ±.1 .XX ±.02 .XXX ±.005 ANGLES ±1°	CAD GENERATED DRAWING. DO NOT MANUALLY UPDATE
MATERIAL See notes	APPROVALS / DATE
FINISH --	DRAWN D. Brancazio 1/14/99
DO NOT SCALE DRAWING	REVISION 2 2/8/99; 3 4/1/99

Massachusetts Institute of Technology
Lab for Manufacturing and Productivity
3DP project

Heater Plate, Middle

SIZE	DWG. NO.	REV.
A	FUR007	3

SCALE	CAD FILE:	SHEET OF
1/2	heater8.slddrw	1 1

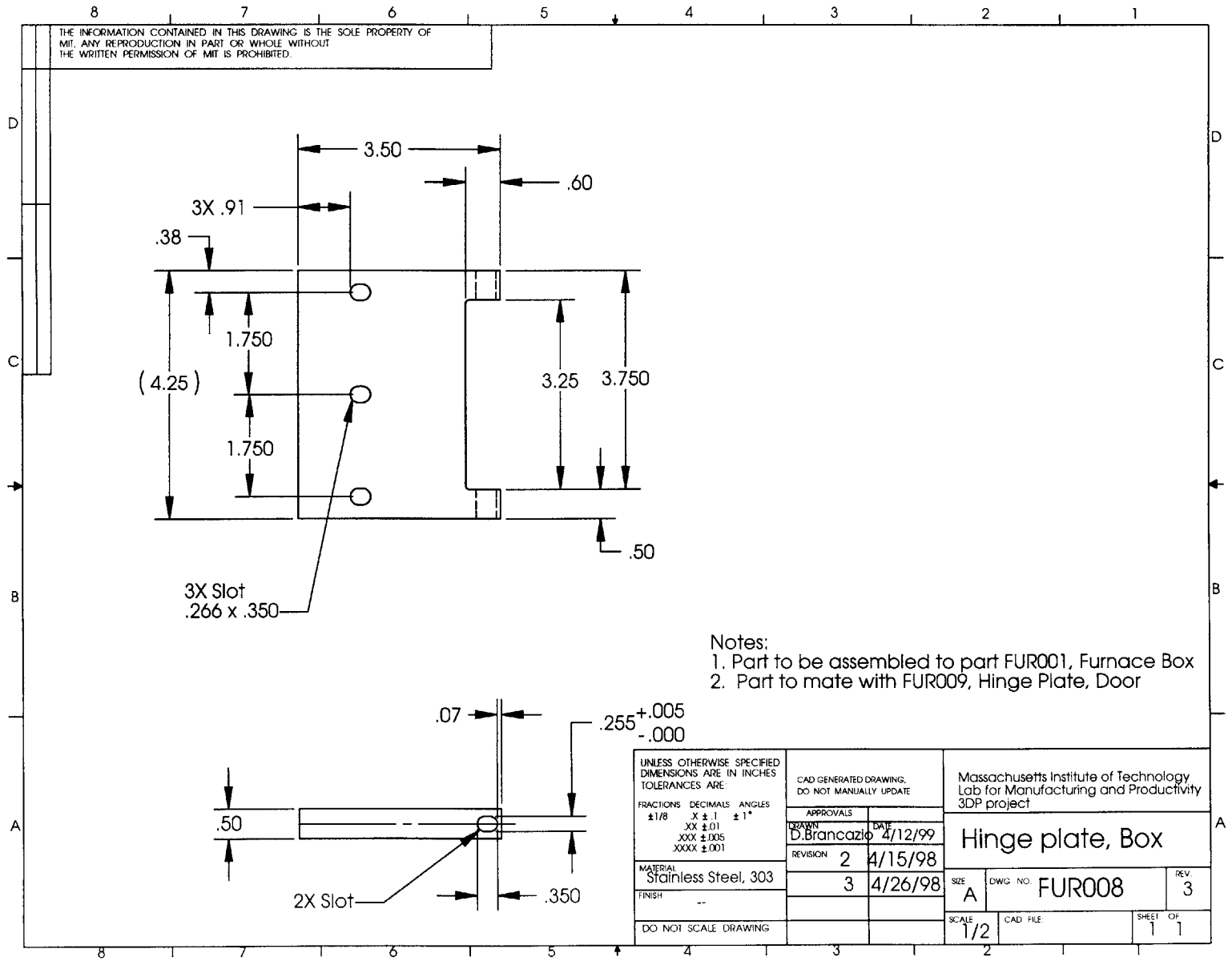
THE INFORMATION CONTAINED IN THIS DRAWING IS THE SOLE PROPERTY OF MIT. ANY REPRODUCTION IN PART OR WHOLE WITHOUT THE WRITTEN PERMISSION OF MIT IS PROHIBITED.
3.50
.60
3X .91
.38
1.750
(4.25)
1.750
3.25
3.750
.50
3X Slot
.266 x .350
.07
.255 +.005 -.000
.50
2X Slot
.350
Notes:
1. Part to be assembled to part FUR001, Furnace Box
2. Part to mate with FUR009, Hinge Plate, Door
UNLESS OTHERWISE SPECIFIED DIMENSIONS ARE IN INCHES TOLERANCES ARE:
FRACTIONS ±1/8 DECIMALS .X ±.1 .XX ±.01 .XXX ±.005 .XXXX ±.001 ANGLES ±1°
MATERIAL Stainless Steel, 303
FINISH --
DO NOT SCALE DRAWING
CAD GENERATED DRAWING. DO NOT MANUALLY UPDATE
APPROVALS
DRAWN D.Brancazio 4/12/99
REVISION 2 4/15/98
3 4/26/98
Massachusetts Institute of Technology
Lab for Manufacturing and Productivity
3DP project
Hinge plate, Box
SIZE A
DWG NO. FUR008
REV. 3
SCALE 1/2
CAD FILE
SHEET 1 OF 1

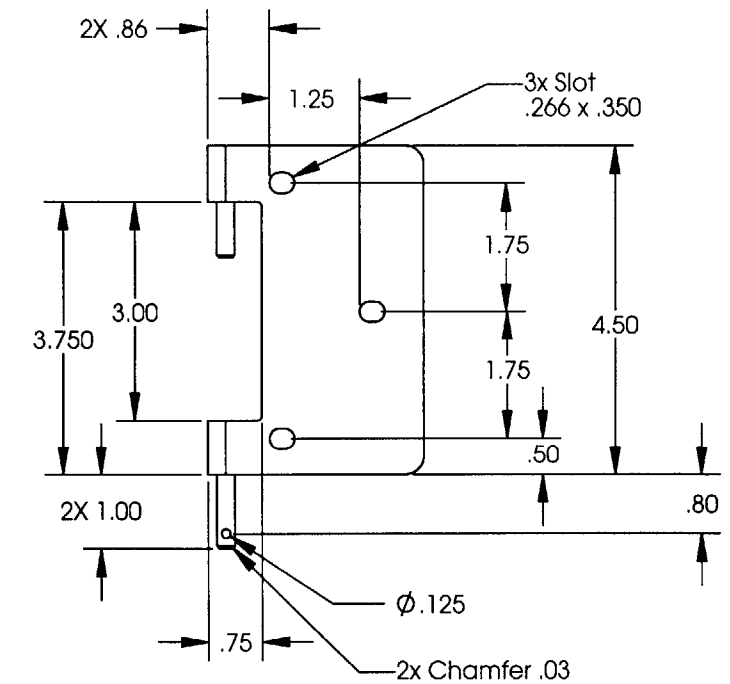

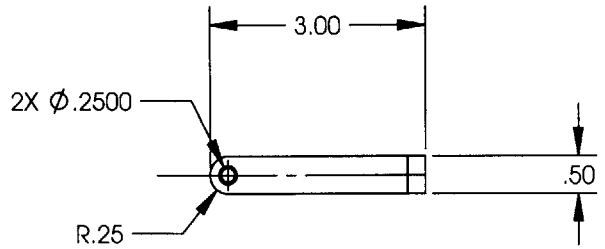

Notes:
1. Part to be assembled to parts FUR002, Door 1 and FUR010, Door 2 (Quantity 2)
2. Part to mate with FUR008, Hinge Plate, Box

UNLESS OTHERWISE SPECIFIED DIMENSIONS ARE IN INCHES TOLERANCES ARE: FRACTIONS ±1/8 DECIMALS .X ±.1 .XX ±.01 .XXX ±.005 .XXXX ±.001 ANGLES ±1°	CAD GENERATED DRAWING. DO NOT MANUALLY UPDATE	Massachusetts Institute of Technology Lab for Manufacturing and Productivity 3DP project
	APPROVALS / DATE	
	DRAWN D.Brancazio 4/12/99	Hinge plate, Door
	REVISION 2 4/15/99	
MATERIAL Stainless Steel, 303	3 4/26/99	SIZE A DWG. NO. FUR009 REV 3
FINISH --		SCALE 1/1 CAD FILE: SHEET 1 OF 1
DO NOT SCALE DRAWING		

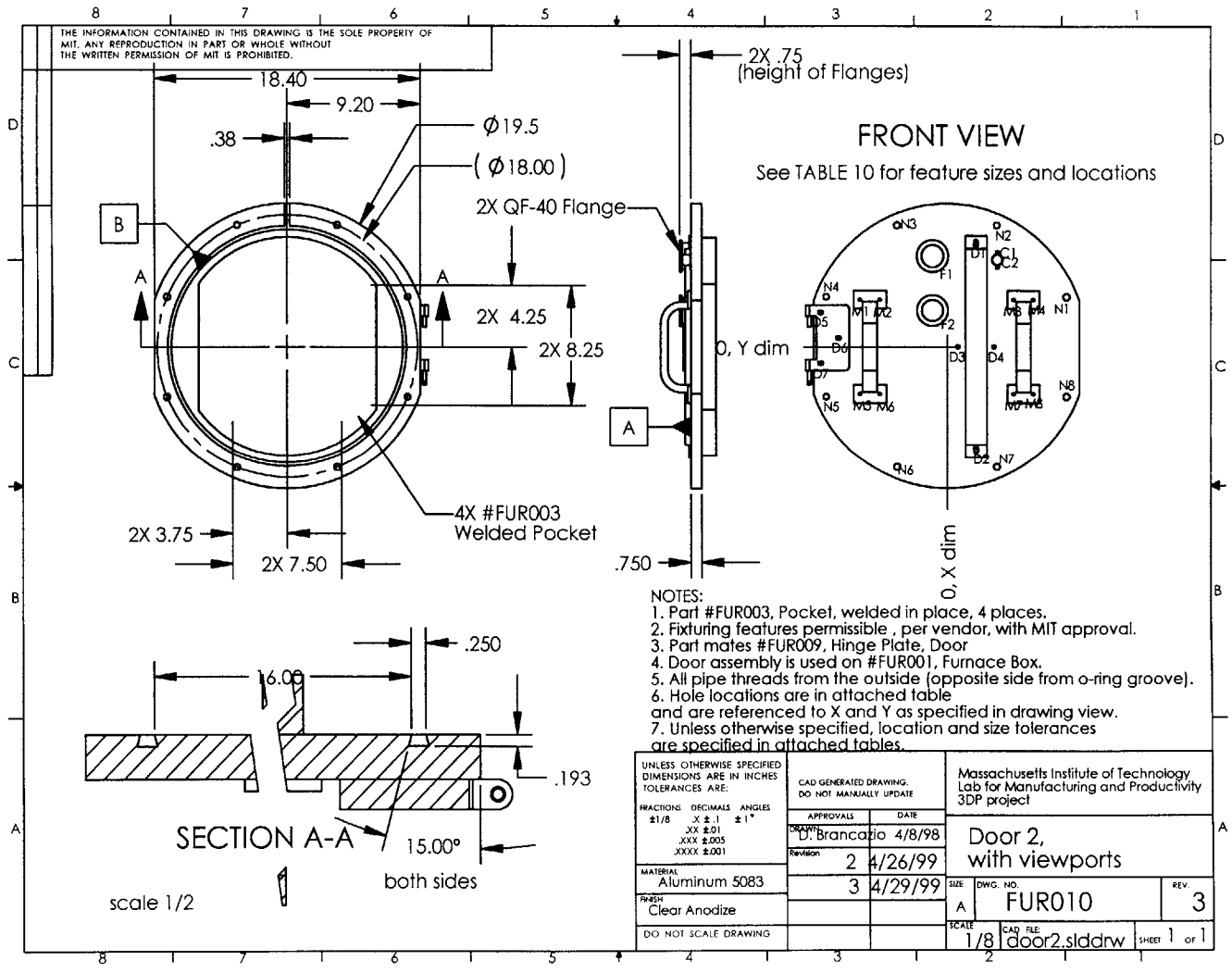
THE INFORMATION CONTAINED IN THIS DRAWING IS THE SOLE PROPERTY OF MIT. ANY REPRODUCTION IN PART OR WHOLE WITHOUT THE WRITTEN PERMISSION OF MIT IS PROHIBITED.
18.40
9.20
.38
Ø19.5
(Ø18.00)
2X QF-40 Flange
2X .75
(height of Flanges)
FRONT VIEW
See TABLE 10 for feature sizes and locations
2X 4.25
2X 8.25
0, Y dim
0, X dim
2X 3.75
2X 7.50
4X #FUR003
Welded Pocket
.750
.250
16.00
.193
SECTION A-A
15.00°
both sides
scale 1/2
NOTES:
1. Part #FUR003, Pocket, welded in place, 4 places.
2. Fixturing features permissible , per vendor, with MIT approval.
3. Part mates #FUR009, Hinge Plate, Door
4. Door assembly is used on #FUR001, Furnace Box.
5. All pipe threads from the outside (opposite side from o-ring groove).
6. Hole locations are in attached table
and are referenced to X and Y as specified in drawing view.
7. Unless otherwise specified, location and size tolerances
are specified in attached tables.
UNLESS OTHERWISE SPECIFIED DIMENSIONS ARE IN INCHES TOLERANCES ARE:
FRACTIONS ±1/8 DECIMALS .X ±.1 .XX ±.01 .XXX ±.005 .XXXX ±.001 ANGLES ±1°
MATERIAL Aluminum 5083
FINISH Clear Anodize
DO NOT SCALE DRAWING
CAD GENERATED DRAWING. DO NOT MANUALLY UPDATE
APPROVALS DATE
DRAWN D. Brancazio 4/8/98
Revision 2 4/26/99
3 4/29/99
Massachusetts Institute of Technology
Lab for Manufacturing and Productivity
3DP project
Door 2,
with viewports
SIZE A
DWG. NO. FUR010
REV. 3
SCALE 1/8
CAD FILE: door2.slddrw
SHEET 1 OF 1

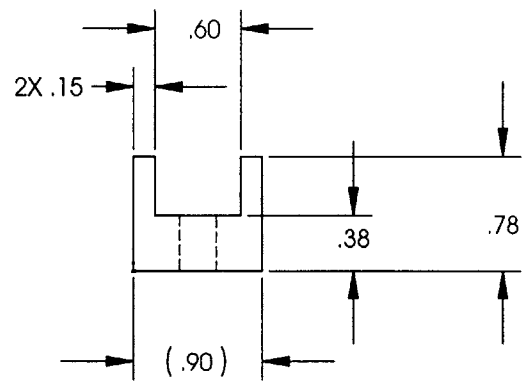

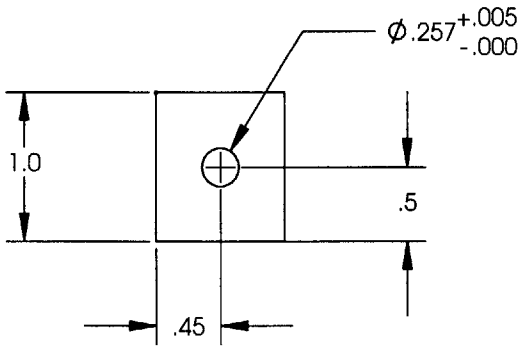

Notes:
1. Quantity: 14

UNLESS OTHERWISE SPECIFIED DIMENSIONS ARE IN INCHES TOLERANCES ARE: FRACTIONS ±1/8 DECIMALS .X ±.1 .XX ±.01 .XXX ±.005 .XXXX ±.001 ANGLES ±1°	CAD GENERATED DRAWING. DO NOT MANUALLY UPDATE	Massachusetts Institute of Technology Lab for Manufacturing and Productivity 3DP project
	APPROVALS / DATE	
	DRAWN D. Brancazio 4/13/99	Mount, Heater, Lower
	REVISION 2 6/8/99	
MATERIAL Inconel 600		SIZE A / DWG NO FUR011 / REV. 2
FINISH --		
DO NOT SCALE DRAWING		SCALE 1/1 / CAD FILE / SHEET 1 OF 1

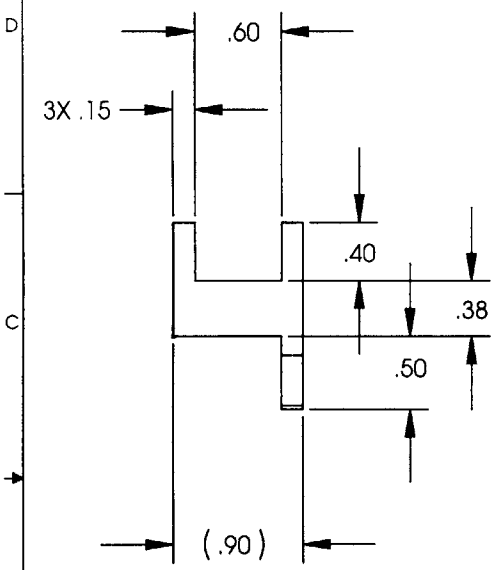

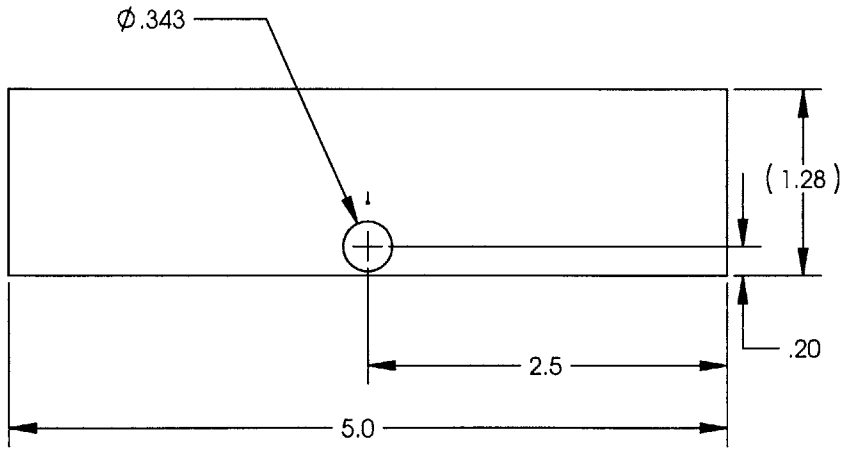

Notes:
1. Quantity: 6

UNLESS OTHERWISE SPECIFIED DIMENSIONS ARE IN INCHES TOLERANCES ARE: FRACTIONS ±1/8 DECIMALS .X ±.1 .XX ±.01 .XXX ±.005 .XXXX ±.001 ANGLES ±1°	CAD GENERATED DRAWING, DO NOT MANUALLY UPDATE	Massachusetts Institute of Technology Lab for Manufacturing and Productivity 3DP project	
	APPROVALS / DRAWN: D. Brancazio 4/13/99 / APPROVED		Mount, Heater, Upper
MATERIAL Inconel 600	REVISION 2 6/8/99	SIZE A	DWG. NO FUR012 REV 2
FINISH --		SCALE 1/1	CAD FILE SHEET 1 OF 1
DO NOT SCALE DRAWING			

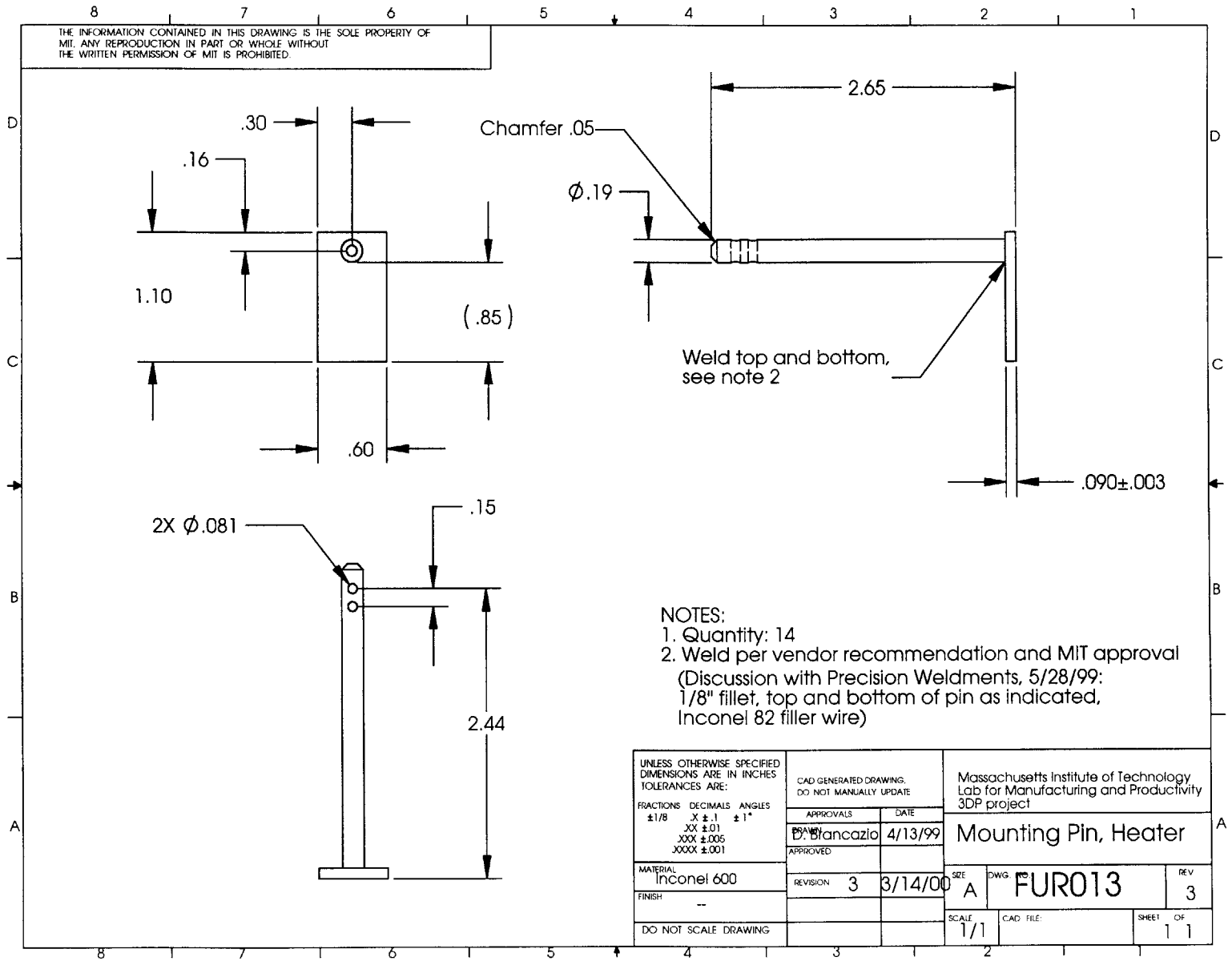

NOTES:
1. Quantity: 14
2. Weld per vendor recommendation and MIT approval
   (Discussion with Precision Weldments, 5/28/99:
   1/8" fillet, top and bottom of pin as indicated,
   Inconel 82 filler wire)

UNLESS OTHERWISE SPECIFIED DIMENSIONS ARE IN INCHES TOLERANCES ARE: FRACTIONS ±1/8 DECIMALS X ±.1 XX ±.01 XXX ±.005 XXXX ±.001 ANGLES ±1°	CAD GENERATED DRAWING. DO NOT MANUALLY UPDATE	Massachusetts Institute of Technology Lab for Manufacturing and Productivity 3DP project
	APPROVALS / DRAWN: D. Biancazio 4/13/99 / APPROVED	Mounting Pin, Heater
MATERIAL Inconel 600	REVISION 3 3/14/00	SIZE A DWG. NO. FUR013 REV 3
FINISH --		SCALE 1/1 CAD FILE: SHEET 1 OF 1
DO NOT SCALE DRAWING		

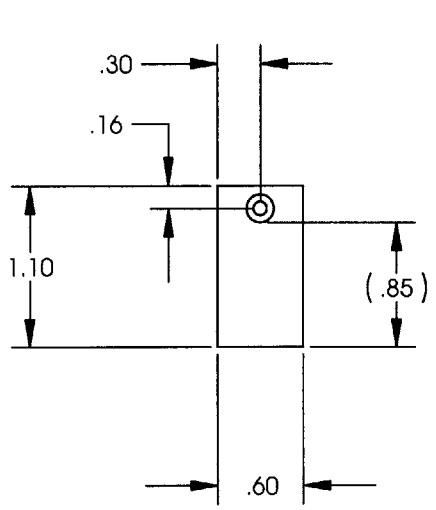

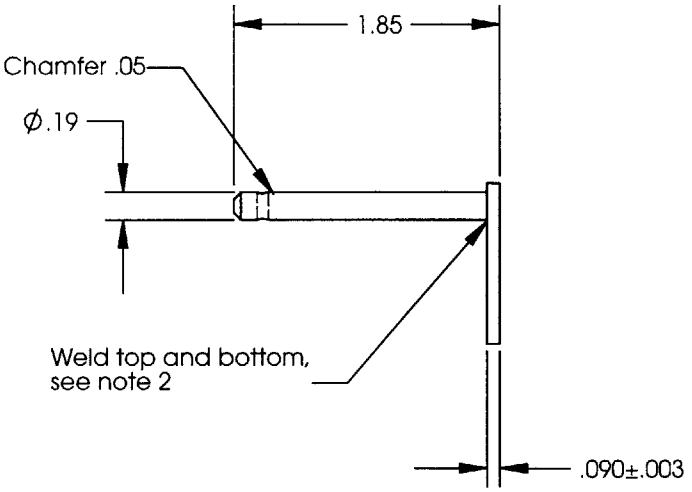

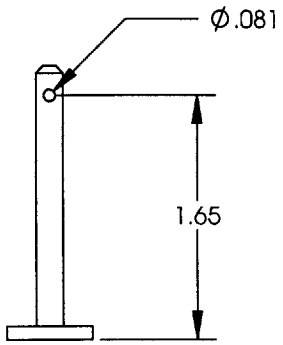

Notes:
1. Quantity: 24
2. Weld per vendor recommendation and MIT approval (Discussion with Precision Weldments, 5/28/99: 1/8" fillet, top and bottom of pin as indicated, Inconel 82 filler wire)

UNLESS OTHERWISE SPECIFIED DIMENSIONS ARE IN INCHES TOLERANCES ARE: FRACTIONS ±1/8 DECIMALS .X ±.1 .XX ±.01 .XXX ±.005 .XXXX ±.001 ANGLES ±1°	CAD GENERATED DRAWING. DO NOT MANUALLY UPDATE	Massachusetts Institute of Technology Lab for Manufacturing and Productivity 3DP project	
	APPROVALS / DRAWN: D. Biancazio	DATE 4/13/99	Mounting Pin, Insulation
MATERIAL Inconel 600	APPROVED		SIZE A / DWG. NO. FUR014 / REV. 3
FINISH --	REVISION 3	3/14/00	
DO NOT SCALE DRAWING			SCALE 1/1 / CAD FILE: / SHEET 1 OF 1

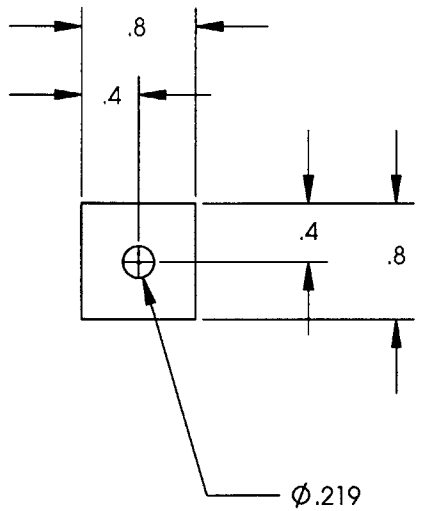

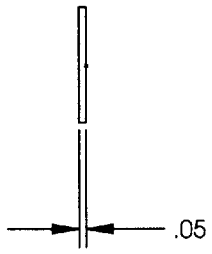

Notes;
1. Quantity: 42

UNLESS OTHERWISE SPECIFIED DIMENSIONS ARE IN INCHES TOLERANCES ARE: FRACTIONS ±1/8 DECIMALS .X ±.1 .XX ±.01 .XXX ±.005 .XXXX ±.001 ANGLES ±1°	CAD GENERATED DRAWING. DO NOT MANUALLY UPDATE	Massachusetts Institute of Technology Lab for Manufacturing and Productivity 3DP project	
MATERIAL Inconel 600	APPROVALS / DRAWN D. Brancazio	DATE 5/4/99	Washer, inconel
FINISH --	APPROVED		
DO NOT SCALE DRAWING	REVISION 2	6/8/99	SIZE A / DWG NO. FUR015 / REV. 2
			SCALE 1/1 / CAD FILE / SHEET 1 OF 1

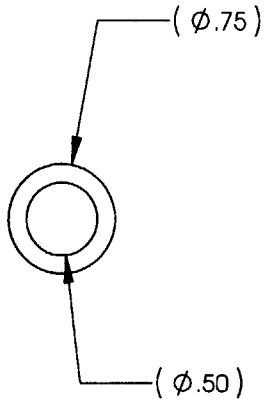

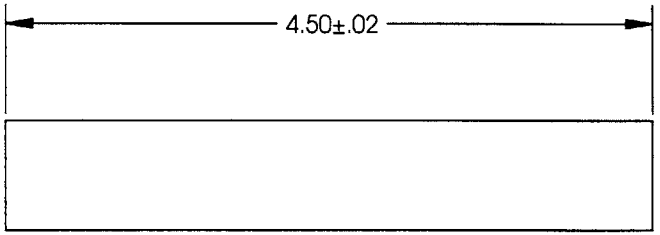

Quantity: 8

UNLESS OTHERWISE SPECIFIED DIMENSIONS ARE IN INCHES
TOLERANCES ARE:
FRACTIONS DECIMALS ANGLES
±1/8 .X ±.1 ±1°
.XX ±.01
.XXX ±.005
.XXXX ±.001

MATERIAL: Mullite
FINISH: --
DO NOT SCALE DRAWING

CAD GENERATED DRAWING.
DO NOT MANUALLY UPDATE

APPROVALS	DATE
DRAWN D. Brancazio	4/13/99
APPROVED	
REVISION	

Massachusetts Institute of Technology
Lab for Manufacturing and Productivity
3DP project

Ceramic Tube, hearthplate support

SIZE	DWG NO	REV
A	FUR016	1

SCALE	CAD FILE	SHEET OF
1/1		1 1

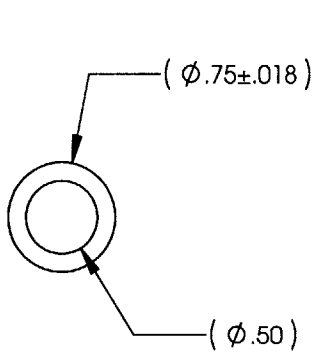

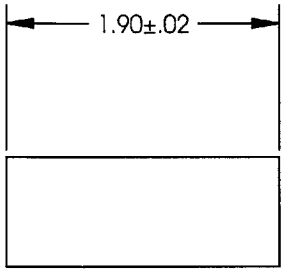

Quantity; 30

UNLESS OTHERWISE SPECIFIED DIMENSIONS ARE IN INCHES TOLERANCES ARE: FRACTIONS ±1/8 DECIMALS .X ±.1 .XX ±.01 .XXX ±.005 .XXXX ±.001 ANGLES ± 1°	CAD GENERATED DRAWING. DO NOT MANUALLY UPDATE	Massachusetts Institute of Technology Lab for Manufacturing and Productivity 3DP project	
	APPROVALS / DATE		
	DRAWN D. Brancazio 4/13/99	Ceramic Tube, electrical insulation	
	APPROVED		
MATERIAL Mullite	REVISION	SIZE A / DWG. NO. FUR017	REV. 1
FINISH --		SCALE 1/1 / CAD FILE	SHEET 1 OF 1
DO NOT SCALE DRAWING			

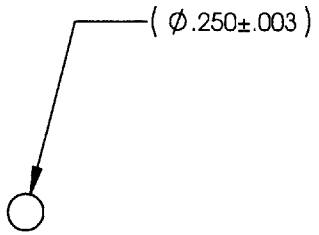

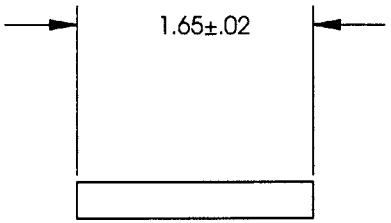

Notes:
1. Quantity: 15
2. Requires high precision rod for close fit, use High Purity Alumina (94%) Rod

UNLESS OTHERWISE SPECIFIED DIMENSIONS ARE IN INCHES TOLERANCES ARE: FRACTIONS ±1/8 DECIMALS .X ±.1 .XX ±.01 .XXX ±.005 .XXXX ±.001 ANGLES ±1°	CAD GENERATED DRAWING. DO NOT MANUALLY UPDATE	Massachusetts Institute of Technology Lab for Manufacturing and Productivity 3DP project
	APPROVALS / DATE	
	DRAWN D. Brancazio 4/13/99	Ceramic Rod, heater location
	REVISION 2 5/4/99	
MATERIAL see note 2		SIZE A DWG NO FUR018 REV 2
FINISH —		SCALE 1/1 CAD FILE: SHEET 1 OF 1
DO NOT SCALE DRAWING		

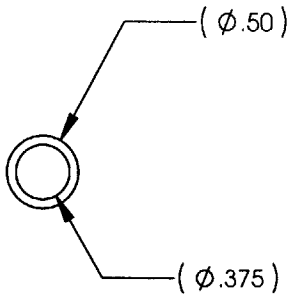

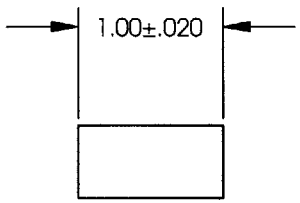

Quantity: 15

UNLESS OTHERWISE SPECIFIED DIMENSIONS ARE IN INCHES TOLERANCES ARE: FRACTIONS ±1/8 DECIMALS .X ±.1 .XX ±.01 .XXX ±.005 .XXXX ±.001 ANGLES ±1°	CAD GENERATED DRAWING. DO NOT MANUALLY UPDATE	Massachusetts Institute of Technology Lab for Manufacturing and Productivity 3DP project
	APPROVALS / DATE	
	DRAWN D. Brancazio 4/13/99	CeramicTube, Heater Support
	APPROVED	
MATERIAL Mullite	REVISION	SIZE A / DWG. NO. FUR019 / REV. 1
FINISH --		SCALE 1/1 / CAD FILE. / SHEET 1 OF 1
DO NOT SCALE DRAWING		

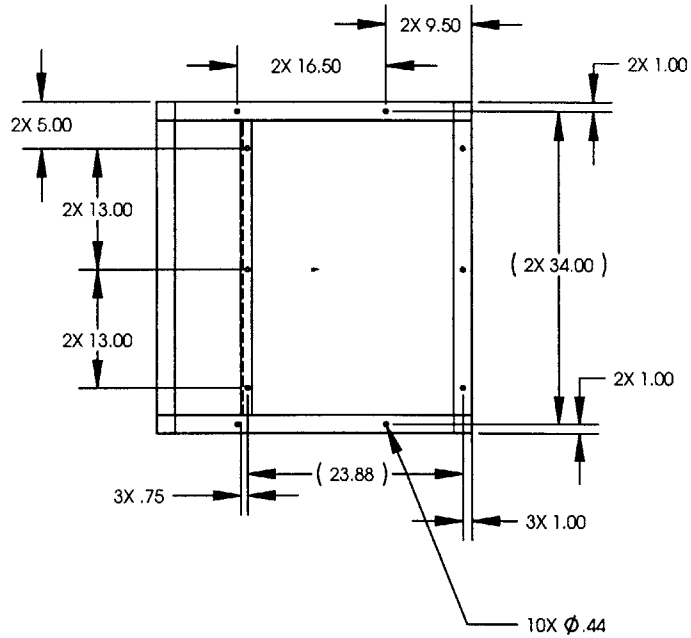

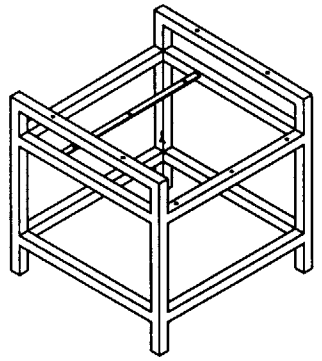

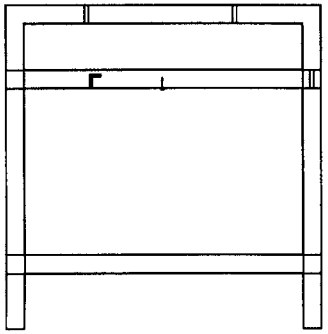

UNLESS OTHERWISE SPECIFIED DIMENSIONS ARE IN INCHES TOLERANCES ARE: FRACTIONS DECIMALS ANGLES ±1/8 .X ±.1 ±1° .XX ±.01 .XXX ±.005 .XXXX ±.001	CAD GENERATED DRAWING. DO NOT MANUALLY UPDATE	Massachusetts Institute of Technology Lab for Manufacturing and Productivity 3DP project
	APPROVALS / DATE	
	DRAWN D. Brancazio 6/29/99	FRAME MODIFICATIONS
	APPROVED	
MATERIAL	REVISION	SIZE A / DWG. NO. FUR020 / REV 1
FINISH --		SCALE 1/16 / CAD FILE: / SHEET 1 OF 1
DO NOT SCALE DRAWING		

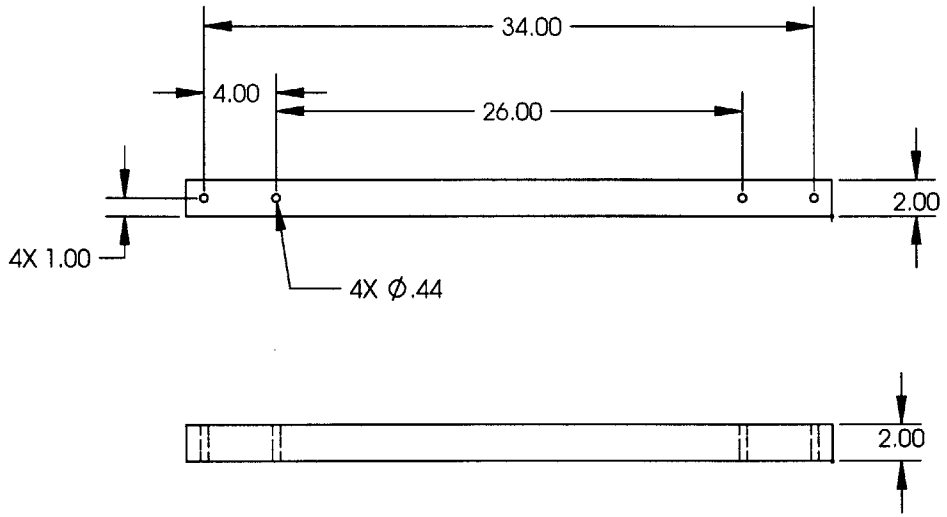

UNLESS OTHERWISE SPECIFIED DIMENSIONS ARE IN INCHES
TOLERANCES ARE:
FRACTIONS ±1/8 DECIMALS .X ±.1 .XX ±.01 .XXX ±.005 .XXXX ±.001 ANGLES ±1°

MATERIAL: Steel Square Tubing
FINISH: --
DO NOT SCALE DRAWING

CAD GENERATED DRAWING. DO NOT MANUALLY UPDATE

APPROVALS	DATE
DRAWN D. Brancazio	6/29/99
APPROVED	
REVISION	

Massachusetts Institute of Technology
Lab for Manufacturing and Productivity
3DP project

FRAME PIECES, NEW

SIZE	DWG. NO	REV.
A	FUR021	1

SCALE	CAD FILE	SHEET 1 OF 1
1/8		

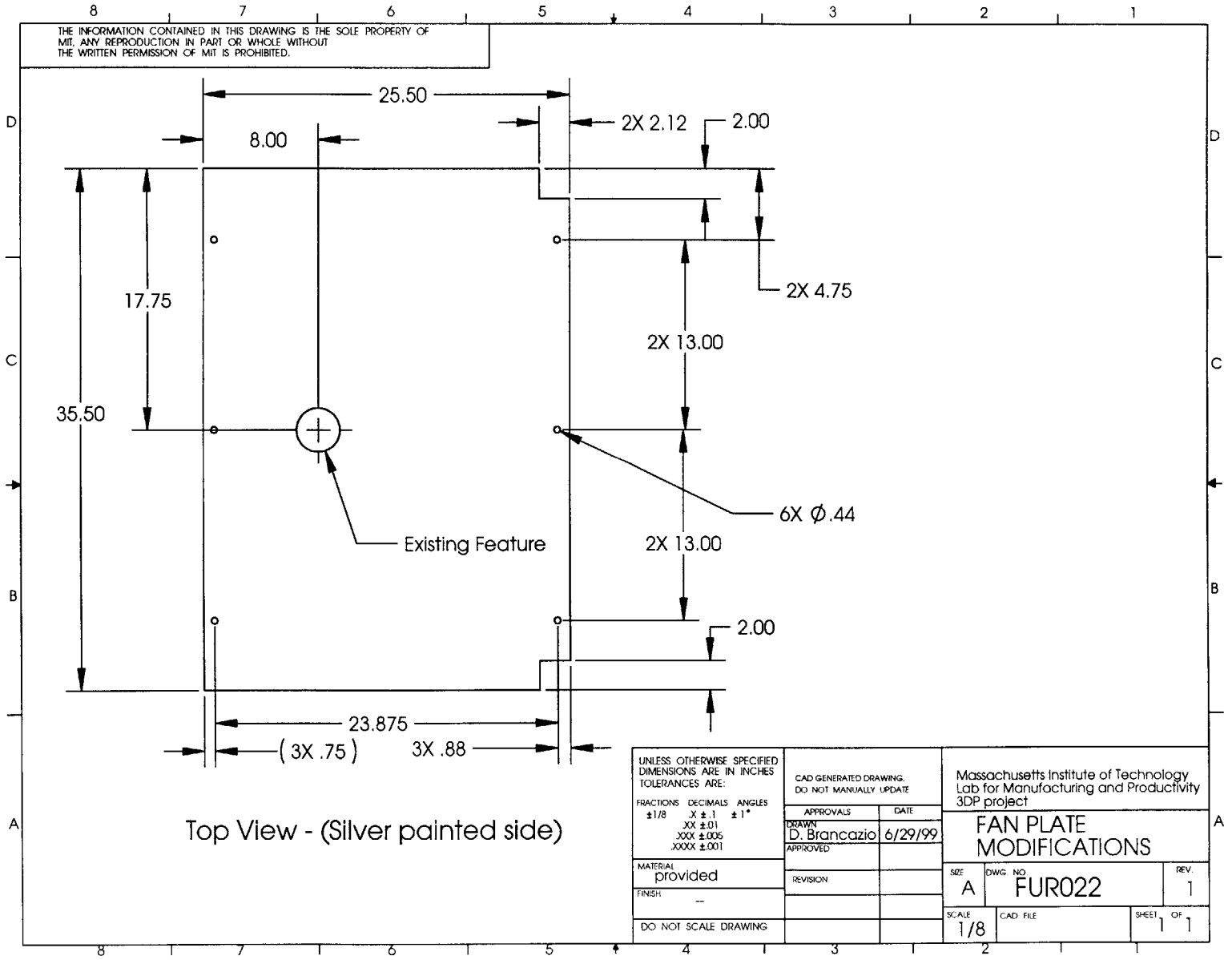
THE INFORMATION CONTAINED IN THIS DRAWING IS THE SOLE PROPERTY OF MIT. ANY REPRODUCTION IN PART OR WHOLE WITHOUT THE WRITTEN PERMISSION OF MIT IS PROHIBITED.
25.50
8.00
2X 2.12
2.00
17.75
2X 4.75
2X 13.00
35.50
Existing Feature
6X Ø.44
2X 13.00
2.00
23.875
(3X .75)
3X .88
Top View - (Silver painted side)
UNLESS OTHERWISE SPECIFIED DIMENSIONS ARE IN INCHES
TOLERANCES ARE:
FRACTIONS DECIMALS ANGLES
±1/8 .X ±.1 ±1°
.XX ±.01
.XXX ±.005
.XXXX ±.001
MATERIAL provided
FINISH --
DO NOT SCALE DRAWING
CAD GENERATED DRAWING. DO NOT MANUALLY UPDATE
APPROVALS DATE
DRAWN D. Brancazio 6/29/99
APPROVED
REVISION
Massachusetts Institute of Technology
Lab for Manufacturing and Productivity
3DP project
FAN PLATE MODIFICATIONS
SIZE A
DWG NO FUR022
REV. 1
SCALE 1/8
CAD FILE
SHEET 1 OF 1

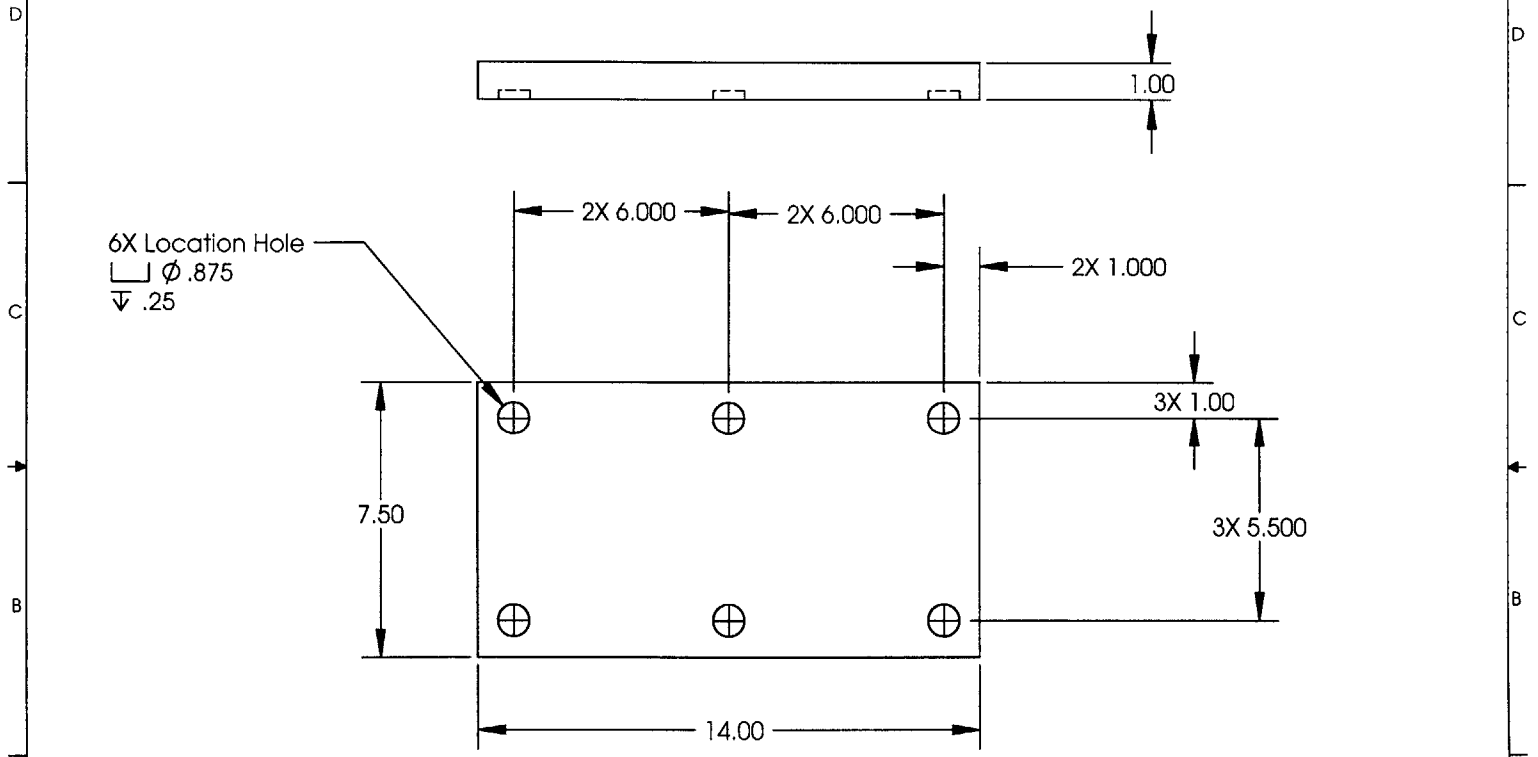

UNLESS OTHERWISE SPECIFIED DIMENSIONS ARE IN INCHES
TOLERANCES ARE:
FRACTIONS ±1/8 DECIMALS .X ±.1 .XX ±.01 .XXX ±.005 .XXXX ±.001 ANGLES ±1°
MATERIAL G r
FINISH - -
D O N O T S C

CAD GENERATED DRAWING. DO NOT MANUALLY UPDATE

APPROVALS	DATE
DRAWN D. Brancazio	7/6/99
APPROVED	
REVISION 3	3/14/00

Massachusetts Institute of Technology
Lab for Manufacturing and Productivity
3DP project

Hearthplate

SIZE A | DWG. NO. FUR023 | REV. 3

SCALE A 1/4 | CAD FILE: E D R A W I N G | SHEET 1 OF 1

REVISIONS

REV	DESCRIPTION	DATE	APPROVED

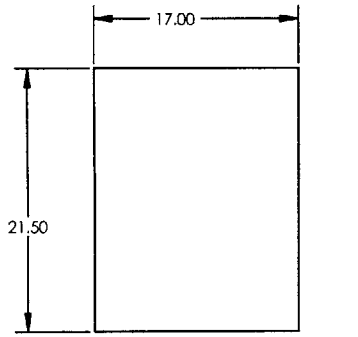

TOP Insulation
Qty: 1

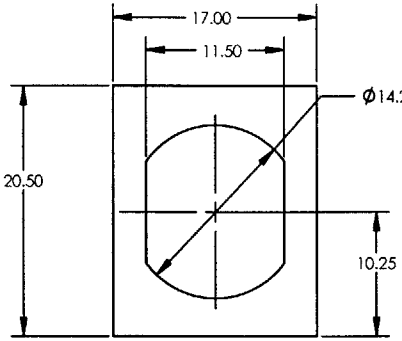

FRONT Insulation
Qty: 1

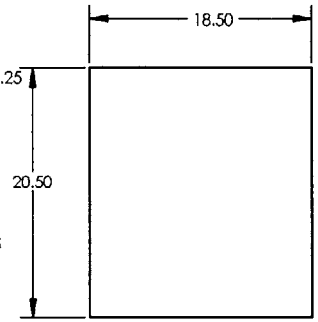

Left/Right Insulation
Qty: 2

Material Information

Manufacturer: Zircar Products, Inc.
Alumina Blanket, Type AB
Approx. thickness: 1 inch
96% Alumina, 4% Silica

Order of Installation in Box

1. Front
2. Top
3. Back
4. Bottom
5. 6. Left and Right

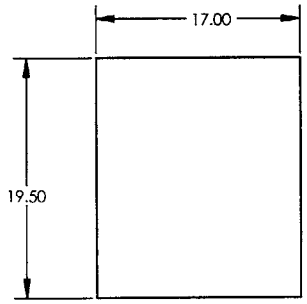

BACK Insulation
Qty: 1

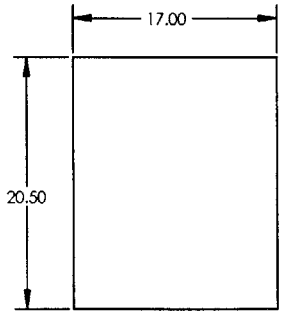

BOTTOM Insulation
Qty: 1

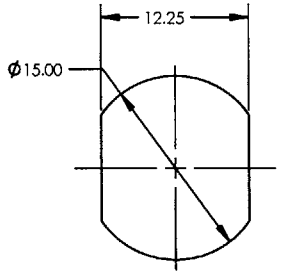

DOOR Insulation
Qty: 2

Massachusetts Institute of Technology
Lab for Manufacturing and Productivity
3DP project

Alumina Insulation, Furnace

SIZE	DWG. NO.	REV
B	FUR024	1
SCALE: 1/8	CAD FILE	SHEET 1 OF 1

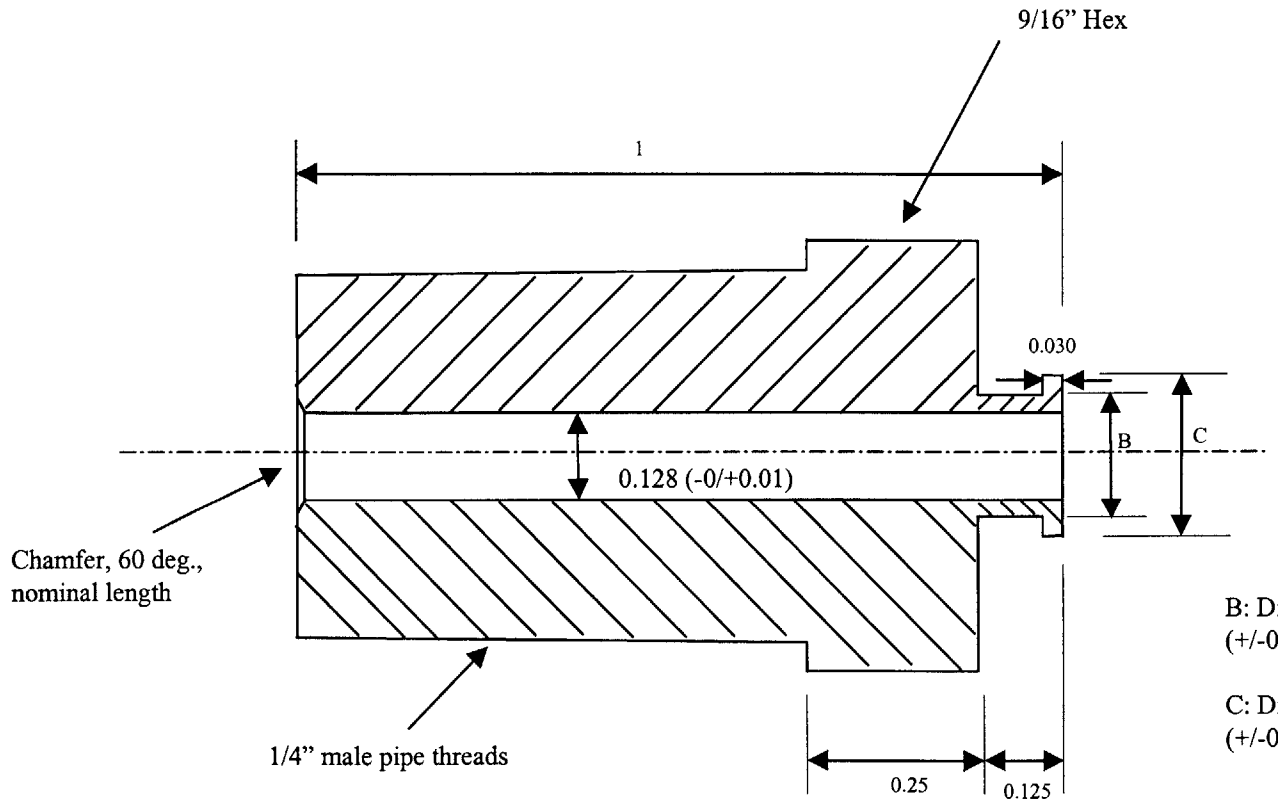

Note: All tolerances +-0.005", unless otherwise stated

Drawing #FUR025	
Ultem power feed through	All dimensions in inches
Scale: 4/1	

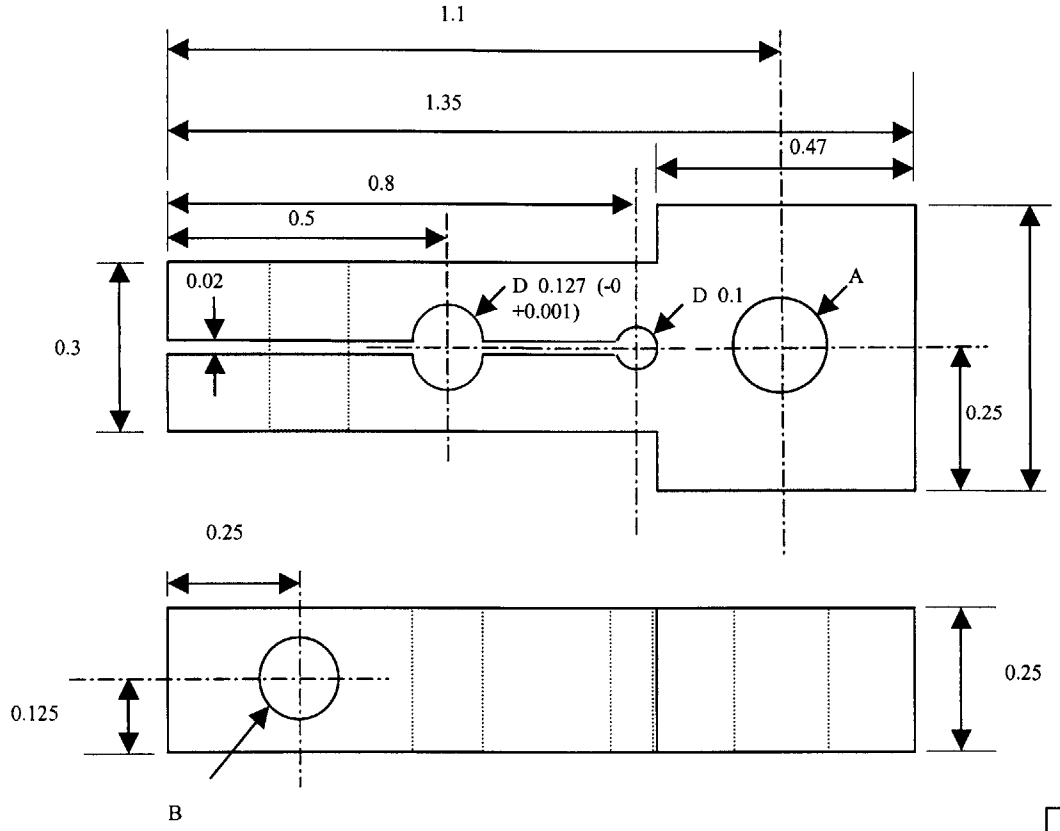

A: Clearance hole for 8-32 screw

B: Clearance hole for 6-32 screw

Note: All tolerances +-0.005" unless otherwise stated

Drawing #FUR026	
Brass electrical connector	All dimensions in inches
Scale: 4/1	

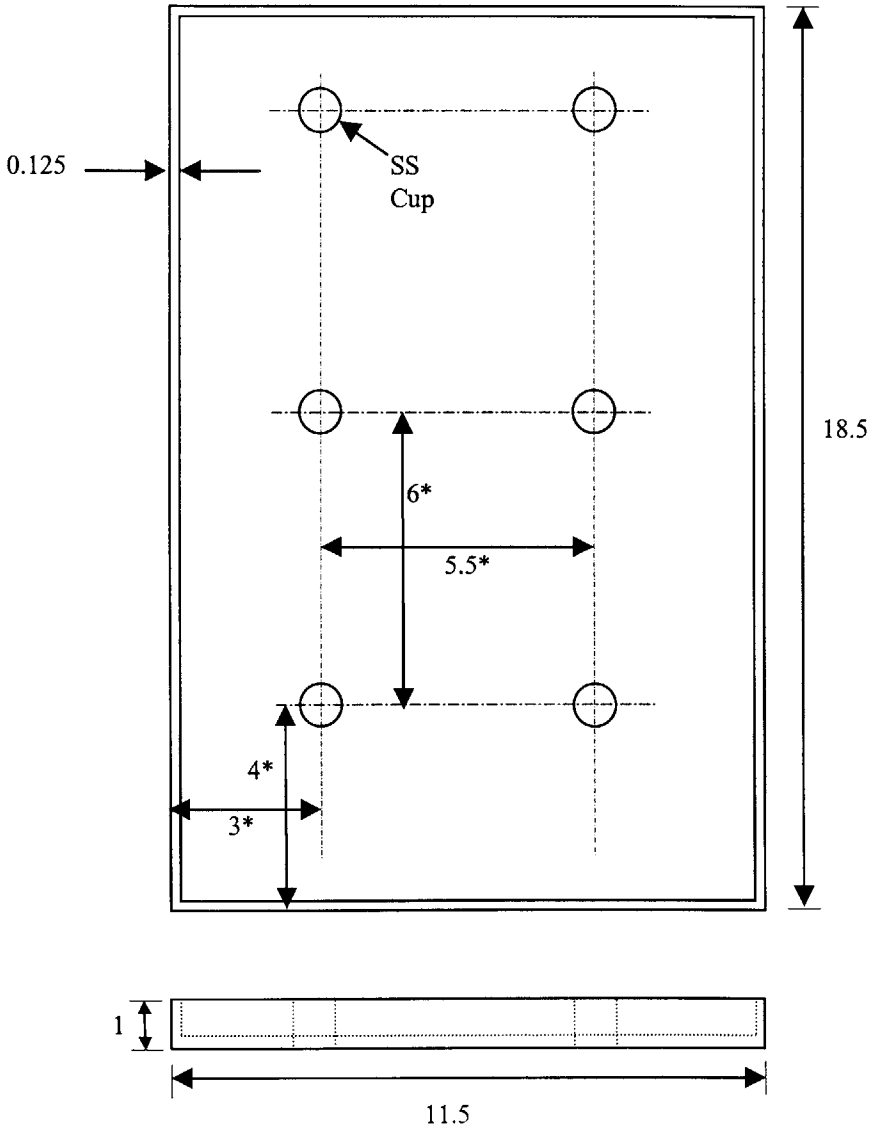

Note 1: Tolerance on * dimensions is +-0.01"

Note 2: SS cups are welded to the frame

Drawing #FUR027	
SS Catch tray	All dimensions in inches
Scale: 4/1	

Appendix 3: Sample Program for the Large Scale Furnace

The controller can store up to 49 different programs in memory. After choosing a program number that the user wants to program into, pressing the "func" and the "prog" keys on the controller panel enables the user to write into the program. A typical program that was used in a furnace run to sinter SS420 powder is presented here. This program was used to carry out run 5 that is described in Chapter 7.

Segment #	Set point	Time	Event 2	Event 3	Event 4	Event 5	PID #
1	10	5 sec					1
2	10	1 min	on	on	on	on	1
3	170	2 min	on	on	on	on	1
4	170	120 min	on	on	on	on	1
5	200	1 min	on	on			1
6	500	60 min	on	on			1
7	1000	100 min	on	on			2
8	1200	40 min	on	on			3
9	1200	60 min	on	on			3
10	20	10 min	on				3
11	20	480 min	on				3

Notes:

1. Segments 1 and 2 are dummy segments. If the very first segment of the program has the contents of segment 3, i.e. SP = 170 C, Time = 2 min, the controller interprets this to mean that it has to stay at 170 C for 2 minutes, and NOT as " ramp to 170 C in 2 minutes". However, the presence of dummy segment 2 before segment 3 causes the furnace to ramp to 170 C in 2 minutes starting at the end of segment 2 as desired.

2. Event 2 turns on the flow of Forming gas (and shuts off the flow of Argon), events 3 and 4 turn banks 1 and 2 respectively of external heaters on. Event 5 turns the top six internal heaters off.

3. Event 5 is on in segments 2 to 4. This causes power to be supplied only to the bottom zone of internal heaters. Also, the set point in segments 3 and 4 was chosen to be 170 C and not 200 C, which is the recommended purging temperature. This was done in order to account for the lag between the control thermocouple that is located in the top heater zone and the bottom heaters that are heating the furnace. This lag causes the bottom zone to overheat above the set point. It was found that a set point of 170 C proved right for the steady state furnace temperature during the purge to settle at around 200 C.

4. Note that segment 4 has been programmed to be 2 hours long. However, during the actual run, the "hold" key on the controller was pressed while the furnace run was in this segment. Once the dew point in the furnace got to below –25 C (which happened around 3 hours after the beginning of this segment in run 5 discussed in Chapter 7), the program was advanced to segment 5 by pressing the "prog" and "disp" keys on the controller together.

5. From segment 5 onwards, bank 2 of the external heaters are shut off and both zones of internal heaters are turned on (event 5 is off).

6. The ramp to 1200 C occurs at a rate of 5 C/min. Note that the ramp has been split into three sections, each of which has a different PID variable for control. PID1 is used for segments with a set point (SP) <= 500 C, PID2 for segments with 500 C< SP<=1000 C and PID 3 for segments with SP>1000 C.

7. The furnace is held at 1200 C for 60 minutes, during which time the SS420 powder sinters.

8. In segment 10, the furnace has been set to cool from 1200 C to 20 C in 10 minutes. Obviously, this is not possible (or desirable) since the only way the part can cool is by losing heat by natural convection. Thus natural convection limits the cooling rate of the furnace.

9. In segment 11, gas flow has been programmed to be left on for 8 hours after the furnace starts to cool down. Eight hours is enough time for the furnace to cool down to a temperature (< 250 C) at which there is no risk of oxidizing the SS part if flow of Forming gas is turned off.

Appendix 4: Using a Nextel Lined SS Crucible for Infiltrating Parts

In the course of performing experiments on directional solidification (Chapter 4), it was found that Graphite crucibles used for melting the infiltrant often used to crack due to thermal expansion induced stresses. Also, the Boron nitride coating that was used to coat the inside of a Graphite crucible would sometimes crack and cause the infiltrant to stick to the Graphite, rendering the crucible useless for future use.

Ideally, one would want to use a SS crucible (which would be much less likely to crack than Graphite) to melt the infiltrant. However, the only issue is that the infiltrant (typically Copper or Bronze) sticks to SS. Nextel, the fabric that was used extensively in the large scale furnace (see section 5.3.3 of Chapter 5), has the property that Copper or Bronze do not wet it. Thus, it was decided to line the inside of a SS crucible with Nextel BF20 fabric (see Appendix 1 for vendor listing) in order to carry out infiltrations. Molten infiltrant does not leak through the Nextel lining, which acts like a bag and contains the melt within itself. It is important to use unsized Nextel (sizing is a chemical coating applied to Nextel fabric to make sewing easy). Otherwise, vapor generated when the sizing burns off during a furnace run will contaminate the furnace atmosphere.

The picture below shows a Nextel lined SS crucible that was used to infiltrate parts in the large scale furnace (the part shown in Figure 7.8 of Chapter 7 was infiltrated using this crucible).

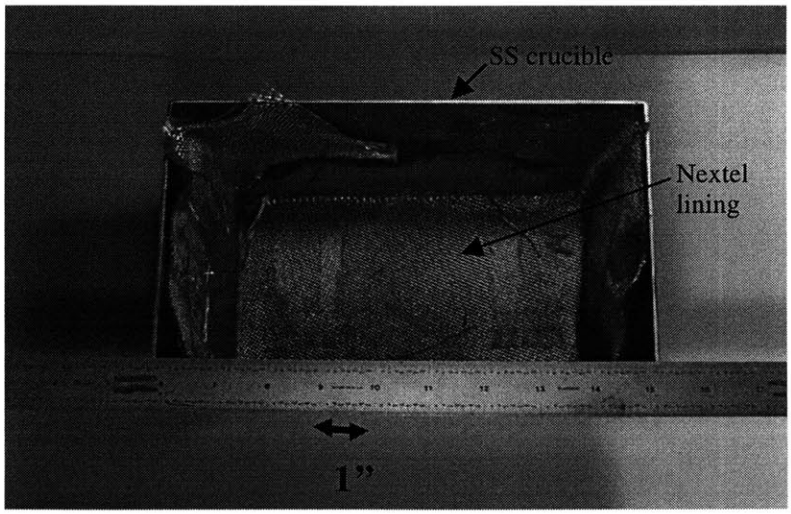

References

1. CRC Handbook of Chemistry and Physics, 80th ed., CRC Press, New York, 1999.

2. German, R.: Powder Metallurgy Science, 2nd ed., Metal Powder Industries Federation, Princeton, NJ, 1994.

3. Guo, Honglin.: " Alloy Design for Three- Dimensional Printing of Hardenable Tool Materials", Ph.D. Thesis, Massachusetts Institute of Technology, 1998.

4. Lorenz, A. M.: " Economical Furnace Processing for 3-D Printed Metal Parts", SM Thesis, Massachusetts Institute of Technology, 1998.

5. Mark's Standard Handbook for Mechanical Engineers, 10th ed., McGraw-Hill, Inc., New York, 1996.

6. Mills, A. F.: Heat Transfer, 2nd ed., Prentice Hall, NJ, 1999.

7. Shames, I. H.: Mechanics of Fluids, 3rd ed., McGraw-Hill, Inc., New York, 1992.

8. Strehlow, R. A.: Combustion Fundamentals, McGraw-Hill, Inc., New York, 1984.